Developing new diagnostic and therapeutic approaches in adrenocortical carcinoma

by

Vasileios Chortis

A thesis submitted to The University of Birmingham

for the degree of

DOCTOR OF PHILOSOPHY

Institute of Metabolism and Systems Research

College of Medical and Dental Sciences

The University of Birmingham

January 2017

Abstract

Adrenocortical carcinoma (ACC) is an aggressive malignancy with high recurrence rates and poor response to chemotherapy. With this work, we have evaluated a potential new treatment target focusing on the mitochondrial NADPH generator Nicotinamide Nucleotide Transhydrogenase (NNT). NNT has a central role within the mitochondrial antioxidant pathways, which protect cells from oxidative stress. Our hypothesis was that NNT silencing will expose cells to cytotoxic levels of oxidative stress. We knocked down NNT transiently in NCI-H295R ACC cells *in vitro*; this led to an increase in cellular oxidative stress and a strong cytotoxic and cytostatic effect. With stable NNT knockdown, we observed the emergence of a partially compensated phenotype over the course of time, with restored redox balance. Surprisingly, steroidogenesis was stimulated by transient NNT loss, challenging current perceptions about the impact of oxidative stress on steroidogenesis.

In our clinical study, we evaluated a new diagnostic tool for biochemical detection of ACC recurrence. Serial post-operative urine samples were collected from a large cohort of patients who had undergone complete ACC resection. Standardised review of longitudinal steroid measurements resulted in detection of disease recurrence prior to or concurrently with imaging with high sensitivity in cases where a pre-operative steroid profile had been provided.

Acknowledgements

I would like to thank my supervisors, Professor Wiebke Arlt and Dr Paul Foster, for all their support during my fellowship. Wiebke has been a never-failing source of inspiration and guidance since my very first steps in the world of scientific research. Paul has been an exemplary supervisor and with his experience and accessibility he has helped me greatly to develop my skills as a budding basic scientist.

I am grateful to a number of current and past IMSR members for their assistance and contributions in various parts of this work, including Angela Taylor, Irina Bancos, Craig Doig, Ian Rose, Lorna Gilligan, Anastasia Arvaniti, Hannah Ivison, Mick O'Reilly and Anne-Marie Hewitt. I would also like to thank Lou Metherell and Eirini Meimaridou at Queen Mary University of London for their collaboration in the *in vitro* work, as well as all European collaborators from the European Network for the Study of Adrenal Tumours who collectively contributed a large number of urine samples to facilitate our clinical study in a very rare disease.

Finally, I would like to dedicate this thesis to my parents, Konstantinos and Evgenia, to whom I owe both the 'life' and the 'good life', and to my partner, Emily, for all her love and support.

Table of Contents

Figures and Tables

Abbreviations

5-PD	pregnenediol
5-PT	pregnenetriol
ACA	adrenocortical adenoma
ACC	adrenocortical carcinoma
An	androsterone
ATP	adenosine triphosphate
B	corticosterone
Bcl2	B-cell lymphoma 2
BSO	buthionine sulfoximine
CRH	corticotropin releasing hormone
CT	computed tomography
CYP11A1	cholesterol side-chain cleaving enzyme
CYP11B1	11β-hydroxylase
CYP11B2	aldosterone synthase
CYP17A1	17α-hydroxylase- 17/20 lyase
CYP21A2	21-hydroxylase
DHEA	dehydroepiandrosterone
E	cortisone
ENSAT	European Network for the Study of adrenal Tumours
ETC	electron transfer chain
Etio	etiocholanolone
F	cortisol
FCCP	carbonyl cyanide-p-trifluoromethoxyphenylhydrazone
FDG-PET	fluorodeoxyglucose proton emission tomography
FGD	familial glucocorticoid deficiency
G6PD	glucose-6-Phosphate dehydrogenase
GC-MS	gas chromatography- mass spectrometry
GPX1	glutathione peroxidase 1
GPX3	peroxiredoxin 3
GSH	reduced glutathione
GSR	glutathione reductase
GSSG	oxidised glutathione
H_2O_2	hydrogen peroxide
HIF-1	hypoxia inducible factor 1
HSD11B1	cortisone reductase
HSD17B3	17β-hydroxysteroid dehydrogenase type III
HSD3B2	3β-hydroxysteroid dehydrogenase type II
HU	Hounsfiled Units
ICDH	isocitrate dehydrogenase

IGF2	insulin-like growth factor 2
IGF2R	IGF2 receptor
IMAZA	[$^{123/131}$I] azetidinylamide
IMTO	[$^{123/131}$I]iodometomidate
IQR	interquartile range
KD	knockdown
LC-MS/MS	liquid chromatography-tandem mass spectrometry
LND	lymph node dissection
MPTP	mitochondrial permeability transition pore
MRI	magnetic resonance imaging
MTHFD	methylene-THF reductase
NAD^+	nicotinamide adenine dinucleotide
NADH	reduced nioctinamide adenine dinucleotide phosphate
$NADP^+$	nioctinamide adenine dinucleotide phosphate
NADPH	reduced nioctinamide adenine dinucleotide phosphate
Nf-κB	nuclear-factor-kappa-light-chain enhancer of activated B cells
NNT	nicotinamide nucleotide transhyrogenase
Nrf2	nuclear factor E2- related factor 2
o,p'-DDD	mitotane
$O2^-$	superoxide
OAA	oxaloacetate
PD	pregnanediol
PHD	prolyl hydroxylase
POR	P450 oxidoreductase
PT	pregnanetriol
ROS	reactive oxygen species
S	deoxycortisol
SCR	scramble
SEM	standard error of the mean
SHMT2	serine hydroxymethyltransferase 2
shRNA	short-hairpin RNA
siRNA	small interfering RNA
SRD5A	5α-reductase
StAR	steroidogenesis acute regulatory protein
TCA	tricarboxylic acid cycle
THDOC	tetrahydrodeoxycorticosterone
THF	tetrahydrofolate
TP53	tumour protein p53
TXN	oxidised thioredoxin
TXN-$(SH)_2$	reduced thioredoxin
TXNRD2	thioredoxin reductase 2
VDAC	voltage-dependent ion channel
VLCFA	very long chain fatty acids
α-KG	α-ketoglutarate

1 General Introduction

1.1 The organ: the adrenal gland and adrenal steroidogenesis

1.1.1 Development and anatomy of the adrenal gland

The adrenal glands, first described by Eustachius in 1563, are two endocrine glands located in the retroperitoneal space above the kidneys. The right adrenal is pyramidal in shape, while the somewhat larger left gland is semilunar. Normal adrenal glands do not size more than 5x3 cm and do not weigh more than 7-10 g. Each gland consists of two parts, the outer cortex and the inner medulla, with distinct embryogenic extractions and biosynthetic orientations. The adrenal cortex arises from the urogenital ridge of the mesoderm during early foetal life, thus sharing the same origin as testicular Leydig cells. Conversely, the medulla arises from the neural crest, part of the ectoderm, and eventually migrates to the adrenal primordium around gestational week seven. The foetal adrenal cortex consists of two zones: the temporary foetal zone, which undergoes apoptotic demise after birth, and the definitive adult zone. Molecular pathways which have been implicated in the embryonic development of the adrenal gland include the β-catenin and sonic hedgehog pathways (Wood and Hammer, 2011).

The adult adrenal cortex consists of three parts, named according to their microscopic structure:

a) The outer zona glomerulosa, site of mineralocorticoid hormone secretion
b) The central zona fasciculata, site of glucocorticoid secretion
c) The inner zona reticularis, site of sex steroid precursor secretion

The adrenal medulla specialises in the synthesis of catecholamines (adrenalin, noradrenalin and dopamine).

Arterial blood supply to the adrenal gland is provided through three main branches: the superior suprarenal artery (from the inferior phrenic artery), the middle suprarenal artery (directly from the aorta) and the inferior suprarenal artery (from the renal artery). Venous drainage is through a central adrenal vein; on the right this is short and drains directly to the inferior vena cava, while on the left venous flow follows a longer route, the adrenal vein draining to the left renal vein (**Fig. 1-1, 1-2**).

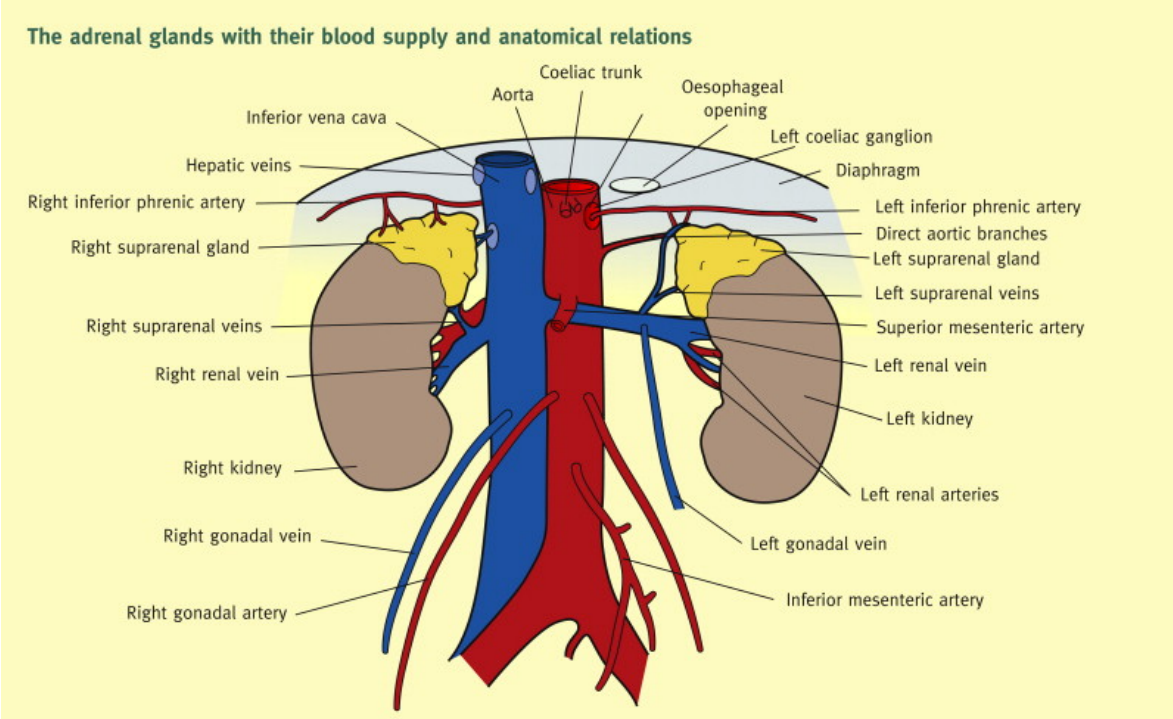

Figure 1-1. The adrenal glands. Source:(Ritchie and Balasubramanian, 2011). Reproduced with permission of Elsevier.

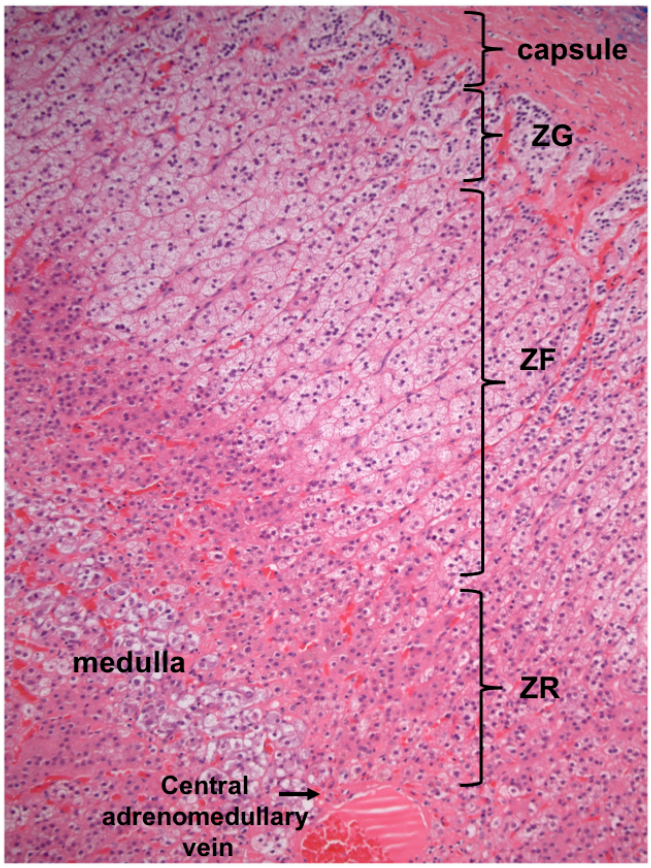

Figure 1-2 Adrenal histology. The adrenal cortex consists of 3 distinct zones, each specialising in the secretion of a different class of steroid hormones: the outer zona glomerulosa (ZG - mineralocorticoids), the intermediate zona fasciculata (ZF - glucocorticoids) and the inner zona reticularis (ZR - androgens). This nomenclature springs from the respective microscopic appearance of each zone. The adrenal medulla comprises the core of the gland and synthesizes catecholamines (adrenalin/noradrenalin/ dopamine). Image provided by Dr K Skordilis from her personal archive.

1.1.2 Steroidogenesis

1.1.1.1 Regulation

Steroid synthesis in each zone of the adrenal cortex is regulated by distinct trophic hormones and negative feedback loops.

a) Zona glomerulosa. Mineralocorticoid (e.g. aldosterone) synthesis in the external zone of the adrenal cortex occurs within the context of the renin-angiotensin-aldosterone axis. Briefly, renin is generated in the juxtaglomerular cells of the kidneys and mediates the cleavage of angiotensin I in the liver. Angiotensin I is converted to angiotensin II by the angiotensin-converting enzyme, and binds to the angiotensin type II receptor in the adrenal cortex to stimulate aldosterone synthesis. Aldosterone stimulates sodium reabsorption and potassium excretion in the renal tubules; the same electrolytes regulate renin production, closing the feedback loop.

b) Zona fasciculata. Glucocorticoid (e.g. cortisol) synthesis in this middle zone of the adrenal cortex is stimulated by the pituitary peptide adrenocorticotropic hormone (ACTH), which is released in response to the hypothalamic hormone CRH (corticotropin-releasing hormone). ACTH release follows a pulsatile pattern which underpins the characteristic circadian rhythm of cortisol excretion by the adrenal glands. Circulating glucocorticoids exert negative feedback on the hypothalamus (CRH) and the pituitary (ACTH), completing the loop. Stressful stimuli (trauma, sepsis, surgery, psychological stress) can acutely potentiate ACTH excretion and, consequently, augment glucocorticoid synthesis.

c) Zona reticularis. The release of adrenal androgen precursors DHEA and androstenedione is also regulated by ACTH; those can be converted in the periphery to active androgens and oestrogens.

1.1.2.1 Adrenal steroidogenic pathways

Adrenal steroidogenesis is a complex, multi-stage biosynthetic process leading to the generation of mineralocorticoids (aldosterone, zona glomerulosa), glucocorticoids (cortisol, zona fasciculata) and androgen precursors (DHEA/androstenedione, zona reticularis) from the common initial precursor cholesterol. ACTH is implicated in the first stages of cholesterol handling by the adrenocortical cells: ACTH interaction with the melanocortin 2 receptor (MC2R) stimulates intracellular cyclic AMP (cAMP) formation, triggering the protein kinase A signalling pathway; this accelerates both ingress of cholesterol esters into adrenocortical cells and intracellular cleavage of esters to cholesterol. The ensuing steps of cholesterol metabolism are mediated by two broad categories of enzymes: a) cytochrome P450 enzymes and b) hydroxysteroid dehydrogenases. The former can be further grouped into mitochondrial (type I) P450 enzymes (side chain cleavage enzyme, CYP11A1; 11β-hydroxylase, CYP11B1; aldosterone synthase, CYP11B2) and microsomal (type II) P450 enzymes (17α-hydroxylase, CYP17A1; 21-hydroxylase, CYP21A2; aromatase, CYP19A1) (Miller, 2005, Payne and Hales, 2004). All P450 enzymes catalyse monooxygenase reactions, inserting one atom of oxygen into organic substrates while the other oxygen atom is reduced to water; for this they require co-factor proteins which supply the essential electrons. Adrenodoxin/ adrenodoxin reductase (also referred to as ferrodoxin/ ferrodoxin reductase) is the protein couple donating electrons to all mitochondrial P450 enzymes, using reduced nicotinamide adenine dinucleotide (NADPH) as their cofactor. Endoplasmic reticulum-based P450 enzymes receive

their essential electron flow from P450 oxidoreductase (POR) (Miller, 2005). Cholesterol (27 carbons) is transported across the mitochondrial membrane by the steroid acute regulatory protein (StAR), where it is converted to pregnenolone (21 carbons) by the cholesterol side-chain cleavage enzyme (CYP11A1) in a reaction requiring three oxygen molecules and three NADPH molecules. The glucocorticoid pathway involves conversion of pregnenolone to progesterone by 3β-hydroxysteroid dehydrogenase type II (HSD3B2) activity, hydroxylation to 17-hydroxyprogesterone by 17α-hydroxylase (CYP17A1), further hydroxylation at carbon 21 by 21-hydroxylase (CYP21A2) and, finally, 11β-hydroxylation by 11β-hydroxylase (CYP11B1) to form cortisol. In the mineralocorticoid pathway, progesterone is first converted to deoxycorticosterone by 21-hydroxylase activity, followed by three CYP11B2-mediated hydroxylation steps leading to the ultimate generation of aldosterone via the intermediate precursors corticosterone and 18-hydroxycorticosterone. Finally, androgen synthesis requires consecutive 17α-hydroxylase and 17-20 lyase activities of the enzyme CYP17A1, which utilises its dual enzymatic potential to successively hydroxylate pregnenolone to 17-hydroxypregnenolone and then convert the latter to dehydroepiandrostenedione (DHEA). DHEA is predominantly secreted by the adrenal in the form of its sulfate ester, DHEAS, generated from unconjugated DHEA by DHEA sulfotransferase (SULT2A1). Glucocorticoid and mineralocorticoid hormones consist of 21 carbon atoms, while androgens consist of 19 and oestrogens of 18 carbon atoms. A schematic outline of adrenal steroidogenesis is provided in **Fig. 1-3**. **Table 1-1** summarises the characteristics of adrenal steroidogenic enzymes.

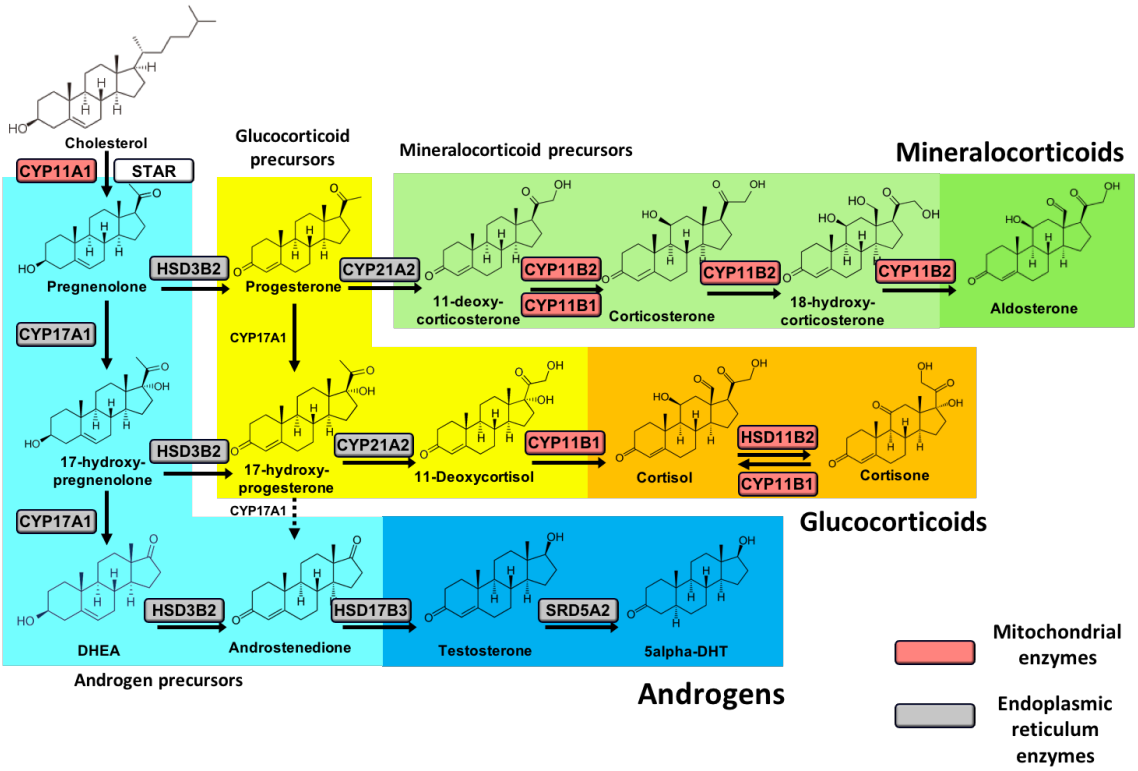

Figure 1-3. Steroidogenesis includes three biosynthetic pathways: the mineralocorticoid pathway (zona glomerulosa), the glucocorticoid pathway (zona fasciculata) and the androgen pathway (zona reticularis). Each pathway involves steps mediated by endoplasmic reticulum (ER) enzymes and mitochondrial enzymes.

Table 1-1 Enzymes participating in adrenal steroidogenesis

Gene	Enzyme	Protein	Tissue expression	Subcellular localization
CYP11A1	Cholesterol side-chain cleaving enzyme	CYP11A1, P450scc	Adrenal cortex, ovary, testis, placenta	Mitochondria
CYP11B1	11β-hydroxylase	CYP11B1, P450c11	Adrenal cortex (zona fasciculata/ reticularis)	Mitochondria
CYP11B2	Aldosterone synthase	CYP11B2, P450c18	Adrenal cortex (zona glomerulosa)	Mitochondria
CYP17A1	17α-hydroxylase-17/20 lyase	CYP17A1, P450c17	Adrenal cortex, ovary, testis	Endoplasmic reticulum
CYP21A2	21-hydroxylase	CYP21A2, P450c21	Adrenal cortex	Endoplasmic reticulum
HSD3B2	3β-hydroxysteroid dehydrogenase type II	HSD3B2, 3β-HSDII	Adrenal cortex	Endoplasmic reticulum

1.2 The disease: Adrenocortical Carcinoma

1.2.1 Epidemiology of adrenocortical carcinoma

Adrenocortical carcinoma (ACC) is a rare but aggressive malignancy arising from the adrenal cortex. The exact incidence of ACC is unknown, but data from cancer registries in the United States and Europe suggest an estimate of 0.7-2 cases per million population per year (1975, Kerkhofs et al., 2013, Fassnacht et al., 2011). This statistic is in striking contrast to the high prevalence of adrenal masses in general, which are encountered in 3-10% of the population according to radiological and autopsy series and are usually benign (Bovio et al., 2006, Kloos

et al., 1995, Fassnacht et al., 2016). A singularity in global ACC epidemiology is observed in Southern Brazil, an area afflicted by a 2.9-4.2 case-per-million incidence of paediatric ACC (worldwide incidence = 0.2 cases per million per year), largely due to the correspondingly high prevalence of mutations in the tumour suppressor gene TP53 (Custodio et al., 2012). ACC appears to have a bimodal age distribution, with a relative peak in the first decade of life and a second, higher peak in the fourth and fifth decade (Wajchenberg et al., 2000). Gender distribution is characterised by female preponderance (1.5:1). Interestingly, this predilection for the female sex seems to apply exclusively to hormonally functional tumours (Wooten and King, 1993, Fassnacht and Allolio, 2009). Limited observational data suggest that long-term use of oral contraceptives may be an additional risk factor (hazard ratio = 1.8, confidence interval 1-3.2) (Hsing et al., 1996). This suggests oestrogens may be involved in the pathogenesis of ACC in some cases; indeed, there is *in vitro* evidence of a pro-proliferative effect of oestrogens on ACC cells (Montanaro et al., 2005, Somjen et al., 2003). The same case-control study identified smoking history as a risk factor in male patients (hazard ratio 2, 95% confidence interval 1-4.4). This finding was corroborated by another series of 250,000 US veterans, as well as rodent studies involving tobacco exposure; the paucity of histological confirmation of ACC in the aforementioned clinical studies, however, mandates caution in the interpretation of these data (Hsing et al., 1996, Chow et al., 1996, Dalbey et al., 1980). Another interesting, and thus far unexplained, epidemiological feature of ACC is the predominance of left-sided tumours over right-sided ones. A literature review of 14 recent publications identified 2607 left-sided vs. 2169 right-sided (Mihai, 2015). Selection bias has been proposed as a potential explanation for this disparity: right-sided tumours are more often inoperable due to liver invasion or vena cava involvement, which may render them less likely

to be reported (Mihai, 2015). Bilateral ACCs are extremely rare and it is usually unclear whether they represent independent tumours or metastases to the contralateral adrenal gland.

1.2.2 Presentation

The majority (45-60%) of new ACC patients present with symptoms of hormone excess, most commonly glucocorticoid (50-80% of hormone secreting ACCs) and/or androgen hormone-related (40-60% of hormone secreting ACCs) (Else et al., 2014, Allolio and Fassnacht, 2006, Luton et al., 1990). Clinical manifestations of glucocorticoid excess (Cushing's syndrome) include centripetal obesity, supraclavicular/ dorsocervical fat pads, facial plethora, skin atrophy, easy bruising, violaceous abdominal striae, oligomenorrhoea (<9 menstrual periods per year), amenorrhoea (total cessation of menses for more than 6 months), diabetes mellitus, osteoporosis with pathological fractures and psychiatric symptoms of depressive or psychotic character (Fassnacht et al., 2011, Else et al., 2014, Libe, 2015). Hypertension and hypokalaemia are often observed in the context of glucocorticoid excess, as the overabundant cortisol can saturate the protective renal enzyme 11β-hydroxysteroid dehydrogenase type II (inactivates cortisol to cortisone) and activate the mineralocorticoid receptor. Androgen excess can become clinically manifest in female patients as hirsutism, acne or, in more extreme cases, virilism (androgenetic alopecia, voice masculinisation, clitoromegaly) (**Fig. 1-4**). In men, overall androgen activity is predominated by testicular testosterone, which obscures the incipient adrenal androgen excess. Oestrogen excess is uncommon (1-5% of cases) and can present as feminisation (gynaecomastia, loss of libido, testicular atrophy) in males or menstrual perturbations in female patients (Allolio and Fassnacht, 2006, Else et al., 2014). Concurrent secretion of glucocorticoids and androgens is not uncommon

(approximately 50% of functional ACCs) and portends underlying adrenocortical malignancy (Else et al., 2014). Aldosterone-producing ACCs are rarely encountered; in such cases, drug-resistant hypertension is the clinical hallmark of mineralocorticoid excess (Seccia et al., 2005, Abiven et al., 2006) .

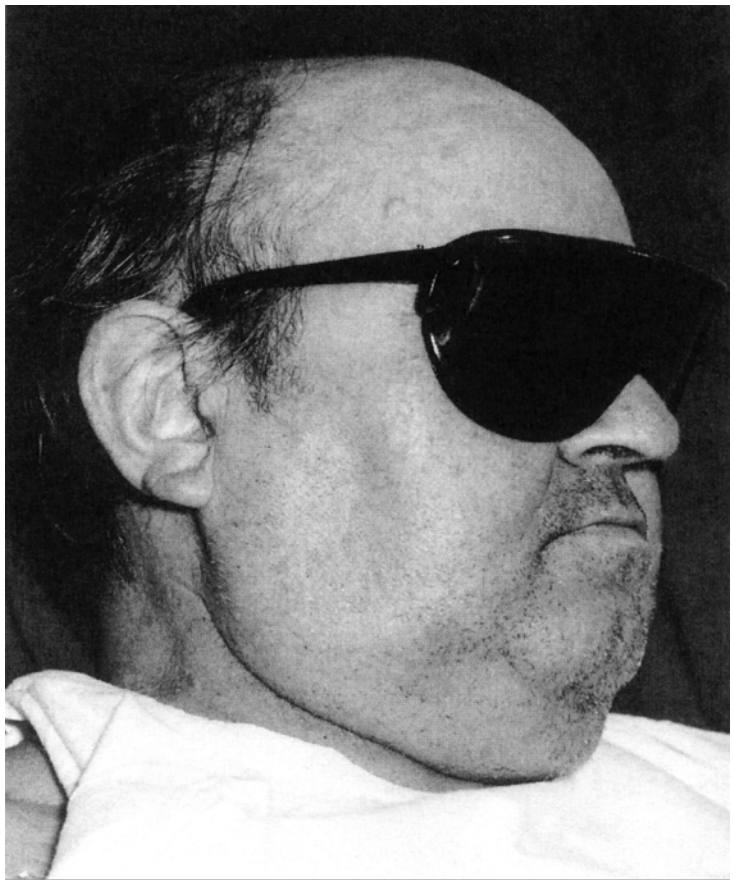

Figure 1-4 Severe virilisation in a female patient with cortisol and androgen- producing ACC. Reproduced with permission of Prof W. Arlt from her personal archive with patient consent.

Loco-regional manifestations due to mass expansion occur at diagnosis in about 20% of ACC patients, including abdominal discomfort, nausea and vomiting (Berruti et al., 2010, Luton et

al., 1990, Else et al., 2014). Nonspecific symptoms of malignancy (fever, weight loss, myalgia, malaise) are rarely the presenting complaint. Pathological fractures as a result of bone metastases can be the initial symptom in patients presenting with advanced disease. Finally, about 10-20% of new ACCs are discovered incidentally in the context of abdominal cross-sectional imaging requested for reasons other than the suspicion of adrenal disease (adrenal incidentalomas) (Fassnacht and Allolio, 2011). This proportion is expected to rise progressively with the ever-increasing use of computed tomography (CT) and magnetic resonance imaging (MRI).

ACCs are generally large tumours at presentation, averaging 10-13 cm in diameter (Berruti et al., 2010, Abiven et al., 2006, Sturgeon et al., 2006). Since 2009, the European Network for the Study of Adrenal Tumours (ENSAT) classification has replaced the International Union Against Cancer (UICC) staging classification, as it demonstrated a higher prognostic accuracy with respect to disease recurrence and overall survival. The new classification emerged from the study of 492 ACC patients from the German Registry (mean follow-up of 36 months) and was subsequently validated in a North American Population of 573 patients (Fassnacht et al., 2009, Lughezzani et al., 2010). According to this system (**Table 1-2**), malignant adrenal tumours associated with periadrenal fat extension, adjacent organ invasion or local lymph node involvement are classified as stage III disease and are associated with poorer prognosis than localised tumours of any size. Stage IV consists solely of patients with distant metastases and is associated with a very poor prognosis. A modified version of this classification system was recently proposed by Libe et al. This involves a) a shift of all tumours with local lymph node involvement to stage IV, as this is a finding with dismal prognostic implications and b) definition of three stage IV subgroups depending on the number of organs that are affected

(IVa: 2 organs, IVb: 3 organs, IVc: > 3 organs; primary tumour and local lymph node involvement count as one organ each) (Libe et al., 2015).

As with many other malignancies, the percentage of patients presenting with advanced tumours has decreased in recent decades with the widespread use of cross-sectional imaging, which allows earlier diagnosis. In a meta-analysis of studies published from 1952-1992, 49% of patients presented with metastatic disease, while less than a third of patients presented with localised tumour (stage I or II) (Wooten and King, 1993). In more recent series, 25-30% of ACC patients appear to present with metastatic disease, and stage II disease has become the most common stage at presentation. ACCs measuring less than 5 cm at presentation remain uncommon (about 5% of cases at presentation) (Fassnacht and Allolio, 2011, Else et al., 2014). In patients with advanced disease, the lungs and the liver are the most common metastatic sites (each affecting 40-80% of metastatic cases), followed by the skeleton (5-20%) (Bilimoria et al., 2008, Fassnacht and Allolio, 2011).

Table 1-2 ENSAT ACC Classification

ENSAT ACC Classification System		
Stage	**TNM classification**	**TNM Definitions**
I	**T1, N0, M0**	T1, tumor ≤5 cm N0, no positive lymph node M0, no distant metastases
II	**T2, N0, M0**	T2, tumor >5 cm N0, no positive lymph node M0, no distant metastases
III	**T1–T2, N1, M0** **T3–T4, N0–N1, M0**	N1, positive lymph node(s) M0, no distant metastases T3, tumor infiltration into surrounding tissue T4, tumor invasion into adjacent organs ***or*** venous tumor thrombus in vena cava or renal vein
IV	**T1–T4, N0–N1, M1**	M1, presence of distant metastases

1.2.3 Diagnosis

1.2.3.1 Biochemistry

Securing a thorough adrenal hormone profile is indispensable in the work-up of newly discovered adrenal lesions for a number of clinical reasons. Firstly, the functional status of the tumour will often inform management decisions (surgical vs. conservative management) and can accurately diagnose medullary lesions (phaeochromocytomas). Secondly, it is imperative to identify patients with glucocorticoid excess before surgery: these patients are at very high risk of post-operative adrenal suppression, which can lead to a life-threatening 'adrenal crisis' if appropriate hydrocortisone replacement is not in place. Finally, routine evaluation of

adrenal steroidogenesis can sometimes provide helpful diagnostic clues to the underlying nature of the lesion (benign adenoma vs ACC), as androgen and/or oestrogen production is extremely uncommon in benign adenomas. Urinary adrenal steroid profiling by mass spectrometry-based techniques represents an emerging diagnostic tool to differentiate benign from malignant adrenocortical tumours, with very promising results in retrospective studies (Arlt et al., 2011).

A comprehensive way of excluding adrenal hormone excess is described in **Table 1-3**. Screening for glucocorticoid hypersecretion is typically based on the overnight dexamethasone suppression test (ONDST), which involves morning serum cortisol measurement after night-time administration of 1mg dexamethasone; the drug's potent glucocorticoid activity suppresses endogenous cortisol in healthy individuals, generally to a serum concentration of <50 nmol/L. Abnormal ONDSTs should be corroborated by second-line tests such as 24-hour urinary free cortisol and salivary midnight cortisol. Morning or random serum cortisol is of little diagnostic value. Most patients with autonomous adrenal glucocorticoid hypersecretion will also have a suppressed plasma ACTH (Nieman et al., 2015, Fassnacht et al., 2016).

Screening for mineralocorticoid excess is mandatory in patients with adrenal tumours and concurrent hypertension or hypokalaemia but should always be done if ACC is suspected. High plasma aldosterone with suppressed renin is suggestive of mineralocorticoid excess (Conn's syndrome) (Nieman et al., 2015, Fassnacht et al., 2016). Screening for adrenal sex steroid excess includes plasma DHEAS, androstenedione, oestradiol, testosterone and 17-hydroxyprogesterone and should be performed in all patients with clinical evidence of hyperandrogenism/ hyperoestrogenism or in patients with high clinical/ radiological suspicion

of ACC (Fassnacht et al., 2016). Analysis of 24-h urine samples by Gas Chromatography-Mass Spectrometry (GC-MS) is a more sensitive means of detecting androgen excess, but is not readily available in all centres at present (Arlt et al., 2011, Kerkhofs et al., 2015). Finally, exclusion of a medullary chromaffin tumour (phaeochromocytoma) is essential in all patients with adrenal masses, not least because of the risk of a potentially fatal adrenergic crisis if surgery is attempted without prior institution of alpha adrenergic receptor blockade. Plasma or urine metanephrines (metabolites of adrenalin and noradrenalin) have overtaken urine catecholamines as the best performing screening test, able to detect phaeochromocytomas with a sensitivity of 98% and specificities above 90% (Lenders et al., 2014).

Table 1-3 Overview of adrenal steroidogenesis

Adrenal zone	Hormone class	Screening tests	Comments
Zona glomerulosa	Mineralocorticoids	Aldosterone, renin	Essential if concurrent hypertension or suspicion of ACC
Zona fasciculata	Glucocorticoids	Overnight dexamethasone suppression test (ONDST) 24-hour urine free cortisol (UFC) Paired (day/night) salivary cortisol ACTH	Abnormal response in ONDST should be confirmed by second-line tests
Zona reticularis	Androgens, oestrogens	Testosterone, DHEAS, Androstenedione, 17-OH-Progesterone, Oestradiol, Progesterone	Essential if clinical suspicion of sex hormone excess or ACC
Adrenal medulla	Catecholamines	Plasma or urine metanephrines	Repeat in supine position if modestly raised

1.2.3.2 Imaging

Adrenal lesions are most commonly discovered in the context of cross-sectional imaging undertaken for reasons other than the suspicion of adrenal pathology (adrenal incidentalomas). Imaging remains instrumental in the diagnostic work-up of a new adrenal lesion, providing useful clues that aid the differentiation of benign adrenocortical adenomas (ACAs) from ACCs and other adrenal pathologies (e.g. phaeochromocytomas, metastases, myelolipomas). Imaging-based characterisation is largely based on the tendency of ACCs to be larger than ACAs and lipid-poor.

Computed tomography (*CT)* is the most commonly used imaging modality in the work-up of adrenal lesions. Generally, adrenal adenomas tend to have a diameter of < 4cm (mean size 3.5cm) while ACCs tend to measure > 6 cm; however, it is worth noting that no more than 25% of adrenal masses > 6 cm turn out to be ACCs (Mantero et al., 2000, Adams et al., 1983). A diagnostic cut-off of > 4 cm provides a sensitivity of 97% for ACC detection, but its specificity is disappointingly low at 52%. Raising the cut-off to 6cm improves specificity to 80% at the cost of a diminished sensitivity of 91%, which is unsatisfactory for definitive cancer diagnostics (Sturgeon et al., 2006). Non-contrast attenuation reflects the lipid content of the lesion; lesions with attenuation < 10 Hounsfield Units (HU) are lipid-rich, a trait which is common in adrenal adenomas but is never encountered in ACCs. Consequently, baseline attenuation lower than 10 HU is 100% specific for benignity and can be safely relied on to exclude malignancy (Dinnes et al., 2016). However, it should be noted that up to 30% of adenomas have an attenuation of >10 HU (lipid-poor adenomas), which is diagnostically unavailing. In patients with previous history of extra-adrenal malignancies and, consequently, higher risk of adrenal metastasis from the primary tumour, false-negatives (i.e. missed cases of malignancy) can occur using >10 HU as a diagnostic cut-off (estimated up to 7%) (Dinnes

et al., 2016). Heterogeneity is most commonly a feature of ACCs, due to the frequent presence of necrosis, haemorrhage or calcification within the malignant tumour, as is irregularity of tumour perimeter.

In cases where attenuation cannot help to differentiate between benign and malignant tumours, contrast washout studies can provide further diagnostic clues, as contrast retention within the tumour tends to be more prolonged with malignancy. Contrast washout of > 50% after 15 mins is suggestive of ACA, but available evidence on the test's performance is poor (Dinnes et al., 2016). Finally, CT of chest, abdomen and pelvis including intravenous contrast remains the first-line investigation to exclude metastases and stage ACC in most centres.

Magnetic Resonance Imaging (MRI) can also be of value in the characterisation of adrenal tumours. ACCs appear isointense to hypo-intense relative to the liver parenchyma on T1-weighted images and hyper-intense relative to the liver parenchyma on T2-weighted images. A particularly useful feature is the loss of signal intensity comparing in-phase to out-of-phase T1-weighted imaging with chemical-shift MRIs, indicative of high lipid content. Persistence of signal intensity on out-of-phase imaging provided a sensitivity of 90% and specificity of 85% for malignancy detection in a small study (Ream et al., 2015), but further studies are required to establish the actual diagnostic performance of this imaging modality (Dinnes et al., 2016).

Fluorodeoxyglucose- Positron Emission Tomography/ Computed Tomography (^{18}F-FDG-PET/CT). ^{18}F-FDG-PET/CT technology has been increasingly used in diagnostic oncology in recent years, predicated on the principle that malignant cells tend to have higher glycolytic rates than healthy cells (Warburg effect). Consequently, administered glucose will be taken up by malignant masses, which will appear as 'hot spots' on the scan (Kunikowska et al., 2014).

3 small studies have explored the diagnostic performance of ^{18}F-FDG-PET/CT in the work-up of adrenal tumours; pooled estimates suggest a sensitivity of 84% and specificity of 90% but evidence quality remains poor (Dinnes et al., 2016).

In summary, no single imaging modality appears to display sufficient accuracy to function independently as a reliable diagnostic test in a high-stake clinical context (considerable pre-test probability of malignancy). Moreover, most relevant studies are plagued by poor methodology and/or small sample size. On this background, the only diagnostic strategy really supported by good quality evidence is excluding malignancy in lesions with non-contrast attenuation of <10 HU in patients with no previous history of malignancy. In moderate/ high attenuation lesions, clinicians and patients still have to live with uncertainty, precariously placed on a clinical field covered by a very thin ground of evidence.

1.2.3.3 Pathology

As in all malignancies, histopathology provides the conclusive diagnosis of ACC; nevertheless, the differentiation between benign and malignant adrenal tumours can often be challenging even on a microscopic level. A recent retrospective study suggested that 13% of adrenocortical tumours assessed in Germany are incorrectly classified on surgical histology (Johanssen et al., 2010). Importantly, transcutaneous core biopsy of an adrenal lesion cannot differentiate between ACA and ACC in the absence of metastases and may lead to disease dissemination (needle canal seeding); therefore its role in the work-up of patients with suspected ACC is very limited (Fassnacht et al., 2016, Bancos et al., 2016). In whole-tumour specimens provided post-operatively, a number of features are used to diagnose ACC, including nuclear grade, mitotic rates, atypical mitoses, cytoplasmic morphology, microscopic

architecture, necrosis, venous or sinusoidal invasion and capsular invasion (**Fig. 1-5**). These have been incorporated in validated scoring systems that are widely used to diagnose ACC, most notably the Weiss scoring system (Table 1-4) (Weiss et al., 1989). Tumours with a Weiss score of 3 or above are considered malignant, while scores 0-2 are diagnostic of ACA. Aubert et al. subsequently proposed a modification of the Weiss system, excluding four criteria with substantial inter-observer variability (**Table 1-4**) (Aubert et al., 2002); despite its claim to diagnostic superiority, however, the modified Weiss model has not managed to overtake its predecessor in clinical practice (Papotti et al., 2011).

Ki67 is a proliferation marker that is also diagnostically relevant, as the vast majority of ACCs have a Ki67 value of > 3% (Libe, 2015). High Ki67 values are generally associated with more aggressive behaviour, although rare cases of metastatic ACCs with Ki67 <1% have also been described (Libe et al., 2015, Berruti et al., 2012, Beuschlein et al., 2015). Immunohistochemical features that are employed to distinguish adrenocortical from medullary tumours include positivity for steroidogenic factor 1 (SF1), inhibin, melan A, calretinin and synaptophysin, and negativity for chromogranin A, epithelial membrane antigen and cytokeratin (Weiss, 1984, Papotti et al., 2011, Sbiera et al., 2010).

Histologic variants of ACC include oncocytic ACC, myxoid ACC and sarcomatoid ACC. Oncocytic ACC is the most common of the three and is characterised by an abundance of cells with granular cytoplasm due to accumulation of mitochondria and endoplasmic reticulum (Wong et al., 2011, Macchi et al., 1998). The Weiss score is less accurate in this context and can lead to over-diagnosis of malignancy (Else et al., 2014).

Table 1-4 Weiss criteria for histologic ACC diagnosis, as per a) the classical Weiss model (Weiss et al, 1989) and b) its subsequent modification by Aubert et al (Aubert et al, 2002). Each criterion scores one point if present. Total scores ≥ 3 are diagnostic of ACC.

Histologic criteria	Comments	Score (Weiss system)	Score (Aubert modification)
Nuclear grade 3 or 4 (Fuhrman criteria)		1	Not included
>5 mitoses per 50 high-power visual fields			2
Atypical mitoses	Defined by abnormal distribution of chromosomes or excessive number of mitotic spindles	1	1
<25% of tumour cells are clear cells	Resembling the normal zona fasciculata	1	2
Diffuse architecture	More than one third of tumours forming patternless sheets of cells	1	Not included
Necroses		1	1
Venous invasion	Tumour cells within endothelium-lined vessel with smooth muscle as wall component	1	Not included
Sinusoidal invasion	Tumour cells within endothelium-lined vessel with little or no supporting tissue	1	Not included
Capsular invasion		1	1
Maximum score		9	7

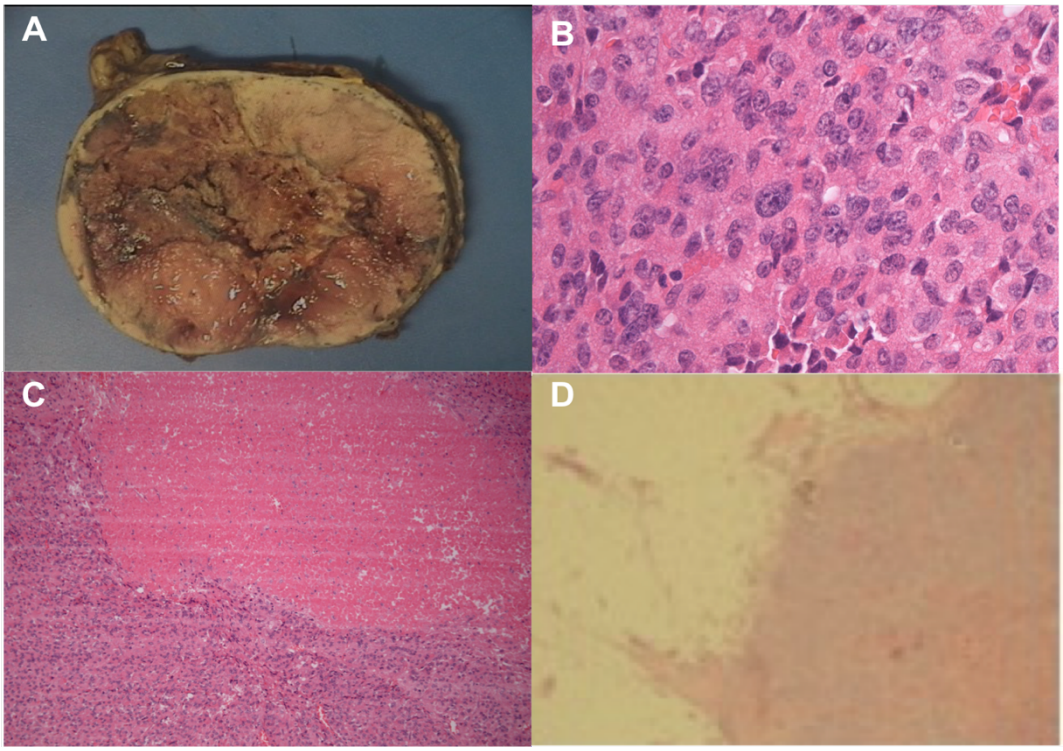

Figure 1-5 ACC histology. A) Macroscopic view of an excised ACC; B) High-grade ACC with nuclear polymorphism; C) ACC with necrotic area; D) ACC (brown) with capsular invasion and infiltration of surrounding fat (yellow). Images provided by Dr K. Skordilis from her personal archive.

1.2.3.4 Emerging modalities – urinary steroid profiling

An intriguing alternative approach which has gained impetus in recent years utilises biochemistry to distinguish between benign and malignant lesions, employing mass spectrometry-based approaches which can overcome the major limitations of routine biochemistry (cross-reactivity, low specificity) and provide a much more comprehensive steroid profile (Taylor et al., 2015). 24-h urine collections analysed by mass spectrometry allow quantification of steroid hormones whose plasma concentration is too low, and also neutralise the effects of diurnal variation which can be significant in adrenal biochemistry. ACCs present an inefficient pattern of steroidogenesis, characterised by relative abundance of

precursor steroids produced during the intermediate steps of steroidogenesis. This distinct steroid fingerprint, attributed to the typical dedifferentiation, and therefore relative immaturity, of malignant adrenocortical cells, can be of diagnostic value (Arlt et al., 2011). Sporadic case reports published over 60 years ago noted the excretion of 'atypical' steroid hormones in ACC patients, most notably the glucocorticoid precursor metabolite 11-tetrahydrodeoxycorisol (THS) and the androgen metabolite pregnenetriol (5-PT), corresponding to intermediate steps of steroidogenesis (Hirschmann and Hirschmann, 1950, Touchstone et al., 1954, Okada et al., 1959). Similar findings were reproduced independently in two small case series comparing ACAs to ACCs, published over the next three decades (Biglieri et al., 1963, Minowada et al., 1985). A subsequent small study compared plasma levels of 11-deoxycorticosterone, corticosterone, 11-deoxycortisol and cortisol between 4 paediatric patients with ACC and 4 with ACA. The ratio of corticosterone/ 11-deoxycorticosterone was lower in ACC and increased post-operatively, suggesting 11β-hydroxylase deficiency (Doerr et al., 1987). Grondal et al. analysed the urinary steroid profile of 24 patients with ACCs, comparing them to ACAs and healthy controls. 23/24 ACCs displayed increased excretion of 3 beta-hydroxy-5-ene steroids and cortisol precursor metabolites, indicative of 3 beta-hydroxysteroid dehydrogenase/delta isomerase and 11β-hydroxylase deficiency (Grondal et al., 1990). Similar findings were reported in a series of 5 ACC patients, revealing low ratios of cortisol metabolites/ tetrahydrocortisol metabolites and high levels of the androgen metabolite pregnenetriol (Tiu et al., 2009). Obviously, the small cohorts used in these studies represent a major limitation. This was overcome in a recent international retrospective study, which managed to recruit a sizeable cohort of 102 ACA and 45 ACC patients (Arlt et al., 2011). Urinary steroid profiling using gas chromatography-mass spectrometry provided an extensive panel of 32 steroid metabolites. Computational analysis

generated a machine learning-based prediction algorithm able to differentiate ACCs from ACAs with a sensitivity and specificity of 90%, a performance superior to that of any available imaging modality (Arlt et al., 2011). Nine steroid biomarkers were selected as the most diagnostically relevant ones in this context, and utilisation of their values alone yielded a sensitivity/specificity of 90% (**Fig. 1-6**). These results were corroborated in a subsequent smaller retrospective study (27 ACCs, 107 ACAs) also demonstrating disparate urinary steroid excretion patterns between benign and malignant adrenocortical tumours. THS was the biomarker with the highest accuracy at discriminating ACCs from ACAs (Kerkhofs et al., 2015). Finally, a recent retrospective study in a similar cohort (31 ACCs, 108 ACAs) also ascertained increased urinary excretion of THS and DHEAS in ACCs, as well as evidence of lower CYP11A1 and CYP11B1 activity based on product/substrate ratios (Velikanova et al., 2016). An ongoing prospective study (EURINE-ACT) will endeavour to validate these results and establish urine steroid metabolomics as a diagnostic tool for the differential diagnosis of adrenal tumours, in a cohort exceeding 2,000 patients.

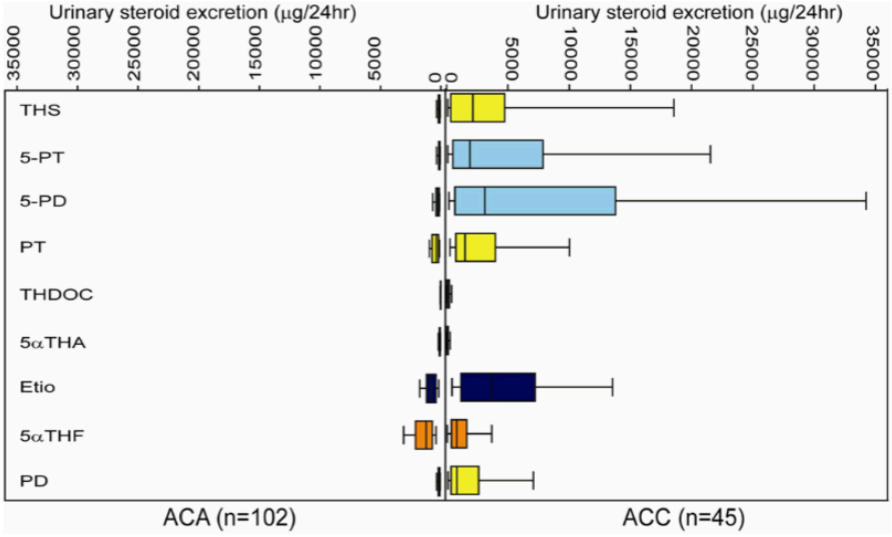

Figure 1-6 Differences in secretion of 9 urinary steroid metabolites between ACAs and ACCs. THS: tetrahydrodeoxycortisol; 5-PT: 5-pregnenetriol; 5-PD: pregnenediol; PT: pregnanetriol; THDOC: tetrahydrocorticosterone; 5α-THA: 5α-tetrahydro-11-deoxycorticosterone; Etio: etiocholanolone; 5a-THF: 5a-tetrahydrocortisol; PD: pregnanediol. Source: (Arlt et al., 2011). Reproduced with permission of the Endocrine Society.

1.2.4 Prognosis

ACC is generally a disease with poor prognosis, with overall 5-year survival rates ranging from 16-44% in different series (Fassnacht and Allolio, 2009). This considerable inter-study variability has been ascribed to selection bias leading to under-reporting of operated patients in some series with particularly grim survival estimates.

The ENSAT staging system has been the foundation of prognostication in ACC patients in the last decade. Stage I is associated with the highest 5-year survival rates (66-82%); this drops to 58-64% for stage II and 24-50% for stage III. Prognosis is extremely poor for patients with metastatic disease, with reported 5-year survival rates in the range of 0-17% (Fassnacht et al., 2009, Icard et al., 1992, Kerkhofs et al., 2013, Lughezzani et al., 2010) **(Fig. 1-7)**.

Importantly, lymph node involvement is a particularly ominous sign, associated with 13% 5-year survival in a recent retrospective study in the North American population (Bilimoria et al., 2008). Patients younger than 55 years of age display higher survival rates than their older counterparts (Bilimoria et al., 2008).

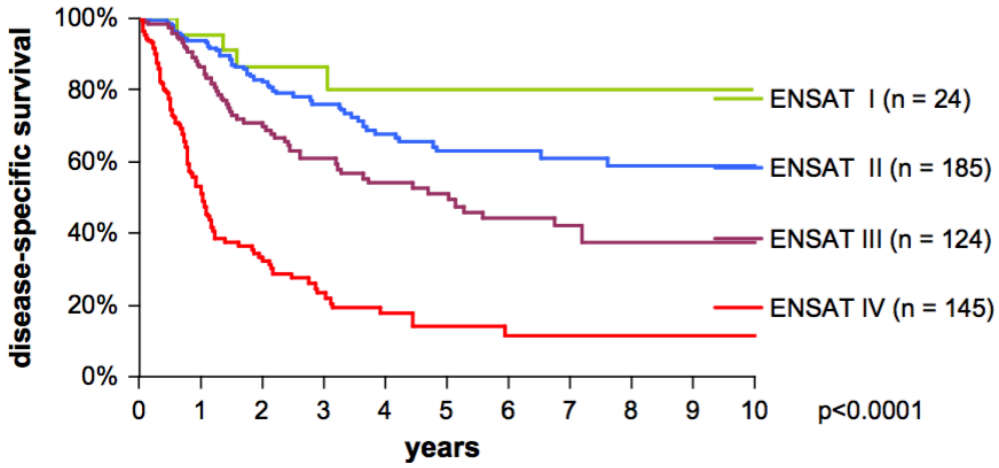

Figure 1-7 Disease-specific survival according to ENSAT stage, based on data from the German Registry. Source: (Fassnacht and Allolio, 2009). Reproduced with permission of the Endocrine Society.

Post-operatively, tumour resection status appears to be the most important predictor of outcome. Microscopically complete (R0) resection is associated with 50% 5-year survival, while prognosis for patients with microscopically (R1) or macroscopically (R2) incomplete resection is clearly poorer (5-year survival 20% and 15%, respectively) (Bilimoria et al., 2008). Amongst patients who have undergone complete resection, the proliferation marker Ki67 is the most significant predictor of recurrence-free and overall survival, as demonstrated recently in a large retrospective study including 2 independent European cohorts (Beuschlein et al., 2015). In another recent retrospective study in patients with advanced ACC (stage III-

IV), poor prognosis was portended by the following factors: patient age > 50 years, symptomatic disease at presentation, incomplete resection, presence of multiple metastatic sites and high tumour grade (Weiss score ≥ 6 and/or Ki67 ≥ 20%) (Libe et al., 2015).

Genomic and epigenomic markers of prognostic relevance (hyper-methylation status, driver gene mutations, miRNA profile) have recently started to emerge and represent a dynamic field of high potential in ACC research (Assie et al., 2014).

1.2.5 Molecular pathology

The last 2 decades have seen radical progress in our understanding of the molecular basis of ACC, although this has not, as yet, been translated into changes in the clinical management of these patients.

1.2.5.1 Clonality and chromosomal aberrations

ACCs consist of a monoclonal cell population; this suggests a biological history of clonal expansion in response to genetic mutations, eventually leading to cancer formation (Beuschlein et al., 1994, Gicquel et al., 1994). Aneuploidy is highly prevalent in ACCs and rare in ACAs, but it is as yet unclear whether the resulting genomic instability is a driver of carcinogenesis. Phenotypically, diploidy was associated with poor prognosis in one study (Haak et al., 1993). Structural chromosomic defects are also more frequent in ACCs than in ACAs, as revealed by a number of comparative genomic hybridisation (CGH) studies. Chromosomal gains at chromosome 5, 7, 12, 16, 19, and 20, as well as losses at chromosome 13 and 22, appear to be the most common aberrations observed in ACCs at this level

(Kjellman et al., 1996, Kjellman et al., 1999, Gicquel et al., 2001, Dohna et al., 2000, Barreau et al., 2013).

1.2.5.2 Gene expression

Global gene expression studies (gene expression arrays) have identified a number of foci and patterns of altered gene expression in ACCs. A study comparing 33 ACCs to 22 ACAs distinguished chromosomal regions of enhanced (12q and 5q) or repressed (11q, 1p, 17p) expression (Giordano et al., 2009). Increased expression of genes involved in cellular proliferation is an important feature of ACC; this is contrary to the pattern of increased expression of steroidogenic genes which characterises ACAs (de Fraipont et al., 2005). Interestingly, two distinct clusters of gene expression were discovered in ACCs in a subsequent study, each carrying different prognostic implications. Increased expression of genes involved in cellular proliferation was associated with poor patient survival, while overexpression of genes involved in cell differentiation, metabolism, and intracellular transport resulted in a less aggressive clinical phenotype (de Reynies et al., 2009). Combined overexpression of BUB1B and PINK1, genes involved in cell cycle regulation, was independently associated with poor outcome, a finding which was corroborated in a subsequent independent study (de Reynies et al., 2009, Fragoso et al., 2012).

1.2.5.3 Gene mutations

ACC is a genetically diverse malignancy. The most commonly reported somatic mutations on loss of heterozygosity (LOH) studies involve *TP53* (tumour protein p53), *MEN1* (menin),

IGF2 (insulin-like growth factor 2), *IGF2R* (IGF2 receptor), *p16/INK4A (CDKN2A)* and *CTNNB1* (β-catenin) (Else et al., 2014). The tumour suppressor gene *TP53*, involved in the molecular pathogenesis of several cancer types, is the most commonly affected gene, with mutations found in about a third of ACC patients (Barzon et al., 2001, Ohgaki et al., 1993, Reincke et al., 1994, Reincke et al., 1996). TP53 is involved in cell cycle control, impeding cell cycle progression in response to certain insults. It has a pivotal role within the apoptotic pathways, affecting the expression of genes that facilitate mitochondrial apoptosis or increasing the expression of cell death receptors. Molecular inducers of *TP53* mutations include DNA damage by UV light, redox stress and chemotherapy (Else et al., 2014, Malkin et al., 1990). Loss of TP53 function results in uncontrolled cellular proliferation, with failure to respond to apoptotic triggers. TP53 mutations in ACC can be either somatic or, less commonly, germline mutations in the context of Li-Fraumeni syndrome (Malkin et al., 1990, Wu et al., 2006). Germline mutations are rare in adult ACC patients (4%) but the commonest mutation in paediatric ACC (50-80% of cases) (Fassnacht et al., 2011). Li-Fraumeni patients have an exceedingly high lifetime cancer risk (> 70% in males, almost 100% in females) (Wu et al., 2006).

Insulin growth factors 1 and 2 (IGF-1 and IGF-2) are important inducers of adrenal cell proliferation and steroidogenesis. High IGF-2 and/or IGF-1 levels are encountered in >80% of sporadic ACCs and are associated with a more aggressive clinical behaviour with high recurrence rates (Gicquel et al., 2001, de Reynies et al., 2009). Overgrowth syndromes driven by mutations in the IGF-2 locus leading to up-regulation of IGF-2 (Beckwith-Wiedemann syndrome and Idiopathic Hemihypertrophy) are also associated with a higher risk of ACC, which appears to comprise 7-15% of malignant tumours observed in such patients

(Lapunzina, 2005, Wiedemann, 1997). Overgrowth syndromes are also associated with a high prevalence of adrenocortical adenomas and cysts (Lapunzina, 2005).

The WNT/beta-catenin pathway is instrumental in foetal adrenal development. Activating mutations in the catenin gene *CTNNB1* are present in at least 25% of both ACCs and ACAs (Gaujoux et al., 2008, Tadjine et al., 2008). WNT/beta-catenin signalling can lead to mesenchymal transformation promoting cell invasion, and beta-catenin overexpression portended aggressive disease course in one study of ACC patients (Ragazzon et al., 2010). Cases of ACC have been reported in patients with Familial Adenomatous Polyposis, an inherited syndrome of multiple intestinal polyps which is molecularly underpinned by constitutive beta-catenin activation, but it is unclear whether this reflects a genuine association or mere statistical coincidence of two rare conditions (Else, 2012).

Other genetic syndromes for whom an association with a higher ACC risk has been suggested include Multiple Endocrine Neoplasia type 1 (*MENIN* gene) and Neurofibromatosis type 1 (neurofibromatin gene); however, the epidemiological evidence supporting these associations is so far less than convincing (Else, 2012).

1.2.5.4 Recent advances - Epigenetic changes and integrated genomic characterisation

On an epigenetic level, gene promoter hyper-methylation leading to altered gene expression was ascertained in a series of 51 ACCs and was correlated with poor clinical outcomes (Barreau et al., 2013).

Two recent studies applied state-of-the-art integrated genomic analysis and identified discrete clusters of ACCs. Assie et al. analysed a group of 45 ACCs and identified two subgroups: a

group characterised by high number of mutations and methylation alterations (C1A) and a group defined by specific deregulation of two miRNA clusters (C1B) (Assie et al., 2014). Clinical outcomes were disparate between the two groups, C1A tumours being associated with poor prognosis. Two years later, genomic analysis in a cohort of 76 ACCs identified three broad molecular clusters of ACCs, integrating data from four platforms (DNA copy number, DNA methylation, mRNA expression, miRNA expression) (Zheng et al., 2016). Importantly, each cluster was associated with different outcomes **(Fig. 1-8)**.

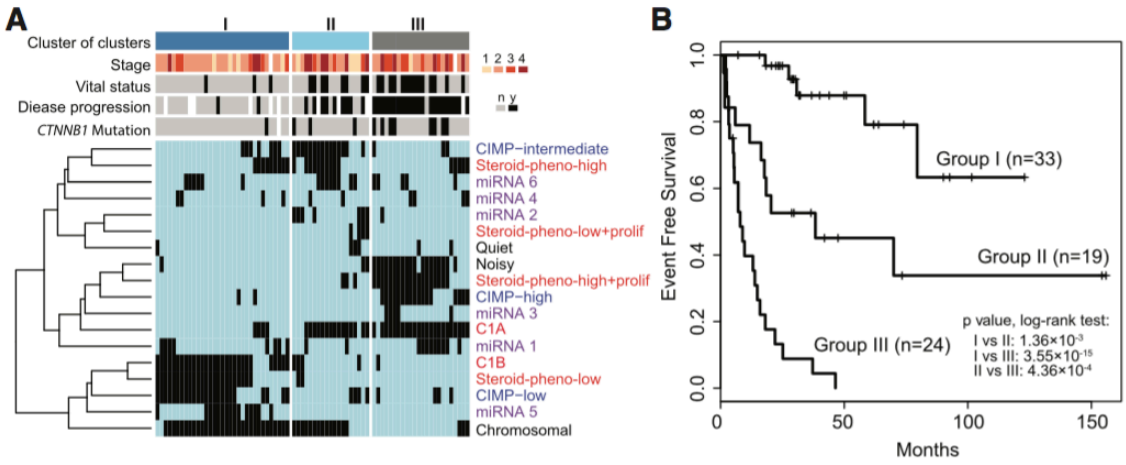

Figure 1-8 Cluster of clusters molecular analysis in a cohort of 76 ACC patients (source: Zheng et al., 2016). A) Cluster of clusters analysis integrating data from four different platforms (DNA copy number, black; MRNA expression, red; DNA methylation, blue; miRNA expression, purple) identifies three distinct clusters (groups). Black bars represent sample positivity for the corresponding molecular parameter. CIMP: CpG island methylation phenotype. C1A and C1B refer to the gene expression profiles defined by de Reynies et al, 2009 B) Event-free survival analysis of the three groups shows correlation of molecular clustering with patient outcomes. Reproduced with permission of Elsevier.

1.2.6 Management

1.2.6.1 Surgery

Surgery for primary tumours. The only hope of cure for ACC patients is complete (R0) tumour resection. Radical surgery with curative intent should be offered to all fit for surgery patients with localised, resectable tumours. This includes all patients with ENSAT stage I-II disease and most patients with stage III disease (Mihai, 2015, Fassnacht and Allolio, 2009). There is still debate as to the optional mode (open vs. laparoscopic) and extent of surgery (e.g. inclusion of local lymph nodes). There is no definitive clinical evidence for the superiority of an open vs a laparoscopic approach; however, most experts would advocate open adrenalectomy in suspicious adrenal tumours, especially if the size is such that renders full excision without breach of the tumour capsule technically challenging (e.g. tumour diameter > 5-6 cm), or if there is radiological suspicion of locally infiltrative disease with lymph node involvement (Berruti et al., 2010, Libe, 2015, Mihai, 2015). Lymph node dissection (LND) is not a formal part of radical adrenalectomy but has become more topical in recent years, after a retrospective study demonstrating reduced recurrence rates in ACC patients having undergone LND (Reibetanz et al., 2012).

In cases where complete tumour resection is not feasible, debulking surgery may have a role in functional tumours associated with clinically distressing hormone excess (e.g. glucocorticoids) that is difficult to control medically (Mihai, 2015). There is no evidence to support the value of debulking resection in non-functional tumours, although some authors suggest it should be considered in slow-growing tumours (low Ki67) where over 90% of total tumour load can be resected (Schteingart et al., 2005).

Surgery for local recurrence or metastasis. Surgery also has a role in select patients who develop recurrent or metastatic disease after primary tumour resection. Three retrospective studies have suggested that resection of locally recurrent disease can improve survival, especially in cases where complete resection of the recurrent tumour is possible or patients who recurred more than 12 months after resection of the primary tumour (Schulick and Brennan, 1999, Erdogan et al., 2013, Dy et al., 2013). The role of metastasectomy in patients with low-volume distant metastatic disease (e.g. 1-2 small metastatic foci) is contentious and the number of described cases in the literature remains low. Data from small retrospective studies suggest some survival benefit may be conferred on patients with fully resectable lung or liver metastases, particularly if the metastasis occurred more than 12 months after the first surgery (Mihai, 2015, Assie et al., 2007, Di Carlo et al., 2006, op den Winkel et al., 2011, Datrice et al., 2012). Patients who recur less than 12 months from surgery have very poor prognosis and metastasectomy does not appear to have a role, as emergence of disseminated, multi-focal disease is all but inexorable (Mihai, 2015).

1.2.6.2 Mitotane

Mitotane (o,p'-DDD) is an analogue of the insecticide dichlorodiphenydichloroethane (DDD). It has been well established as the first line of recurrent/metastatic ACC management since the 1960s and, more than 5 decades later, remains the only drug specifically approved for this use by the Food and Drug Agency and the European Medicine Executive Agency (Hahner and Fassnacht, 2005, Terzolo, 2012). Mitotane is used as monotherapy in patients with inoperable recurrent disease of limited volume, or within combination chemotherapy regimens in patients with more advanced and/or aggressive disease. Despite its long history of

use, evidence supporting the efficacy of mitotane actually emanates from retrospective or small prospective studies, many of which used hormonal control rather than radiographic or survival data as indicator of clinical response. No randomised-controlled trial has ever formally compared mitotane to other treatment options (Hahner and Fassnacht, 2005, Berruti et al., 2010, Terzolo, 2012). Within these methodological limitations, available evidence suggests modest response rates ranging from 13-33% of treated patients; results tend to be short-lived. Mitotane has a narrow therapeutic window, as blood levels of at least 14 mg/l have to be attained to facilitate satisfactory anti-tumour activity, while levels above 20 mg/l are associated with high rates of toxicity (Terzolo, 2012, Else et al., 2014). In clinical practice, tolerability is highly variable, with some patients developing toxicity in sub-therapeutic levels while others tolerating levels above 20 mg/l perfectly well. Adverse effects include gastrointestinal manifestations (nausea, vomiting, diarrhoea), hepatotoxicity and neurotoxicity (dysarthria, ataxic gait, confusion) (Hahner and Fassnacht, 2005). Hypogonadism and gynaecomastia are often observed, due to disturbance of testicular steroidogenesis, elevation of the steroid hormone binding globulin and inhibition of 5a-reductase (Hahner and Fassnacht, 2005, Chortis et al., 2013). Another important feature of mitotane treatment is the invariable induction of adrenal insufficiency. This has been ascribed both to the drug's adrenolytic activity (i.e. damage of the healthy adrenal gland) and to CYP3A4 enzyme induction leading to acceleration of cortisol breakdown. High-dose hydrocortisone replacement is therefore essential to avoid a life-threatening adrenal crisis (Chortis et al., 2013). Induction of the microsomal CYP3A4 enzymatic system by mitotane is also inopportune in view of its effects on other medications ACC patients may receive. Indeed, more than 50% of current formulary drugs are metabolised by this system, and dose adjustments may be necessary to avoid treatment failure. This includes several of the most

commonly used cytotoxic chemotherapy options in these patients (Chortis et al., 2013, Kroiss et al., 2011).

Aside from its role in the treatment of active disease, mitotane is commonly used as adjuvant treatment after primary tumour resection. The ability of adjuvant mitotane to reduce recurrence rates in patients with surgically excised ACC was demonstrated in a large retrospective study comparing three cohorts of patients who had undergone complete tumour resection. One group received mitotane treatment post-operatively, while the other two were placed on observation only. Recurrence-free survival was significantly higher in the mitotane-treated group; overall survival was significantly higher only with reference to one of the two control groups (Terzolo et al., 2007). It is now widely accepted that adjuvant mitotane should be the norm in patients with high-risk features (proliferation marker Ki67 >10%, macroscopically or microscopically incomplete resection). An ongoing international, randomised prospective trial (ADIUVO) is exploring the value of mitotane administration post-operatively in the select group of patients with complete resection and low proliferation index (Ki67 <10%).

1.2.6.3 Systemic chemotherapy

Monotherapy. A number of cytotoxic drugs have been tried as single-agent treatment in ACC patients, mostly in the context of small case series or case reports. Modest clinical response has been displayed in case reports or series with doxorubicin, alkylating-like agents and cisplatin (Berruti, 2012). Doxorubicin (Adriamycin) is an anthracycline compound which causes DNA damage, cell cycle arrest and apoptotic cell death. Limited data from small case series and a phase II study suggest modest response rates of 19-25% (Berruti, 2012, Decker et

al., 1991, Haq et al., 1980, Pommier and Brennan, 1992). Administration to patients who had failed to respond to mitotane was to no avail in this cohort of cases. Cisplatin, a platinum-based compound, is the agent with the highest efficacy as monotherapy against advanced ACC. It induces programmed cell death interfering with DNA replication. Out of 13 patients with advanced ACC included in three small series, seven showed initial response to treatment (Chun et al., 1983, Tattersall et al., 1980, Terzolo, 2012). Promising results were initially achieved by suramin, a polyanionic compound with adrenolytic activity, in vitro and in small case series; however, a subsequent stage II study revealed only modest, short-lived anti-tumour effects with unacceptable toxicity (La Rocca et al., 1990a, La Rocca et al., 1990b, Arlt et al., 1994). Gossipol, a plant toxin with promising *in vitro* and *in vivo* effects in pre-clinical ACC models, was used in a phase II clinical trial in advanced ACC patients who failed to respond to mitotane chemotherapy. 3/18 patients showed clinical response which lasted several months; after these results the drug never found its way to clinical practice. Finally, paclitaxel is an agent with considerable *in vitro* efficacy against adrenocortical cancer cell lines, but very scant clinical evidence to support its application in advanced ACC, with only isolated case reports and a phase I study. Overall, mitotane remains the undisputed first-line monotherapy option in routine clinical practice, primarily by virtue of its favourable side-effects profile in comparison to systemic cytotoxic chemotherapy.

Combination chemotherapy. Combination chemotherapy is offered to ACC patients who either present with advanced malignancy of high tumour load or fail to respond to mitotane monotherapy (Terzolo, 2012) (**Table 1-5**). Mitotane is usually employed in combination with one or more cytotoxic agents. Multidrug resistance is a common clinical feature of ACC and has been associated with high levels of expression of multidrug resistance genes (*MDR1*, *ABCB1*), which enhance drug efflux from cancer cells. Mitotane has displayed an opportune

capacity to interfere with this resistance mechanism and increase intratumoural drug accumulation, which provides a strong rationale for including it in combination chemotherapy (Bates et al., 1991). A pertinent caveat is the CYP3A4-inducing effect of mitotane which can accelerate the breakdown of numerous drugs in the liver, as alluded to earlier (Chortis et al., 2013, Kroiss et al., 2011). A number of cytotoxic regimens including mitotane have been evaluated in phase II clinical trials (Table 1-5), with response rates varying from 9-48%. The two best performing regimens, Mitotane + Etoposide/ Doxorubicin/Cisplatin (M+EDP) and Mitotane + Streptozotocin (M+S) were recently compared in the first ever randomised prospective study in ACC (n=304 patients with metastatic disease), through collaboration of several European Centres affiliated with the European Network for the Study of Adrenal Tumours (Fassnacht et al., 2012). M+EDP afforded better progression-free survival (5 months vs 2.1 months) and objective response rates (23.2% vs 9.2%) than M+S. Importantly, the effect on overall survival was meagre and not statistically different between the two regimens (15 vs 12 months) **(Fig. 1-9)**. In light of these results, M+EDP is now considered the first-line cytotoxic chemotherapy option in patients not responding to mitotane monotherapy, for want of more effective treatment options. In non-responding cases, the combination of gemcitabine and capecitabine has been proposed as salvage chemotherapy, leading to disease stabilization for at least 6 months in 29% of patients when offered as second-line chemotherapy according to a phase II trial (Sperone et al., 2010)

*Table 1-5 Prospective studies of combination chemotherapy in ACC. * randomized-controlled trial. Abbreviations: CP: cyclophosphamide; P: cisplatin; D: doxorubicin; 5FU: 5-Fluoruracil; E: Etoposide; M: Mitotane; S: Streptozotocin; V: Vincristin; I: Irinotecan; G: Gemcitabine; Cap: Capecitabin. Source: (Else et al., 2014). Adapted and reproduced with permission of the Endocrine Society.*

Study	Drugs	Patient n	% patients with response	% patients with response or stable disease	Response duration (months)
(van Slooten and van Oosterom, 1983)	CP/ P/ D	11	18	73	10-23
(Schlumberger et al., 1991)	5FU/ P/ D	13	31	54	6-42
(Bukowski et al., 1993)	M/ P	37	30	NR	8 (median)
(Bonacci et al., 1998)	E/ P/ (M)	18	33	44	9-26
(Berruti et al., 1998)	M/ E/ D/ P	28	54	82	24 (median)
(Williamson et al., 2000)	E/ P	37	14		NR
(Khan et al., 2000)	M/ S	23	30	52	7 (median)
(Abraham et al., 2002)	M/ E/ D/ V	35	23	NR	12 (mean)
(Baudin et al., 2002)	M/ I	12	0	25	NR
(Khan et al., 2004)	CP/ V/ C/ T	11	18	82	7 (median)
(Berruti et al., 2005)	M/ E/ D/ P	72	49	NR	18 (median)
(Sperone et al., 2010)	M/ G/ 5FU or Cap	28	7	46	10 (median)
*(Fassnacht et al., 2012)**	M/ E/ D/ P	151	21	56	5 (median)
*(Fassnacht et al., 2012)**	M/ S	153	8	30	2 (median)

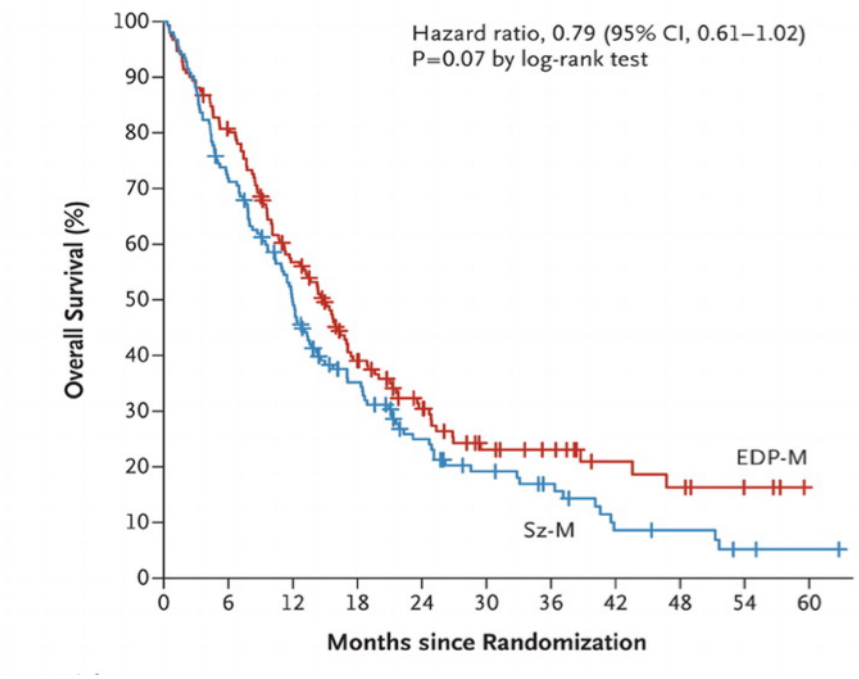

Figure 1-9 Overall survival in patients with metastatic ACC randomized to combination chemotherapy with Mitotane, Etoposide, Doxorubicin and Cisplatin (EDP-M) or Mitotane and Streptozotocin (Sz-M) (Fassnacht et al., 2012). Reproduced with permission of the Massachusetts Medical Society.

In recent years, considerable effort has been expended towards the development of targeted therapies for ACC, mostly focusing on proteins that are highly expressed in malignant adrenocortical tumours. The epidermal growth factor receptor (EGFR) and the vascular endothelial growth factor (VEGF) were the first two genes to be targeted. In both cases the clinical results were disappointing with failure to yield any objective response, at least in patients with chemotherapy-resistant disease (Quinkler et al., 2008, Wortmann et al., 2010). A trial with the multi-tyrosine kinase inhibitor sorafenib in combination with paclitaxel had to be abandoned upon recruitment of 10 patients, as all demonstrated disease progression on first clinical evaluation (Berruti et al., 2012). Another tyrosine kinase inhibitor, sunitinib, was

evaluated in a phase II study on patients with metastatic ACC who failed to respond to mitotane and first-line chemotherapy; only 5 out of 35 patients achieved disease stabilisation (14%) (Kroiss et al., 2012).

More recently, Insulin Growth Factor-I Receptor (IGF1-R) inhibitors have been tried in clinical studies. Cixutumumab showed some modest success in combination with temsirolomus (inhibitor of mechanistic targets of Rapamycin - mTOR) with 42% of patients achieving stable disease (Naing et al., 2013). Combination treatment with Cixutumumab and mitotane, however, failed to show any effectiveness in a phase II study (Lerario et al., 2014). A similar agent (linstinib, IGF1-R inhibitor) was overall no better than placebo at yielding clinical response in a recent phase III trial, although a small group of patients enjoyed sustained response over long periods (Fassnacht et al., 2015). Overall, despite rather auspicious pre-clinical data, targeted therapies so far have failed to demonstrate effectiveness in clinical studies and improve the outcome of patients with advanced disease.

1.2.6.4 Medical treatment to control hormone excess

Medical control of the detrimental hormone excess is often a secondary treatment aim in ACC. Glucocorticoid excess is the most common hormonal perturbation emanating from ACCs and its clinical sequelae involve the classic constellation of symptoms and signs comprising Cushing's syndrome. Aside from its adrenolytic activity, mitotane has additional adrenostatic effects, i.e. direct inhibitory effects on steroidogenesis. These include CYP11A1 inhibition, as well as cortisol breakdown through CYP3A4 induction (Chortis et al., 2013, Else et al., 2014). Of note, mitotane can inhibit steroidogenesis at lower levels than the threshold for its antineoplastic effect (Baudry et al., 2012, Nieman et al., 2015).

Metyrapone is a specific inhibitor of CYP11B1 which is commonly used in the medical control of cortisol excess. It has a rather favourable side-effect profile (mainly mild gastrointestinal symptoms), with the caveat that it can exacerbate underlying androgen excess and induce adrenal insufficiency (Daniel et al., 2015).

Ketoconazole inhibits CYP17A1, CYP11A1 and CYP11B1 and is still used in many countries, but carries a risk of severe idiosyncratic hepatotoxicity and interacts with other drugs through inhibition of liver microsomal enzymes (e.g. CYP3A4) (Nieman et al., 2015).

Etomidate is an anaesthetic agent which can inhibit CYP11A1 and CYP11B1 even at low doses. It is used as intravenous infusion at non-anaesthetic doses for rapid control of glucocorticoid excess in some centres in challenging cases of florid Cushing's, but requires close inpatient monitoring (Schulte et al., 1990).

Finally, mifepristone is a glucocorticoid receptor antagonist which completes the modern armamentarium for Cushing's syndrome control. Its main disadvantage is its inability to block the action of excessive cortisol on the mineralocorticoid receptor, which can cause hypertension and hypokalaemia. Therefore, additional treatment with mineralocorticoid receptor blockers (e.g. spironolactone) may be required (Nieman et al., 2015). In challenging cases, recourse to combination therapy with two or even three of the above agents is common, as the success rates of any monotherapy in mitigating overwhelming glucocorticoid excess are limited (Nieman et al., 2015) (**Fig. 1-10**).

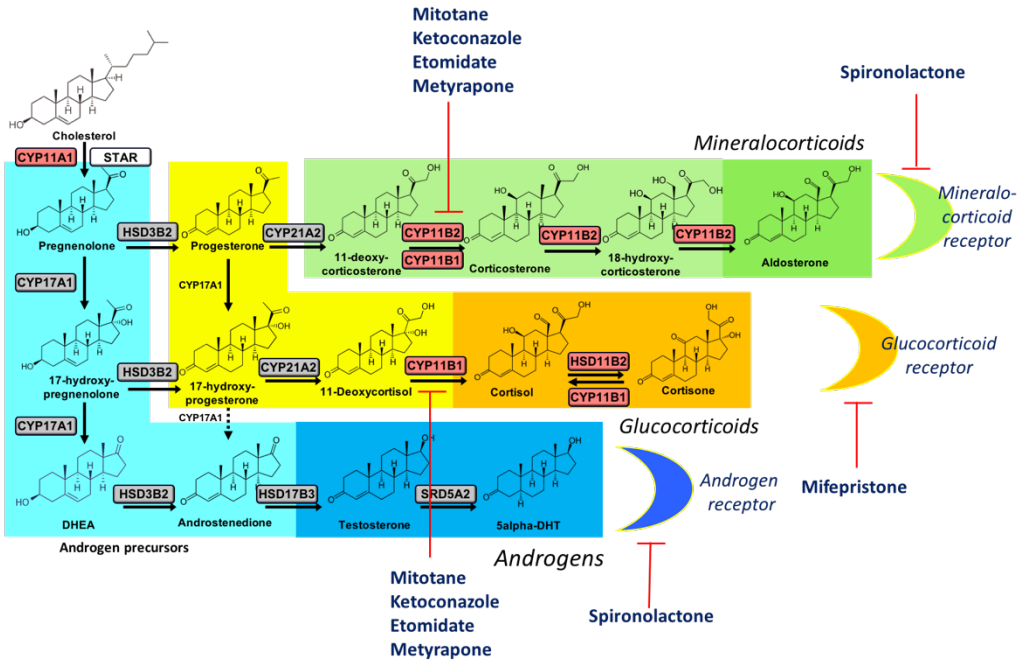

Figure 1-10 Effects of adrenostatic agents on adrenal steroidogenesis. Red lines indicate inhibition.

Androgen excess may require medical treatment when it manifests itself clinically as severe hirsutism or virilisation in female patients. Options include a number of agents with anti-androgenic effects, including spironolactone (mineralocorticoid and androgen receptor blocker), finasteride (5α-reductase inhibitor) and flutamide (Else et al., 2014). Furthermore, it has been shown that mitotane is a powerful inhibitor of 5α-reductase activity, thereby reducing the activation of testosterone to 5α-dihydrotestosterone and ameliorating androgen excess, but also compromising androgen action in male patients without androgen excess (Chortis, 2013).

Oestrogen excess causing severe gynaecomastia in male patients can be addressed by institution of aromatase inhibitors or oestrogen receptor antagonists, although this is very rarely encountered in clinical practice (Else et al., 2014).

1.2.6.5 Other treatment options

Radiotherapy has not found a wide application in ACC, but is occasionally employed either as adjuvant treatment post-operatively or to palliate patients with advanced disease. Adjuvant radiotherapy administration has only been explored in three retrospective studies, all based on small patient cohorts (< 20 patients). Two of the studies showed reduced incidence of local recurrence; however, no improvement in overall survival was demonstrated (Else et al., 2014, Fassnacht et al., 2006, Habra et al., 2013). No firm conclusions can be drawn on the ground of such slender evidence. Some experts advocate the use of radiotherapy in cases of incomplete tumour resection (Berruti et al., 2010). There may be a role for radiotherapy in patients with metastatic disease of limited volume, but pertinent evidence is so far limited to small retrospective studies (Polat et al., 2009, Ho et al., 2013, Hermsen et al., 2010). Effective pain alleviation has been reported in a number of small case series, especially in the event of spinal metastases (Else et al., 2014). Successful control of hormone excess has also been reported in a small case series (Magee et al., 1987).

Radiofrequency ablation is occasionally employed in cases with isolated local or distal disease recurrence of low volume, especially in patients who are considered poor surgical candidates in view of poor overall performance status and/or comorbidities. Successful applications (e.g. in liver metastases) have been reported, but no clinical trials have formally assessed the performance of this intervention (Ripley et al., 2011). Generally, primary ACCs (high bleeding risk) and proximity to large vessels constitute contra-indications (Ripley et al., 2011). Topical arterial chemoembolization is not widely used but may have a role in the palliative treatment of small (<3 cm) disease foci of high lipidol uptake (Soga et al., 2009).

Finally, following up on the discovery that [$^{123/131}$I]iodometomidate (IMTO) tracer is taken up avidly by adrenocortical tissue on single-photon emission CT, radionuclide treatment with

[$^{123/131}$I]IMTO was recently attempted in a small cohort of 11 ACC patients. The results were promising, with one patient achieving partial remission and five patients achieving disease stabilisation for a median period of 14 months (Hahner et al., 2012). [$^{123/131}$I] azetidinylamide (IMAZA), an IMTO metabolite, was recently introduced, boasting the relative advantage of more selective and durable adrenal uptake (Hahner, 2015).

1.2.7 Follow-up

The optimal protocol for the post-operative follow-up of patients with complete ACC resection has not been established, the low disease prevalence having hampered the development of evidence-based guidance. Empirically devised protocols are imaging-centred and aim to detect recurrences as early as possible, so that prompt treatment can be instigated. In principle, the high risk of disease recurrence, especially in the first two post-operative years, has to be weighed against the high radiation exposure which is ineluctably associated with regular whole-body CT scans. A commonly followed protocol involves contrasted CT scans of chest and abdomen (or CT chest with MRI of abdomen and pelvis in less parsimonious healthcare systems) every three months for the first two post-operative years, followed by six-monthly imaging for the next three years (Fassnacht and Allolio, 2009, Else et al., 2014, Arlt et al., 2011). FDG-PET scans are also employed in some centres as a more sensitive but costly surveillance method. (Fassnacht and Allolio, 2009). In post-operative years 6-10, a period associated with a very low recurrence risk (<5%), imaging typically takes place on an annual basis (Else et al., 2014). A typical modern ACC managing algorithm, representative of our practice at the Queen Elizabeth Hospital Birmingham, is displayed in **Fig. 1-11**.

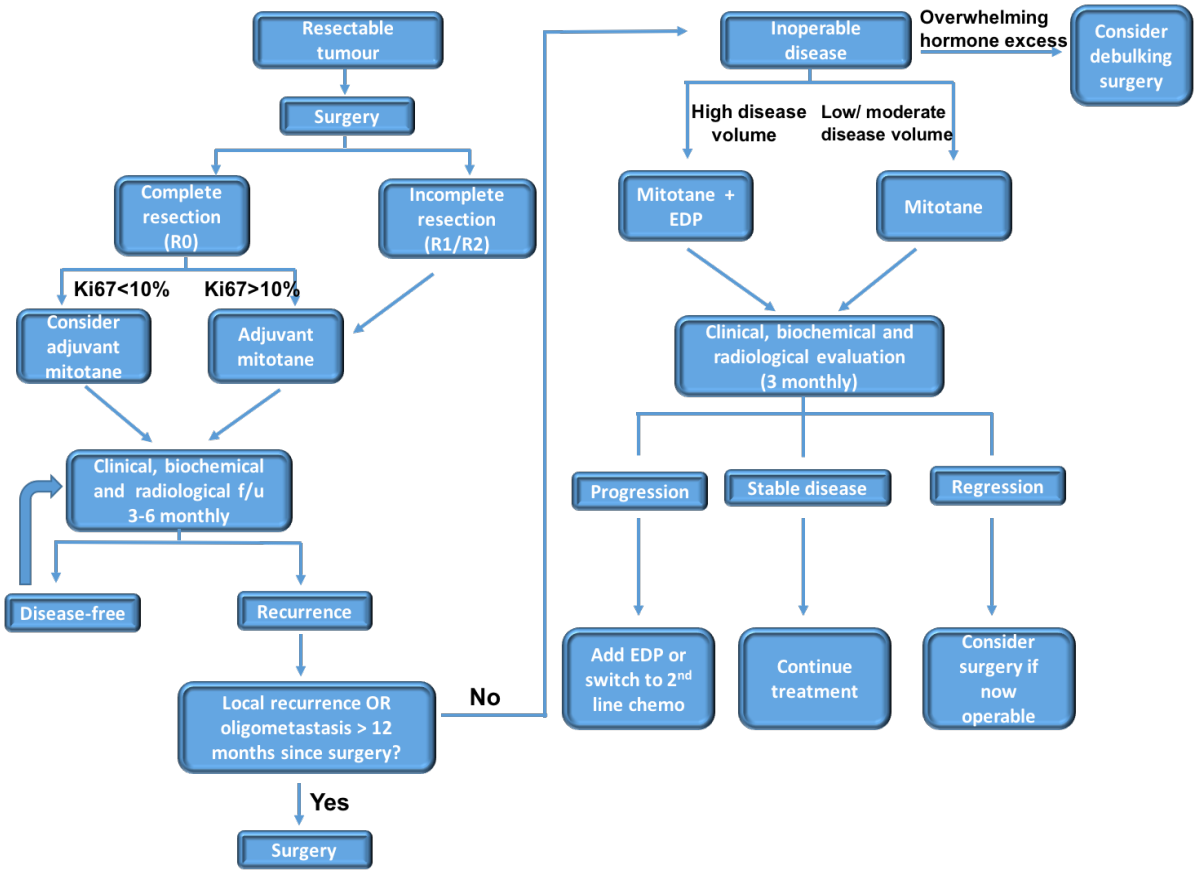

Figure 1-11 ACC management algorithm. EDP: combination chemotherapy with Etoposide, Doxorubicin and Cisplatin

Biochemical follow-up to detect recurrent adrenal steroid hormone excess has an ancillary role in the post-operative surveillance of ACC, with the important limitation that capturing the hormonal output of minuscule metastatic lesions in routine clinical biochemistry is difficult and usually radiological manifestation of recurrent disease precedes the development of deranged biochemistry. Routine clinical biochemistry in patients with history of ACC includes serum androgens, 17-hydroxyprogesterone, oestradiol, aldosterone and urinary free cortisol.

Diagnostic ambiguity in early stages of recurrence/ metastasis is not uncommon and may lead to delays in reaching a firm diagnosis and commencing treatment. FDG-PET scans or percutaneous biopsies are sometimes employed in such cases (Fassnacht and Allolio, 2009, Else et al., 2014).

Urinary steroid profiling holds some promise as a future monitoring tool in operated patients. Disturbed steroidogenesis in the context of ACC and the emerging ability of urine steroid profiling by mass spectrometry to capture such changes and distinguish benign from malignant adrenal tumours has been discussed in previous sections. It may be reasonable to apply the same principle in the clinical context of recurrent ACC, anticipating that this will be accompanied by similar, progressive perturbations of steroidogenesis, possibly recapitulating the pre-operative profile. In a case series, Wangberg et al. obtained pre-operative and serial post-operative urinary steroid profiles from five operated patients with ACC. In two of them, disease recurrence was heralded biochemically by the re-emergence of the pre-operative secretion pattern (Wangberg et al., 2010). Interestingly, in one patient presenting with liver metastases and combined androgen-glucocorticoid excess, removal of the primary tumour was followed by a shift in the steroidogenic fingerprint, with persistence of glucocorticoid excess but disappearance of androgen excess. No other studies have attempted to formally evaluate the role of steroid profiling as a post-operative surveillance tool so far.

1.3 The target: Nicotinamide Nucleotide Transhydrogenase

1.3.1 Nicotinamide Nucleotide Transhydrogenase and Familial Glucocorticoid Deficiency.

In the search for novel therapeutic approaches in ACC, useful insights may be provided by recent advances in our understanding of adrenal pathophysiology. In 2012, SNP array genotyping studies revealed that antioxidant pathway defects are causally implicated in a rare form of hereditary primary adrenal insufficiency called Familial Glucocorticoid Deficiency (FGD) (Meimaridou et al., 2012). FGD is a rare autosomal recessive disorder which is characterised by congenital inability of the adrenal glands to produce sufficient amounts of cortisol despite sufficient ACTH stimulation by the pituitary (Meimaridou et al., 2013). Patients typically present in the first months of life with recurrent infections, failure to thrive, hypoglycaemic episodes, seizures or haemodynamic instability. Adrenal biochemistry characteristically reveals very low or undetectable cortisol with high ACTH and failure to respond to ACTH stimulation (short SYNACTHEN test), indicating primary adrenal insufficiency (Clark et al., 2009, Metherell et al., 2005). Renin and aldosterone tend to be normal. Until recently, three gene mutations had been identified in association with this condition, accounting for 50% of reported cases. These included genes encoding proteins that mediate the transport of cholesterol to the adrenal cells (MC2R, MRAP and StAR), which represents the first step of steroidogenesis in response to ACTH stimulation (Clark et al., 2009, Metherell et al., 2005). In their 2012 study, Meimaridou et al. identified a new genetic cause performing targeted exome sequencing in cryptogenic FGD patients of consanguineous parentage (Meimaridou et al., 2012). The new culprit, the chromosome 5-situated gene *NNT*, encodes a mitochondrial proton pump called Nicotinamide Nucleotide Transhydrogenase (NNT). NNT serves as one of the major mitochondrial generators of reduced nicotinamide

adenine dinucleotide phosphate (NADPH) and constitutes an essential component of the mitochondrial antioxidant pathways (Rydstrom, 2006, Leung et al., 2015). In the original study, 19 *NNT* mutations were identified in 13 individuals, out of a total cohort of 100 patients with FGD of unknown cause (Meimaridou et al., 2012). All affected individuals were homozygotes or compound heterozygotes, indicating an autosomal recessive pattern of inheritance. No *NNT* mutations had hitherto been discovered in humans, but since this discovery 34 *NNT* mutations have been reported in 41 patients with unexplained glucocorticoid deficiency. The majority of discovered mutations are either nonsense or frameshift mutations, predicted to lead to premature protein truncation; the rest comprise missense mutations affecting vital protein domains (Yamaguchi et al., 2013, Novoselova et al., 2015, Weinberg-Shukron et al., 2015, Jazayeri et al., 2015, Roucher-Boulez et al., 2016, Hershkovitz et al., 2015, Meimaridou et al., 2012). In a minority of described cases there was co-existent aldosterone deficiency (high renin, low aldosterone), consistent with global adrenal insufficiency (Weinberg-Shukron et al., 2015, Roucher-Boulez et al., 2016).

Despite NNT's ubiquitous expression in all human tissues (Meimaridou et al., 2012), the clinical phenotype associated with inactivating *NNT* mutations is remarkably specific, only affecting the adrenal glands in the vast majority of patients. This interesting clinical observation indicates a selective susceptibility of adrenocortical cells to NNT loss. Rare extra-adrenal ailments described in these patients include testicular adrenal rest tumours, likely secondary to high ACTH (2 cases); cryptorchidism (2 cases); Leydig cell adenoma of the testicles (2 cases); congenital hypothyroidism (2 cases) and left ventricular hypertrophy (1 case) (Hershkovitz et al., 2015, Roucher-Boulez et al., 2016).

1.3.2 Structure and physiology

Current knowledge of NNT physiology provides putative biological mechanisms to explain this novel association. NNT is a redox-driven proton pump with inherent enzymatic activity, which resides in the inner mitochondrial membrane of eukaryotic cells, catalysing the reversible reduction of $NADP^+$ to NADPH according to the reaction:

$$NADH + NADP^+ + H^+_{intermembrane} \leftrightarrow NAD^+ + NADPH + H^+_{matrix}$$

The physiological transmembrane proton gradient shifts the reaction strongly to the right, maintaining a high mitochondrial ratio of $NADPH/NADP^+$ under physiological conditions (Arkblad et al., 2005, Rydstrom, 1974, Rydstrom, 2006, Rydstrom et al., 1998). Reversal of the direction of the reaction, so that NADH can be produced from NADPH with concurrent H^+ pumping against the transmembrane gradient, appears to be possible under hypoxic conditions (Ying, 2008). In normoxic conditions, however, the biological role of NNT is to replenish the mitochondrial pool of NADPH, powered by the transmembrane proton gradient.

NNT (molecular weight 114 kD) is a homodimer; each half consists of a lipophilic, membrane-embedded domain (DII) and two hydrophilic domains (DI and DIII) protruding into the inner mitochondrial matrix (eukaryotic cells) or cytosol (bacteria) (Yamaguchi et al., 1988, Leung et al., 2015). DI binds NAD(H), while DIII binds NADP(H) (**Fig. 1-12**). The structure of the hydrophilic domains has been successfully studied in a number of species, including Homo sapiens, but the structure of the transmembrane domain that facilitates proton pumping remained elusive. Recently, Leung et al. managed to elucidate the whole protein structure in *Thermus thermophilus*, using a combination of crystallography and cryo-electron microscopy (Leung et al., 2015). This elegant study revealed a peculiar pattern: while the two membrane-bound domains (DII) are symmetrical, each containing a putative proton channel,

NNT as a whole displays a striking asymmetry as the two DIII domains have opposite orientations. The authors hypothesised that this asymmetry facilitates division of labour between the two subunits in alternating cycles, so that one of the two DIII domains mediates hydride transfer from NADH to NADPH, while its counterpart participates in proton transfer.

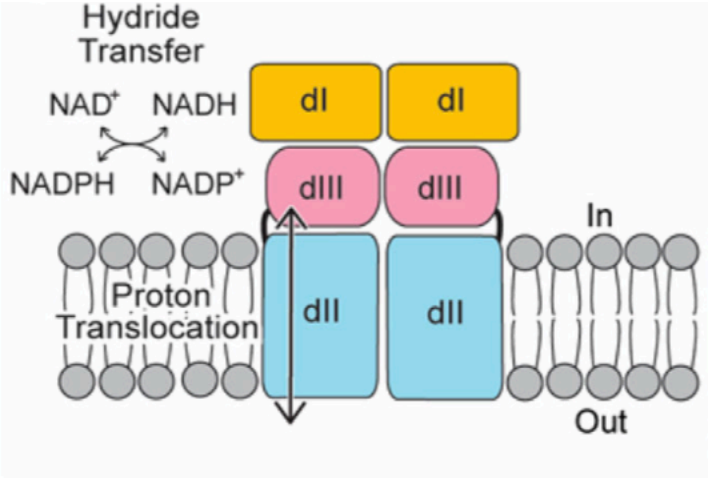

Figure 1-12 Schematic representation of NNT structure and function. The NAD(H) binding domain (dI) and the NADP(H) binding domain (dIII) catalyse hydride transfer between nicotinamide nucleotides, with concurrent translocation of protons to the mitochondrial matrix. Source: (Leung et al., 2015). Reproduced with permission of the American Association for the Advancement of Science.

It is still unknown what percentage of the total mitochondrial NADPH pool is contributed by NNT. Studies on redox balance in *Escherichia coli* suggested that NNT generates approximately 45% of the total NADPH pool (Rydstrom, 2006, Sauer et al., 2004), but more recent studies have underscored the complexity of NADPH-generating networks in eukaryotic cells and indicated that the relative contribution of each pathway can vary according to cell type and metabolic circumstances (Lewis et al., 2014, Fan et al., 2014). Our current

understanding of cytosolic and mitochondrial pathways of NADPH synthesis is described separately in the succeeding section.

The existence of many redundant biosynthetic pathways generating NADPH is explained by the important biological roles of this versatile electron carrier. Contrary to NADH, which predominantly acts as an electron donor to the mitochondrial electron transfer chain to fuel ATP synthesis, NADPH is involved in two distinct areas: reductive biosynthesis and antioxidant defence. Maintaining a constant NADPH supply to fuel lipid, aminoacid and nucleotide biosynthesis is of major importance in highly proliferating cells (Fan et al., 2014, Vander Heiden et al., 2009). With regard to its second role as a safeguard of cellular redox homeostasis, NADPH acts as an essential electron donor to the two most important antioxidant pathways: the glutathione pathway and the thioredoxin pathway, both of which mediate the detoxification of chemically reactive oxygen molecules (reactive oxygen species, ROS) to H_2O (Prasad et al., 2014b). ROS are constantly generated intracellularly as by-products of aerobic metabolism, and their efficient scavenging represents an existential need for all cells (Gupta et al., 2012). Reduced glutathione (GSH) has a well-established, central role in the mitochondrial redox balance system as it is involved in the detoxification of the major ROS molecule hydrogen peroxide (H_2O_2), both directly and through the action of glutathione peroxidise (GPX) (Prasad et al., 2014a, Mari et al., 2009, Andreyev et al., 2005). The second major mitochondrial antioxidant system (thioredoxin pathway) involves reduction of mitochondrial thioredoxin by thioredoxin reductase (TXNRD2), using two electrons from NADPH. Reduced thioredoxin in its turn regenerates reduced peroxiredoxin 3 (PRDX3) from its oxidised form. Two molecules of reduced PRDX3 can then serve to reduce H_2O_2 to H_2O, while they are oxidized to a disulfide-linked peroxiredoxin dimer (Mustacich and Powis, 2000).

In summary, NNT generates NADPH to support anabolic processes and fuel the mitochondrial antioxidant defence network with reducing equivalents, preventing oxidative damage caused by excessive ROS accumulation (oxidative stress) (**Fig. 1-13**). A more thorough description of ROS and their scavenging pathways is provided in subsequent sections.

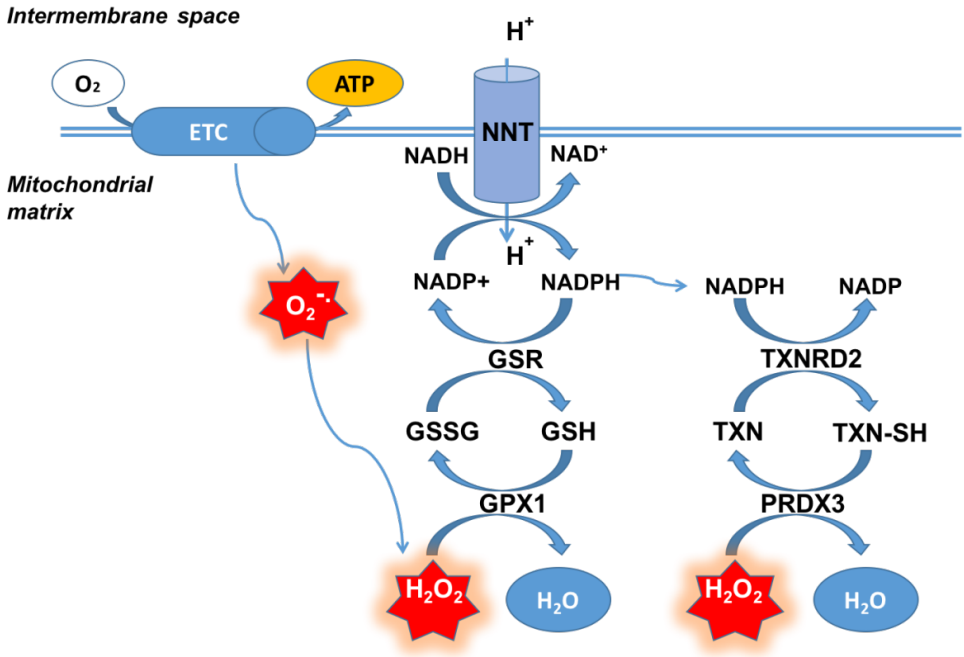

Figure 1-13 Interaction between NNT and the mitochondrial antioxidant pathways. ETC: electron transfer chain; ATP: adenosine triphosphate; GSR: glutathione reductase; GSSG: oxidised glutathione; GSH: reduced glutathione; GPX1: Glutathione peroxidase 1; TXNRD2: thioredoxin reductase 2; TXN: oxidised thioredoxin; TXN-SH: reduced thioredoxin; GPX3: peroxiredoxin 3; $O_2^{\cdot-}$: superoxide; H_2O_2: hydrogen peroxide

As expected, NNT inhibition has been shown to compromise NADPH synthesis, hamper ROS scavenging and alter the cellular redox status (i.e. the balance between oxidising and reducing

elements) in various cell lines, as indicated by a number of pertinent metabolic parameters (NADPH/$NADP^+$ ratio, reduced/oxidised glutathione ratio, ROS concentration) (Ripoll et al., 2012, Arkblad et al., 2005, Meimaridou et al., 2012, Yin et al., 2012). Transient knockdown (KD) of NNT in PC12 rat phaeochromocytoma cells also resulted in impaired mitochondrial metabolism, most notably inhibition of oxidative phosphorylation with decreased oxygen consumption rates (Yin et al., 2012). This was ascribed to the paradoxically decreased ratio of NADH/NAD^+ observed in the aftermath of NNT inhibition, potentially due to inhibition of the Kreb's cycle enzyme pyruvate dehydrogenase through redox-controlled signalling (e.g. JNK-mediated). Perturbation of mitochondrial respiration was accompanied by increased levels of apoptosis. In an elegant metabolic *in vitro* study on melanoma and renal carcinoma cells, Gameiro et al. showed that NNT KD impedes glutamine utilisation in Kreb's cycle, due to functional inhibition of isocitrate dehydrogenase by the low NADH/NAD^+ ratio (Gameiro et al., 2013). This increased the dependence of malignant melanoma cells on glucose to derive anabolic carbons for their proliferation. Indeed, NNT-KD cells were more sensitive to glucose deprivation. Overexpression of NNT had the opposite effects, increasing reductive carboxylation of glutamine. Finally, xenografts derived from NNT-KD melanoma cells showed at least a tendency towards lower proliferation than their controls (Gameiro et al., 2013). In another recent study on neuronal cells, NNT KD disrupted the thioredoxin pathway, limiting reduced peroxiredoxin availability and, consequently, increasing ROS levels. This enhanced cellular susceptibility to chemically-induced oxidative stress (paraquat treatment) (Lopert and Patel, 2014)

A number of *in vivo* studies have explored the sequelae of NNT dysfunction in rodents. Rather opportunely, a spontaneous loss-of-function *Nnt* mutation was discovered in C57BL/6J mice in 2005 (Toye et al., 2005). The first metabolic perturbation identified in this

mouse strain was impaired glucose tolerance, as a result of deficient insulin secretion (Freeman et al., 2006, Shimomura et al., 2009, Toye et al., 2005). The same phenotype was reproduced in a different mouse strain upon *Nnt* knockout. The mechanism underlying this association remains elusive (Parker et al., 2009). Ronchi et al. evaluated the metabolic effects of *Nnt* mutation in the same strain with *ex vivo* studies on liver mitochondria. In keeping with *in vitro* data, they showed that *Nnt* mutant mice had liver mitochondria with a lower ratio of NADPH/NAPD, impaired redox balance (decreased reduced/ oxidised glutathione ratio) and inability to detoxify exogenous ROS, when compared to a BL6 strain with wild-type *Nnt*. Of note, the ratio of NADH/NAD^+ was higher in *Nnt* mutant mice, which is at odds with the results of the aforementioned *in vitro* studies (Ronchi et al., 2013). Meimaridou et al. demonstrated a decrease in circulating corticosterone (the major glucocorticoid and mineralocorticoid hormone in rodents) in *Nnt* mutant mice, underpinned by histological findings of disorganised structure and increased apoptosis in the zona fasciculata of the mouse adrenals (Meimaridou et al., 2012). Blunted corticosterone response to restrain stress was observed in NNT knockout mice by Picard et al., as well as augmentation of the hyperglycaemic response to stress due to deficient insulin secretion (Picard et al., 2015).

Recently, the first study evaluating the effects of *NNT* mutations in FGD patients (homozygotes) and carriers (heterozygotes) *ex vivo* using circulating lymphocytes was published. Suppression of NNT activity to <60% of normal (homozygotes and heterozygotes) resulted in decreased mitochondrial mass and mitochondrial DNA copies. Suppression to <30% of normal activity (homozygotes only) additionally resulted in impaired oxidative phosphorylation and high rates of mitochondrial gene deletions, presumably reflecting oxidative DNA damage (Fujisawa et al., 2015).

Interestingly, it has been long known that NADPH (and by inference NNT) also serves as an essential electron donor to a number of steroidogenic cytochrome P450 enzymes that reside in the mitochondria (CYP11A1, CYP11B1, CYP11B2) (Hanukoglu, 2006). This provides a putative mechanism to explain the association of NNT dysfunction with adrenal insufficiency, alongside the possibility of adrenal cortex damage due to oxidative stress.

1.3.3 NADPH metabolism

The role of NNT as a mitochondrial NADPH generator is best appreciated if considered within the complete network of biosynthetic pathways that can produce NADPH alongside it. The total NADPH pool can be divided into cytosolic NADPH and NADPH located within intracellular orgenelles (most notably mitochondria). Cellular membranes appear to be impermeable to NADP(H) and NAD(H), and transfer of reducing equivalents across them requires multi-step reaction pathways such as the malic acid cycle (Nikiforov et al., 2011, Pollak et al., 2007). The ability to rapidly reduce NADP to NADPH in response to oxidative stimuli or starvation is important. This can be facilitated by a number of enzymes:

a) ***Isocitrate dehydrogenase (ICDH).*** ICDHs catalyse the oxidative decarboxylation of isocitrate to a-ketoglutarate in the tricarboxylic acid (TCA) cycle, a reaction during which NAD(P)H is generated. Three isoforms of ICDH have been described in mammals: mitochondrial NAD^+-dependent ICDH (IDH), mitochondrial $NADP^+$-dependent dehydrogenase (IDPm) and cytosolic $NADP^+$-dependent dehydrogenase (IDPc). IDPm, also known as ICDH type II, catalyses the following reaction, contributing to the mitochondrial NADPH pool:

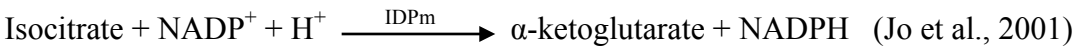

(Jo et al., 2001)

b) ***Malic enzyme.*** Malate dehydrogenase or NADP-malic enzyme is an oxidoreductase catalysing the carboxylation of malate to pyruvate, generating NADPH.

(S)-malate + $NADP^+$ $\xrightarrow{\text{malic enzyme}}$ pyruvate + CO_2 + NADPH (Peron et al., 1975)

Malate and pyruvate can be transported across the mitochondrial membrane, thus allowing some flexibility in reducing power shifts between the cytosol and the mitochondria (malate-pyruvate shuttle). For instance, cells can invest cytosolic NADPH to generate malate and transport it to the mitochondria, where it can be used by malic enzyme to generate NADPH locally (Fan et al., 2014).

c) ***Glucose-6-Phosphate dehydrogenase (G6PD).*** This enzyme is considered the major cytosolic NADPH generator, but is not expressed in mammalian mitochondria. It catalyses the first and rate-limiting step of the Pentose Phosphate Pathway:

Glucose-6-Phosphate + $NADP^+$ + H^+ $\xrightarrow{\text{G6PD}}$ 6-Phosphoglucono-delta-lactose + NADPH (Frederiks et al., 2007, Ursini et al., 1997).

G6PD is the sole NADPH generator in red cells. G6PD deficiency is the most common enzyme deficiency in humans and is particularly prevalent in Asian, African and Mediterranean populations due to the phenotype of partial resistance to malaria it confers to carriers. Clinically, it only appears to be associated with haemolytic anaemia in response to oxidative stress triggered by various agents (fava beans, drugs, ketoacidosis), while patients with mild deficiency are completely asymptomatic (Beutler, 1996).

d) ***Tetrahydrofolate reductase.*** The importance of folate-dependent NADPH synthesis has been highlighted by modern metabolic mammalian cell studies based on hydrogen tracing. Folate-dependent NADPH-generating pathways involve transfer of a single carbon from serine to tetrahydrofolate (THF) to produce methylene-THF. The latter is subsequently oxidised by methylene-THF reductase (MTHFD) to form the purine precursor formyl-THF, in a reaction involving NADPH generation. MTHFD exists in both a cytosolic and a mitochondrial form. Recent studies suggest this pathway may contribute up to a quarter of the total NADPH pool in mammalian cells (Fan et al., 2014, Lewis et al., 2014).

An overview of known sources of mitochondrial NADPH is provided in **Figure 1-14**.

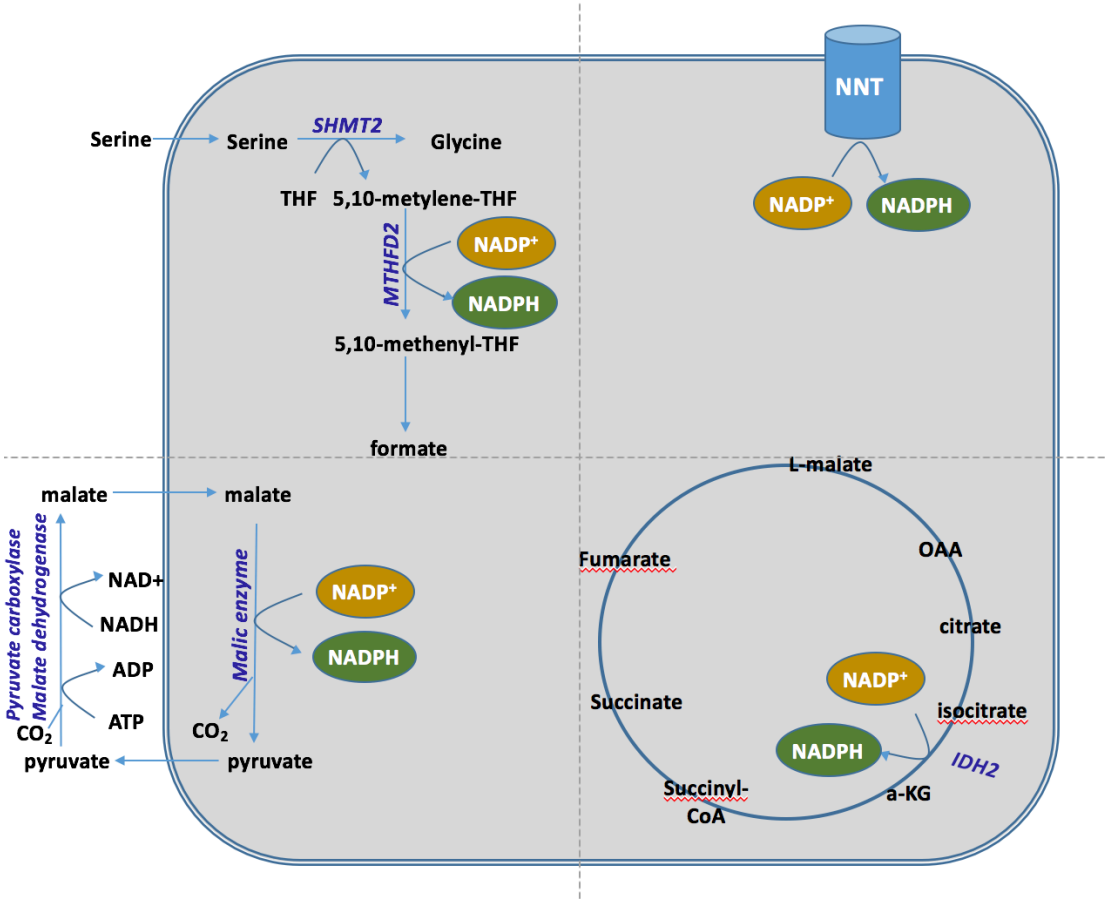

Figure 1-14 Mitochondrial sources of NADPH. THF: tetrahydrofolate; SHMT2: serine hydroxymethyltransferase 2; MTHFD2: methylenetetrahydrofolate dehydrogenase; IDH2: isocitrate dehydrogenase type II; a-KG: alpha-ketoglutarate; OAA: oxaloacetate

1.3.4 Reactive oxygen species (ROS) – basic physiology

Reactive oxygen species (ROS) are chemically reactive, oxygen-containing molecules which can be further subdivided into radical ROS [containing one or more unpaired electrons, such as superoxide (O_2^-), hydrocyl radical (OH^-), nitric oxide (NO)] and non-radical ROS [hydrogen peroxide (H_2O_2), ozone (O3), organic hydroxyperoxide (Fruehauf and Meyskens, 2007, Gupta et al., 2012). ROS are constantly generated within cells, their production

ineluctably intertwined with aerobic metabolism entailing electron transfer reactions. The main intracellular generation loci include

Peroxisomes: xanthine oxidase and other oxidases generate superoxide and hydroxyl radicals (del Rio et al., 1992)

Cell membrane: Membrane-bound enzymes from the NADPH oxidase (NOX) family generate ROS (Bedard and Krause, 2007)

Endoplasmic reticulum (ER): ROS are generated within the ER during protein folding and disulphide bond formation by oxidoreductin 1, disulphide isomerase and NOX4 (Gupta et al., 2012).

Mitochondria: The major ROS generating area within eukaryotic cells. A number of mitochondrial sources of ROS can be enumerated:

The tricarboxylic acid cycle (TCA cycle) or Kreb's cycle. The TCA cycle (**Fig. 1-15**) is a series of reactions oxidising carbohydrates, fats and proteins to generate CO_2 and energy (ATP). NADH and NADPH are generated during the cycle and serve as electron transporters from TCA substrates to the electron transfer chain. Several TCA enzymes can produce ROS as by-products during electron transfer (NADH dehydrogenase, pyruvate dehydrogenase, a-ketoglutarate dehydrogenase, succinate dehydrogenase). All these enzymes use flavin-containing groups to facilitate electron transfer; during this process some electrons remain stranded in the flavin groups and eventually leak generating superoxide (Sabharwal and Schumacker, 2014). Consequently, inhibition of any enzymatic step along the TCA cycle results in increased ROS generation as more free electrons accumulate (Sabharwal and Schumacker, 2014).

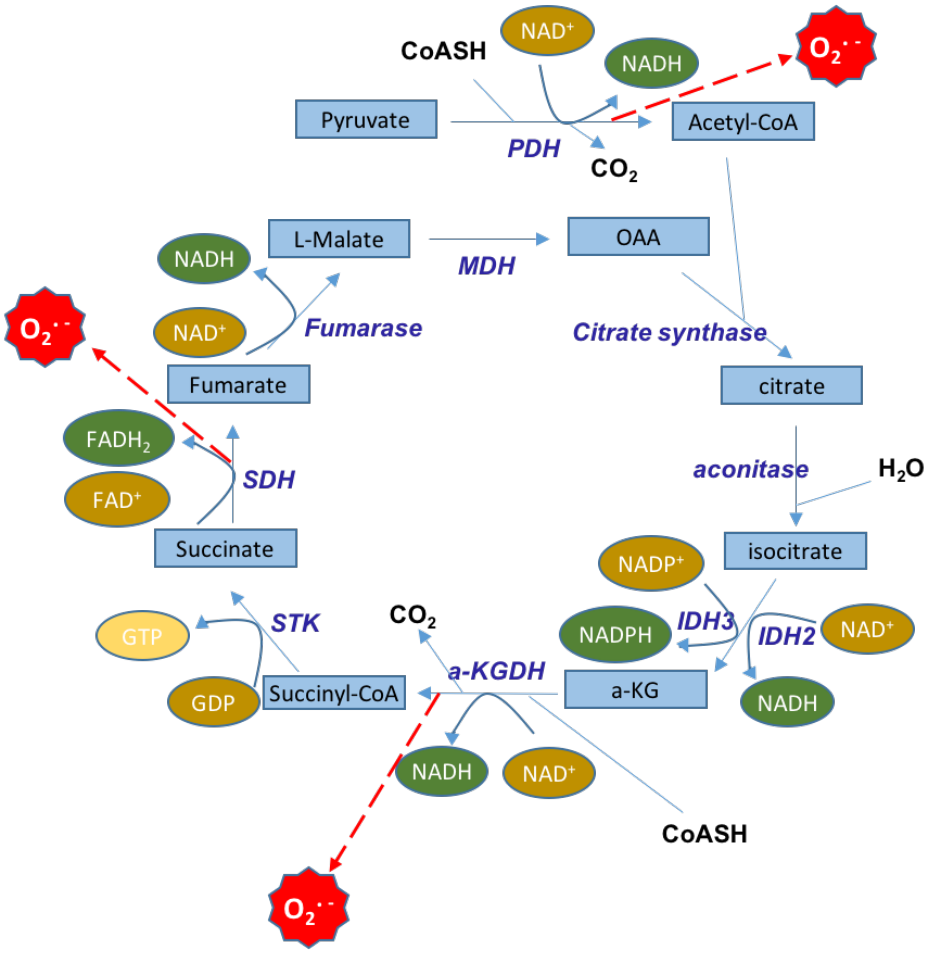

Figure 1-15 ROS production in the TCA cycle. CoASH: coenzyme A; PDH: pyruvate dehydrogenase; IDH: isocitrate dehydrogenase; a-KG: alpha-ketoglutarate; a-KGDH: alpha-ketoglutarate dehydrogenase; SCoA-S: SuccinylCoenzyme A synthase; MDH: malate dehydrogenase; OAA: oxaloacetate; GDP: guanosine diphosphate; GTP: guanosine triphosphate

The Electron transport chain (ETC). The ETC involves a series of mitochondrial membrane-abiding enzymes (complexes I-V) which mediate the transfer of electrons generated in the TCA cycle to O_2, with synchronous generation of energy in the form of ATP (oxidative

phosphorylation). ROS (superoxide) are generated during this process through premature, single electron transfer to O_2 in complexes I (NADH dehydrogenase) and III (Cytochrome C reductase) (Sabharwal and Schumacker, 2014). Depending on the exact site of their generation, ETC-derived ROS may be directed to the mitochondrial matrix or the mitochondrial intermembrane space. Escape from the matrix to the intermembrane space and from there to the cytosol can also occur, as ROS can cross membranes through aquaporins and anion channels (Sabharwal and Schumacker, 2014, Bienert et al., 2007, Han et al., 2003).

Mitochondrial CYP450 Type I enzymes. These include the cholesterol side chain cleavage enzyme (CYP11A1 or P450scc), 11β-hydroxylase (CYP11B1 or P450c11) and its isoenzyme aldosterone synthase (CYP11B2 or P450c11AS). The hydroxylation reactions catalysed by these enzymes involve electron transfer from NADPH, which can lead to electron leakage to O_2 generating superoxide. The interaction between ROS and steroidogenesis is complex and is analysed in more details in a subsequent section.

Cytochrome b5 reductase. This outer mitochondrial membrane enzyme oxidises NAD(P)H and reduces cytochrome b5. Superoxide production at high rates has been reported (Whatley et al., 1998, Andreyev et al., 2005).

Monoamine oxidases A and B. Also located in the outer mitochondrial membrane, these enzymes catalyze the oxidation of biogenic amines. Hydrogen peroxide is produced during this reaction (Andreyev et al., 2005) (**Fig. 1-16**).

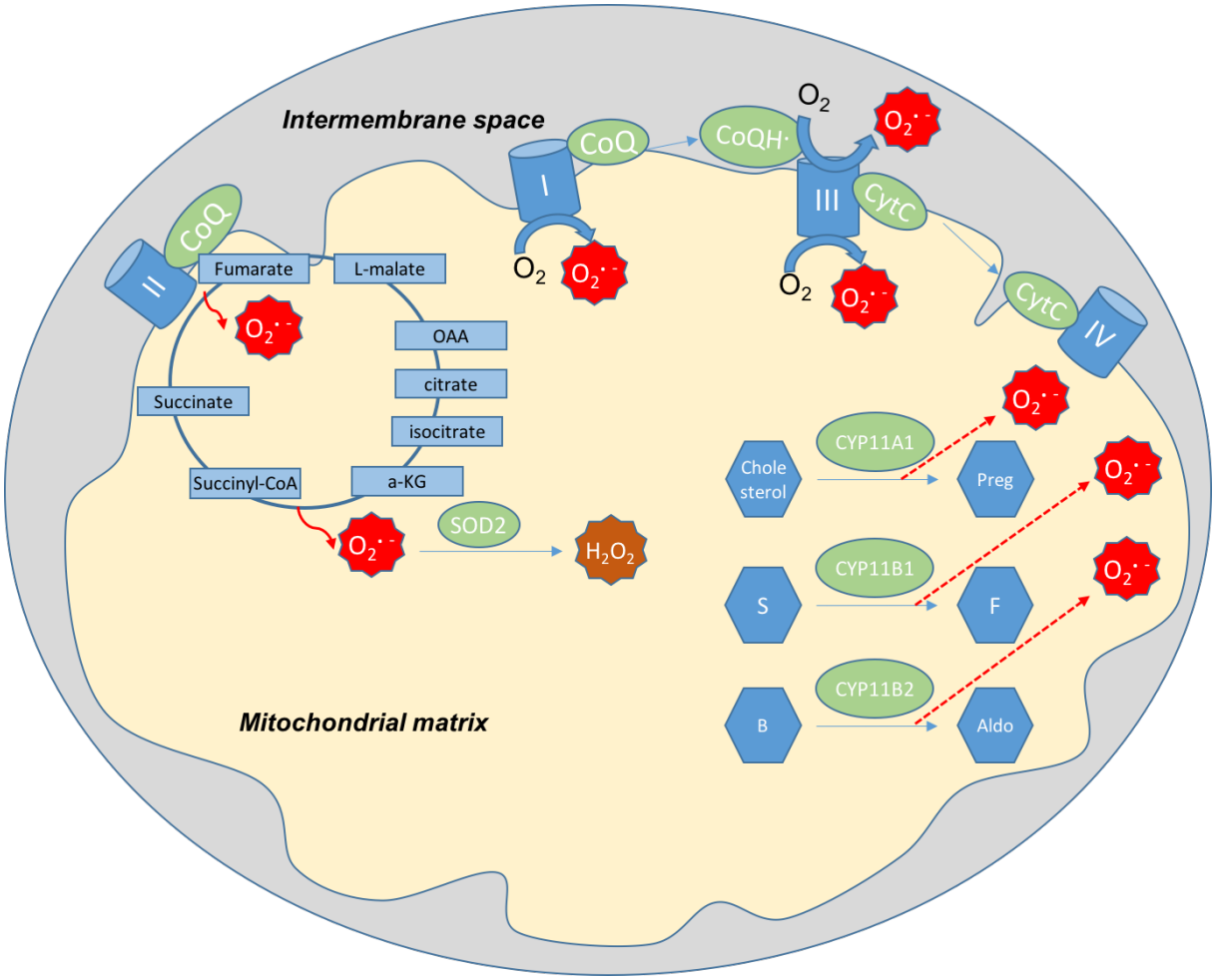

Figure 1-16 *Main sources of ROS in adrenal mitochondria. Superoxide is produced during electron leakage in respiratory chain complexes I - III, mitochondrial steroidogenesis (P450 monooxygenases) and the TCA cycle. CoQ: coenzyme Q; CytC: cytochrome C; Preg: pregnenolone; S: deoxycortisol; F: cortisol; B: corticosterone; Aldo: aldosterone; SOD2: mitochondrial superoxide dismutase*

Aside from these intracellular sources, ROS can be generated by a plenitude of external/ environmental triggers, including smoking, asbestos, inflammation, hypoxia, chemotherapy and radiotherapy (Gupta et al., 2012). Increased levels of ROS can cause oxidative damage to

DNA, proteins and lipids, disrupting cellular function and, in severe cases, triggering cell death. This deleterious impact of high intracellular ROS levels is commonly referred to as *oxidative stress*, and can be a result of high endogenous ROS production, exogenous insults or impaired scavenging mechanisms (antioxidant pathways) (Gupta et al., 2012, Fruehauf and Meyskens, 2007, Schieber and Chandel, 2014). Different ROS display different degrees of reactivity with cell macromolecules. Superoxide (O_2^-) is the most commonly produced intracellular ROS and is only mildly reactive. It is rapidly converted to hydrogen peroxide (H_2O_2) by superoxide dismutase 1 (cytosol, mitochondrial intermembrane space) or 2 (mitochondrial matrix). H_2O_2 is moderately reactive with cellular macromolecules. When allowed to accumulate inordinately, it can be converted to highly reactive hydroxyl radicals (Schieber and Chandel, 2014, Sabharwal and Schumacker, 2014).

In the last two decades, it has become increasingly evident that oxidative stress is but one dimension of ROS (patho)physiology, which is mainly pertinent in the context of ROS excess. When present in moderation, ROS are involved in various signalling pathways (redox signalling), hence serving a useful biological role as mediators of adaptive cellular responses to various environmental stress inducers (Schieber and Chandel, 2014). A good example of this 'virtuous to vicious' spectrum of ROS activity can be found in their interaction with proteins. Low-level hydrogen peroxide (H_2O_2) oxidises cysteine residues to sulfenic anions (Cys-SOH). This triggers allosteric changes in protein structure that modify their function and can initiate signalling cascades. Sulfenic anions can be reduced back to thiolate anions ($Cys-S^-$) by thioredoxin reductase and glutaredoxin; hence, this reversible oxidation can serve as a temporary signalling transduction mechanism. When H_2O_2 is allowed to accumulate excessively, however, it causes irreversible oxidation of cysteine residues to sulfinic (SO_2H) or sulfonic (SO_3H) species, permanently damaging the affected protein (Schieber and

Chandel, 2014). Redox signalling regulates numerous cell processes including proliferation, survival, angiogenesis, lipid metabolism, immune response and aging (Schieber and Chandel, 2014, Gupta et al., 2012).

The following sections focus on the role of ROS in steroidogenesis and cancer pathophysiology, which are most relevant to this work.

1.3.5 ROS and steroidogenesis

The interaction between ROS and steroidogenesis has yet to be fully elucidated, but appears to be bidirectional. Mitochondrial steroidogenesis is ineluctably associated with ROS generation in the reactions catalyzed by CYP11A1, CYP11B1 and CYP11B2, all cytochrome P450 monooxygenases which transfer reducing equivalents and an oxygen atom to steroid substrates, according to the following hydroxylation reaction:

$$\text{Substrate-H} + \text{NADPH} + H^+ + O_2 \rightarrow \text{Substrate-OH} + NADP^+ + H_2O$$ (Hornsby, 1980, Hanukoglu and Hanukoglu, 1986)

Electron transfer from NADPH to the steroid substrate occurs via two intermediate electron transfer proteins, adrenodoxin reductase (FAD-containing flavoenzyme) and adrenodoxin (ferrodoxin-type iron-sulfur protein) (Grinberg et al., 2000, Ziegler et al., 1999). Adrenodoxin and adrenodoxin reductase are ubiquitously expressed, but predominantly so in the adrenal cortex and corpus luteum (Brentano and Miller, 1992, Hanukoglu and Hanukoglu, 1986). Of note, they are not substrate-specific, i.e. a single form of adrenodoxin reductase and

adrenodoxin react with all mitochondrial P450 steroidogenic enzymes. The order of electron transfer is always the same:

NADPH ⟶ Adrenodoxin reductase⟶ Adrenodoxin ⟶ P450 (Hanukoglu, 2006)

The efficiency of this process, however, is never 100%, and superoxide (O_2^-) is also generated as a by-product when an unpaired electron is transferred to O_2. This is often described as 'electron leakage' or 'uncoupling of electron transfer'. Electron leakage has been studied in reconstituted forms of CYP11A1 and CYP11B1, which showed that about 15% and 40% of the total electron flow through each enzymic system, respectively, is directed to ROS formation (Rapoport et al., 1995). By comparison, leakage within the mitochondrial electron transfer chain occurs at an estimated rate of only 0.15% of the total electron flow (St-Pierre et al., 2002). Interestingly, uncoupling of CYP11A1 appears to be inversely proportional to substrate availability, while in CYP11B1 uncoupling increases with increasing concentrations of deoxycorticosterone (Rapoport et al., 1995). Within the adrenal cortex, expression of P450 mitochondrial enzymes is much higher (up to ten-fold) than the expression of other electron transfer chain enzymes or microsomal P450 enzymes (Hanukoglu and Hanukoglu, 1986). Therefore, it can be surmised that they account for a substantial proportion of total ROS generation within adrenocortical cells. This fact can potentially explain the higher concentration of antioxidants (e.g. Vitamin C, selenium) in the adrenal gland in comparison to other tissues (Prasad et al., 2014a). Derouet-Humbert et al. were able to demonstrate ROS-associated mitochondrial apoptosis is various cell lines overexpressing adrenodoxin or CYP11A1 (Derouet-Humbert et al., 2005).

The opposite direction of this interaction, i.e. the impact of oxidative stress on steroidogenesis, has been explored in a small number of *in vitro* studies, often with conflicting results. In 1980, Hornsby et al., working on cultured bovine adrenocortical cells, showed that treatment with antioxidants can ameliorate the decrease in CYP11B1 activity that is seen in response to treatment with cortisol, and augment the stimulation of CYP11B1 activity seen in response to ACTH treatment (Hornsby, 1980). 10 years later, Behrman et al. found that hydrogen peroxide (H_2O_2) has a specific inhibitory effect on cholesterol transport to the mitochondria in rat luteal cells, but did not seem to affect downstream steroidogenesis (Behrman and Aten, 1991). In another study, an inhibitory effect of H_2O_2 on 3beta-hydroxysteroid dehydrogenase was demonstrated in MA-10 Leydig tumour cells (Stocco and Ascoli, 1993). Similarly, Diemer et al. showed that treatment of MA-10 Leydig tumour cells with H_2O_2 suppressed CYP11A1 activity after 3h of cAMP stimulation in a dose-dependent manner, as evidenced by lower progesterone synthesis, although CYP11A1 expression was not affected. Exogenous xanthine oxidase administration, leading to superoxide generation, was associated with down-regulation of StAR and suppression of progesterone production (Diemer et al., 2003). Interestingly, Zhao et al. demonstrated a biphasic relationship between chemically induced oxidative stress and steroidogenesis in rat Leydig cells. Moderate oxidative stress increased testosterone synthesis activating CYP11A1, 3β-HSD and 17β-HSD, while higher levels had the opposite effect (Zhao et al., 2012).

There is hardly any evidence on the effects of oxidative stress on mineralocorticoid synthesis. The only relevant *in vitro* study of aldosterone synthesis on NCI-H295R (ACC) cells surprisingly showed that CYP11B2 (aldosterone synthase) is actually up-regulated by oxidative stress (Rajamohan et al., 2012).

In clinical medicine, a number of familial forms of adrenal insufficiency have been associated with impaired redox status, including triple A syndrome, X-linked adrenoleukodystrophy and, as discussed previously, Familial Glucocorticoid Deficiency (FGD) (Prasad et al., 2014b). Triple A syndrome (Allgrove's syndrome) is an autosomal recessive disease characterized by the clinical constellation of alacrima (absence of tears), oesophageal achalasia and primary adrenal insufficiency. This is often accompanied by a progressive neurodegenerative process (Allgrove et al., 1978). The genetic culprit, *AAAS,* encodes a nucleoporin (ALADIN) whose exact role has yet to be elucidated. Dermal fibroblasts from Triple A patients display high levels of ROS. It is unclear what drives this oxidative stress and to what extent this is causally linked to the clinical syndrome. Histological evidence of atrophic zona fasciculata and reticularis have been reported (Prasad et al., 2014b, Allgrove et al., 1978). In a recent study, stable knockdown of *Aaas* in NCI-H295R ACC cells increased oxidative stress and led to a suppression of cortisol synthesis and expression of CYP11B1 and StAR; CYP11A1 did not appear to be affected (Prasad et al., 2013). These results were subsequently contradicted by Juhlen et al., who found that ALADIN knockdown in NCI-H295R-S1 (substrain 1) cells only has an impact on the CYP450 type II microsomal enzymes CYP17A1 and CYP21A2, and their electron donor enzyme POR. Steroidogenically, only 17-hydroxyprogesterone, 11-deoxycortisol and androstenedione were significantly suppressed (Juhlen et al., 2015). Interestingly, *Aaas* knockout in mice fails to reproduce the features of human patients (Huebner et al., 2006).

Adrenoleukodystrophy is another rare genetic disease (X-linked) afflicting the central nervous system (progressive demyelination) and the adrenal glands (primary adrenal insufficiency). It is caused by mutations of *ABCD1,* a gene encoding the ALP protein, which mediates intracellular transfer of very long chain fatty acids (VLCFA) into the peroxisomes for beta-

oxidation (van Roermund et al., 2008). Accumulation of VLFCA results in ROS generation, although the exact mechanism is poorly understood (Ivashchenko et al., 2011). *Abcd1* knockout mice, however, have a much milder phenotype and the adrenal glands are spared (Forss-Petter et al., 1997, Prasad et al., 2014b).

In 2014, whole exon sequencing in three related patients with FGD revealed they all shared an inactivating mutation of mitochondrial thioredoxin reductase type 2 (Prasad et al., 2014a). This discovery of a second gene (after *NNT*) participating in the mitochondrial antioxidant defence network in FGD patients consolidated the importance of redox homeostasis for the adrenal gland. Whether glucocorticoid deficiency in these patients arises as a consequence of ROS-induced adrenal cell damage, developmental failure of adrenal cortex formation due to aberrant redox signalling or functional inhibition of steroidogenic enzymes remains unknown (Prasad et al., 2014a).

1.3.6 ROS and cancer

The multi-layered relationship between ROS and cancer has been extensively explored in the last two decades and several levels of interaction have been identified. It is now recognised that ROS are involved in signalling pathways implicated in oncogenesis (malignant cellular transformation), response to hypoxia, cell proliferation, cell viability and angiogenesis, all important parameters of malignant pathophysiology (Fruehauf and Meyskens, 2007, Gupta et al., 2012, Schumacker, 2006) (**Fig. 1-17**).

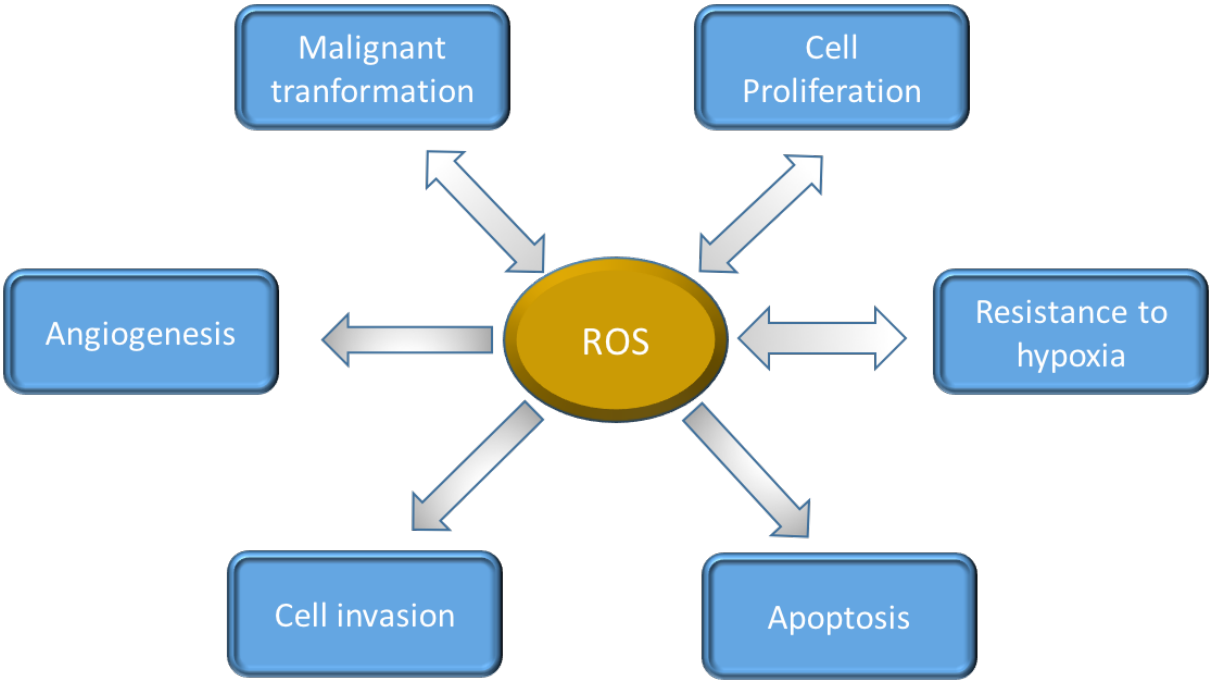

Figure 1-17 Interaction between ROS and important cellular processes involved in cancer pathophysiology. Double arrows represent bidirectional relationships.

1.3.6.1 ROS and malignant transformation

Oncogenesis or malignant cellular transformation refers to the process whereby healthy cells acquire properties of malignant cells, either through activation of oncogenes or inactivation of tumour suppressor genes. Our understanding of ROS involvement in malignant cell transformation is still incomplete, but an ever-increasing body of work has accrued evidence supporting ROS involvement in this process (Fruehauf and Meyskens, 2007, Sabharwal and Schumacker, 2014, Schumacker, 2006, Gupta et al., 2012). Stimulation of malignant transformation by oxidising agents (Radisky et al., 2005, Azad et al., 2010) and suppression of malignant transformation by antioxidants (Wang et al., 2011, Irani et al., 1997, Yan et al., 2009) have been demonstrated *in vitro*. ROS-induced DNA damage leading to genomic

instability and oncogene activation is a putative pathophysiological link (Gupta et al., 2012, Fruehauf and Meyskens, 2007). Mitochondrial DNA is particularly susceptible to ROS-induced damage owing to its proximity to the electron transfer chain, and its mutations can lead to loss of function of crucial cell cycle 'checkpoints', a hallmark feature of malignant cells (Schumacker, 2006).

Malignant cells generally have higher levels of oxidative stress than normal cells. This difference is partly due to the higher metabolic rates of cancer cells, leading to higher rates of ROS generation in the electron transfer chain. Elegant *in vitro* studies involving immortalised benign cell lines as controls, however, indicated that the increased oxidative stress of malignant cells is probably an attribute related to the malignant transformation itself, even allowing for the differences in metabolic rates between malignant and healthy cells (Trachootham et al., 2006). Maintaining modestly elevated ROS levels may be beneficial to malignant cells in a number of ways, including accelerated proliferation, resilience to hypoxia and stimulation of angiogenesis, as detailed in the following paragraphs.

1.3.6.2 ROS and hypoxia

Dealing with a hypoxic microenvironment is a challenge almost invariably facing cancer cells. Malignant cell response to hypoxic stress is mediated by the hypoxia-inducible factor 1 (HIF-1). HIF-1 is a cytosolic heterodimer consisting of HIF-1α and HIF-1β. In response to hypoxia, it translocates to the nucleus and induces the transcription of a number of target genes; the end effect is enhanced cell proliferation and stimulation of angiogenesis. Under normoxic conditions, HIF-1 is quickly inactivated through hydroxylation of proline residues by PHD (prolyl hydroxylase), followed by degradation by the ubiquitin–proteasome system.

PHD uses O_2 as a substrate and thus its action is inhibited by hypoxia, allowing free expression of HIF-1 and, consequently, the whole panel of hypoxia-response genes which mediate cellular resistance to hypoxic conditions (Pugh and Ratcliffe, 2003). The effect of ROS on HIF-1 is not as yet fully elucidated and existing evidence is contradictory. A series of *in vitro* studies have demonstrated that both exogenous and endogenous ROS can augment HIF-1a stabilization and binding and, consequently, augment cell survival, proliferation and angiogenesis (Duyndam et al., 2001, Brauchle et al., 1996, Chandel et al., 2000, Guzy et al., 2007, Wang et al., 1995). However, other studies have demonstrated diametrically different results, with exposure to exogenous or endogenous excessive ROS inhibiting HIF-1a stabilization and/or binding (Huang et al., 1996, Hellfritsch et al., 2015). From an alternative perspective, it has been ascertained that hypoxia itself paradoxically stimulates mitochondrial ROS production, enhancing electron leakage in the ETC (Guzy and Schumacker, 2006).

1.3.6.3 Role of ROS in cellular proliferation.

The ability of ROS to enhance cellular proliferation has been demonstrated in a large number of *in vitro* and *in vivo* studies using various cancer types. This also applies to healthy cells, as redox signalling can augment growth factor-mediated cellular proliferation (Schumacker, 2006). Molecular targets through which the proliferative effect of excess ROS is facilitated include ERK (extracellular signal-regulated kinases), Nf-κB (nuclear-factor-kappa-light-chain enhancer of activated B cells), Cyclin E, EGFR, JNK (c-Jun N-terminal kinases) and others (Fruehauf and Meyskens, 2007, Gupta et al., 2012, Liu et al., 2002, Ruiz-Ramos et al., 2009). In cancer studies, exogenous H_2O_2 stimulated proliferation in hepatoma cells through activation of protein kinase B (Liu et al., 2002), while arsenite-induced ROS reproduced the

same effect on breast cancer cells (Ruiz-Ramos et al., 2009). Similarly, increase in endogenous ROS production has been associated with enhanced proliferation in lung cancer, breast cancer and ovarian cancer cells (Hu et al., 2005, Na et al., 2008). In keeping with these findings, treatment with ROS scavengers (e.g. catalase, N-acetylcysteine) has demonstrated anti-proliferative effects *in vitro* (Saunders et al., 2010, Martin et al., 2007, Policastro et al., 2004). Conversely, a smaller number of studies have demonstrated suppression of cellular proliferation in response to ROS loads, suggesting that the net effect of ROS on cellular proliferation may be dose-dependent, with modest rises stimulating and steep elevations inhibiting proliferation (Koka et al., 2010, Donadelli et al., 2007, Qu et al., 2011).

1.3.6.4 ROS and cell death

ROS excess can trigger cell death by apoptosis, necrosis or autophagy. Apoptosis is a controlled form of cell death induced either by the mitochondria (intrinsic pathway) or non-mitochondrial death receptors (extrinsic pathway) (Gupta et al., 2012). ROS can induce apoptosis through the extrinsic pathway: death receptor Fas can be activated by ROS, eventually leading to caspase 8 activation and apoptosis (Denning et al., 2002, Medan et al., 2005, Reinehr et al., 2005, Uchikura et al., 2004). Mitochondrial ROS-dependent apoptosis involves opening of the mitochondrial permeability transition pore complex (MPTP), a multimeric channel consisting of adenine nucleotide translocase, cyclophilin D, creatine kinase and a voltage dependent ion channel (VDAC). ROS-induced pore opening is mediated by activation of pore-destabilising proteins (Bcl-2-associated X protein, Bcl-2 homologous antagonist) as well as inactivation of pore-stabilising proteins (Bcl-2 and Bcl-Xl) (Martindale and Holbrook, 2002). MPTP opening is followed by cytochrome c release, apoptosome

formation and caspase activation, effectuating the apoptotic demise of the cell (Martindale and Holbrook, 2002, Gupta et al., 2012) (**Fig 1-18**). When ROS accumulation becomes even more excessive, it can act as a trigger of necrosis rather than apoptosis, in a caspase-independent fashion. Necrosis is a rapid and uncontrolled form of cell death, involving disruption of cell membranes and release of cell contents to the extracellular space (Krysko et al., 2008). The capacity of excessive ROS to act as triggers of necrosis has been demonstrated in a number of cell lines *in vitro*, including Jurkat T-lymphocytes, multiple myeloma, lymphoma and prostate cancer cells (Nair et al., 2009, Hampton and Orrenius, 1997, Garbarino et al., 2007). A third mode of cell death associated with ROS excess is autophagy. Autophagy comprises a self-catabolic process of lysosomic degradation of cellular organelles and proteins. Autophagy in response to ROS accumulation has been demonstrated in various cancer types *in vitro*, including colon cancer, gliomas, glioblastomas and breast cancer (Chen et al., 2008, Xie et al., 2011, Shrivastava et al., 2011, Park et al., 2011).

As with proliferation, the interaction between ROS and cell death is not entirely straight-forward, and more modest levels of ROS have been shown, in a smaller number of studies, to have the opposite effects, promoting cell survival (Yang et al., 2007, Brar et al., 2003). Sub-cellular localisation also seems to be important, with moderate elevations in cytoplasmic ROS supporting cell survival while mitochondrial ROS inducing apoptosis (Deshpande et al., 2003). Overall, there appears to be a multi-phasic relationship between ROS and cellular growth kinetics, whereby low ROS levels can promote cell survival and stimulate proliferation, higher (supra-physiological) levels trigger apoptosis and more overwhelming rises can directly induce necrosis or autophagy (Gupta et al., 2012, Schafer and Buettner, 2001).

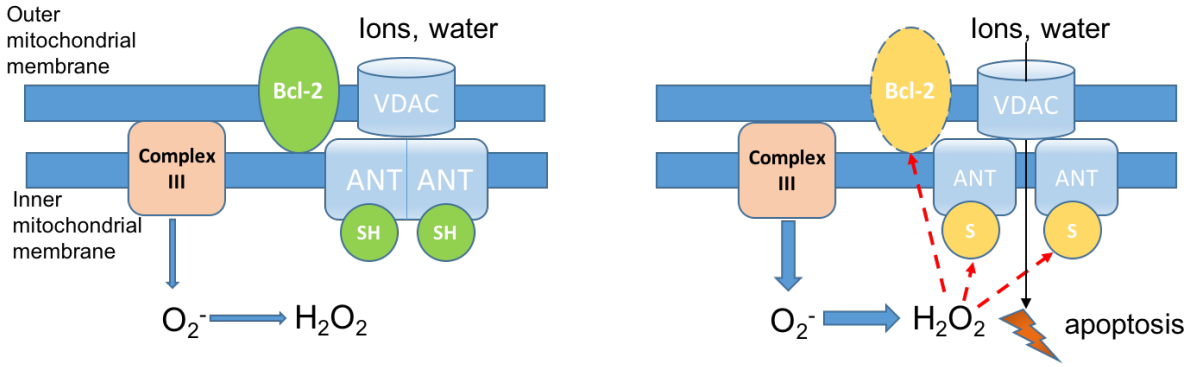

Figure 1-18 H_2O_2-induced apoptosis through mitochondrial permeability transition pore (MPTP) opening. H_2O_2 destabilises MTP through direct oxidation of ANT (adenine nucleotide translocase) and/or the pore-stabilising protein Bcl-2. Resulting VDAC (voltage-dependent anion channel) opening allows influx of anions and water into the mitochondria, cytochrome c activation and, eventually, apoptosis. Source: (Fruehauf and Meyskens, 2007) . Adapted and reproduced with permission of the American Association of Cancer Research.

1.3.6.5 ROS and cell invasion/ angiogenesis

Similar to their effect on cell proliferation, modest ROS rises can also promote angiogenesis and tissue invasion and enhance the metastatic potential of malignant cells *in vitro* and *in vivo*. Signalling pathways mediating this effect include mitogen-activated protein kinase (MAPK), CXC chemokine receptor, VEGF and VEGF receptors 1 and 2 (Ho et al., 2011, Arbiser et al., 2002, Chetram et al., 2011). Suppression of invasion/ angiogenesis by ROS has also been described in a smaller number of studies, suggesting that, as with other previously

described effects, this impact may also be dosage/location-dependent (Adhikary et al., 2010, Qu et al., 2011, Hellfritsch et al., 2015).

1.3.6.6 ROS and resistance to chemotherapy

Adaptation to chronic exogenous oxidative stress has been observed in various cancer cell lines *in vitro* (Trachootham et al., 2009, Gupta et al., 2012). This can be explained by two interacting factors:

a) The toxicity (to the extent of cell death) of excessive ROS accumulation creates a selective pressure under which cells that manage to adapt (e.g. by strengthening their antioxidant pathways) have an advantage and dominate the population.
b) An oxidized intracellular microenvironment creates genomic instability due to oxidative DNA damage and defective DNA repair, augmenting the genetic plasticity of malignant cells and accelerating their adaptation to new metabolic challenges.

Molecular pathways through which adaptation to oxidative stress is achieved often involve Nf-κB, Nrf-2 (nuclear factor E2- related factor 2) and HIF-1 (hypoxia inducible factor 1); all of them converge to the up-regulation of antioxidant genes (Trachootham et al., 2009). Redox adaptation can be a dynamic process following a 'vicious cycle' pattern, eventually resulting in late-stage cancer cells that manage to survive despite high endogenous ROS by virtue of their hypertrophic antioxidant defence mechanisms. Not only does successful redox adaptation allow malignant cells to survive despite high ROS levels, but it can often enhance their resilience to chemotherapy, especially when it comes to drugs that exert part of their cytotoxic effect through oxidative stress (**Fig.1-19**) (Trachootham et al., 2009). From a

different perspective, the dependence of such cells on their antioxidant capacity may represent a metabolic 'Achilles' heel' that can be targeted therapeutically. This is discussed comprehensively in a separate section, after an overview of the antioxidant defence mechanisms.

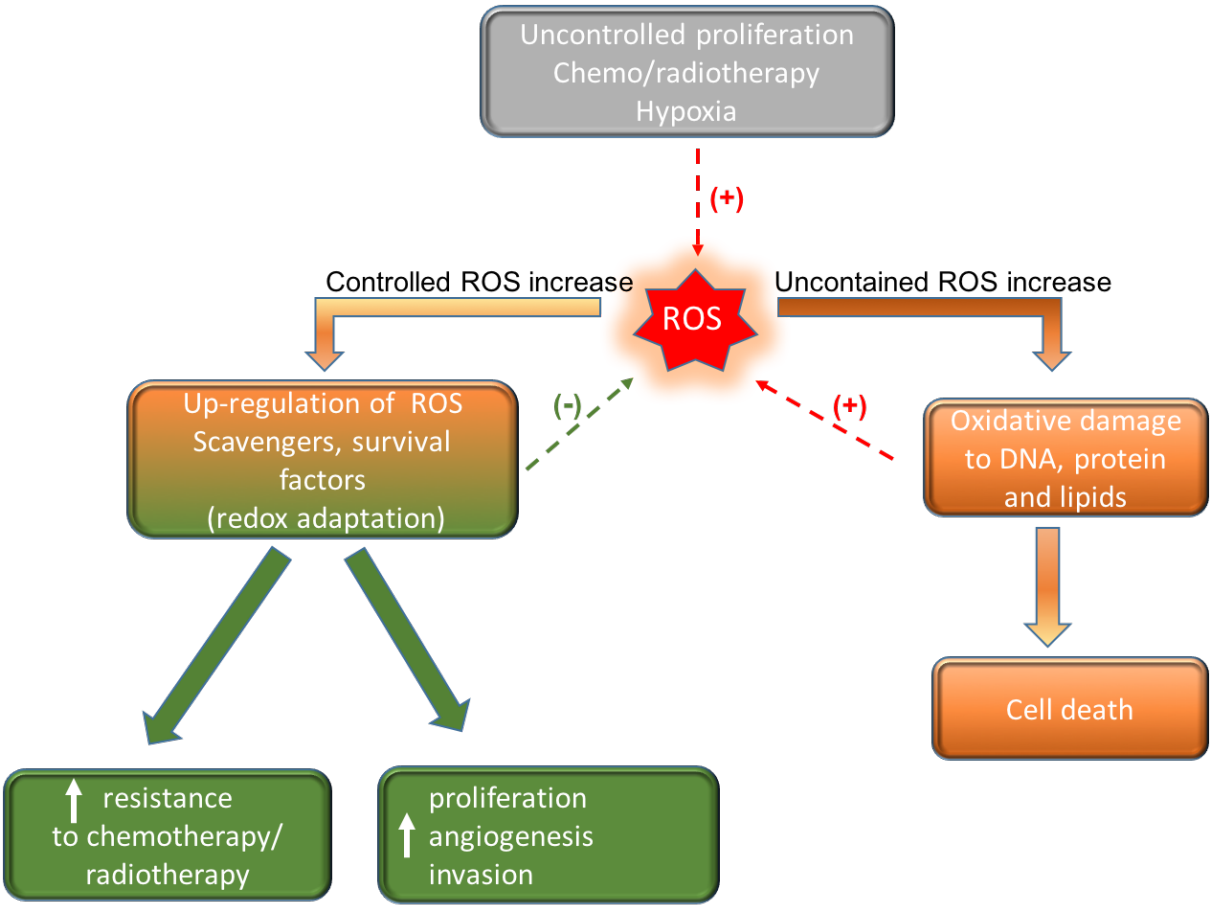

Figure 1-19 ROS as a double-edged sword in cancer pathophysiology. Increase in intracellular ROS levels in cancer cells, both constitutively and exogenously, can lead to diametrically different outcomes. Excessive/ uncontrolled rises can induce lethal oxidising toxicity, leading directly to cell death. With more modest increases cells may manage to adapt to the increased oxidative stress, upregulating ROS scavenging pathways and survival agents (e.g. Bcl-2). This response is often orchestrated by multi-target transcription factors such as NF-κB and/or Nrf2. When successful, this response may lead to a more aggressive phenotype, characterised by chemo- and radio-resistance and rapid proliferation.

1.3.7 ROS scavenging (antioxidant pathways)

Given the versatile role of ROS in intracellular signalling and cell viability, a number of antioxidant pathways have evolved to create an efficient buffering system that can maintain these potentially toxic metabolic by-products at sustainable levels and respond promptly to exogenous stressors. The key players in these systems are described below:

Superoxide dismutases (SODs). SODs catalyse the dismutation of superoxide (O_2^-) to hydrogen peroxide (H_2O_2), in order to protect mitochondrial iron-sulfur cluster-containing enzymes from superoxide toxicity (Andreyev et al., 2005). Two isoforms of SOD can be distinguished in mammalian cells: Cu,Zn-SOD (cytoplasm, nucleus) and MnSOD (mitochondria). SODs cannot act as ROS scavengers independently, as they require systems that can react with H_2O_2. Expression of MnSOD is often low in malignant cells, and cell lines overexpressing SOD have reduced proliferation rates and cellular viability *in vitro* and *in vivo,* presumably due to accumulation of H_2O_2 (Andreyev et al., 2005). In mice, homozygous MnSOD mutations result in a lethal phenotype, but MnSOD overexpression is also

detrimental, begetting a phenotype of developmental delay and subfertility (Li et al., 1995, Raineri et al., 2001).

The glutathione pathway. Glutathione (L-c-glutamyl-L-cysteinyl-glycine or GSH) is the most abundant antioxidant molecule in most tissues (Lee et al., 2008). It is a tripeptide with a thiol (–SH) group in its cysteine residue when at a reduced state. GSH synthesis is performed in the cytoplasm via the action of c-glutamylcysteine ligase (GCL) and GSH synthetase, which are ubiquitously expressed in all tissues. From there it can be transferred to cellular organelles, including the mitochondria, through numerous transporters and carriers (Andreyev et al., 2005). Glutathione peroxidases (GPXs) use reduced glutathione as an electron donor to reduce H_2O_2 to H_2O. GPXs are selenoproteins which possess redox-active selenocysteine residues at their catalytic sites (Mari et al., 2009, Lee et al., 2008). Overall, reduced glutathione is a versatile antioxidant molecule which acts to maintain cellular redox balance in the following ways:

a) It serves as a substrate to glutathione peroxidase type 1 (GPX1) and peroxiredoxin in reactions that detoxify H_2O_2 to H_2O, both in the cytosol and the mitochondrial matrix
b) It protects mitochondrial membrane lipids from oxidative damage through reduction of hydroperoxide groups, in reactions that are catalysed by mitochondrial glutathione-S-transferases and glutathione peroxidase type 4 (GPX4). This reaction is of vital importance, as indicated by the fact that GPX4 knockout in mice results in embryonal lethality, while GPX1 knockout is viable.
c) It can react non-enzymatically with toxic electrophilic compounds (endogenous or exogenous).

d) It serves as a substrate to glutaredoxin, a disulfide oxidoreductase able to reduce disulfides in various proteins to prevent oxidative damage (cytosol and mitochondria) (Mari et al., 2009).

Upon reducing ROS or oxidised protein/ lipids, either enzymatically or non-enzymatically, glutathione switches to its oxidised form (GSSG). The ratio of reduced to oxidised glutathione is a widely-used marker of cellular antioxidant capacity. Within the mitochondria, approximately 90% of total glutathione is at its reduced form (Mari et al., 2009, Andreyev et al., 2005). Importantly, GSSG cannot cross the mitochondrial membrane; therefore, mitochondria are dependent on NADPH to reduce GSSG back to GSH within the mitochondrial matrix, in a reaction catalysed by glutathione reductase (Andreyev et al., 2005) (**Fig. 1-20**).

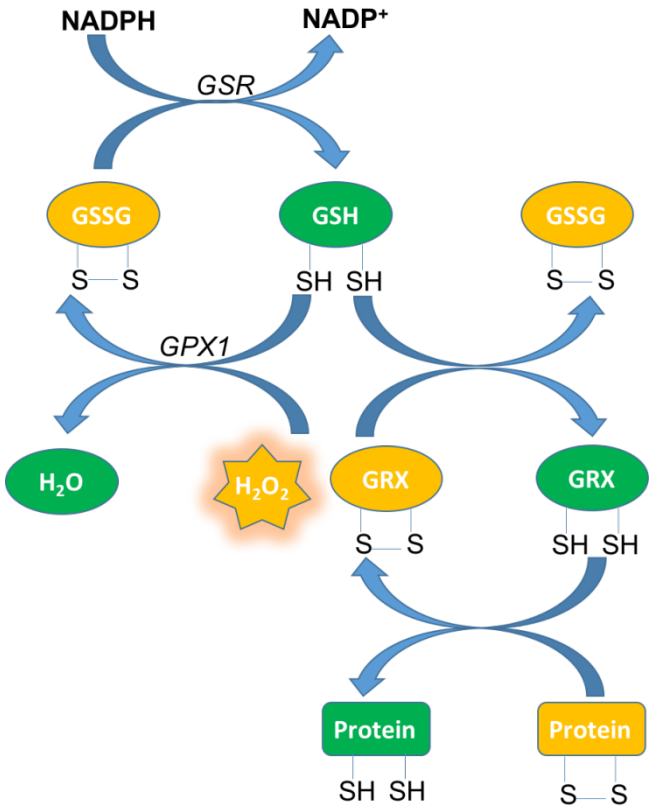

Figure 1-20 The glutathione pathway. Oxidised and reduced molecules are presented in yellow and green, respectively. Reduced glutathione (GSH) is regenerated from oxidised glutathione (GSSG) by glutathione reductase (GSR), using NADPH as a donor of reducing equivalents. GSH can be used by glutathione peroxidase type I (GPX1) to reduce H_2O_2 to H_2O, or interact with oxidised glutaredoxin (GRX-S_2) to generate its reduced form (GRX-$(SH)_2$). GRX-$(SH)_2$ can act non-enzymatically to break disulphide bonds in proteins to reverse oxidative damage.

The thioredoxin pathway. Thioredoxins are a group of small, redox-active proteins characterised by the presence of a conserved -Trp-Cys-Gly-Pro-Cys-Lys- catalytic site that can undergo oxidation/reduction of the two Cys residues reversibly, with concurrent transfer of reducing equivalents to or from a disulfide substrate. Oxidised thioredoxin (TXN-S_2) can be reduced back to its reduced form (TXN-$(SH)_2$) by thioredoxin reductase (TXNRD), in a reaction requiring electron donation by NADPH.

$$TXN\text{-}(SH)_2 + X\text{-}S_2 \longleftrightarrow TXN\text{-}S_2 + X(SH)_2$$

$$TXN\text{-}S_2 + NADPH \longleftrightarrow TXN\text{-}(SH)_2 + NADP^+$$

Two isoforms of thioredoxin reductase have been described: thioredoxin reductase 1 (cytosolic) and thioredoxin reductase 2 (mitochondrial) (Powis and Montfort, 2001, Mustacich and Powis, 2000). Reduced thioredoxin in its turn offers its reducing equivalents to peroxiredoxins type 1-5 (PRDX 1-5). Peroxiredoxins can then act directly with H_2O_2 and detoxify it to H_2O, in a reaction during which two reduced PRDX subunits are converted to an oxidised disulphide-linked dimer. PRDX type 3 and, to a lesser extent, PRDX type 5 are located in the mitochondria, the former being mitochondria-specific (Prasad et al., 2014b, Powis and Montfort, 2001). Like glutathione peroxidase, peroxiredoxins are also involved in the detoxification of lipid peroxides, protecting the mitochondrial membrane. Kinetic analysis has suggested that peroxiredoxin type 3 reacts with 90% of the total H_2O_2 concentration within the mitochondrial matrix (Cox et al., 2010). Of note, regeneration of reduced peroxiredoxin can be alternatively facilitated by glutaredoxin, in which case reduced glutathione acts as the reducing agent (Cox et al., 2010). Thioredoxin reductase type 2 knockout (but not peroxiredoxin knockout) is lethal in mice (Andreyev et al., 2005) (**Fig. 1-21**).

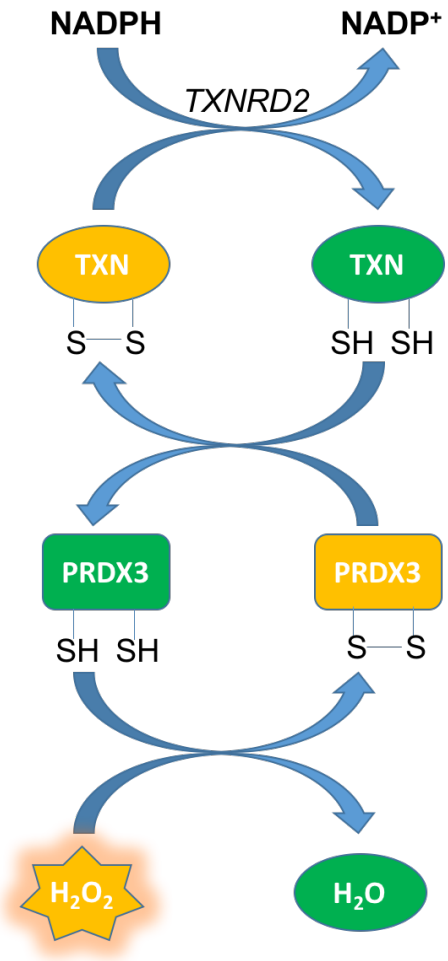

Figure 1-21 The mitochondrial thioredoxin pathway. TXN: thioredoxin; TXNRD2: thioredoxin reductase 2; PRDX3: peroxiredoxin 3; H_2O_2: hydrogen peroxide.

Taken together, the glutathione and thioredoxin/peroxiredoxin pathways comprise the bulk of the antioxidant armamentarium of eukaryotic mitochondria. Some important points to consider regarding their interaction are the following: a) both pathways use NADPH as an essential donor of reducing equivalents – therefore, the antioxidant capacity of mitochondria

is vitally dependent on their ability to produce ample NADPH; b) each of the two pathways can be up-regulated to compensate for dysfunctions in the other pathway (redundancy) (Ueda et al., 2002) and c) exogenous oxidants as well as certain endogenous oxidative stress-inducing agents may occasionally preferentially interact with one of the two pathways, indicating that this redundancy is not complete (Halvey et al., 2005, Hansen et al., 2006).

Catalase. Catalase is a non-NADPH-dependent, enzymatic ROS scavenger. Structurally, it is a tetrameric molecule with four haeme groups, through which its antioxidant activity is facilitated (Nagem et al., 1999). Catalase is ubiquitously expressed in all major organs, but predominantly in the liver, kidneys and erythrocytes. The main catalatic reaction involves detoxification of H_2O_2 to H_2O and O_2. Intracellularly, catalase is mostly expressed in the peroxisomes and the cytoplasm (Glorieux et al., 2015). Catalase expression in low concentrations has also been detected in rat heart and liver mitochondria, as well as the cytoplasmic membrane of cancer cells (Bauer, 2012, Glorieux et al., 2015). Catalase expression in malignant cells is variable. Suppressed catalase levels in comparison to healthy cells of the corresponding organ have been observed in a number of malignancies; conversely, high catalase expression has been demonstrated in certain aggressive malignancies with pronounced resistance to chemotherapy and radiotherapy (gliomas, mesotheliomas). Of note, up-regulation of catalase seems to mediate resistance to prolonged treatment with oxidising agents (cisplatin, ionising radiation, bleomycin) *in vitro* (Glorieux et al., 2015).

1.3.8 ROS modulation as a treatment strategy in oncology

1.3.8.1 Chemotherapy

Cytotoxic chemotherapy has been the mainstay of advanced cancer treatment since 1945. A broad range of chemotherapy agents have been developed since then, with various molecular mechanisms of action largely converging to a single output: inhibition of cell division. A number of commonly used cytotoxic chemotherapy agents have the additional capacity to induce oxidative stress, an effect to which part of their therapeutic potential has been ascribed (**Table 1-6**). It should be noted that these drugs' impact on redox balance is rather a secondary effect, alongside the primary molecular toxicity mechanisms on whose grounds they were originally developed (e.g. disruption of DNA replication, disruption of mitotic spindle). Consequently, it is difficult to ascertain how much of the cytotoxic effect is directly attributable to oxidative stress. A classic example of a routinely used chemotherapy agent which also acts as oxidative stressor is doxorubicin. Doxorubicin is an anthracycline compound used in the treatment of various cancer types, including ACC, by virtue of its ability to disrupt DNA synthesis. It has also been shown that doxorubicin acts as a 'redox cycler': it reacts with flavoprotein reductases (e.g. NADPH:quinine oxidoredictase – NQO1) and generates superoxide, especially when intracellular NADPH is low. Doxorubicin also contributes to intracellular iron chelation, which may eventually generate highly reactive hydroxyl radicals through a Fenton type reaction (Kotamraju et al., 2002).

Table 1-6 Approved chemotherapy agents which can induce oxidative stress. Source: (Montero and Jassem, 2011). Adapted and reproduced with permission of Springer.

Drug	Effect on redox balance	Other cytotoxic effects	Reference
Arsenic trioxide	ROS generation, oxidation of reduced glutathione	Degradation of the promyelocytic leukaemia protein	(Fruehauf and Meyskens, 2007, Lu et al., 2007)
Bleomycin	Metal-dependent ROS generation	Disruption of cellular division	(Chen and Stubbe, 2005, Chow et al., 2008)
Cisplatin	ROS generation, ROS-triggered apoptosis	DNA damage	(Berndtsson et al., 2007)
Anthracyclines (doxorubicin, epirubicin)	ROS generation, ROS-triggered apoptosis	Disruption of cellular division	(Wondrak, 2009)
Topoisomerase II inhibitors (etoposide)	ROS generation, ROS-triggered apoptosis	Inhibition of DNA replication	(Oh et al., 2007)
Taxanes (paclitaxel, docetaxel)	ROS generation, ROS-triggered apoptosis	Inhibition of mitotic spindle formation	(Alexandre et al., 2006, Alexandre et al., 2007)

Chemical induction of oxidative stress with a view to inducing cell death has been used as a strategy to develop novel anti-cancer agents in experimental oncology in the last two decades. This can be effectuated either through direct ROS generation or abrogation of antioxidant

pathways. As described above, malignant cells are characterised by higher baseline ROS levels than healthy cells, which brings them closer to the toxic threshold beyond which cell death is triggered. Therefore this treatment strategy is expected to exert a selective toxic effect on cancer cells (Gupta et al., 2012, Fruehauf and Meyskens, 2007, Trachootham et al., 2006). Novel agents currently under study which act as exogenous ROS inducers include redox cyclers (MGd), iron chelators (Dp44mT) and electron transfer chain modulators (arsenic trioxide) (Trachootham et al., 2009). Elesclomol is another ROS generator that received considerable attention after prolonging recurrence-free survival in malignant melanoma patients (phase II trial). The drug (used in combination with paclitaxel) had to be withdrawn due to concerns regarding unacceptable toxicity in phase III trials (Kirshner et al., 2008).

The limitation of exogenous ROS induction in oncology is that cancer cells, especially in aggressive/ advanced disease types, can be notoriously adaptable to environmental challenges, including oxidative stress. Up-regulation of antioxidant defence mechanisms can result in the development of resistant phenotypes (Fruehauf and Meyskens, 2007, Trachootham et al., 2009). An alternative ROS-centred strategy involves antioxidant pathway inhibition, aiming to provoke a gradual accumulation of endogenous ROS. This option has been explored both as monotherapy and as part of combination chemotherapy, with a view to enhancing cellular sensitivity to oxidative stress (Fruehauf and Meyskens, 2007, Watson, 2013). ROS scavenging pathways targeted so far include:

The glutathione pathway, largely considered the most important pillar of cellular antioxidant defence. Up-regulation of glutathione synthesis (e.g. glutathione sulfotransferase) often accompanies malignancy and is associated with tumour aggressiveness (Hsu et al., 2002). A number of agents have been developed to target glutathione synthesis and action (Renschler,

2004, Trachootham et al., 2006, Trachootham et al., 2009). BSO (buthionine sulfoximine) is an inhibitor of GSH synthesis which has demonstrated *in vitro* ability to suppress growth in pancreatic cancer cells, reverse BCL-2-mediated cisplatin resistance in breast cancer cells and enhance oxidative stress-induced cytotoxicity in leukemic cells (Schnelldorfer et al., 2000, Rudin et al., 2003). *In vivo*, BSO enhanced the cytotoxic effects of melphalan and arsenic trioxide (both intracellular ROS inducers) in xenograft models of multiple myeloma and solid tumours (Tagde et al., 2014, Maeda et al., 2004). Beta-phenylethyl-isothiocyanate. (PEITC) is another agent which depletes reduced glutathione and inhibits glutathione peroxidase. Anti-tumour activity has been demonstrated *in vitro* in ovarian cancer, leukaemia and osteosarcoma models (Trachootham et al., 2009, Gupta et al., 2012). NOV-002 is a compound that decreases the intracellular ratio of reduced to oxidised glutathione. It has demonstrated an *in vitro* capacity to suppress cellular proliferation and invasion, through interference with redox signalling pathways. Clinically, it has shown promising cytotoxic effects in combination treatment regimens in phase II clinical trials on non-small cell lung cancer, breast cancer and ovarian cancer. In a phase III trial however, it failed to demonstrate any additional cytotoxic activity in combination with paclitaxel and carboplatin in non-small cell cancer patients (Uys et al., 2010, Townsend and Tew, 2009, Montero et al., 2012, Gumireddy et al., 2013, Montero and Jassem, 2011).

Drugs inhibiting glutathione-S-transferase have also been developed: canfosfamide and ezatiostat hydrochloride. Confosfamide was used successfully in combination with carboplatin/ paclitaxel for advanced non-small cell carcinoma, but failed to demonstrate superiority to routine chemotherapy as third line chemotherapy in advanced ovarian carcinoma (Sequist et al., 2009, Vergote et al., 2009). Ezatiostat has been applied in the treatment of myelodysplastic symptoms and was beneficial improving haematological

parameters and reducing transfusion needs in a substantial proportion of patients (Raza et al., 2009). Finally, Imexon is another developing agent that depletes reduced glutathione. Correlation of efficiency against beta-cell lymphoma with tumour expression levels of glutathione peroxidase and superoxide dismutase 2 has been demonstrated (Barr et al., 2014).

The thioredoxin pathway. Considerable effort has been recently expended on targeting this antioxidant pathway, given its habitual up-regulation in cancer cells which is associated with a more aggressive clinical course (Trachootham et al., 2009, Ceccarelli et al., 2008, Kaimul et al., 2007). Agents targeting this pathway include PX-12, Dimensa, motexafin gadolinium and arsenic trioxide (Montero and Jassem, 2011, Gupta et al., 2012, Trachootham et al., 2009). PX-12 irreversibly inhibits thioredoxin type I. It has been used in clinical trials (phase II) against advanced pancreatic cancer; its effect on progression-free survival, however, was evidently inferior to standard second line chemotherapy agents (Kona et al., 2011, Baker et al., 2013). Auranofin, a gold complex agent traditionally used in rheumatoid arthritis, is also able to act as a thioredoxin reductase inhibitor. It has displayed cytotoxicity against a number of cell lines *in vitro* (e.g. melanoma, leukemia, lung cancer) as well as lung cancer *in vivo* (Cox et al., 2008, Gandin et al., 2010, Park and Kim, 2005, Talbot et al., 2008). Dimensa is a novel disulphide drug which inhibits thioredoxin reductase and glutathione reductase. It has demonstrated clinical efficacy at prolonging progression-free and overall survival in patients with metastatic non-small cell lung carcinoma in phase II and III clinical trials (Montero and Jassem, 2011). Motexafin gadolinium inhibits thioredoxin reductase and transfers electrons from antioxidant molecules (NADPH, glutathione, ascorbate) to oxygen. A phase III clinical trial of motexafin in combination with radiotherapy in non-small cell lung cancer patients with brain metastases showed promising results (Mehta et al., 2009). Finally, arsenic trioxide (As_2O_3) is a cytotoxic agent which can induce major redox perturbations through superoxide

generation, thioredoxin reductase inhibition and interference with mitochondrial respiration (Jing et al., 1999, Maeda et al., 2004, Niu et al., 1999, Shen et al., 1997, Pelicano et al., 2003, Lu et al., 2007). As_2O_3 efficacy against promyelocytic leukaemia has been demonstrated in a number of *in vitro* studies, as well as phase III clinical trials (Lo-Coco et al., 2013). *In vitro*, it has also been used successful against other types of CLL and ALL, as well as in neuronal, liver and lung cancer cell lines (Gupta et al., 2012).

Superoxide dismutase (SOD). SOD catalyses the conversion of superoxide to hydrogen peroxide, which can then be detoxified to water by the various antioxidant pathways (glutathione, peroxiredoxin, catalase). SOD inhibitors used in clinical trials include ATN-224 and 2-methoxyestradiol. ATN-224 has displayed modest efficacy against recurrent prostate cancer in phase II clinical trials (Lin et al., 2013). 2-methoxyestradiol (2-ME) showed some anti-tumour effect against metastatic carcinoid tumours in combination with procarbazine in phase II clinical trials; conversely, it failed to show clinical efficacy against metastatic renal cell carcinoma and recurrent prostate cancer (James et al., 2007, Sweeney et al., 2005).

Another intriguing strategy which has been tentatively explored in recent years involves combination of two redox 'hits' to limit the possibility of successful metabolic adaptation, especially in highly resistant tumour types. A classic example of this approach is the use of ascorbic acid -resulting in glutathione depletion- to enhance arsenic trioxide cytotoxicity in refractory multiple myeloma (Bahlis et al., 2002). *In vitro*, introduction of arsenic trioxide alongside 2-ME reversed leukemia cell resistance to 2-ME (Zhou et al., 2003). Similarly, the combination of BSO with auranofin (thioredoxin reductase inhibitor) resulted in impressive synergy against glioblastoma cells (Sobhakumari et al., 2012). An obvious concern with such

approaches is the potential side effects of combined redox manipulation; future clinical data will be required before this question can be convincingly answered.

1.3.8.2 Radiotherapy

Radiotherapy is used in oncology to suppress proliferation and induce apoptotic death of malignant cells. A number of *in vitro* and *in vivo* studies in various cancer types (breast, lung, prostate cancer) have indicated that part of this cytotoxic effect is due to oxidative stress induction by radiotherapy (Di Pietro et al., 2006, Gordan et al., 2007, Shil et al., 2005, Gupta et al., 2012). Findings from clinical studies have also been in support of this concept (Bhosle et al., 2002, Gupta et al., 2010, Jones et al., 2011). On these grounds, employing drugs that generate ROS or interfere with antioxidant pathways may be an attractive ancillary strategy to enhance radiotherapy sensitivity. This concept has been successfully applied in a range of tumours in recent studies (Gupta et al., 2012).

1.4 Summary, hypotheses and project objectives

1.4.1 *In vitro* work to evaluate NNT as a novel therapeutic target in ACC

ACC is a rare but aggressive malignancy, with the majority of patients presenting with, or eventually developing, metastatic disease (Libe, 2015, Else et al., 2014, Fassnacht and Allolio, 2011). No current medical treatments are particularly efficient at controlling disease progression. A recent randomised-controlled trial revealed a dismal median survival of < 15 months for patients with disseminated disease receiving combination chemotherapy,

underscoring the urgent need to develop more effective management strategies (Fassnacht et al., 2012). Unfortunately, the rapid progress in our understanding of the genetic make-up and molecular biology of ACC in the last two decades has so far failed to enrich the meagre pharmacological armamentarium of attending clinicians (Libe, 2015).

Recent studies revealed that inactivating mutations of genes encoding mitochondrial antioxidant enzymes *(NNT, TXNRD2)* cause a rare, hereditary form of primary adrenal insufficiency (Familial Glucocorticoid Deficiency), interestingly manifesting in isolation without involvement of other target organs (Meimaridou et al., 2012, Prasad et al., 2014a). These findings suggest a selective susceptibility of the adrenal glands to oxidative stress. It is still unclear whether the adrenal insufficiency of these patients results from oxidative stress-induced adrenocortical cell death, functional inhibition of steroidogenesis or a combination thereof. Oxidative stress also represents a known area of metabolic vulnerability in cancer cell biology. Malignant cells have constitutively higher levels of oxidative stress than healthy cells; antioxidant pathway targeting has been employed successfully as a treatment strategy in a number of *in vitro* and *in vivo* studies in various cancer types, but never in ACC (Gupta et al., 2012, Trachootham et al., 2009). The objective of such approaches is to increase intracellular oxidative stress, leading to oxidative cell toxicity and, eventually, triggering cell death.

Within this context, the first aim of this project is to explore the value of antioxidant targeting as a therapeutic approach in ACC, focusing on NNT as a putative treatment target. Therapeutic merit may be afforded either by inhibition of cell proliferation or suppression of steroidogenesis. My specific hypotheses are outlined below:

Hypothesis 1: NNT silencing in ACC cells will induce deleterious oxidative stress, resulting in cell death and/or impaired cellular proliferation (Fig. 1-21).

I will explore this hypothesis *in vitro* using NCI-H295R ACC cells, the only existing human immortalised ACC cell line, with the following approaches juxtaposing different temporal frames:

a) I will *acutely* inhibit NNT expression [transient NNT knockdown by small interfering RNA (siRNA) transfection] and evaluate the immediate effects of this manipulation on cellular redox balance, mitochondrial respiration, cell proliferation and apoptotic rates.

b) I will *chronically* inhibit NNT expression [stable NNT knockdown by short hairpin RNA (shRNA) transfection] and evaluate the longer-term effects of this manipulation on the same outputs.

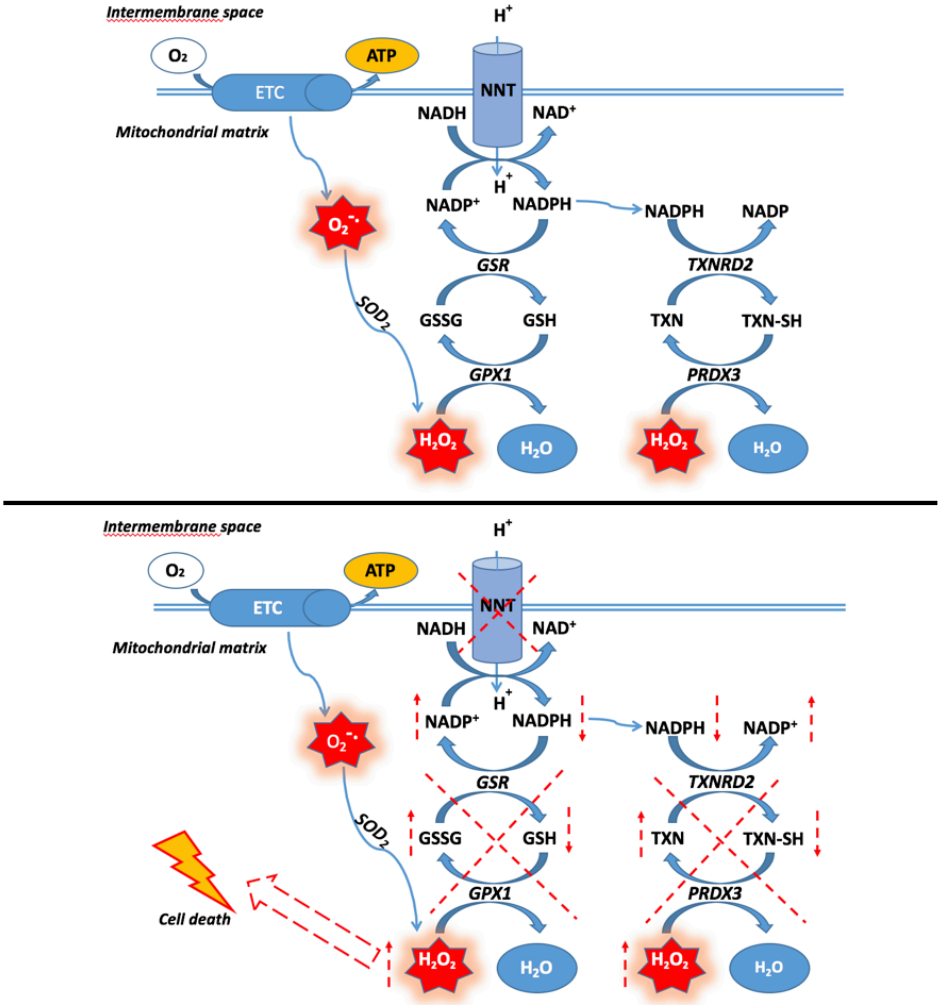

Figure 1-22 A) NNT as a mitochondrial NADPH generator feeding the antioxidant pathways B) Hypothesis 1: NNT inhibition is expected to compromise the mitochondrial pool of NADPH, disrupting the function of the mitochondrial antioxidant pathways. The consequent accumulation of H_2O_2 will increase oxidative stress and eventually trigger cellular apoptosis. ETC: electron transfer chain; ATP: adenosine triphosphate; GSR: glutathione reductase; GSSG: oxidised glutathione; GSH: reduced glutathione; GPX1: Glutathione peroxidase 1; TXNRD2: thioredoxin reductase 2; TXN: oxidised thioredoxin; TXN-SH: reduced thioredoxin; GPX3: peroxiredoxin 3; $O_2^{\cdot-}$: superoxide; H_2O_2: hydrogen peroxide

Hypothesis 2: NNT silencing in ACC cells will inhibit steroidogenesis

I propose to explore this hypothesis *in vitro* using NCI-H295R ACC cells, which have long been established as the main cell model of human adrenal steroidogenesis, using the following approaches:

a) I will *acutely* inhibit NNT expression (transient NNT KD by siRNA transfection) and evaluate the immediate impact of this manipulation on steroidogenesis through a combination of gene expression analysis (real-time PCR) and comprehensive steroid profiling in cell media by liquid chromatography/ tandem mass spectrometry (LC-MS/MS).

b) I will *chronically* inhibit NNT expression (stable NNT KD by shRNA transfection – duration: weeks/months) and evaluate the longer-term effects of this manipulation on steroidogenesis by gene expression analysis and steroid profiling (**Fig. 1-22**).

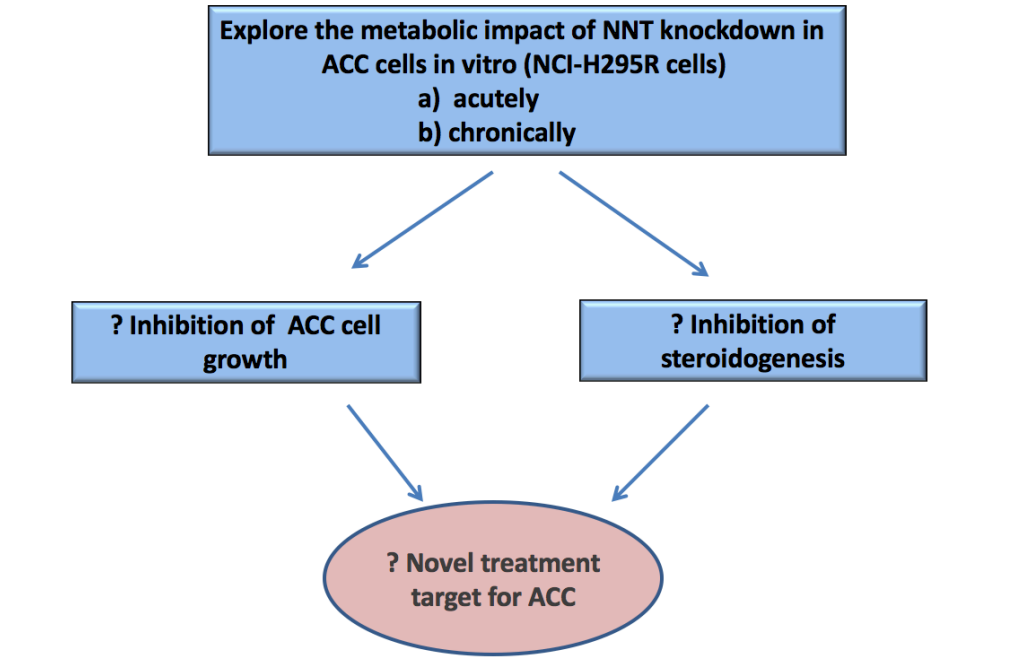

Figure 1-23 Overview of in vitro project objectives

1.4.2 Clinical study to provide proof-of-concept for the use of urine steroid metabolomics in detecting ACC recurrence

Adrenocortical carcinoma is a rare (incidence 1-2 cases/ million/ year) but aggressive malignancy. Disease recurrence rates are high, exceeding 50% even in patients with microscopically complete (R0) resection, necessitating close follow-up in all cases for several years (Libe, 2015, Else et al., 2014). Cross-sectional imaging remains the mainstay of the surveillance strategy, but has important disadvantages including cost, prolonged radiation exposure and frequent diagnostic ambiguity in early stages of recurrent/ metastatic disease (Cawood et al., 2009). Early detection of disease recurrence is important, as it may allow either radical re-do surgery in cases of limited metastatic disease volume, or early institution of mitotane and/or cytotoxic chemotherapy, potentially prolonging survival (Libe, 2015, Else et al., 2014, Erdogan et al., 2013, Datrice et al., 2012, Mihai, 2015, Schulick and Brennan, 1999).

Most ACCs are biochemically active, but tend to present an immature steroidogenic pattern characterized by abundance of steroid precursor metabolites (Arlt et al., 2011). This pattern appears to be a distinguishing feature of ACC that can be diagnostically relevant. Urine steroid profiling by gas chromatography-mass spectrometry (GC-MS) in conjunction with sophisticated machine learning analysis (steroid metabolomics) has recently been introduced as a sensitive and specific biomarker tool for the original diagnosis of primary ACCs in a large retrospective study (Arlt et al., 2011). Building on these promising results, I intend to explore the value of this approach as a surveillance tool to detect disease recurrence in patients who have undergone complete ACC resection.

Hypothesis 3: Urine steroid metabolomics can be employed diagnostically to detect disease recurrence in patients who have undergone complete ACC resection.

To test this hypothesis, we collected longitudinal 24-h urine samples from ACC patients having undergone complete (R0) resection of their tumour and used gas chromatography/ mass spectrometry to derive comprehensive steroid profiles. Collaboration with several major adrenal centres in Europe facilitated the accretion of a sizeable cohort of operated ACC patients. I will evaluate the diagnostic performance of machine learning analysis of these profiles at detecting disease recurrence by the time of its first radiological manifestation.

2 General Methods

2.1 Description of adrenocortical carcinoma cell line (NCI-H295R) and cell line validation

NCI-H295R adrenocortical carcinoma cells were provided as a gift by Professor Enzo Lali (University of Nice, France). This cell line was initially established in late 1980s from a female patient with ACC, which later metastasised (Gazdar et al, 1990). The parental cell line (NCI-H295) represented a mixed cell population from the original tumour; to circumvent the problem presented by the slow growth of these cells, a sub-population of cells able to grow in a monolayer was selected over a period of 3 months during which cells were repeatedly flushed with growth medium. The new cell line (NCI-H295R) expresses all major human steroidogenic enzymes, including CYP11A1, CYP11B1, CYP17A1, CYP21A2, CYP11B2 and HSD3B2, and secretes all 3 classes of adrenocortical steroid hormones (glucocorticoids, mineralocorticoids and androgens) (Wang and Rainey, 2012, Xing et al., 2011). NCI-H295R cells respond well to angiotensin II and K^+ as inducers of mineralocorticoid synthesis but are minimally responsive to ACTH. This problem can be overcome by use of either forskolin (adenyl cyclase activator) or $_C$AMP analogues. NCI-H295R cells were cultured under standard conditions using Dulbecco's Modified Eagle's Medium (DMEM)/Ham's F-12 medium (Gibco, Thermo Fisher) supplemented with 2.5% Nu serum (Sigma), 1% penicillin-streptomycin (Gibco, Thermo Fisher) and 1% ITS+ universal cell culture premix (BD Biosciences). ITS+ is a proliferation-promoting supplement containing human insulin, human transferrin, selenous acid, BSA and linoleic acid. Media was refreshed twice weekly. Cells were grown in 25cm^2 or 75 cm^2 cell culture flasks (Corning) and split to new flasks when they reached 70-80% confluence. Splitting involved washing with Phosphate-Buffered Saline (Sigma) followed by addition of 2 ml trypsin (Thermo Fisher) and incubation at 37^{o}C for 2 min. Trypsin was inactivated by addition of cell media; cells were centrifuged at 12,000 rpm

for 5 min. The resulting pellet was re-suspended in cell media and transferred to new flasks using a 1:3–1:5 ratio. During experimental work described in the succeeding sections, 6-well plates (Corning) and 96-well (Falcon) cell culture plates were also used. All experiments were performed using passage numbers 10-25.

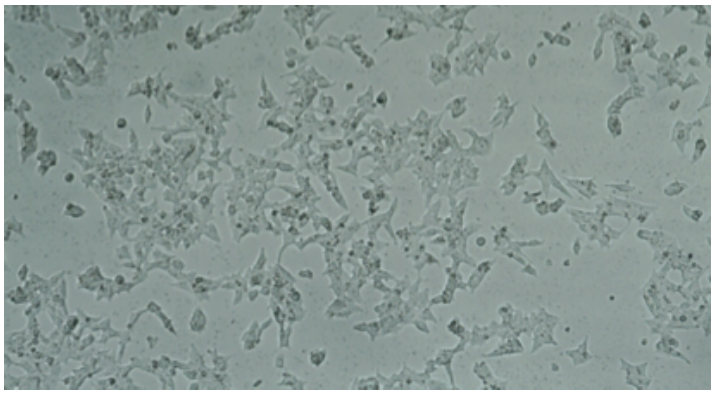

Figure 2-1 Microscopic caption (10x) of NCI-H295R cells growing in a 6-well plate.

Cell line identity was confirmed through Short Tandem Repeat (STR) genetic analysis performed by the DNA Diagnostics Company (London, UK) followed by comparison to genetic profiles provided by the American Tissue Culture Collection (ATCC) (http://www.lgcstandards-atcc.org). STRs are microsatellite DNA areas consisting of series of 2-13 nucleotides repeated several times in a row. Analysis identifies the number of repeats for each STR; combination of multiple STRs generates a profile which is unique for each cell line.

Marker	Allele 1	Allele 2
AMEL	X	
D3S1358	15	16
D1S1656	12	
D2S441	11	
D10S1248	14	
D13S317	13	
Penta E	5	
D16S539	11	
D18S51	17	
D2S1338	25	
CSF1PO	10	12
Penta D	8	
TH01	9.3	
vWA	17	18
D21S11	32.2	
D7S820	9	12
D5S818	12	
TPOX	8	
D8S1179	13	
D12S391	19	20
D19S433	13	
FGA	19.2	24
D22S1045	15	

Figure 2-2. Genetic STR analysis of H295R cells used in this project, including 22 highly polymorphic areas (loci). Number of sequence repeats is indicated for each locus.

2.2 Gene expression

2.2.1 RNA extraction

RNA extraction was performed using the RNeasy mini kit (Qiagen) following the manufacturer's instructions. The kit uses a silica-based membrane and a high-salt buffer system which allows purification of RNA molecules comprising > 200 nucleotides from cell lysates. Cells were grown in 6-well plates at loading concentrations of 300,000 – 500,000 cells/ well, and cultured for 1-9 days prior to RNA extraction. At the selected time-points, cells were washed with Phosphate Buffered Saline and detached by tapping after incubation with 500 µl trypsin for 2 minutes at 37^{o}C. Trypsin was inactivated by addition of quadruple volumes of serum-replete culture media and cells were pelleted with 5-10 min centrifugation

at room temperature (12,000 rpm). Supernatant was removed and pelleted cells were disrupted by mixing with 350 µl RLT buffer, supplemented with 1% β-mercaptoethanol (Sigma-Aldrich). Cells were homogenised using a sterile, 21-gauge needle (10 aspirations per sample) and then diluted with 350 µl of 70% ethanol in de-ionised H_2O to promote selective binding of RNA to the RNeasy membrane. Samples were transferred to spin columns and centrifuged at 15,000 rpm for 15 seconds. Subsequently, 700 µl RW1 buffer was added to each column and samples were centrifuged at 15,000 rpm for 15 seconds. 500 µl of RPE buffer was next loaded to each column, followed by centrifugation at 15,000 rpm for 15 seconds and, after reloading 500 µl RPE, for 2 min. The follow-through was decanted after each centrifugation. To minimise ethanol carry-over, spin columns were then transferred to new microtubes and centrifuged for an additional minute. Finally, 30 µl of RNase-free water was added to each column and centrifuged at 15,000 rpm for 1 minute. The follow-through solutions, containing all eluted RNA, were collected in 1.5 ml Eppendorf tubes and stored at -20^{o}C, or -80^{o}C for prolonged storage. RNA concentration was determined by spectrophotometry (Labtech Nanodrop Spectrophotometer ND-1000), by addition of 1.5 µl of each RNA sample. A 260/280 nm absorbance ratio of at least 2 was considered suggestive of satisfactory RNA purity.

2.2.2 Reverse transcription

Reverse transcription to generate complementary DNA ($_C$DNA) was carried out using the TetrocDNA Synthesis Kit (Bioline), following the manufacturer's instructions. 200ng - 2µg $_C$DNA (volume up to 12 µl) were added to 8 µl of a reaction mix, consisting of 1µl reverse transcriptase, 1µl oligo(dT)18 primer, 1 µl dNTP mix, 1 µl Ribosafe RNAse inhibitor and 4 µl

Reverse Transcription Buffer. Total volume was complemented to 20 µl by addition of nuclease-free water if required. Reactions were incubated at 45°C for 30 min, followed by heat-blocking at 85°C for 5 min to terminate. All handling of RNA and cDNA samples was performed on ice, to avoid nucleic acid degradation.

2.2.3 cDNA concentration measurement

cDNA concentration was measured using a fluorescent DNA dye (Picogreen assay®, Invitrogen). The assay is based on a fluorescent DNA dye (Quant-iT™ PicoGreen® dsDNA reagent) which allows accurate estimation of cDNA concentration by comparison of sample fluorescence to the fluorescence exhibited by a dilution series of DNA samples with known concentrations (standard curve). Samples to be measured were loaded to a flat-bottomed 96-well plate with transparent wells (Corning) at a volume of 1 µl/ well, and diluted in 99 µl of buffering solution (1xTE). A standard curve was prepared by serial dilutions of a stock cDNA solution (2 mcg/ml) in 1x TE buffer, to end-concentrations of 0, 10, 100 and 1,000 ng/ml. The fluorescent DNA dye was diluted 200x in TE and added to all wells at a volume of 100 µl/ well. After 5 min incubation at room temperature, fluorescence was measured (excitation 480 nm, emission 520 nm) (Wallac Victor 1420 multilabel counter) and cDNA concentrations were determined based on fluorescence readings, using an equation derived from the standard curve. Results were multiplied by 200 to derive the cDNA concentration in the samples of interest.

2.2.4 Real-time PCR

Gene expression (NNT and steroidogenic enzymes) was quantified by Real-Time polymerase chain reaction (qPCR), using Taqman^{TM} Gene Expression Assays (Thermo Fisher). With Real-Time PCR, the DNA template of interest is subjected to consecutive cycles of replication by use of sequence-specific primers, with synchronous measurement of the end-product at the end of each cycle by fluorescence. The higher the concentration of the specific sequence (template) in the original sample, the earlier the cycle in which fluorescence first becomes detectable. With this principle, serial measurements of template fluorescence during the exponential replication phase allow reliable estimation of DNA concentration in the original sample.

Each replication cycle consists of 3 steps:

- Denaturation. During this step, high temperature is applied (typically 95^{o}C) to 'melt' double-stranded DNA to single-stranded DNA.
- Annealing. This step allows the primers to hybridize with their complementary sequences within the single strands of DNA. The temperature in this stage must be lower than the melting temperature of the primers.
- Extension. At this stage DNA polymerase extends the primers, leading to replication of the sequence/ gene of interest. Typical temperatures at this stage range from 60-72^{o}C. In this project, annealing and extension stages were combined to a 1 min incubation at 60^{o}C per cycle.

With TaqMan technology, fluorescence emission is accomplished by use of specially designed probes. Each probe is complementary to a sequence within the gene of interest, where it promptly binds during annealing, downstream of the primer. The 5' end of the probe

has an attached 'reporter' fluorescent dye, while the 3' end has a 'quencher' dye of different wavelength, which quenches the reporter fluorescence. During replication cycles, DNA polymerase cleaves the probes that are attached to the DNA template releasing the reporter, whose fluorescence can now be emitted. The earliest cycle in which emitted fluorescence exceeds the threshold of 'significant' detection is termed Ct, and is inversely related to the original template concentration in the sample of interest. Gene expression is normalised to a housekeeping gene, i.e. a gene which is constitutively expressed in high levels in all human tissues.

All reactions were carried out at a total volume of 12 µl, comprising:

- 1-4 µl of cDNA (10-100 ng)
- 8-11 µl of a reagent mix consisting of 2xTaqman Universal PCR Master mix (Thermo-Fisher), probe-primer mix for gene of interest and housekeeping gene RPLPO (Thermo-Fisher) and nuclease-free water, using the following ratio: 6.25 µl Taqman Master Mix: 0.625 µl probes: 4 µl nuclease-free water.

10-50 ng of cDNA were used per reaction, with the proviso that loading cDNA mass in all wells should be equal within each plate. Reactions were run in a 7500 ABI qPCR analyser [50^{o}C incubation for 2 minutes, 95^{o}C incubation for 10 minutes, followed by 40 cycles of 95^{o}C incubation for 15 seconds (denaturation) then 60^{o}C for 1 minute (annealing-extension)]. All reactions were normalised against the housekeeping gene RPLPO (large ribosomal protein). Data were expressed as the cycle number at which logarithmic PCR plots cross a calculated threshold line (Ct values) and used to determine ΔCt values [ΔCt= (Ct of the target gene) – (Ct of the housekeeping gene)]. To compare gene expression between a sample of interest and a control sample, ΔΔCt values were used, defined as ΔΔCt= ΔCt (sample) – ΔCt

(control). Results were also expressed as fold change in gene expression to control, derived using the equation fold change = $2^{-\Delta Ct}$.

2.3 Protein expression

2.3.1 Protein lysate generation

Protein lysates were generated applying RIPA buffer (Sigma) with protease inhibitor cocktail (Sigma) to adherent cells grown in 6-well plates (30 µl of protease inhibitor cocktail per 1ml RIPA Buffer; 150 µl RIPA per well). Wells were washed with PBS before RIPA addition. Plates with RIPA were incubated on ice for 5 min. Cells were then detached by scraping and stores at -80^{o}C for at least 1 h. Samples were subsequently thawed on ice and centrifuged for 10 minutes at 8,000 g (4^{o}C), followed by collection of the supernatant. Lysates were stored at -80^{o}C.

2.3.2 Protein concentration measurement

Total protein concentration was determined colorimetrically using the BCA Protein Assay Kit (Thermo Fisher) as per the manufacturer's instructions. The reaction on which the assay is based involves protein-mediated reduction of Cu^{2+} to Cu^{+} in an alkaline environment; bicinchoninic acid (BCA) then reacts with Cu^{+} to generate an end-product that can be detected colorimetrically, generating strong absorbance at 562 nm. 4 µl of each protein sample were loaded to flat-bottomed, transparent-walled 96-well plates. A standard curve was prepared using serial dilutions of a stock protein solution to generate concentrations of 0 – 2,000 µg/ml.

BCA reagent B was added to reagent A using a 1:50 ratio, and the mix was added to wells at a volume of 76 µl/ well. After 30 min incubation at 37^{o}C for 30 min, absorbance was measured at 560 nm using a Wallac Victor 1420 multilabel counter.

2.3.3 Western Blotting

Protein expression was assessed using Western Blotting. Western Blotting involves separation of denatured proteins as they travel through a gel across an electric current, followed by detection of the protein of interest by use of protein-specific antibodies.

Sample volumes corresponding to 7.5 - 15 µg of protein were mixed with equal volumes of 1x Laemmli buffer (Bio-rad), containing SDS (sodium dodecyl sulfate) detergent [475 ml 1x Laemmli buffer (Bio-rad) mixed with 25 µl 2-mercaptoethanol (Sigma)]. SDS induces protein denaturation and gives polypeptides a negative charge to facilitate separation; 2-mercaptoethanol is added to reduce intra- and inter- molecular bonds. Samples were loaded to 10% SDS-PAGE (polyacrylamide) Gels (Thermo Fisher) and subjected to electrophoresis at 80 V for 15 min and 140 V for 90 min; this step achieves protein separation along the gel according to molecular weight. A mix of ten multicolour recombinant protein standards (Precision Plus Protein^{TM} Kaleidoscope^{TM} Standards, Bio-Rad) was used as a guide ('ladder') to indicate molecular weight. Proteins were then transferred to a nitrocellulose membrane using the iBLOT^{TM} Dry Transfer System (Thermo Fisher), a method which allows buffer-free transfer within 7 min.

Membranes were washed with Tris-Buffered saline with Tween 20 (TBS-T; recipe: 50 ml Tris-HCL, 20g NaCl, 0.625 ml Tween80, 2447 ml deionized H_2O), followed by overnight

incubation in TBS-T with 5% milk at 4^{o}C overnight to reduce non-specific antibody binding. The next day, after 3 x 5 min washes with TBS-T, membranes were probed for 60 minutes with anti-NNT antibody produced in rabbit (HPA004829, Sigma), and diluted in tris-buffered TBS-T at a 1:500 dilution. After 3x15 min washes with TBS-T, membranes were probed with secondary anti-rabbit antibody, horseradish peroxidase (HPR) and alkaline phosphatase-conjugated (sc-2030, Santa-Cruz), for 60 min (1:2000 dilution in TBS-T). After a further series of TBS-T washes, membranes were imbued with ECL. ECL is a chemiluminescent agent that reacts with HPR, allowing detection of the primary-secondary antibody complexes attached to the membrane. This was accomplished simply by exposing an X-Ray film to the membrane in a cassette protected from light, followed by film developing. Developing times of 20-30 mins were usually required to produce strong bands.

B-actin was used as control protein, to normalise NNT expression to the actual protein load. Primary and secondary antibodies were stripped off by 2x10 min washes in a stripping buffer (15g Glycine, 1g SDS, 2.5 ml Tween80, 1L deionised H_2O), followed by incubation with milk and antibodies as detailed above. Primary antibody for β-actin (produced in mice) was purchased from Sigma and used at a 1:10,000 dilution in TBS-T. Secondary antibody (anti-mouse) was purchased from Santa-Cruz and was used at 1: 20,000 dilution.

Initial Western Blotting attempts were unsuccessful, with no NNT bands despite strong β-actin binding. These attempts involved a boiling step, whereby protein samples in Laemmli buffer were boiled at 95^{o}C for 5 min before loading to the gel, to complete the process of protein denaturation and render the sample easier to load to the gel (less viscous). The problem resolved, and NNT bands started to appear, once this step was omitted from the protocol.

2.4 Redox state

The ratio of reduced to oxidized glutathione was used as a marker of intracellular oxidative stress in this work; the ratio is inversely proportional to oxidative stress (Sun et al., 1997, Rebrin and Sohal, 2008). Reduced glutathione (GSH), oxidized glutathione (GSSG) and total glutathione were measured by luminescence, using the GSH/GSSG-Glo^{TM} Assay (Promega) according to the manufacturer's instructions. The assay takes place in white, opaque-walled 96-well plates (Perkin-Elmer) and generates a luminescent signal which is proportional to the amount of reduced glutathione present in the well. This is achieved by use of a GSH-dependent luciferin probe according to the following series of reactions:

$$\text{GSH + Luciferin-NT} \xrightarrow{\text{Glutathione sulfotransferase}} \text{GSH-NT + Luciferin}$$

$$\text{Luciferin} \xrightarrow{\text{Ultra-Glo rLuciferase + ATP}} \text{Light}$$

These reactions are used to measure total glutathione or oxidised glutathione separately, using two distinct biochemical manipulations after cell lysis (**Fig. 2-3**). To measure total glutathione, oxidised glutathione is first reduced to GSH, so that the end amount of GSH within the well represents the original sum of intracellular GSH and GSSG. To measure GSSG, GSH is blocked with N-ethylmaleidine (NEM), followed by GSSG reduction to GSH. This way, luminescence eventually reflects intracellular GSSG only.

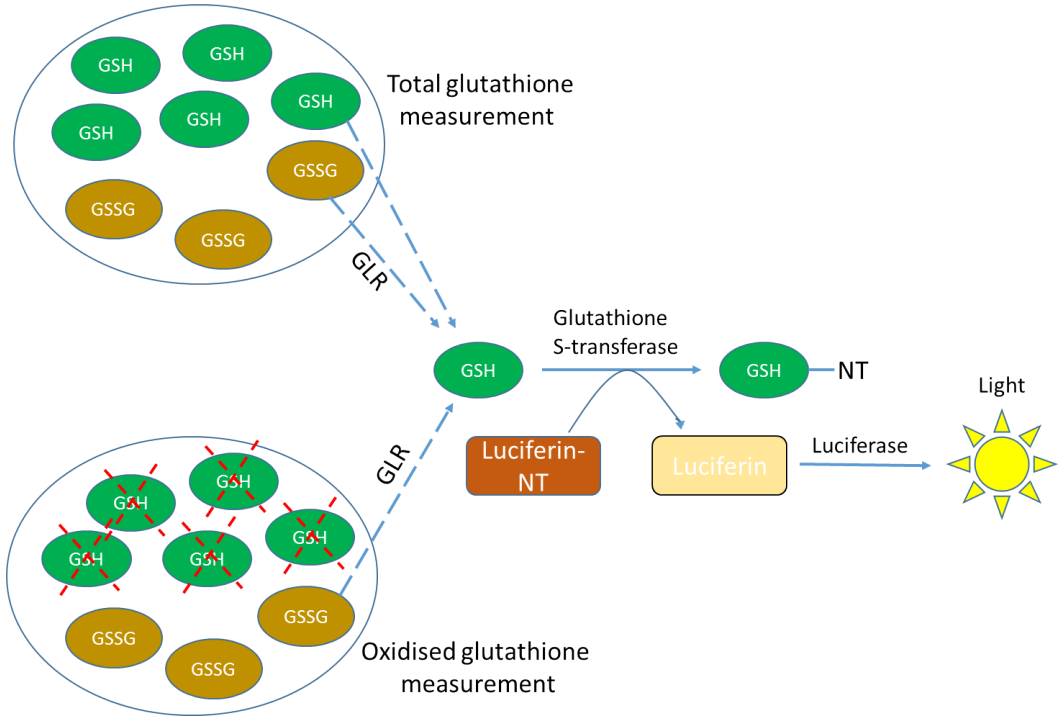

Figure 2-3 The GSH/GSSG-Glo™ assay (Promega). GSH: reduced glutathione; GSSG: oxidized glutathione; GLR: glutathione lysis reagent. Adapted and reproduced with permission of Promega.

Before the assay, NCI-H295R cells were grown in white, opaque-walled 96-well plates. Triplicate samples were assayed for total glutathione or GSSG after medium removal. 2 wells were pre-treated with Menadione (Sigma) 40 µM for 2 hours to induce oxidative stress as positive controls. First, cells were lysed by addition of 50 µl of either Total Glutathione Reagent (1 µl Luciferin-NT + 10 µl Passive Lysis Buffer + 39 µl deionised H_2O) or Oxidised Glutathione Reagent (1 µl Luciferin-NT + 10 µl Passive Lysis Buffer + 0.5 µl NEM + 38.5 µl deionized H_2O). After 5 minutes, an equal volume of Luciferin Generation Reagent was added, consisting of 1.25 µl 100 mm DTT, 3 µl Glutathione-S-Transferase and 45.75 µl Glutathione Reaction Buffer. After 30 min incubation, wells were treated with Luciferin Detection Reagent (100 µl/well) for 15 mins and luminescence was measured in a Wallac

Victor 1420 multilabel counter. Blank measurements (no cells) were subtracted from sample values to produce net results. GSH /GSSG ratios were calculated directly from Net Relative Luminescence Units (RLU) measurements using the equation GSH/GSSG ratio = [Net total glutathione RLU-Net GSSG RLU]/ [Net GSSG RLU/2].

2.5 Metabolic Flux Analysis (Seahorse XF)

Metabolic Flux analysis was employed to assess the effect of NNT knockdown on mitochondrial bioenergetics, using the Seahorse XF 24 Analyser. Seahorse Analysers have the ability to measure changes in oxygen and proton concentration in a minute volume (< 2 µL) of medium above a cell monolayer within a microplate, by use of solid-state sensor probes residing 200 microns above the cell monolayer. Changes in oxygen concentration provide the oxygen consumption rate (OCR), reflective of mitochondrial respiration. Changes in proton concentration (or pH) provide the extracellular acidification rate (ECAR), reflective of the rate of anaerobic glycolysis (glycolysis leads to the production of lactate, which increases extracellular proton concentration). Measurements are taken automatically at intervals of approximately 5-8 minutes until the rate of change is linear; the slope is then calculated and used to determine OCR and ECAR. Once a measurement is completed, the probes lift to allow the larger supernatant medium volume to mix with the medium in the 'transient microchamber', restoring cell values to baseline. Up to four treatment compounds can be added sequentially at regular intervals through an integrated drug delivery system. For this project, the Seahorse XF Cell Mito Stress Test was used to measure a number of key parameters (Basal respiration, ATP-linked respiration, H^+ (Proton) Leak, Maximal Respiration, Spare Respiratory Capacity, and Non-mitochondrial respiration). This is

achieved through serial treatments with the following reagents, each inhibiting a different complex within the mitochondrial electron transfer chain (**Fig. 2-4**):

a) Oligomycin, inhibitor of ATP synthase (complex V). Oligomycin triggers a decline in OCR, as stage 3 oxidative phosphorylation has been blocked. This OCR decline reflects the component of oxygen consumption that is used for ATP production. ECAR increases as cells resort to anaerobic glycolysis, which releases lactic acid.

b) FCCP (Carbonyl cyanide-p-trifluoromethoxyphenylhydrazone), mitochondrial membrane uncoupler. FCCP causes proton leak from the mitochondrial intermembrane space to the mitochondrial matrix, resulting in a collapse of the mitochondrial membrane potential. Under these conditions, oxygen flow through the electron transfer chain is uninhibited and oxygen is maximally consumed by complex IV in an attempt to restore the proton gradient across the inner mitochondrial membrane. The difference between this stimulated OCR and baseline OCR provides the spare respiratory capacity, a measure of cellular ability to cope with increased energy demands. ECAR remains higher than baseline as anaerobic glycolysis is still employed to make up for the diminished aerobic energy production.

c) Mix of rotenone and antimycin A, inhibitors of complex I and III, respectively. This combination generates a total inhibition of mitochondrial respiration. Remaining oxygen consumption reflects non-mitochondrial respiration. ECAR remains high (www.agilent.com).

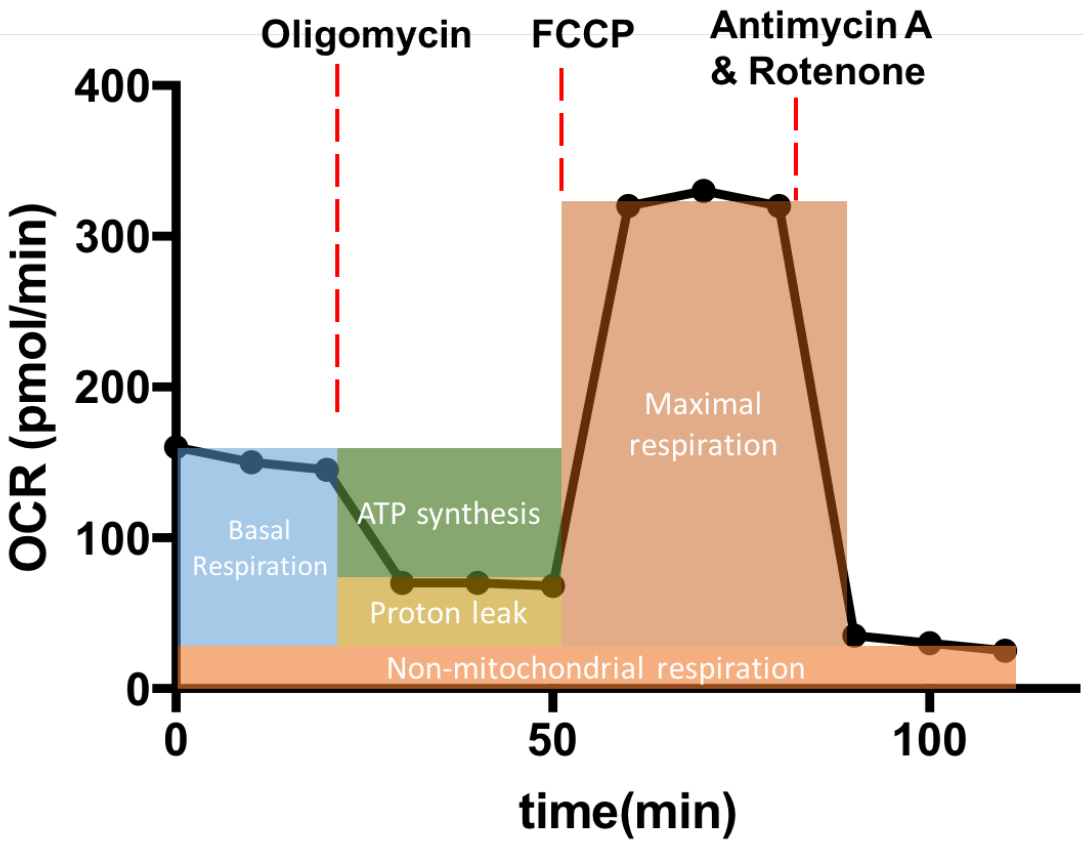

Figure 2-4 The Seahorse XF Cell Mito Stress Test. Serial injections of Oligomycin, FCCP and Antimycin A-Rotenone alter mitochondrial respiration, generating characteristic, measurable changes in oxygen consumption. FCCP: Carbonyl cyanide-p-trifluoromethoxyphenylhydrazone. Source: www.agilent.com. Adapted and reproduced with permission of Agilent.

One day before the planned metabolic flux analysis, NCI-H295R cells were trypsinised and transferred to Seahorse XF-24 plates at a density of 100,000 cells/well. Typical cell culture media volume per well was 100-150 µl. On the day of metabolic flux analysis, media was replaced with a DMEM-based medium supplemented with 25 mM glucose, 2 mM sodium pyruvate, 31 mM NaCl, 2 mM GlutaMax (pH 7.4) and incubated at 37 °C in a non-CO2

incubator for 60 min. Baseline oxygen consumption rate (OCR, measured by oxygen concentration change) and extracellular acidification rate (ECAR, measured by pH change) were measured, followed by serial treatment with the following mitochondrial inhibitors: oligomycin (ATP synthase inhibitor, 2 μM), FCCP (mitochondrial respiration uncoupler, 1 μM), and rotenone and antimycin A (Complex I inhibitor, 1 μM). After the assays, plates were stored at -80 C to be used for protein concentration measurements as surrogate markers of cell density. Results were normalised to protein concentration, measured by the BCA Protein Assay Kit (Thermo-Fisher).

2.6 Cellular Proliferation

Cellular proliferation was assessed after culturing cells in flat-bottomed, transparent-walled 96-well plates, using the CyQUANT® Proliferation Assay Kit (Thermo Fisher) and following the manufacturer's instructions. CyQUANT® uses of a proprietary green fluorescent dye, CyQUANT® GR, which exhibits strong fluorescence enhancement when bound to cellular nucleic acids after cell lysis. The fluorescence emitted by a given well is therefore proportional to the total amount of DNA, which in its turn is proportional to cell number before lysis. The linear detection range is wide (500 – 50,000 cells).

In proliferation time-courses, NCI-H295R cells were grown in transparent, flat-bottomed 96-well plates (Falcon), loaded at a concentration of 8,000 cells/well and cultured in 200 μl of plain culture media or treatment media. At least 5 biological replicates (wells) per group of cells were used in each experiment. Media was refreshed every 48h by removal and addition of 100 μl fresh media. At pre-determined time points, the media was removed and cells were

frozen at -80°C. The beginning of treatment was used as the baseline time point (t=0) at each proliferation series.

On the day of the assay, plates were defrosted in room temperature for 30 min and a mastermix was freshly prepared, containing 19 ml of dH_2O, 1 ml Lysis Buffer and 50 µl CyQUANT® GR fluorescent dye for every 100 wells to be assayed. After vortexing, 180 µl of the mastermix were added to each well. Blank wells were also used to measure background fluorescence. Plates were then run in a Wallac Victor 1420 multilabel counter using 480 nm excitation/ 520 nm emission maxima.

2.7 Cellular apoptosis

Cellular apoptosis was assessed after growing cells in white, opaque-walled 96-well plates, using the Caspase-Glo 3/7™ Assay kit (Promega). The Caspase-Glo 3/7™ assay measures the activity of the effector caspases 3 and 7, which are activated during programmed cell death (apoptosis) through proteolytic cleavage by initiator caspases. Once activated, caspases 3 and 7 swiftly proceed with proteolytic degradation of intracellular proteins, executing programmed cell death (Garcia-Calvo et al., 1999). The assay provides a luminogenic substance with a tetrapeptide sequence which is cleaved by caspases, releasing a substrate for luciferase. Therefore, emitted luminescence is proportional to caspase activity in the corresponding well.

To perform this assay, cells were grown in white, opaque-walled, flat-bottomed 96-well plates (Perkin-Elmer) in 200 µl of growth media. At least 10 biological replicates were used per group of cells. At the assaying time-point, 4 wells/ group were randomly chosen to measure

caspase activity. 100 µl media were removed and replaced by 100 µl of a solution of the luminogenic Caspase-Glo 3/7 substrate in Caspase-Glo 3/7 buffer (Caspase-Glo 3/7 Reagent). The buffer facilitates cell lysis and also contains a thermostable luciferase. Plates were incubated at room temperature for 50 min after shaking briefly, protected from light. This period allows cell lysis to occur, followed by caspase 3 and 7-mediated cleavage and release of the luminogenic substrate. Luminescence was measured in a Wallac Victor 1420 multilabel counter. A blank well containing cell media and Caspase-Glo 3/7 Reagent only was also included, its luminescence deducted from sample measurements to produce net luminescence values.

At the end of the assay, media and reagents were removed from all wells and stored at -80^{o}C. The next day, relative quantification of cell number in the remaining wells (i.e. wells not used for caspase activity measurement) was performed by use of the CyQuant® Proliferation Assay Kit (Thermo Fisher), as described above. Luminescence values obtained in the apoptosis assay were normalised to the fluorescence results of the proliferation assay.

During the course of this work, the above protocol was modified to allow culture of cells in transparent-walled plates, which allow microscopic evaluation of cell growth and are more suitable for fluorescence measurement. With the new protocol, cells were loaded and cultured in transparent-walled 96-well plates, using at least 10 biological replicates/ plate. On the day of the assay, the luminogenic solution was added to 4 wells/ group (100 µl of the solution replacing 100 µl of cell media) and, after 5 min of gentle shaking, solution and media were transferred to a white, opaque-walled plate. Caspase activity was measured as described above. The transparent-walled plate was frozen at -80^{o}C and subsequently used for cell number quantification with the CyQuant® Proliferation Assay Kit.

2.8 In vitro steroid profiling by liquid chromatography and tandem mass spectrometry (LC-MS/MS)

The impact of NNT loss on the hormonal output of ACC cells was delineated by use of comprehensive steroid profiling in cell media by LC-MS/MS. LC-MS/MS is a powerful analytical tool which combines the ability of liquid chromatography to separate substances in a sample according to their chemical properties with the capacity of mass spectrometry for separation according to mass. With modern liquid chromatography (also called high-performance LC – HPLC), the sample is carried through a column by a liquid (mobile phase). The column is equipped with a lining ('stationary phase') which binds the various molecules within the sample (analytes) with a strength that depends on the molecule polarity. The polarity of the mobile phase then increases progressively, leading to sequential elution of the analyte detachment at different times (retention times) according to their polarity (Taylor et al., 2015).

Having been separated according to their polarity, analytes enter the mass spectrometry analysers. In LC-MS/MS, two sequential MS analysers are employed to enhance overall specificity. Entering the first MS analyser, sample analytes are ionised and travel through a quadrupole at times that are determined by their mass-to-charge ratio. In the second analyser, molecules undergo fragmentation into smaller particles in a special collision cell; generated ionised fragments are then selected according to their mass-to-charge ratio with a second quadrupole. This results in highly specific detection, as the various analytes beget unique fragmented ions, leaving their very specific analytical fingerprint (Taylor et al., 2015).

Modern mass spectrometry-based techniques (be it LC-MS/MS or GC-MS) have been established as the most sensitive and specific method of steroid hormone analysis, outperforming the traditional immunoassays with their significant analytical lacunae (cross-

reactivity between similar analytes, low sensitivity, poor inter-lab standardisation) (Taylor et al., 2015). LC-MS/MS has distinct advantages over GC-MS as a high-throughput analytical test, by virtue of its short running times and relatively low cost.

To explore steroidogenesis in our *in vitro* cell model, NCI-H295R cells were incubated in 6-well plates in 1 ml of serum-free DMEM/Ham's F-12 medium (Gibco, Thermo Fisher), supplemented with 1% penicillin-streptomycin and 1% ITS universal cell culture premix. Serum-free media was used as serum itself contains steroids which may confound results. Media was collected after 48 h incubation (120 hours post transfection) to silinised glass tubes and stored at -20^{o}C.

To extract steroid hormones from cell media, 20 µl of serum steroid internal standard solution was transferred to each tube and vortexed briefly, followed by addition of 3 ml Methyl tert-butyl ether (MTBE, Sigma). After vigorous vortexing, samples were frozen at -20^{o}C for at least 1 hour. The top layer (liquid phase) was transferred to a 96-well plate using Pasteur pipettes. MTBE was evaporated to dryness at 55^{o}C and samples were reconstituted in 125 µl of 1:1 H_2O/methanol. Steroid metabolite identification and quantification was performed by liquid chromatography/tandem mass spectrometry (LC/MS/MS), with reference to a linear calibration series and appropriate internal standards (AcquityTM Ultra Performance Liquid Chromatographer, Xevo TQ Mass Spectrometer) as described previously (Juhlen et al., 2015, Haring et al., 2013) (Table 2-1).

Table 2-1 Calibration series used to quantify steroid metabolites in cell media samples by LC-MS/MS

Calibration number	Added volume of serum steroid stock (1µg/ml)	Added volume of cell media (µl)	Concentration (ng/ml)
C0	0	1000	0
C1	0.5	999.5	0.5
C2	1	999	1
C3	5	995	5
C4	10	990	10
C5	25	975	25
C6	50	950	50
C7	100	900	100
C8	250	750	250
C9	500	500	500

2.9 Statistical analysis

Statistical analysis and schematic depiction of data was completed using GraphPad Prism Software. Data are represented as mean ± standard error (mean ± SEM) values, unless otherwise stated. Data that are not normally distributed are presented as median ± interquartile range (IQR). Two-group comparisons were made using Student's paired t-test for normally distributed data or Wilcoxon's signed-rank test for data not following a Gaussian distribution. Multiple comparisons (paraquat, BSO and auranofin treatment courses) were performed by one-way ANOVA followed by post-hoc multiple comparison testing (Turkey's test).

3 Effects of transient NNT knockdown on ACC cell metabolism, proliferation and steroidogenesis

3.1 Introduction

NNT is a proton pump of the inner mitochondrial membrane that transfers reducing equivalents from NADH to $NADP^+$, fuelling the main mitochondrial antioxidant pathways as well as anabolic cellular metabolism (Rydstrom, 2006, Leung et al., 2015). NNT inactivation in a number of *in vitro* cell models has been associated with a multifaceted metabolic impact, including induction of oxidative stress, disruption of mitochondrial respiration and inhibition of glutamine utilisation in the TCA cycle (Arkblad et al., 2005, Meimaridou et al., 2012, Ripoll et al., 2012, Lopert and Patel, 2014, Yin et al., 2012, Gameiro et al., 2013). Limited pre-clinical data suggest an adverse effect of NNT inactivation on the proliferation and viability of certain malignant cell lines (apoptosis in PC12 rat phaeochromocytoma cells *in vitro*, suppression of melanoma xenografts in rodents), presumably due to the deleterious effects of high oxidative stress (Yin et al., 2012, Gameiro et al., 2013). Recent human genetic studies underscored the importance of NNT in adrenal (patho)physiology, demonstrating that NNT mutations underlie a rare hereditary form of primary adrenal insufficiency (Familial Glucocorticoid Deficiency) (Meimaridou et al., 2012, Roucher-Boulez et al., 2016). In keeping with this, 2-month-old *Nnt* mutant mice have low circulating levels of corticosterone; on histology, their adrenal glands displayed disorganised zonae fasciculatae with high levels of apoptosis (Meimaridou et al., 2012). The clinical phenotype of patients with inactivating NNT mutations is remarkably specific: the adrenals glands are the only affected organs in the majority of described cases, suggesting a particular vulnerability of adrenal cells to NNT loss. The roots of this vulnerability may be putatively traced down to the high metabolic activity of the adrenal cortex and its steroidogenic commitment, both incurring a high oxidative toll on the adrenal mitochondria (Hanukoglu, 2006, Prasad et al., 2014b). On this background,

NNT emerges as an attractive treatment target in the clinical condition in which adrenocortical cell damage is most desirable therapeutically, i.e. ACC.

Antioxidant enzyme targeting with a view to curtailing the capacity of malignant cells to deal with their high endogenous ROS levels is not new under the sun in the world of Experimental Oncology. Promising results have been delivered in preclinical models and a limited number of clinical studies (Gupta et al., 2012, Watson, 2013, Fruehauf and Meyskens, 2007, Trachootham et al., 2009). NNT has not been explored as a oncologic treatment target so far, with the only exception of recent pre-clinical studies on malignant melanoma where a detrimental effect of NNT inhibition was demonstrable both *in vitro and in vivo* (Gameiro et al., 2013).

3.2 Methods

3.2.1 Research strategy

In this Chapter, we will explore the acute effects of NNT silencing on ACC redox balance and mitochondrial bioenergetics, and try to ascertain whether these may have a detrimental impact on ACC tumour growth (increased cell death and/or suppressed proliferation) and steroid biosynthesis. Transient NNT silencing will be achieved through anti-NNT siRNA transfection of NCI-H295R ACC cells, using Viromers as transfection vehicles. Viromers are synthetic polymers emulating the structure of the influenza virus haemaglutinin, which can bind siRNA molecules forming complexes that are naturally taken up by cells through endocytosis. This way, they facilitate the introduction of the siRNA molecules directly into cells without compromising cell function and viability. SiRNA molecules break down the mRNA of their target gene, leading to temporary gene expression silencing (gene knock-down) for a period which typically lasts a few days. Having transiently knocked down NNT in NCI-H295 cells, we will explore the immediate ramifications of NNT loss with respect to

a) Cellular redox balance, as reflected on the ratio of reduced to oxidised glutathione
b) Mitochondrial bioenergetics, focusing on mitochondrial oxygen consumption rates and glycolytic rates (extracellular flux analysis – Seahorse XF)
c) Cellular proliferation, using longitudinal assessment of cell numbers under routine cell culture conditions as well as under metabolic stressors (oxidative stress, glucose deprivation)
d) Cellular apoptosis, measuring caspase 3 and 7 activity
e) Steroidogenesis, through a combination of Real-Time PCR and steroid profiling by LC-MS/MS

All experiments were paired, NNT knockdown cells being plated and treated alongside their controls, to mitigate the confounding effects of inter-experiment variability and enhance the power of statistical analysis.

3.2.2 SiRNA transfection

Transient NNT gene silencing was achieved with introduction of small interfering RNA (siRNA) molecules into NCI-H295R cells. SiRNAs are short (20-25 base pairs), double-stranded RNA molecules which are able to effect post-transcriptional silencing of their target gene through a process known as RNA interference (Agrawal et al., 2003). Once introduced into the cell, the two strands of each molecule are separated after binding of a protein complex called RNA-induced silencing complex (RISC). Following this, RISC is guided by the siRNA to its complementary sequence within the target mRNA; if base pairing is precise, RISC degrades the mRNA, leading to silencing of the corresponding gene. This effect lasts until the siRNA molecules become themselves degraded, typically a few days. RNA inhibition by siRNA transfection is a cost-effective way of inhibiting gene function *in vitro*, with the limitation that the effect is short-lived and may not necessarily recapitulate the long-term sequelae of the particular gene loss. A second caveat is that inadvertent silencing of other genes with partially complementary sequences may also occur, especially with high transfection concentrations (Jackson and Linsley, 2010). This phenomenon is widely known as 'off target effects' and suggests that the biological effect seen with a given siRNA may not be caused by the target gene of interest. This risk can be mitigated through independent application of two different siRNAs targeting different areas of the gene of interest.

Viromers (Viromer Blue®, Lipocalyx, Germany) were used as transfection vehicles. Viromers are polymeric molecules which bind siRNAs and introduce them into cells deploying a viral fusion mechanism akin to the one used by the influenza virus (https://viromer-transfection.com). The siRNA-viromer complex is taken up by cells through endocytosis. The acidic environment of the endosomes triggers a structural change whereby the fusion peptide loses its charge, becomes hydrophobic and penetrates the endosomic membrane, escaping into the cytosol. Once in the cytosol, viromers regain charge, which precludes regression into the endosomes. siRNAs then dissociate from them into the cytosol and the process of RNA interference begins.

Three different siRNAs against human NNT were assessed, all purchased from Thermo Fisher:

a) HSS118902 siRNA, targeting exon 21; this siRNA is referred to in the Results section as KD SiRNA1. NCI-H295R cells transfected with SiRNA1 are referred to in the Results section as KD SIRNA1 cells.
b) HSS118901 siRNA, targeting exons 20 and 21; this siRNA is referred to in the results section as KD SiRNA2. NCI-H295R cells transfected with SiRNA2 are referred to in the Results section as KD SIRNA2 cell.
c) HSS118900 siRNA, targeting exons 16 and 17; this siRNA is referred to in the results section as KD SiRNA3.
d) A scramble, non-sense siRNA (Silencer Select 1 negative control) not targeting any genes was used as negative control; this siRNA is referred to in the Results section as SCR SiRNA. NCI-H295R cells transfected with SCR SiRNA are referred to in the Results section as SCR SIRNA.

Viromer transfection was performed according to the following protocol:

NCI-H295R cells were grown in 75 cm^2 flasks (Corning) in full culture media as described in Chapter 2. When 70-80% confluence was attained, media was removed and cells were washed with Phosphate Buffered Saline (PBS, Sigma), followed by 37^oC incubation in 2 ml of Trypsin (Gibco, Thermo Fisher) for 2 min. Cells were detached by gentle tapping and diluted in full media in plastic tubes (Corning) to be centrifuged at 12,000 rpm for 5 min. Pelleted cells were re-suspended in 10-15 ml of full media and cell density was estimated by microscopy. Following this, cells were loaded to a) 6-well plates at a concentration of 300,000 cells/well in 2 ml media, or b) 96-well plates at a concentration of 8,000 cells/ well in 100 µl media, and incubated overnight at 37^oC. The next day, working solutions of siRNAs in Buffer F (Viromer Blue kit, Lipocalyx, pH 7.2) were prepared at a concentration of 11 µM. Working solutions of Viromers in Buffer F were also prepared (by addition of 1000 µl Buffer F to 11 µl Viromer Blue stock solution) and vortexed for 5 sec. The working solutions of Viromers were then added to each siRNA solution (989 µl of diluted Viromers per 100 µl diluted siRNA) and mixed well by pipetting. After 15 min incubation at room temperature to allow formation of siRNA-Viromer complexes, the Viromer-siRNA mix was

a) applied directly to cells in 6-well plates (100-300 µl to 2 ml media for optimisation, 200 µl/ well in subsequent experiments) and mixed by gentle plate rocking or

b) diluted in cell media in falcon tubes at a concentration of 80 µl per 1 ml of media and then added to cells in 96-well plates -after complete removal of old media- at a volume of 108 µl/ well.

Gene knockdown efficiency was assessed by Real-Time PCR and Western Blotting from 2-7 days post-transfection. Media was changed on day 3 post-transfection and every 48 h

thereafter. In 96-well plates, 100 µl of media was added to each well 48 h post transfection to avoid disruption of cell proliferation by media evaporation. 6-well plates were used to assess knockdown efficiency by Real-Time PCR and Western Blotting, as well as for steroid profiling in cell media (LC-MS/MS). 96-well plates were used for proliferation, apoptosis and redox balance assessment.

The above protocol had to be modified temporarily for a period of three months during the course of this project due to changes introduced by the manufacturing company (Lipocalyx). The modification consisted of substitution of Opti-MEM media (Gibco, Thermo Fisher) for Buffer F. SiRNA and Viromer concentrations in the working solution were maintained. Transfection efficiency was not affected. After three months, Lipocalyx reinstated Buffer F and the protocol was resumed as detailed above.

An important problem encountered during 6-well transfection was the eventual loss of cells in the centre of the wells (both in the knockdown and control transfection group), which limited the RNA yield and required pooling of several wells to achieve sufficient RNA concentrations to proceed with cDNA synthesis and quantitative PCR. This problem resolved with a protocol modification whereby cell media was not changed on the day of transfection. This suggested the previously observed cell loss was due to cell detachment during media change on the day of transfection, as H295R cells adhere poorly to the bottom of the wells in the first 24-48 h.

3.2.3 Redox balance assessment

To assess the effect of NNT knockdown on cellular redox balance, NCI-H295R cells (passage 10-20) were loaded onto white opaque-walled, flat-bottomed 96-well plates (Perkin-Elmer) at

a concentration of 8,000 cells/well. The next day, media was removed carefully trying not to disrupt plated cells. Cells were transfected with siRNA-Viromer complexes as described above, using 100 µl media and 8 µl siRNA-Viromer solution per well. 48 h post-transfection, 100 µl growth media was added to each well, and media was refreshed by removal and addition of 100 µl media the next day. 96 h post-transfection, the intracellular ratio of reduced/oxidised glutathione was measured (in triplicates) using the GSH/GSSG-Glo™ assay (Promega) as described in Chapter 2.

3.2.4 Metabolic Flux analysis

NCI-H295R cells were transfected in 6-well plates as described above and cultured for 6 days. On day 6 (144h post-transfection), cells were washed with PBS and collected by trypsinisation. Cell density was measured microscopically and cells were loaded to Seahorse XF 24-well microplates at a loading density of 100,000 cells/well (media volume 100-150 µl). The next day (166 h post-transfection), metabolic flux analysis was completed as described in Chapter 2.

3.2.5 Proliferation time-courses

Assessment of cellular proliferation and viability was performed in flat-bottomed, transparent-walled 96-well plates (Falcon). At the beginning of each proliferation series, NCI-H295R cells (passage 10-25) were loaded onto plates, at a loading concentration of 8,000 cells/ well, in 110 µl of cell media. This loading concentration was selected after optimisation experiments comparing proliferation rates with various loading concentrations (5,000 - 15,000

cells/ well, data not shown). The next day, media was removed carefully trying not to disrupt plated cells and cells were transfected with siRNA as described above, using a total cell media volume of 108 µl of media per well. 48 h post-transfection, 100 µl of growth media was added to each well. At 72 h post-transfection (baseline point), media was replenished and one plate was frozen at -80^{o}C to determine 'baseline' cell numbers. In the remaining plates, cells were cultured for a further 96 h (i.e. until 166 h post-transfection), with intermediate media replenishment at 120 h hour post transfection (removal of 100 µl old media and addition of 100 µl fresh media per well). At least 5 biological replicates (wells) per group (i.e. NNT knock-down or scramble siRNA-transfected cells) were used in each time-course. At the end of the time-course, cell numbers were derived using DNA fluorescence, as described earlier. Proliferation rates were established using the formula

Proliferation rate = %(fluorescence at 166 h – fluorescence at 72 h)/ fluorescence at 72 h.

In some time-courses, concurrent drug treatment or conditioned culture media was applied to evaluate cellular proliferation and viability under special conditions (chemically-induced oxidative stress, adrenotoxic chemotherapy, glucose deprivation). Treatment was started 72h post-transfection (baseline time-point) and lasted 96 h. Treatment courses applied in the course of this project included:

a) Paraquat (N,N′-dimethyl-4,4′-bipyridinium dichloride, Sigma). Paraquat is a herbicide which is widely used as a chemical inducer of oxidative stress (superoxide generation) (Lei et al., 2014). Paraquat was administered for a total duration of 96 h and was replenished once in cell media during the proliferation course (48h). Stock solution of paraquat in sterile-filtered dH_2O was stored in 4^{o}C.

b) Glucose-deplete media (DMEM, L-Glutamine (+), glucose 1 g/dl, sodium pyruvate, catalogue number 11966025, Gibco). Media was supplemented with 2.5% Nu Serum (Sigma) and 1% ITS+ premix (BD Biosciences). This formulation contains 1/3 of the glucose concentration of regular NCI-H295R culture media. Glucose-deplete media was administered for a total duration of 96 h and was replenished once during the proliferation course (48h).

c) L-buthionine sulfoximine (BSO, Cayman Scientific). BSO is a potent, specific inhibitor of g-glutamylcysteine synthetase, the rate-limiting step in glutathione (GSH) biosynthesis (Bailey, 1998). BSO was administered for a total duration of 96 h and was replenished once in cell media during the proliferation course (48h). Doses ranged from 10-4,000 nM. Sterile-filtered solution of BSO in sterile-filtered dH_2O was generated fresh on the day of the experiments, as the substance is unstable in liquid form. Powder BSO was stored at -20^{o}C.

d) Auranofin (Sigma). Auranofin is a gold-complex agent and the most potent inhibitor of thioredoxin reductase. In proliferation series, it was administered for a total duration of 96 h and was replenished once in cell media during the proliferation course (48h). Doses ranged from 200-2,000 nM. Sterile-filtered liquid stock solution of auranofin in DMSO was stored at 4^{o}C.

3.2.6 Apoptosis

To evaluate the effects of NNT knockdown on cellular redox balance and apoptosis, NCI-H295R cells were loaded to opaque-walled, flat-bottomed 96-well plates (Perkin-Elmer) at a loading concentration of 8,000 cells/well, and transfected the next day as described above

(10-15 wells/ transfection group). Media was refreshed on days 2 and 4 post-transfection. On day 5 (120 h post-transfection), caspase activity was measured as described in Chapter 2 (Caspase 3/7-Glo™ assay, Promega) using 4 wells (replicates) per transfection group. After the end of the assay, plates were frozen at -80°C and relative cell density in the remaining wells was assessed the next day using the CyQuant® Cell Proliferation kit (Thermo Fisher).

3.2.7 Steroid profiling by Liquid Chromatography/ Tandem mass spectrometry

To outline the impact of NNT knockdown on steroid production, NCI-H295R cells transfected in 6-well plates were incubated in 1 ml of serum-free media (DMEM/F12 supplemented with 1% ITS+ premix and 1% Penicillin-Sterptomycin) for 48h, starting 72h post-transfection. At the end of the incubation, media was collected in silinised glass tubes and stored at -20°C. Protein was harvested as described in Chapter 2 and used to standardise the results to protein concentration. Steroid extraction from stored cell media was subsequently completed as described in Chapter 2.

3.3 Results

3.3.1 NNT silencing by siRNA transfection

The efficacy and duration of NNT silencing in NCI-H295R cells transfected with siRNA in 6-well plates was evaluated by Western Blotting and Real-Time PCR. Three different siRNAs against NNT were evaluated (KD SiRNA 1, 2 and 3). Scramble, non-sense siRNA was used as negative control (SCR SiRNA). Gene silencing at a translational level was assessed by Western Blotting, from 24 h to 166 h post-transfection (Fig. 3-1). KD SiRNA1 was selected as the siRNA of choice as it displayed the most consistent knockdown efficiency, and was used in all subsequent experiments. KD SiRNA2 was used to corroborate results in proliferation and apoptosis assays, whose results are most likely to be confounded by off-target effects. KD SiRNA3 produced less satisfactory knock-down and thus was not used in subsequent experiments. Real-time PCR was deployed to measure NNT expression at a transcriptional level 72 h – 166 h post-transfection. Good levels of NNT silencing were achieved with both KD SiRNA1 and KD SiRNA 2 throughout this time window (**Fig. 3-1**).

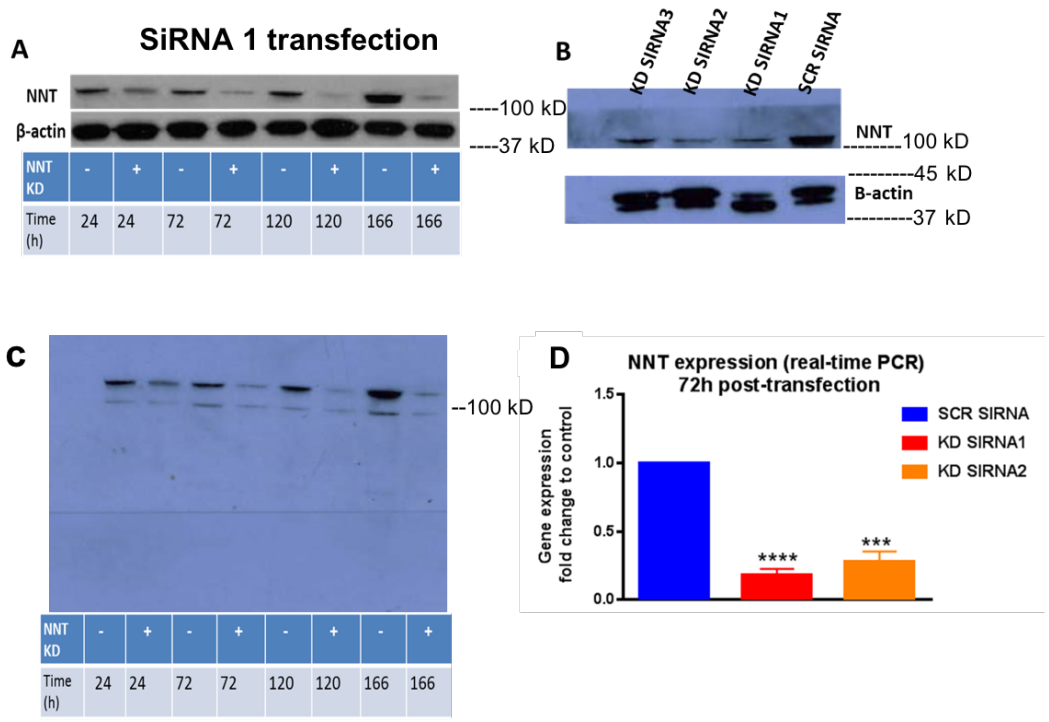

*Figure 3-1 Assessment of NNT knockdown in siRNA-transfected NCI-H295R cells by Western Blotting and Real-Time PCR. A) Protein expression at serial time-points in the first week post-transfection with KD SiRNA 1. Cells transfected with SCR siRNA were used as controls [indicated as (-)]. B) Comparison of NNT expression in cells transfected with scramble, non-sense siRNA (SCR SiRNA, negative control) and three alternative SiRNAs against NNT (KD SiRNA 1, 2 and 3) 72 h post-transfection. C) Whole NNT blot from time-series displayed in panel A, added to demonstrate antibody specificity. D) Real-time PCR comparing NNT expression in SCR SIRNA cells, KD SIRNA1 and KD SIRNA2 cells, 72 h post-transfection. ****p<0.0001, ***p<0.001; n>5 independent experiments.*

3.3.2 Cellular redox balance

The effect of acute NNT silencing on NCI-H295R cellular redox balance was determined by measurement of the cellular ratio of reduced to oxidised glutathione (GSH/GSSG ratio), 96 h post-transfection (GSH/GSSG-Glo^{TM} assay, Promega). Lower GSH/GSSG ratios suggest higher intarcellular levels of oxidative stress and impaired residual antioxidant capacity (Rebrin and Sohal, 2008). In keeping with our hypothesis, NNT silencing by KD SiRNA1 increased intracellular oxidative stress, as suggested by a statistically significant decrease in the GSH/GSSG ratio compared to cells transfected with SCR SiRNA [median (IQR) GSH/GSSG ratio in KD SIRNA1 cells normalised to SCR SIRNA cells 0.83 (0.41 – 0.9); $p<0.05$, n=8 independent experiments] (**Fig. 3-2**).

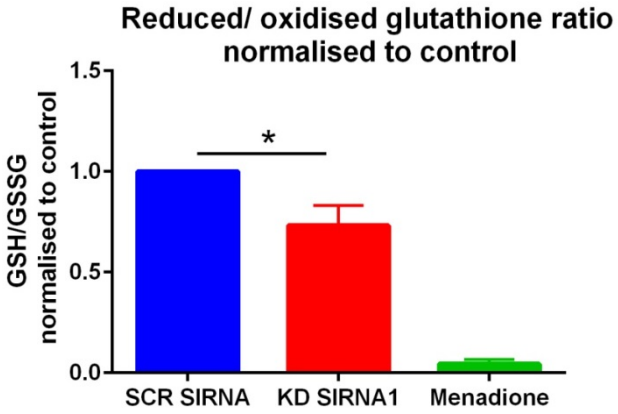

*Figure 3-2 GSH/GSSG ratio in NCI-H295R cells transfected with KD SiRNA1, normalised to the GSH/GSSG ratio of SCR SiRNA-transfected cells. Low GSH/GSSG ratio levels suggest higher intracellular oxidative stress, as a result of NNT loss. Menadione: NCI-H295R cells treated with the potent oxidising agent Menadione (40 μM) for 2h as positive control (*p<0.05, n=8 independent experiments).*

3.3.3 Mitochondrial bioenergetics

Changes in mitochondrial respiration were evaluated by direct measurement of cellular oxygen consumption, using Extracellular Flux analysis (Seahorse XF analyser). We observed no statistically significant difference between SCR SiRNA-transfected cells and KD SiRNA1-transfected cells [median (IQR) oxygen consumption rates 6 (4.4-7.8) and 7 (5-8.2) pmol/min/ μg protein, respectively; n=4 independent experiments, $p>0.05$). After baseline OCR measurement, oligomycin was used to inhibit respiratory chain complex V (ATP synthase); this led to a similar OCR decrease in both transfection groups [post-oligomycin OCR 2.5 (1.9-3.2) in SCR SIRNA wells vs 2.7 (2.2-3.9) pmol/min/ μg protein in KD SIRNA1 cells, $p> 0.05$]. Treatment with the mitochondrial uncoupler FCCP (Carbonyl cyanide-p-trifluoromethoxyphenylhydrazone) led to an expected sharp rise in OCR in both cell groups; again, no differences were observed [post-FCCP OCR 5.3 (3.1-7.3) pmol/min/μg in SCR SIRNA cells vs 5.6 (4-6.7) pmol/min/μg in KD SIRNA1 cells, $p>0.05$]. Of note, the maximal oxygen consumption displayed post-FCCP was similar to the baseline OCR of NCI-H295R cells, an unusual but reproducible finding which may suggest that NCI-H295R cells tend to operate close to their maximal respiratory capacity even under normal growing conditions. Finally, combination treatment with Antimycin A and Rotenone was deployed to inhibit all mitochondrial respiration; residual oxygen consumption (non-mitochondrial respiration) was also comparable between the two groups [1 (0.8-1.2) pmol/min/ μg for SCR SIRNA cells vs 1.1 (0.7-2.3) pmol/min/ μg for KD SIRNA1 cells]. Baseline extracellular acidification rates, representative of baseline glycolytic rates, did not differ between the two groups (0.69 ± 0.13 mpH/min/protein for SCR SiRNA cells vs 0.63 ± 0.08 mpH/min/protein for KD SIRNA1 cells; $p> 0.05$, n=4) (**Fig. 3-3**).

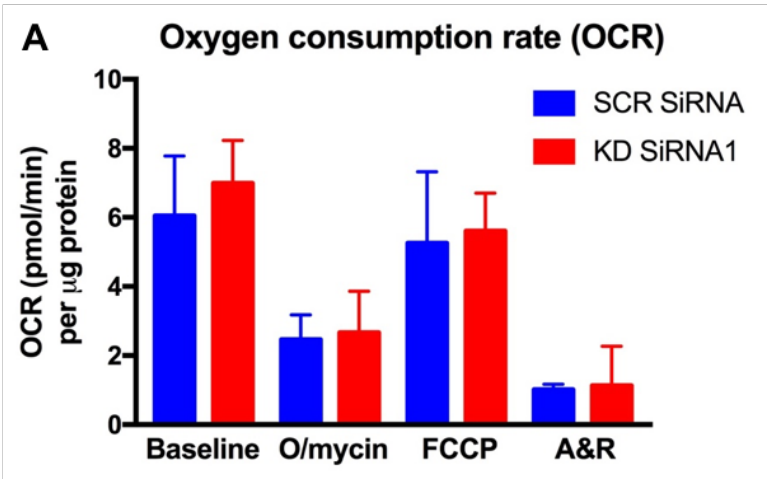

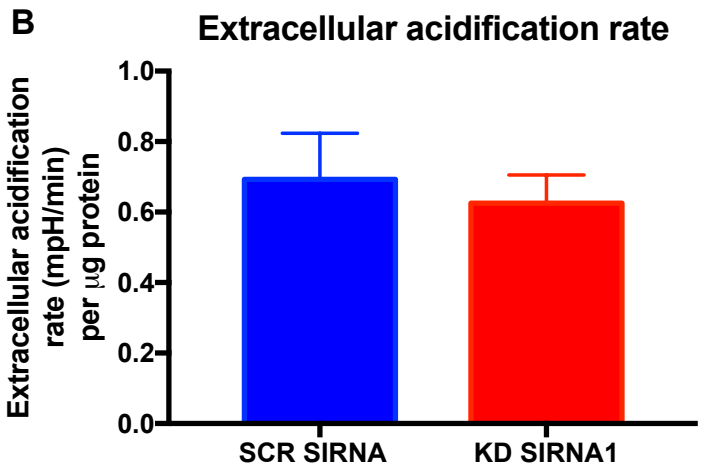

Figure 3-3 A) Seahorse XF24 analysis of cellular oxygen consumption rates (OCR) in siRNA-transfected NCI-H295R cells at baseline and after successive application of three mitochondrial respiration inhibitors. Bars represent median ± IQR values. No significant difference was detected between KD SIRNA1 and SCR SIRNA cells. FCCP: Carbonyl cyanide-p-trifluoromethoxyphenylhydrazone. A&R: Antimycin A plus Rotenone ($p>0.05$, $n= 4$ independent experiments); B) Baseline extracellular acidification rates in siRNA-transfected NCI-H295R cells. Bars represent mean ± SEM values. No significant difference was detected between KD SIRNA1 and SCR SIRNA cells ($p>0.05$, $n= 4$ independent experiments).

3.3.4 Cellular proliferation

Cellular proliferation rates were assessed over the time window from 72h-166 h post-transfection, a period during which consistent NNT knock-down had been confirmed on a protein level. NNT knock-down by KD SiRNA1 transfection led to a decrease in proliferation rates from 111.8% ± 11.3% in SCR SIRNA cells to 39.2% ± 11.3% in KD SIRNA1 cells ($p=0.0001$, n=13 independent experiments). To exclude the possibility that this impact was driven by non-specific, off-target siRNA effects, these results were corroborated by use of a second siRNA against NNT (KD SiRNA2), which had an even more striking effect, completely obliterating cell proliferation (proliferation rate -4.6% ± 15.1% vs 115.0% ± 19.1%; $p<0.01$, n=5 independent experiments) (**Fig. 3-4**).

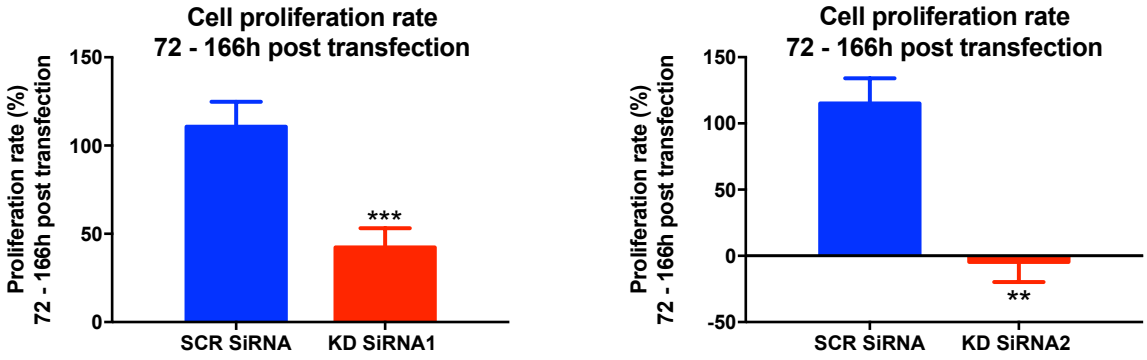

*Figure 3-4 Proliferation rates observed in siRNA-transfected NCI-H295R cells, 72-166 h post-transfection, using DNA fluorescence. NNT knock-down with two different siRNAs suppressed cell proliferation. Proliferation rate = %[(DNA fluorescence emitted at 166 h post-transfection - DNA fluorescence emitted at 72h post-transfection)]/ DNA fluorescence emitted at 72h post-transfection. ***p<0.001, **p<0.01; n≥ 5 independent experiments.*

3.3.5 Apoptosis

In order to establish whether the increased oxidative stress observed with NNT knockdown leads to higher rates of apoptosis -as predicted by ROS physiology- we measured intracellular caspase 3 and 7 activity 120 h post-transfection. We also quantified relative cell numbers (DNA fluorescence) at the same time-point to standardise the results to cell numbers. KD SIRNA1 cells exhibited significantly higher caspase 3/7 activity than SCR SIRNA cells [median (IQR) ratio KD SIRNA1 to SCR SIRNA cells 1.27 (1.05-2.1); p<0.001, n=8 independent experiments], confirming that NNT KD triggers cell death by apoptosis in keeping with our core hypothesis. The effect was even more marked with KD SiRNA2 transfection [median (IQR) ratio KD SIRNA2 to SCR SIRNA cells 3.9 (2-5.4); p<0.05, n=4 independent experiments], paralleling the results of the proliferation assays (**Fig. 3-5**).

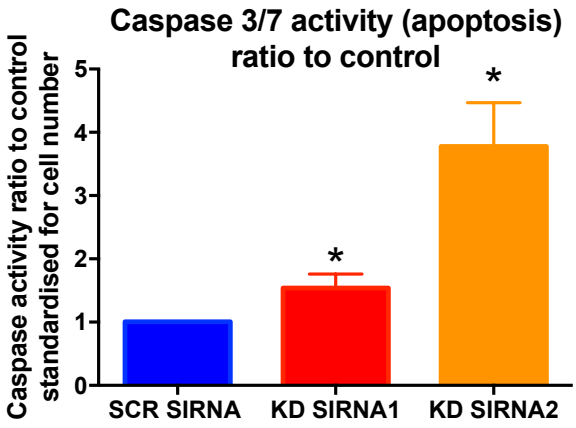

*Figure 3-5 Caspase 3/7 activity ratio in KD SIRNA1 and KD SIRNA2 cells to SCR SIRNA cells, after standardization for cell numbers. Increased caspase activity indicates higher apoptotic rates in KD SIRNA cells (*p<0.05, n≥ 4 independent experiments).*

3.3.6 Proliferation under chemically-induced oxidative stress and glucose deprivation

Given the integral role of NNT in mitochondrial antioxidant defence and the detrimental effect of NNT inhibition on redox balance, we further hypothesised that NNT loss will render NCI-H295R cells more sensitive to chemically induced oxidative stress. To assess this assumption, we treated NCI-H295R cells with a low dose of paraquat, a pesticide which induces oxidative stress *in vitro,* generating superoxide. Treatment with 10 μM of paraquat for 96 h (72 h -166 h post-transfection) led to a statistically significant impairment of cellular proliferation and viability in cells transfected with KD SiRNA1, but not in their counterparts that were treated with SCR SiRNA (ratio of cell fluorescence after 96 h paraquat treatment to cell fluorescence without paraquat treatment 0.98 ± 0.07 in SCR SIRNA cells vs 0.79 ± 0.05 in KD SIRNA1 cells; $p<0.05$, n=6 independent experiments) (**Fig. 3-6**). These results have implications of potential translational importance, suggesting that NNT knockdown may potentiate the cytotoxic effects of chemotherapy agents which induce oxidative stress.

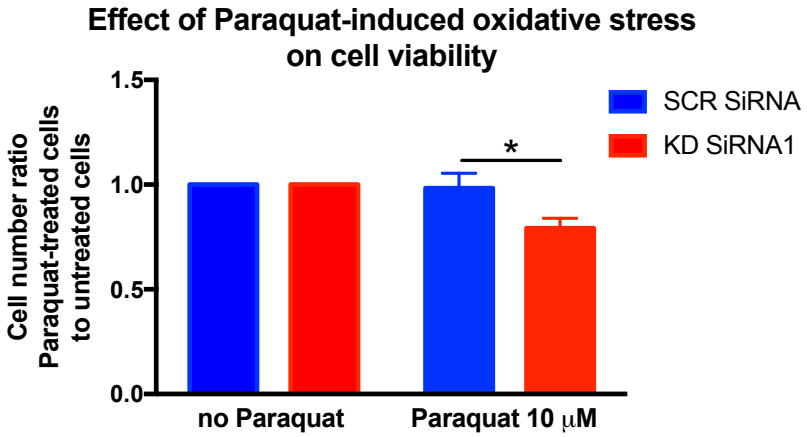

*Figure 3-6 Effect of low-dose Parquat treatment (10 μM) on NCI-H295R cell proliferation, 72-166 h post siRNA transfection. KD SIRNA1 cells are more sensitive to chemically-induced oxidative stress (*p<0.05, n=7 independent experiments).*

Previous work has suggested that NNT inhibition can impede glutamine utilisation in the TCA cycle (Gameiro et al., 2013). In response to this, cells have to resort to glucose to derive the missing carbons to fuel their anabolic needs and continue to proliferate. To establish whether NNT silencing renders ACC cells more sensitive to glucose deprivation, we cultured cells in low-glucose DMEM/F12 media, containing 1/3 of the glucose concentration of regular NCI-H295R culture media (1 g/L vs 3.1 g/L). Culturing cells under these conditions for 96 h (72-166 h post-transfection), we observed a more pronounced effect on the proliferation of KD SIRNA1 cells than of SCR SIRNA cells (**Fig. 3-7**).

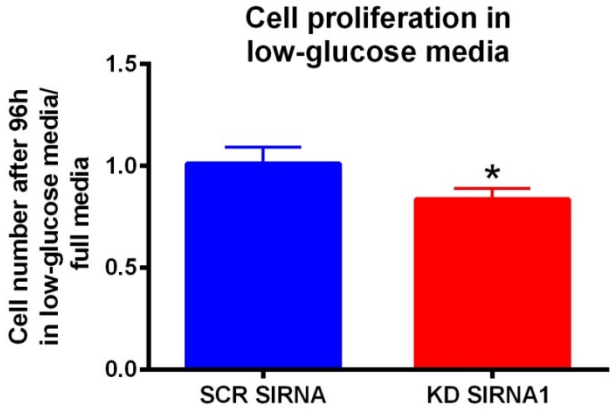

*Figure 3-7 NCI-H295R cell proliferation in low-glucose media, 72-166 h post siRNA transfection. Glucose deprivation suppresses proliferation in KD SIRNA1 cells (*p<0.05, n=5 independent experiments).*

3.3.7 Alternative antioxidant targeting

Given the auspicious effects of NNT inhibition on NCI-H295R cell growth, we went on to evaluate the sensitivity of ACC cells to isolated inhibition of each of the two pillars of cellular antioxidant defence: the glutathione pathway and the thioredoxin pathway. We used buthionine sulfoximine (BSO, a potent inhibitor of the glutathione-producing enzyme c-glutamylcysteine ligase), to deplete intracellular glutathione. BSO has a proven capacity to inhibit > 90% of total glutathione synthesis *in vitro*, with excellent tolerability in clinical studies (Bailey, 1998). We observed a significant cytostatic effect with BSO doses of 200 μM after 96 h of treatment (**Fig. 3-8A**).

Pharmacological manipulation of the alternative mitochondrial antioxidant pathway, the thioredoxin pathway, was achieved by auranofin, a gold complex with well-established capacity to inhibit thioredoxin reductase (Madeira et al., 2012). Auranofin has exhibited anti-tumour effects against certain cancer types in vitro (e.g. leukemia, melanoma, non-small cell

lung cancer) and is currently being studied in clinical trials against leukemia (Gandin et al., 2010, Weir et al., 2012, Sobhakumari et al., 2012). NCI-H295R treatment with auranofin concentrations of 1 μM led to a substantial suppression of proliferation, while higher concentrations effected massive cytotoxicity (**Fig. 3-8B**).

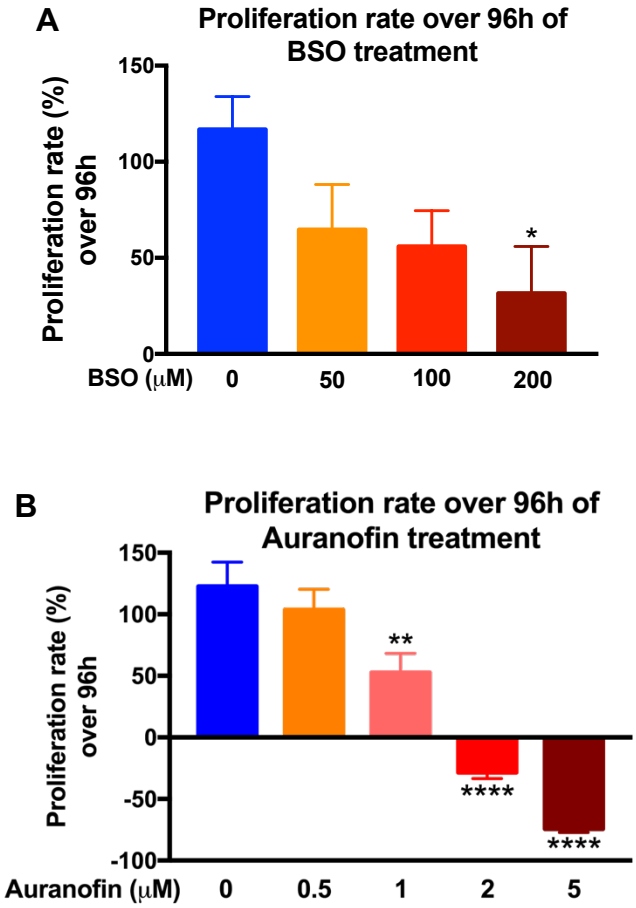

*Figure 3-8 Effects of glutathione and thioredoxin pathway inhibitors on NCI-H295R cell proliferation. A) 96 h treatment with incremental doses of BSO (0-200 μM), inhibitor of glutathione synthesis. Control cells were treated with vehicle only. *p<0.05; n= 9 independent experiments. B) 96 h treatment with incremental doses of auranofin (0-5 μM), thioredoxin reductase inhibitor. Control cells were treated with vehicle only. **p<0.01, ***p<0.001,****p<0.0001; n=8.*

3.3.8 Steroidogenesis

The effects of transient NNT silencing on steroidogenesis were evaluated through comprehensive steroid profiling in cell media by LC-MS/MS, as well as gene expression analysis by Real-Time PCR. We postulated that NNT silencing will disrupt steroidogenesis either depriving mitochondrial steroidogenic monooxygenases -Cholesterol side-chain cleaving enzyme (CYP11A1), 11β-hydroxylase (CYP11B1), aldosterone synthase (CYP11B2)- of their essential electron donor NADPH, or due to oxidative stress-induced down-regulation of key steroidogenic enzymes. Surprisingly, we observed the opposite response in the acute aftermath of NNT inhibition: KD SiRNA1-transfected cells produced significantly more cortisol (0.13 ± 0.03 nM/μg vs 0.05 ± 0.01 nM/μg protein; $p<0.01$, n=5 independent experiments) and androstenedione (1.25 ± 0.29 nM/μg vs 0.57 ± 0.17 nM/μg; $p<0.05$, n=5) than their SCR SiRNA-transfected controls (**Fig. 3-9**). Individual enzyme activity was measured by computation of the corresponding product to substrate ratios for three key steroidogenic enzymes [11β-hydroxylase (CYP11B1), 21-hydroxylase (CY21A2), 17/20-lyase (CYP17A1)]; all three displayed higher activity in KD SiRNA1-transfected cells, in keeping with a paradoxical generalised stimulation of steroidogenesis by acute NNT loss (**Table 3-1**). Interestingly, the ratio of cortisol/cortisone was also consistently higher in NNT KD cells. Other steroid metabolites were below the threshold of quantification in most experiments, therefore no other product-to-substrate ratios could be computated.

We also explored the gene expression alterations underpinning the enhanced steroidogenic capacity of cells transfected with KD SiRNA1, comparing the expression of core steroidogenic genes (STAR, CYP11A1, CYP21A2, CYP17A1, 3βHSD2, CYP11B1, CYP11B2) between KD SIRNA1 and SCR SIRNA cells. There was a statistically significant

increase in the expression of CYP21A2 ($p<0.05$), CYP17A1 ($p<0.05$) and 3βHSD2 ($p<0.01$) in KD SIRNA1 cells (**Table 3-2**). Expression of CYP11B1 and CYP11B2 was below detection in both groups due to low baseline expression levels of these enzymes in NCI-H295R cells.

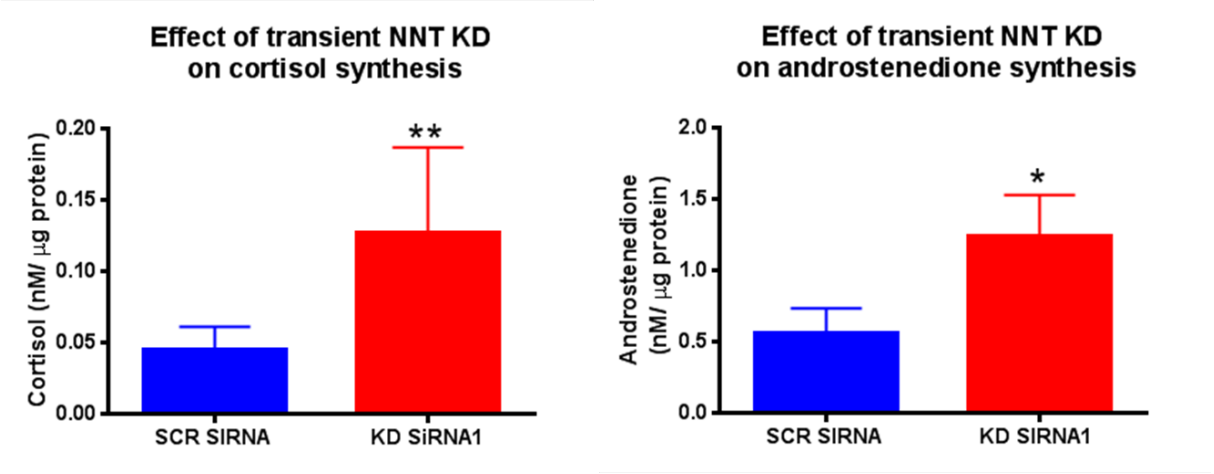

*Figure 3-9 Effect of transient NNT knockdown on NCI-H295R cell cortisol and androstenedione production. NNT knockdown stimulates cortisol and androstenedione synthesis. *p<0.05, **p<0.01; n=5 independent experiments*

Table 3-1 Steroidogenic enzyme activity in SCR SIRNA and KD SIRNA1 cells, derived from product-to-substrate ratios (LC-MS/MS). Results are expressed as mean ± SE values (n=6 independent experiments). HSD11B1: cortisone reductase.

Enzyme	Product/ substrate ratio	SCR SiRNA (nM/µg)	KD SiRNA1 (nM/µg)	P value
CYP11B1	cortisol/ 11-deoxycortisol	0.011±0.001	0.021±0.005	P<0.01
CYP21A2	11-deoxycortisol/ 17-OH-progesterone	37.6±9	81.1±15.2	P<0.01
CYP17A1	androstenedione/ 17-OH-progesterone	4.7±1	17.1±2.5	P<0.01
HSD11B1	cortisol/cortisone	5.1±1.1	13.1±2.9	P<0.001

Table 3-2 Effects of transient NNT KD on steroidogenic enzyme expression as assessed by Real-Time PCR. ΔCt= Ct (NNT) – Ct (RPLPO). n≥ 6 independent experiments

	SCR SIRNA median ΔCt (IQR)	KD SIRNA1 median ΔCt (IQR)	P value	Median fold change KD SIRNA1/ SCR SIRNA
StAR	**4.0 (2.3-6.8)**	**2.2 (1.9 - 3.0)**	**> 0.05**	
CYP11A1	**5.9 (3.3 - 9)**	**4.8 (3.5 - 4.9)**	**> 0.05**	
3βHSD2	**8.7 (7.6 -10.3)**	**8.0 (7.4 - 8.8)**	**< 0.01**	**2**
CYP17A1	**2.8 (1.5 - 5.2)**	**1.8 (0.7 - 2.9)**	**< 0.01**	**2.5**
CYP21A2	**9.3 (4.2 -12.9)**	**6.4 (0.4 - 9.2)**	**< 0.05**	**11.5**

3.4 Discussion

With this work, we explored the immediate impact of NNT silencing on ACC cells with respect to redox balance, mitochondrial bioenergetics and cellular proliferation, using transient NNT knockdown in NCI-H295R cells by siRNA transfection. Our aim was to establish whether NNT inhibition can have therapeutically beneficial effects, limiting tumour growth or suppressing steroidogenesis, as is suggested by the development of adrenal insufficiency in patients with inactivating NNT mutations. We hypothesised that NNT inhibition will compromise the ability of adrenocortical mitochondria to effectively deal with oxidative stress, leading to progressive accumulation of ROS. ROS excess has multiple toxic sequelae, and can directly impair cell viability triggering apoptosis (Gupta et al., 2012, Fruehauf and Meyskens, 2007). We also postulated that NNT inhibition will suppress steroidogenesis.

In the acute setting (transient knockdown), NNT loss increased intracellular oxidative stress, leading to a dramatic suppression of cell proliferation and increased rates of apoptosis. Redox balance perturbations in response to NNT loss have been previously demonstrated in a limited number of cell lines *in vitro* (rat phaechromocytoma, human melanoma) as well as in lymphocytes derived from NNT mutant patients *ex vivo* (Yin et al., 2012, Gameiro et al., 2013, Fujisawa et al., 2015). Meimaridou et al. reported increased levels of oxidative stress in NCI-H295R cells with chronic NNT silencing (shRNA knockdown) (Meimaridou et al., 2012). These findings are in keeping with the biological role of NNT as a major mitochondrial generator of NADPH, which is the essential provider of reducing equivalents to the two main antioxidant pathways (Rydstrom, 2006, Leung et al., 2015). Importantly, NNT silencing led to a swift inhibition of cell proliferation (by > 60% in comparison to controls), with increased rates of apoptotic death. The association between excessive oxidative stress

and mitochondrial apoptosis has been well established in the literature (Martindale and Holbrook, 2002, Nair et al., 2009, Hampton and Orrenius, 1997, Garbarino et al., 2007, Gupta et al., 2012), but data on the effects of NNT loss on cellular proliferation and viability are scarce. Transient NNT silencing increased rates of apoptosis in PC12 (rat phaechromocytoma) cells (Yin et al., 2012). Stable NNT knockdown in human melanoma cells, another cancer type particularly vulnerable to oxidative stress, was associated with reduced cellular viability and high apoptotic rates *in vitro*, as well as deceleration of melanoma xenograft growth in mice (though the latter was statistically significant for only one of the two anti-NNT shRNAs that were used) (Gameiro et al., 2013). Meimaridou et al. reported high levels of apoptosis in the zona fasciculata of adrenals derived from NNT mutant mice, as well as in NCI-H295R cells stably transfected with shRNA against NNT *in vitro;* effects on cell proliferation were not explored in their study (Meimaridou et al., 2012). It is not clear whether the pronounced suppression of cell proliferation we observed with NNT knockdown can be ascribed entirely to the cumulative effects of increased apoptotic death (cytotoxicity), or whether NNT loss had an additional cytostatic effect, suppressing cell division. Although ROS have been typically associated with a stimulation of cellular proliferation, a number of *in vitro* models have demonstrated the opposite effect (suppression of cell division), in a complex relationship that may depend on the magnitude of ROS excess and/or tissue type (Gupta et al., 2012, Koka et al., 2010, Donadelli et al., 2007). NNT inhibition may also interfere with cellular proliferation in a ROS-independent way, curtailing the amount of NADPH available to fuel the voracious anabolic needs of malignant cells.

An additional interesting feature observed in KD SIRNA1 cells, also predicted by our hypothesis, is their sensitivity to chemically induced oxidative stress - even at sub-toxic doses of oxidising agents- as demonstrated by treatment with the superoxide-generating agent

paraquat. This finding is of translational importance, as oxidative stress induction is also a feature of a number of classic chemotherapy agents and is considered to contribute to their cytotoxic effect (Trachootham et al., 2009, Montero and Jassem, 2011). NNT inhibition may thus be envisaged as a meaningful strategy to sensitize ACC to such drugs. Synergy with mitotane would also appear theoretically plausible, as the latter has been associated with endoplasmic reticulum stress induction (Sbiera et al., 2015).

Monitoring of cell growth in low-glucose media suggested that NNT KD renders ACC cells more sensitive to glucose deprivation. This corroborates previous work demonstrating diminution of cell proliferation in melanoma cells under low-glucose culture conditions (Gameiro et al., 2013). The underlying mechanism involved inhibition of glutamine utilisation in the TCA cycle; consequently, cells were more dependent on glucose as an alternative source of anabolic carbons. It should be noted, however, that our Metabolic Flux analysis did not demonstrate a difference in baseline glycolytic rates between KD SIRNA1 and SCR SIRNA cells, which seems to be at odds with the proliferation results. A potential explanation for this ostensible discrepancy arises if we consider cell proliferation as a relevant factor: KD SIRNA1 cells consume glucose at the same rate as the SCR SIRNA cells despite having lower proliferation rates and, consequently, lower overall anabolic needs.

The effects of NNT silencing on NCI-H295R steroidogenesis were surprising and refuted our initial hypothesis. In the acute setting (siRNA knockdown) we observed a generalised stimulation of steroidogenesis leading to increased production of cortisol and androstenedione, respectively the main glucocorticoid and androgen metabolites excreted by these cells. This is contrary to what one would have anticipated considering that mitochondrial NADPH is an essential cofactor to CYP11A1, CYP11B1 and CYP11B2.

Furthermore, most of the few published studies exploring the relationship between ROS and steroidogenesis (mostly on testicular Leydig cell tumour cells) have reported down-regulation of steroidogenic enzymes with oxidative stress (most notably CYP11A1) (Diemer et al., 2003, Stocco et al., 1993, Prasad et al., 2013, Behrman and Aten, 1991, Stocco and Ascoli, 1993, Zhao et al., 2012) (Diemer et al., 2003, Stocco et al., 1993, Prasad et al., 2013, Behrman and Aten, 1991, Stocco and Ascoli, 1993, Zhao et al., 2012) (Diemer et al., 2003, Stocco et al., 1993, Prasad et al., 2013, Behrman and Aten, 1991, Stocco and Ascoli, 1993, Zhao et al., 2012) (Diemer et al., 2003, Stocco et al., 1993, Prasad et al., 2013, Behrman and Aten, 1991, Stocco and Ascoli, 1993, Zhao et al., 2012) (Diemer et al., 2003, Stocco et al., 1993, Prasad et al., 2013, Behrman and Aten, 1991, Stocco and Ascoli, 1993, Zhao et al., 2012) (Diemer et al., 2003, Stocco et al., 1993, Prasad et al., 2013, Behrman and Aten, 1991, Stocco and Ascoli, 1993, Zhao et al., 2012) (Diemer et al., 2003, Stocco et al., 1993, Prasad et al., 2013, Behrman and Aten, 1991, Stocco and Ascoli, 1993, Zhao et al., 2012). Interestingly, Zhao et al. demonstrated a biphasic relationship between ROS and steroidogenesis, which suggests that the direction of the effect may be dose-dependent (Zhao et al., 2012)(Zhao et al., 2012)(Zhao et al., 2012)(Zhao et al., 2012)(Zhao et al., 2012)(Zhao et al., 2012)(Zhao et al., 2012). Two relevant studies on NCI-H295R cells focused on ALADIN, a gene whose dysfunction is associated with a constellation of adrenal insufficiency, neurological disorders and oxidative stress. Prasad et al. reported deficient cortisol synthesis and suppressed expression of CYP11B1 and StAR with ALADIN knockdown in these cells; CYP11A1 did not appear to be affected (Prasad et al., 2013). These results were contradicted by Juhlen et al., who found that ALADIN knockdown in H295R-S1 (substrain 1) cells only has an impact on the CYP450 type II microsomal enzymes CYP17A1 and CYP21A2, and their electron donor POR. Steroidogenically, only 17-hydroxyprogesterone, 11-deoxycortisol and

androstenedione were significantly suppressed, with no demonstrable effect on cortisol production (Juhlen et al., 2015).

Of note, the enhanced steroidogenic output we observed would be expected to incur a substantial oxidative burden on ACC cells, as CYP11B1 and, to a lesser extent, CYP11A1 generate ROS through electron leakage as detailed in Chapter 1. Therefore, this response appears counter-intuitive from a redox economy standpoint. A potential explanation is that the observed stimulation of steroidogenesis is but an incidental event in the context of a generalized acute-phase response to an insult (NNT loss) that threatens cell viability. The possibility of off-target siRNA effects contributing to the observed phenotype cannot be excluded. Despite the limitations of *in vitro* work, NCI-H295R cells remain the most widely used model to study disorders of adrenal steroidogenesis. To the extent that this model can recapitulate *in vivo* adrenal physiology, our data suggest that the degree of NADPH shortage generated by NNT loss is not limiting for adrenal steroidogenesis; furthermore, it indicates that oxidative stress does not functionally inhibit steroidogenesis in the human adrenal cortex. Mechanistic conjectures aside, our results indicate that there is no role for NNT targeting to inhibit adrenal steroidogenesis.

Finally, within the same framework we also explored the anti-tumour potential of alternative antioxidant targets, focusing on the glutathione and thioredoxin pathways. We used buthionine sulfoximine (BSO) to inhibit glutathione synthesis. BSO is a specific and competitive inhibitor of γ-glutamylcysteine synthetase, the rate-limiting enzyme in glutathione synthesis (Bailey, 1998). It has long been known that intratumoural glutathione levels correlate with resistance to cytotoxic chemotherapy (Traverso et al., 2013). BSO has exhibited anti-tumour effects (inhibition of cell proliferation and/ or increased rates of

apoptosis) against neuroblastoma, ovarian cancer, breast cancer, pancreatic cancer and small cell lung cancer *in vitro* (Bailey, 1998, Maeda et al., 2004, Schnelldorfer et al., 2000, Tagde et al., 2014, Anderson et al., 1999). It can also augment cell sensitivity to oxidative stress, especially in combination with alkylating agents such as melphalan (Dusre et al., 1989). *In vivo*, a combination of intravenous BSO and melphalan has been used in three phase I clinical trials, with good tolerability except for a possibly increased incidence of melphalan-induced bone marrow toxicity (Bailey et al., 1994, Bailey, 1998, O'Dwyer et al., 1996, Bailey et al., 1997). Successful intratumoural GSH depletion was demonstrated in these studies. More recently, the same regimen was administered to 38 children with refractory neuroblastoma, inducing a clinical response in six of them (Anderson et al., 2015). In our work, we observed a suppression of NCI-H295R cell growth with doses ≥ 200 μM, i.e. at a dose that is clinically attainable in plasma without substantial toxicity (Bailey, 1998). These findings suggest that ACC is susceptible to the anti-tumour effects of glutathione depletion.

Auranofin, a gold complex-based agent able to inhibit thioredoxin reductase, was used to evaluate the sensitivity of NCI-H295R cells to thioredoxin pathway abrogation. Auranofin was initially applied in the treatment of rheumatoid and psoriatic arthritis in the '80s, by virtue of its versatile anti-inflammatory properties [activation of mitogen-activated protein kinases (MAPK), inhibition of nuclear factor kappa-light-chain-enhancer of activated-B-cells (NF-κB) and suppression of pro-inflammatory cytokines] (Madeira et al., 2012). Chronic administration is very well tolerated, with similar dropout rates to placebo (Glennas et al., 1997). More recently, attention shifted to the drug's newfound ability to inhibit thioredoxin reductase (cytosolic and mitochondrial), thereby inducing oxidative stress and inhibiting DNA synthesis (Brown et al., 2010, Cox et al., 2008, Hill et al., 1997). This has translated into cytotoxicity against a number of cell lines *in vitro* (e.g. melanoma, leukemia, lung

cancer), most notably through mitochondrial apoptosis (Gandin et al., 2010, Li et al., 2016, Sobhakumari et al., 2012, Weir et al., 2012, Park and Kim, 2005). Of note, auranofin has the additional ability to interfere with selenium metabolism, potentially also causing some inhibition of glutathione peroxidase (Talbot et al., 2008). *In vivo*, efficacy was demonstrated against non-small cell lung cancer in a xenograft model (Li et al., 2016). Auranofin is currently being investigated in clinical trials against leukemia, non-small cell lung cancer and ovarian cancer (www.clinicaltrials.gov).

Taken together, our *in vitro* work supports the value of antioxidant targeting as a novel therapeutic approach to suppress tumour growth in ACC. Further work, e.g. in the context of *in vivo* animal studies, will be required to confirm these promising results and identify the most effective of available targets.

4 Effects of stable NNT knockdown on ACC cell metabolism, proliferation and steroidogenesis

4.1 Introduction

In the previous chapter, we explored the acute ramifications of NNT silencing on ACC redox balance, mitochondrial respiration, cell proliferation/ viability and resistance to oxidative stress. We ascertained that NNT knockdown impairs cellular redox balance, suppresses cell proliferation, induces apoptosis and renders cells more susceptible to chemically-induced oxidative stress. We also observed a paradoxical stimulation of steroidogenesis. Our findings support the value of NNT targeting as a novel therapeutic approach to control ACC proliferation and/ or enhance the cytotoxic activity of chemotherapy agents that are associated with oxidative stress. A limitation of our model was that it can only outline the short-term effects of NNT knockdown, as siRNA-induced gene silencing only lasts a few days. The plasticity of malignant cells and their notorious adaptability to exogenous insults is well known to any clinical or experimental oncologist and constitutes a major obstacle to the development of durable treatments (Watson, 2013). The eventual development of resistance to cytotoxic chemotherapy is all but inexorable in the vast majority of solid organ malignancies, ACC being no exception (Gupta et al., 2012, Fassnacht et al., 2012). Interestingly, redox adaptation (that is the ability of cells to adapt to higher ROS scavenging requirements) is now believed to comprise an important part of the molecular changes mediating chemotherapy (and radiotherapy) resistance (Gupta et al., 2012, Trachootham et al., 2009, Watson, 2013). Indeed, cell resistance to pro-oxidant chemotherapy agents such as doxorubicin, paclitaxel or platinum-based agents has been shown to correlate with the endogenous antioxidant capacity of various cell lines *in vitro* (Ramanathan et al., 2005, Hoshida et al., 2007, Trachootham et al., 2009). Redox adaptation, achieved through successful stimulation of various antioxidant pathways, can boost malignant cell survival not only by neutralising chemotherapy or radiotherapy-induced oxidative stress but also by

inhibiting cell death signalling (such as caspases), stimulating pro-survival molecules (such as Bcl-2) and augmenting DNA repair (Trachootham et al., 2009).

In this chapter, we will try to delineate the long-term effects of NNT loss on ACC cell metabolism, proliferation and steroid synthesis, establishing whether progressive redox adaptation is possible and to what extent this can alter the response we described in the transient silencing model of Chapter 3.

4.2 Methods

4.2.1 Research strategy

In order to characterise the chronic effects of NNT silencing on NCI-H295R cells, we used a stable, short-hairpin RNA (shRNA)-mediated knockdown system established by lentiviral transfection. Mirroring the experimental work undertaken with the transient knockdown model, we evaluated the *chronic* effects of NNT knockdown on:

a) Cellular redox balance, as reflected on the ratio of reduced to oxidised glutathione
b) Mitochondrial bioenergetics, focusing on mitochondrial oxygen consumption rates and glycolytic rates (extracellular flux analysis – Seahorse XF)
c) Cellular proliferation, using longitudinal assessment of cell numbers under routine cell culture conditions as well as under metabolic stressors (oxidative stress, glucose deprivation)
d) Cellular apoptosis, measuring caspase 3 and 7 activity
e) Steroidogenesis, by steroid profiling in cell media (LC-MS/MS)

All experiments were paired, NNT knockdown cells being plated and treated alongside their controls.

4.2.2 Lentiviral transfection for shRNA knockdown

ShRNAs are oligonucleotides consisting of two complementary 19–22 base pair RNA sequences connected by a short, hairpin-like loop of 4–11 nucleotides. Stable expression of shRNAs against the gene of interest within cells is accomplished through transfection with

genetically modified lentiviruses containing plasmids into which a shRNA-coding sequence has been introduced. The plasmid integrates into the host cell genome, allowing continuous transcription of shRNA. Within the cytosol, shRNA molecules are recognized by an endogenous Dicer enzyme which processes the shRNAs into siRNA duplexes; following this, silencing of the target gene is effected through the RNA interference mechanism described in Chapter 3 (Moore et al., 2010).

Lentiviruses belong to the the Retroviridae family and are widely used to transfect mammalian cell lines *in vitro* by virtue of their unique biological properties, most notably their ability to infect both dividing and non-dividing cells with high efficiency and integrate permanently into the host cell genome (Ramezani and Hawley, 2002). Most lentiviral vectors are based on the Human Immunodeficiency type I Virus (HIV-1). Plasmids used in lentiviral transfection often also possess an antibiotic resistance gene which allows selection of transfected from non-transfected cells and a green fluorescence protein (GFP) allowing visualization of transfected cells in fluorescent microscopes (https://www.addgene.org). To increase the safety of lentiviral use, the genes required for viral replication are distributed in 3 plasmids (2^{nd} generation lentiviral systems):

- A plasmid expressing the viral envelope
- A packaging plasmid containing the Gag, Pol, Rev and Tat genes, required for viral replication
- A plasmid containing the sequence encoding the shRNA of interest, flanked by long terminal repeats (LTRs) that facilitate integration into the genome of host cells. (https://www.addgene.org).

For this project, the following plasmids were used:

a) Pmd2.g (https://www.addgene.org/12259/)

Purpose: VSV-G envelope expressing plasmid (2nd generation)

This plasmid expresses the VSV-G gene under the control of the human CMV promoter. The gene encodes the Vesicular Stomatitis Virus envelope G glycoprotein (VSV-G) to allow production of a pseudotyped retrovirus with a broad host range. It also contains an ampicillin resistance gene to allow selection of the plasmid in Escherichia Coli.

b) **PCMV delta r8.2** (https://www.addgene.org/12263/)

Purpose: Packaging lentiviral plasmid

This is a packaging plasmid (2nd generation) containing the HIV-1 gag, pol, tat and rev coding sequences, which encode the viral core proteins and replication enzymes required for the formation of the lentiviral structure and for replication and integration of the lentivirus. Expression is controlled by the CMV promoter. The plasmid also encodes an HIV-1 Rev response element (RRE) to allow Rev-dependent expression of the tet genes. An ampicillin resistance gene is also included to allow selection of the plasmid in E.coli. An SV40 early promoter and origin sequence facilitate high-level expression of the selection marker and episomal replication in cells expressing the SV40 large T antigen.

c) **pGIPZ lentiviral vectors** expressing shRNA against NNT (RHS4430-98851990; RHS4430-98913600; RHS4430-98524425; RHS4430-101033169 RHS4430-101025114 from Dharmacon) (http://dharmacon.gelifesciences.com)

Purpose: lentiviral Gateway destination vectors, shRNA expression

These are the lentiviral expression vectors which will express the shRNA of interest in the transfected mammalian cells. They include 2 bacteriophage-derived recombination sites; puromycin resistance genes for plasmid selection in mammalian cell cultures and bacterial cultures, respectively; a turboGFP (green fluorescent protein)-encoding sequence for microscopic confirmation of transfection; an human CMV promoter driving strong trans-gene expression; a packaging sequence; a Rev response element to enhance packaging efficiency. For additional safety, the 3' long terminal repeat (LTR) is self-inactivating. A mix of the 5 different plasmids detailed above was used, all containing anti-NNT shRNAs. Plasmids containing scramble, nonsense shRNA (SCR ShRNA) were used separately to generate negative controls.

All plasmids were kindly donated by Dr Eirini Meimaridou and Dr Lou Metherell from Queen Mary University of London, in the context of collaborative work.

Plasmids were applied to 6-well plates containing HEK-293T (human embryonic kidney tumour) cells. HEK-293T cells contain the SV-40 large T-antigen, thus allowing the fast replication of plasmids containing the SV40 reference sequence. Cells were transfected in Opti-MEM reduced serum media (Thermo Fisher), using the following plasmid quantities (per well) and employing lipofectamine (Thermo Fisher) as transfection vehicle:

a) Pmd2.g: 500 ng
b) PCMV delta r8.2: 1,000 ng
c) ShRNA-expressing plasmids: 1,500 ng
d) Lipofectamin 2000 Reagent (Thermo Fisher): 9 μl

Cells were incubated overnight at 37^{o}C; the next day, media was changed to normal HEK-293T culture media [Dulbecco's Modified Eagle Medium (DMEM - Gibco, Thermo Fisher)

supplemented with 10% Fetal Bovine Serum (Sigma), 2 mM L-glutamine (Sigma) and 1% Penicillin-Streptomycin (Sigma)]. After 24h, media was again changed to NCI-H295R cell culture media (DMEM-F12 supplemented with 2.5% Nu serum, 1% ITS+ Premix and 1% Penicillin-Streptomycin). The next day, media was collected, centrifuged at 1200 rpm, filtered using a 0.2 μm filter and applied to NCI-H295R cells, which had been plated at 6-well plates at 70-80% confluence. At the same time, fresh NCI-H295R media was added to the HEK-293T wells. The next day, the same process was repeated and virus-containing media was again applied to the same NCI-H295R cells. After 3-day incubation, transduction efficiency on microscopic evaluation (% fluorescent cells) exceeded 80%. At that point, selection with Puromycin (4 μg/ml) was commenced, boosting the percentage of fluorescent cells to over 90-95%.

All subsequent experiments/ assays were undertaken from 4-12 weeks post-transfection (passage 17-30, passage from transfection 5-18). 4 weeks was the earliest time-point for which the growth of a cell population sufficient to facilitate the desired experimental work was accomplished. Cells transfected with shRNA against NNT will hence be referred to as KD SHRNA cells, while their controls transfected with non-sense, scramble shRNA will be referred to as SCR SHRNA cells. Puromycin was regularly added to cell media for 1-week periods to maintain high percentage of transfected cells, but was not used during any of the experiments described below.

4.2.3 Redox balance assessment

To assess the effect of NNT knockdown on cellular redox balance, KD SHRNA cells and SCR SHRNA cells were loaded onto white opaque-walled, flat-bottomed 96-well plates at a concentration of 15,000 cells/well. After 24 hours, the intracellular ratio of reduced/ oxidised glutathione was measured (in triplicates) using the GSG/GSSG-Glo^{TM} assay (Promega) as described in Chapter 2. Menadione was applied to a pair of wells as positive control (potent inducer of oxidative stress) 2h before the assay.

4.2.4 Metabolic Flux Analysis

KD SHRNA and SCR SHRNA cells of the same passage growing in flasks were collected by trypsinisation and cell density was established by microscopy. Cells were loaded to Seahorse XF 24-well microplates at a loading density of 100,000 cells/well (media volume 100-150 µl). The next day, metabolic flux analysis was completed as described in Chapter 2.

4.2.5 Proliferation time-courses

Assessment of cellular proliferation and viability was performed in flat-bottomed, transparent-walled 96-well plates. At the beginning of each proliferation series, KD SHRNA and SCR SHRNA cells were loaded at a concentration of 8,000 cells/ well, in 100 µl of cell media. This loading concentration was selected after optimisation experiments comparing proliferation rates observed with various loading concentrations (5,000 – 15,000 cells/ well, data not shown). The next day, media was removed carefully to avoid disruption of plated cells and replaced by 200 µl of fresh media. One plate was frozen down at -80^{O}C to provide

baseline cell numbers (t=0 h). Cells were cultured for a further 96 h; media was replenished at 48h by removal of 100 µl old media and addition of 100 µl fresh media (per well). At least 5 wells per group (i.e. knockdown or control) were used in each time-course. At the end of the time-course, cell numbers were measured using DNA fluorescence, as described earlier (Chapter 2). Proliferation rates were established using the formula

Proliferation rate (%) = %(fluorescence at 96 h – fluorescence at 0 h)/ fluorescence at 0 h

In some time-courses, concurrent drug treatment or special growth media was applied to evaluate cellular proliferation and viability under special conditions (chemically-induced oxidative stress, glucose deprivation). Treatment was started 24h post cell loading (baseline time-point) and lasted 96 h. Treatment courses applied in the course of this project included:

a) Paraquat (N,N′-dimethyl-4,4′-bipyridinium dichloride, Sigma). Paraquat is a herbicide which is widely used as a chemical inducer of oxidative stress (superoxide generation) (Lei et al., 2014). Paraquat was administered for a total duration of 96 h and was replenished once in cell media during the proliferation course (48 h). Doses ranged from 10-30 µM. Stock solution of paraquat in sterile-filtered dH_2O was stored at 4^oC.
b) Glucose-deplete media (DMEM, L-Glutamine (+), glucose 1 g/dl, sodium pyruvate – Gibco, Thermo Fisher). Media was supplemented with 10% Foetal Bovine Serum (Sigma) and 1% ITS+ premix (BD Biosciences). Glucose-deplete media was administered for a total duration of 96 h and was replenished once during the proliferation course (48 h).

4.2.6 Apoptosis

To evaluate the effects of NNT knockdown on cellular apoptosis rates, KD SHRNA and SCR SHRNA cells were loaded to opaque-walled, flat-bottomed 96-well plates (Perkin-Elmer) at a loading concentration of 8,000 cells/well (10 wells/ group). Media was refreshed after 48 h by addition of 100 µl of cell media. Caspase activity was measured as described in Chapter 2 using 4 wells (replicates) per transfection group. At the end of the assay, plates were frozen at -80^{o}C and relative cell density in the remaining wells was assessed the next day using the the CyQuant® Proliferation Assay Kit (Thermo Fisher). Results from the proliferation assay were deployed to normalise the caspase assay results.

4.2.7 Steroid profiling by Liquid Chromatography/ Tandem mass spectrometry

To outline the impact of NNT knockdown on steroid production, stably transfected NCI-H295R cells were loaded to 6-well plates at a concentration of 500,000 cells/ well and incubated at 37^{o}C overnight. The next day, media was carefully removed and replaced by 1 ml of serum-free media (DMEM/F12 supplemented with 1% ITS+ premix and 1% Penicillin-Sterptomycin). Cells were incubated for 48 h at 37^{o}C. At the end of the incubation, media was collected in silinised glass tubes and stored at -20^{o}C. Protein was harvested as described in Chapter 2 and used to standardise the results to protein concentration. Steroid extraction from stored cell media was subsequently completed as described in Chapter 2.

4.3 Results

4.3.1 NNT silencing by shRNA transfection

The efficacy and duration of NNT silencing in NCI-H295R cells transfected with shRNA in 6-well plates was evaluated by Western Blotting and Real-Time PCR. We observed consistent suppression of NNT expression by > 80% in cells transfected with anti-NNT shRNA (KD SHRNA) in comparison to cells transfected with scramble, non-sense shRNA (SCR SHRNA). Gene silencing at a translational level was confirmed by Western Blotting, demonstrating all but complete elimination of the corresponding band (**Fig. 4-1A**). Real-time PCR was used to measure NNT expression at a transcriptional level 2-16 weeks post-transfection (**Fig. 4-1B**). The durability of NNT silencing was confirmed by repeated Real-Time PCR/ Western Blotting at regular intervals and microscopic evaluation confirming green fluorescence emission by > 90% of cultured cells.

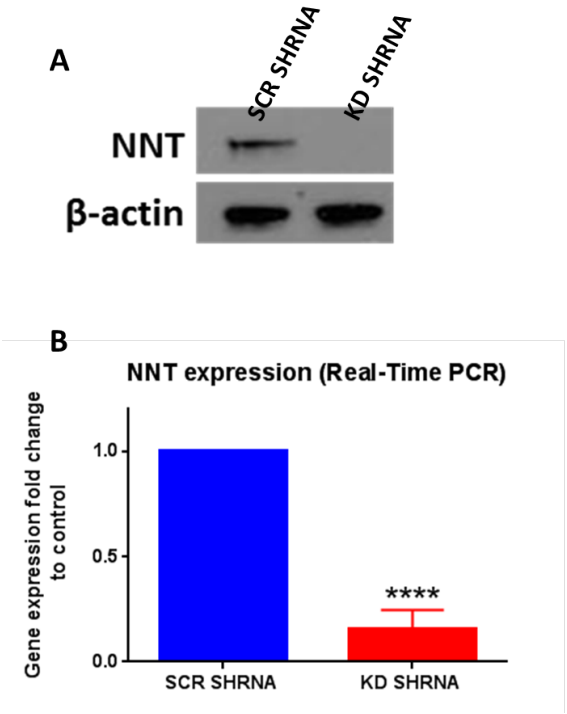

*Figure 4-1. Assessment of NNT knockdown in shRNA-transfected NCI-H295R cells by Real-Time PCR and Western Blotting. A) Western Blotting comparing NNT expression in cells transfected with SCR ShRNA vs KD ShRNA; B) Comparison of NNT mRNA expression in cells transfected with scramble, non-sense shRNA (SCR SHRNA, negative control) and shRNA against NNT (KD SHRNA). Results are expressed as fold-change to control (****p<0.0001; n>10 independent experiments).*

4.3.2 Cellular redox balance

The effect of stable NNT silencing on NCI-H295R cellular redox balance was determined by measurement of the cellular ratio of reduced to oxidised glutathione (GSH/GSSG ratio), 96 h post-transfection (GSH/GSSG-Glo^{TM} assay, Promega). Lower GSH/GSSG ratios suggest higher intracellular levels of oxidative stress and compromised residual antioxidant capacity. Contrary to the phenotype observed in the transient KD model (where acute NNT loss was associated with a decrease in the ratio of reduced/ oxidised glutathione), we observed no

significant differences between the redox status of SCR SHRNA and KD SHRNA cells [median (IQR) GSH/GSSG ratio in KD SHRNA cells normalised to SCR SHRNA cells 0.96 (0.83 – 1.03); p>0.05, n=10 independent experiments] (**Fig. 4-2**). This suggests development of redox adaptation with time in this cell model to compensate for NNT loss.

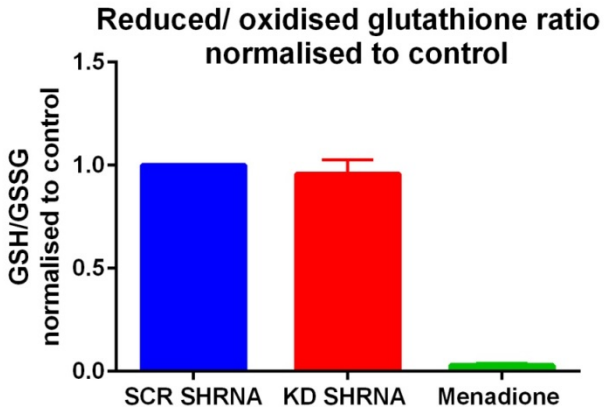

Figure 4-2 GSH-GSSG ratio in stably transfected NCI-H295R cells. No significant difference was observed between KD SHRNA and SCR SHRNA cells. Menadione: NCI-H295R cells treated with Menadione (40 μM) for 2 h as positive control. Bars represent median ± IQR values (p>0.05, n=10 independent experiments).

4.3.3 Mitochondrial bioenergetics

Changes in mitochondrial respiration were evaluated by direct measurement of cellular oxygen consumption, using Extracellular Flux analysis (Seahorse XF analyser). We observed a statistically significant increase in baseline oxygen consumption rates (OCR) in KD SHRNA cells in comparison to SCR SHRNA cells [median (IQR) OCR for SCR SHRNA cells 10 (4.3-11) pmol/l/μg protein, KD SHRNA cells 15 (7.8-16.5) pmol/l/μg; p<0.05, n=7 independent experiments]. This difference was sustained in response to successive

administrations of mitochondrial respiration inhibitors (oligomycin, FCCP, Antimycin A & Rotenone), though narrowly missing statistical significance (**Fig. 4-3A**). Similar to the transient KD model, we observed that the maximal oxygen consumption displayed post-FCCP was similar to the baseline OCR of NCI-H295R cells, although post-FCCP OCRs exhibited considerable variability. There was also a trend towards higher baseline extracellular acidification rates (ECAR), representative of glycolytic rates, with stable NNT KD (1.85 ± 0.24 mpH/min/protein for SCR SHRNA cells vs 2.3 ± 0.30 mpH/min/protein for KD SHRNA cells; p=0.063, n=7) (**Fig. 4-3B**).

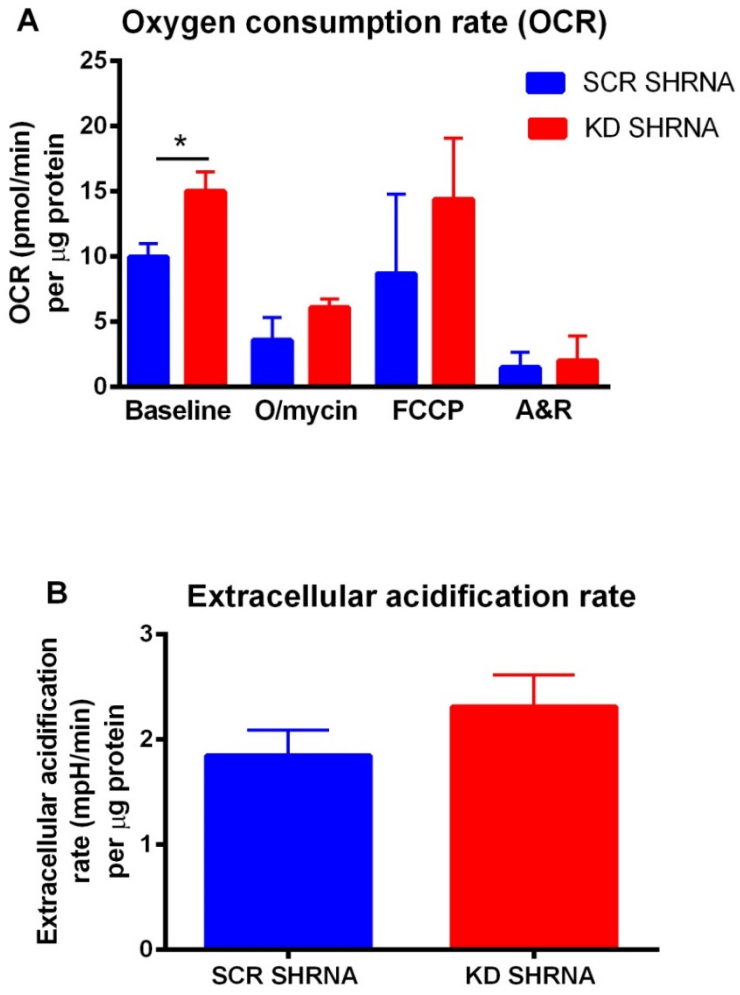

*Figure 4-3 A) Seahorse XF24 analysis of cellular oxygen consumption rate (OCR) in stably transfected NCI-H295R cells, at baseline and after successive application of three mitochondrial respiration inhibitors. Results were standardised for cell number using protein content as a surrogate marker. Bars represent median ± IQR values. KD SHRNA cells displayed higher baseline OCR than their controls. O/mycin: Oligomycin; FCCP: Carbonyl cyanide-p-trifluoromethoxyphenylhydrazone; A&R: Antimycin A plus Rotenone. *P<0.05, n=7 independent experiments. B) Baseline extracellular acidification rate standardised for protein content. Bars represent mean ± SEM values. A tendency towards higher ECAR was observed in KD SHRNA cells, without reaching statistical significance (p=0.06, n=7).*

4.3.4 Cellular proliferation

Cellular proliferation was assessed over a 96h period; repeat experiments were conducted from 4-12 weeks from initial transfection. Proliferation rates were provided by the following ratio: %[(DNA fluorescence emitted at end point - DNA fluorescence emitted at baseline)]/ DNA fluorescence emitted at baseline. In this model, NNT knockdown was also associated with slower proliferation, but the effect was evidently less marked than the one observed in the acute knockdown model (proliferation rate of SCR SHRNA cells 164% ± 17%, KD SHRNA cells 135 ± 17%; $p<0.05$, n=13 independent experiments) (**Fig. 4-4**).

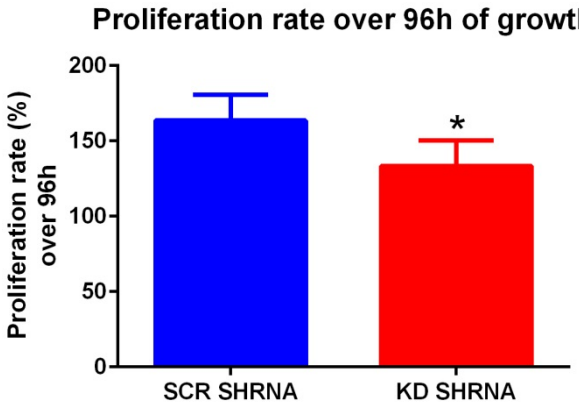

*Figure 4-4 Proliferation rate of NCI-H295R cells over a 96h period of growth, measured by DNA fluorescence. KD SHRNA cells displayed significantly lower proliferation than SCR SHRNA cells. Proliferation rate = %[(DNA fluorescence emitted after 96 h - DNA fluorescence emitted at baseline)/ DNA fluorescence emitted at baseline] (*p<0.05, n=13 independent experiments).*

4.3.5 Apoptosis

We explored the effect of chronic NNT silencing on cell death measuring intracellular activity of caspase 3 and 7, effector caspases of cellular apoptosis. In antithesis with our findings in the transient KD model, we observed no effect of NNT knockdown on cellular apoptosis rates with chronic gene silencing [median (IQR) caspase activity ratio normalised for cell number KD SHRNA vs SCR SHRNA cells 0.925 (0.74-1.15); p>0.05, n=4 independent experiments] (**Fig. 4-5**).

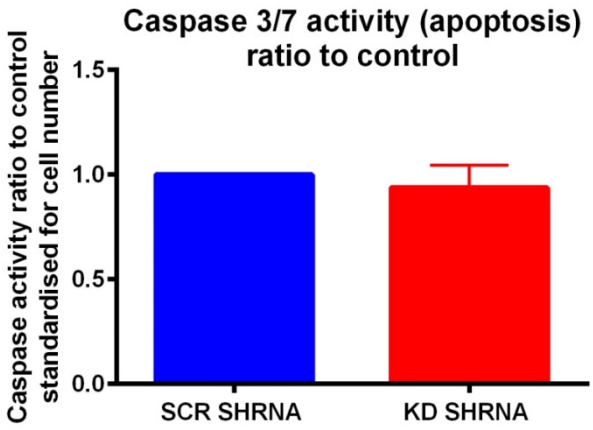

Figure 4-5 Effect of stable NNT knockdown on cellular apoptosis, measured by determination of caspase 3 and 7 activity. No significant difference was observed in apoptotic rates between KD SHRNA and SCR SHRNA cells (p>0.05, n=4 independent experiments).

4.3.6 Proliferation under chemically induced oxidative stress and glucose deprivation

Paraquat was administered over a 96 h period to establish whether chronic NNT silencing renders NCI-H295R cells more sensitive to chemically induced oxidative stress, as was the case with acute NNT knockdown. We observed no difference in cellular proliferation between KD SHRNA and SCR SHRNA cells with either low- or high-dose paraquat exposure (**Fig. 4-**

6). These results are congruous with the evaluation of baseline redox balance in the same model, which also revealed no difference between KD and control cells.

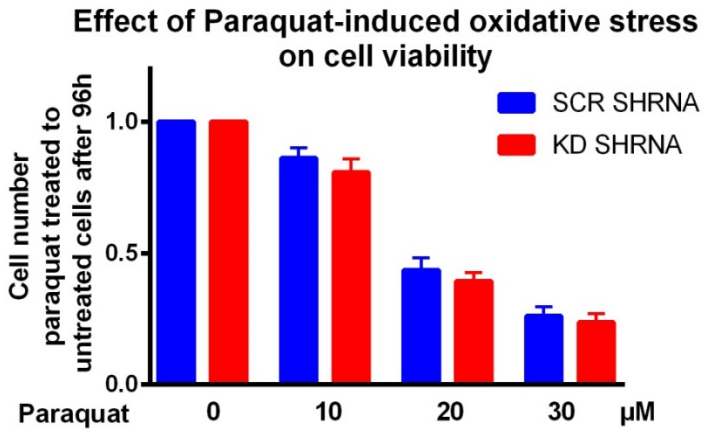

Figure 4-6 Effect of stable NNT KD on cellular response to chemically-induced oxidative stress. The pro-oxidant agent paraquat was administered to KD SHRNA and SCR SHRNA cells for 96 h at incremental doses (10, 20 and 30 μM) and cell proliferation was assessed. No difference was observed between the two groups (p>0.05, n=13 independent experiments).

We also explored the effect of glucose deprivation on ACC cell proliferation, culturing KD SHRNA and SCR SHRNA cells in low-glucose media. We observed that proliferation was similarly suppressed in the two groups of cells, with no statistically significant difference between them (**Fig. 4-7**).

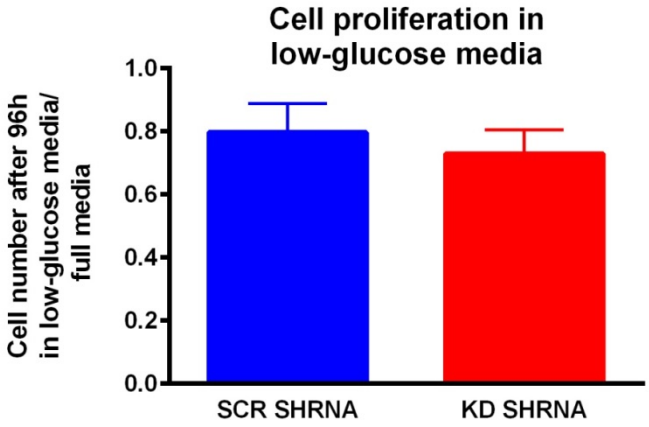

Figure 4-7 Proliferation of stably transfected NCI-H295R cells in low-glucose media. No significant difference was observed between KD SHRNA and SCR SHRNA cells (p>0.05, n=5 independent experiments).

4.3.7 Steroidogenesis

The compensated phenotype we observed with chronic (shRNA-mediated) NNT knockdown extended to steroidogenesis. We observed no statistically significant difference in cortisol (SCR SHRNA cells 0.039 ± 0.008 nM/ µg protein, KD SHRNA 0.049 ± 0.005 nM/ µg protein; p>0.05, n=6 independent experiments) or androstenedione synthesis (SCR SHRNA cells 0.44 ± 0.05 nM/ µg protein, KD SHRNA 0.41 ± 0.05 nM/ µg protein; p>0.05, n=6 independent experiments) between KD SHRNA and SCR SHRNA cells (**Fig. 4-8**), although a trend towards higher cortisol production with NNT KD was noted. Likewise, activity of CYP11B1, CYP21A2 and CYP17 was not significantly different between the two groups, although a trend towards higher CYP11B1 and CYP21A2 activity for KD SHRNA cells was noted (**Table 4-1**).

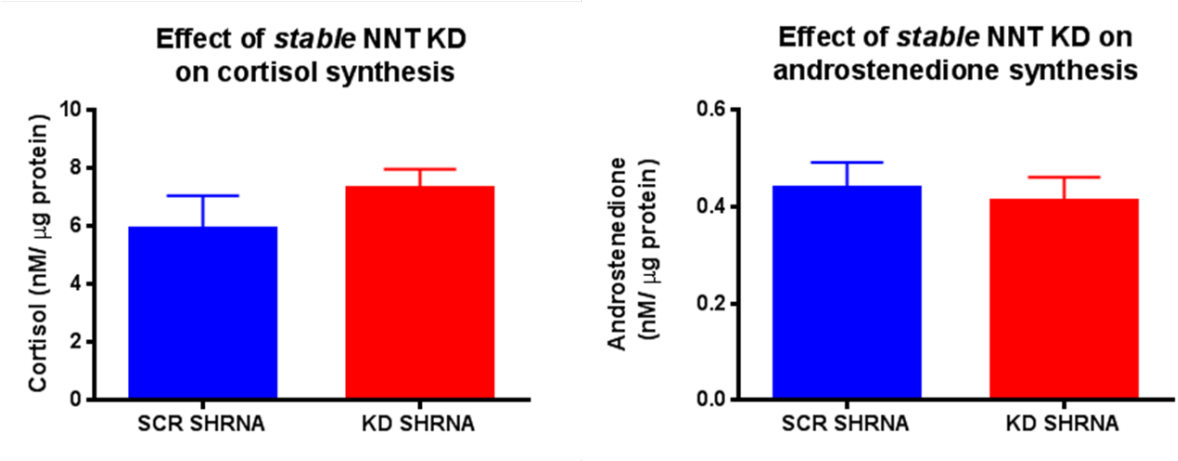

Figure 4-8 Effects of stable NNT knockdown on adrenal glucocorticoid (cortisol) and androgen (androstenedione) synthesis. No differences were observed between KD SHRNA and SCR SHRNA cells (p>0.05, n=6 independent experiments).

Table 4-1 Steroidogenic enzyme activity in SCR SIRNA and KD SIRNA cells, derived from product-to-substrate ratios (LC-MS/MS). Results are expressed as mean ± SEM values (n=6 independent experiments)

Enzyme	Product/ substrate ratio	SCR SiRNA (nM/µg)	KD SiRNA1 (nM/µg)	P value
CYP11B1	cortisol/ 11-deoxycortisol	0.03 ± 0.005	0.04 ± 0.006	p>0.05
CYP21A2	11-deoxycortisol/ 17-OH-progesterone	18.9 ± 4.4	22.9 ± 5	p>0.05
CYP17A1	androstenedione/ 17-OH-progesterone	3.8 ± 0.8	3.8 ± 0.6	p>0.05
HSD11B1	cortisol/ cortisone	6.6 ± 3.7	7.3 ± 2.4	p>0.05

4.4 Discussion

The longer-term effects of NNT loss on ACC cells, as delineated in the stable knockdown model we generated, were disparate from the ones encountered in the acute setting. Importantly, with long-term culture (4-12 weeks) under constant NNT silencing, NCI-H295R cells managed to restore their redox balance. This compensation abrogated the pro-apoptotic early impact of NNT loss. Interestingly, a persistent proliferative handicap was demonstrated, though this was less marked than the one observed in the acute setting. Extracellular flux analysis revealed higher rates of oxygen consumption in KD SHRNA cells, as well as a trend towards higher glycolytic rates. This response may reflect higher energy needs. Of note, these results contradict the findings of Yin et al. and Fuzisawa et al., who reported suppressed oxidative phosphorylation in response to NNT loss in rat phaeochromocytoma cells and human lymphocytes, respectively (Yin et al., 2012, Fujisawa et al., 2015).

Said compensation appears to have developed during the first four weeks of culture post-transfection. Successful knockdown was first confirmed 2 weeks post transfection, but 4 weeks was the first time point at which an adequate bulk of transfected cells had been grown to allow repeat experiments. We observed no differences in the metabolic, proliferative or steroidogenic phenotype of cells from 4-12 weeks post-transfection.

Redox adaptation to chronic oxidative stress has been previously described in tumour models *in vitro*; this process is driven by the strong selective pressure of oxidative toxicity and promoted by the genomic instability (oxidative DNA damage/ impaired DNA repair) which characterises the oxidised intracellular microenvironment (Trachootham et al., 2009). The adaptive response is often orchestrated by versatile transcription factors, most notably Nrf2 and Nf-κB, which can up-regulate the expression of core antioxidant genes (superoxide

dismutase, catalase, glutathione pathway, thioredoxin pathway). Inactivation of apoptotic factors (e.g. caspases) and/or stimulation of pro-survival molecules (e.g. Bcl2) has also been described (Trachootham et al., 2009, Sullivan and Graham, 2008, Chen et al., 2007). In the absence of NNT, potential compensatory mechanisms that may mediate redox adaptation include alternative NADPH resources (e.g. malic enzyme, isocitrate dehydrogenase, tetrahydrofolate reductase) or NADPH-independent ROS scavengers (e.g. catalase). Ongoing work, which has not been completed at the time of submission of this thesis, involves comparative analysis of the complete molecular landscape that is shaped by acute and chronic NNT silencing, through whole-transcriptome RNA sequencing and whole metabolome analysis. This is expected to provide useful insights illuminating the adaptive cell response to NNT loss.

It is noteworthy that no chronic impact of NNT loss on steroidogenesis was apparent in this model, completing the picture of successful metabolic adaptation. These results confirm that NNT deficiency does not functionally inhibit steroidogenesis as a result of the compromised NADPH supply within the mitochondria. This finding could be explained either by compensatory up-regulation of alternative NADPH resources or because the proportion of mitochondrial NADPH that is contributed by NNT is not high enough to constitute a limiting factor for steroidogenic monooxygenases. On the basis of our results, it appears most likely that the adrenal insufficiency of NNT-deficient patients is due to oxidative adrenocortical cell damage, which could potentially evolve already *in utero*. Of relevance, pathways with an integral role in adrenocortical development during embryogenesis (e.g. Sonic Hedgehoc pathway) can be disrupted by oxidative stress (Xiao et al., 2015).

Overall, our *in vitro* work suggests that NNT targeting as a treatment strategy in ACC merits further exploration with *in vivo* pre-clinical models (e.g. xenograft mouse models). It is difficult to predict whether the transient KD or the stable KD model better reflects the anti-tumour potential of NNT silencing *in vivo*, but it is worth noting that the anti-proliferative effect was maintained even with chronic gene silencing, if to a lesser degree. Inducible knockdown may provide the most suitable xenograft model. An alternative option would be to employ pharmacological inhibitors of NNT. A caveat here is that although a number of inhibitors have been described in the literature (adenosine derivatives, palimityl-CoA derivatives, dicyclohexylcarbodiimide, dethylpyrocarbonate), all available data stem from *in vitro* studies (Phelps and Hatefi, 1981, Rydstrom, 1972). A major advantage of NNT targeting is the anticipated low toxicity of such an approach, given the adrenal-specific clinical phenotype of patients with NNT mutations.

5 Urinary steroid profiling as a novel surveillance tool to detect ACC recurrence

5.1 Introduction

Adrenocortical carcinoma is a rare (incidence 1-2 cases/million/year) but aggressive malignancy (Kebebew et al., 2006, Libe et al., 2015). Disease recurrence rates are high, exceeding 50% even in patients with microscopically complete (R0) resection (Pommier and Brennan, 1992, Stojadinovic et al., 2002). Therefore, vigilant surveillance of all operated patients by regular cross-sectional imaging is essential for several years (Libe, 2015, Fassnacht et al., 2013, Else et al., 2014). Although the optimal surveillance protocol has yet to be established, a common approach in expert centres (including University Hospitals Birmingham) involves three-monthly CT scans (thorax and abdomen) in the first two post-operative years, six-monthly CT scans in the next three years and annual scans in years 6-10 post-operatively. This is associated with considerable costs, prolonged radiation exposure and frequent diagnostic ambiguity in early stages of recurrent/ metastatic disease (Cawood et al., 2009). Early detection of disease recurrence is important, as it may allow either radical re-do surgery in cases of limited metastatic disease volume, or early institution of mitotane and/or cytotoxic chemotherapy, potentially prolonging survival (Libe, 2015, Else et al., 2014, Erdogan et al., 2013, Datrice et al., 2012, Mihai, 2015, Schulick and Brennan, 1999). The number of metastatic sites at diagnosis of recurrent disease has been shown to be an independent prognostic factor (Erdogan et al., 2013, Assie et al., 2007).

Most ACCs (45-70%) are biochemically active, usually presenting an inefficient steroidogenic pattern dominated by steroid precursor metabolites (Arlt et al., 2011, Fassnacht and Allolio, 2009, Luton et al., 1990). The cause of this characteristic steroidogenic pattern has not been definitively elucidated, but it has been tentatively attributed to the relative dedifferentiation of malignant cells or the high frequency of mutations within the malignant cellular microenvironment (Arlt et al., 2011, Kerkhofs et al., 2015). Most of these hormones,

which represent intermediate steps along the three biosynthetic pathways, are not detectable in routine clinical biochemistry. Analysis of 24h urine collections by gas chromatography and mass spectrometry (GC-MS), however, can quantify the metabolites of every adrenal steroid (precursor) hormone, providing a truly comprehensive outline of steroidogenesis. This allows the detection of minute changes in steroidogenesis and the illumination of all intermediate steps that tend to be perturbed in the setting of adrenocortical malignancy (Arlt et al., 2011, Kerkhofs et al., 2015). This approach was first explored in a sizeable retrospective patient cohort by Arlt et al. in 2011 with a multi-centre European Study facilitated through the European Network for the Study of Adrenal Tumours (ENSAT) (Arlt et al., 2011). Urinary steroid metabolite profiles from 102 patients with benign adrenocortical adenomas and 56 patients with ACC were compared using computational analysis (machine learning). The nine steroid biomarkers with the highest diagnostic performance were selected and integrated in a diagnostic algorithm which managed to differentiate between benign and malignant tumours with a sensitivity and specificity of 90%. Some degree of adrenal hormone/ hormone precursor hypersecretion was present in 95% of ACCs (Arlt et al., 2011). In this study, we are evaluating the diagnostic performance of this novel approach in a different clinical context: the post-operative surveillance of ACC patients following microscopically complete (R0) tumour resection.

5.2 Methods

5.2.1 Study population

Serial post-operative 24-hour urine samples were prospectively collected from patients with histologically confirmed ACC, who had undergone microscopically complete (R0) tumor resection in 12 clinical specialist referral centers participating in the European Network for the Study of Adrenal Tumors (ENS@T; www.ensat.org), after approval of local ethical review boards and informed patient consent. Participating countries included the UK (Birmingham), Germany (Wurzburg, Munich, Berlin), France (Paris), Italy (Florence, Turin), the Republic of Ireland (Dublin, Galway), Poland (Warsaw), Croatia (Zagreb) and Portugal (Lisbon). Urine samples were collected between 2007 and 2016. Inclusion criteria were defined as a) history of ACC with histological confirmation, b) complete (R0) tumor resection and c) provision of at least one post-operative urine sample at a disease-free state, i.e. before any radiological evidence of disease recurrence, and within two years from surgery. ACC recurrence had to be confirmed by one of the following: a) emergence of new lesions on cross-sectional imaging (CT, MRI) which either enlarge on follow-up scans, or regress in response to chemotherapy, b) emergence of enhancing lesions on PET or PET-CT scans, or c) histological evidence of recurrent/metastatic ACC on percutaneous biopsy or metastasectomy. Participating centres were prompted to provide urine samples every three months, but actual frequency of provided samples did not constitute an exclusion criterion as long as at least one post-operative sample at disease-free state had been provided.

5.2.2 Biochemical analysis

Measurement of 24-h urinary steroid metabolite excretion in 129 recruited ACC patients as well as in a healthy control cohort (50 men, 77 women, age range 20–81 yr) was carried out by GC-MS. Urinary steroid profiling by GC-MS was established 40 years ago by Shackleton et al. (Shackleton and Snodgrass, 1974) and Sjovall (Sjovall, 1975), and still boasts the highest analytical sensitivity for steroid metabolite detection in biological samples (Arlt et al., 2011). The first separation stage (gas chromatography) involves evaporation of purified and chemically processed (derivatised) steroid samples which run -in a gaseous form- through a liquid column (stationary phase) at different speeds according to their affinity to the column. At the end of the column, steroids reach the mass spectrometer, where they are bombarded with electrons and fragmented into molecule-specific ionised particles in a special collision cell. The resulting fragments are then selected according to their mass-to-charge ratio through acceleration within a quadrupole (Arlt et al., 2011, Taylor et al., 2015).

To prepare samples for GC-MS analysis, free and conjugated steroids were extracted from 5 ml urine samples by solid-phase extraction using SepPak columns (Waters, Milford, Ma, USA). Columns were prepared by washes with 4 ml methanol (Sigma) and 4 ml double-distilled water (ddH_2O). After sample loading, the columns were washed with 4 ml ddH_2O and steroids were eluted in 4 ml methanol in a clean biosilicate tube. Samples were left to evaporate in a heat-block (55^oC), aided by N_2 steam. The remaining dry samples (steroids) were incubated for 3 hours at 55^oC in a special hydrolysis buffer (3 ml 0.1M acetate buffer [pH 4.8-5.0] + 10 mg ascorbate + 10 mg sulfatase/glucoronidase; all ingredients purchased from Sigma) to remove glucuronide and sulphate groups (deconjugation). Deconjugated steroids were subsequently reloaded onto SepPak columns and eluted into glass tubes with 4

ml methanol. The final stage of sample preparation consisted in chemical derivatisation, to enhance the sensitivity of mass spectrometry. To achieve this, samples were again evaporated and three drops of 2% methoxyamine-pyridine were added. After vortexing, tubes were incubated at 55^{o}C for one hour, then evaporated under N_2. In the next step, 75 µl of N-trimethylsilylimidazole (Sigma) were added; tubes were vortexed again and incubated at 120^{o}C overnight. Subsequently, samples were extracted by adding 2 ml cyclohexane and 2 ml dH_2O, each step followed by vortexing. After centrifugation (1,000 x g for 5 minutes), the bottom layer was discarded. Another 2 ml dH_2O were added, followed by the same sequence of vortexing, centrifugation and removal of the bottom layer. The top layer, which contained the extracted steroids in cyclohexane, was transferred into injection vials. The samples were then injected into an Agilent 5973 GC mass-spectrometer operating in selected-ion-monitoring (SIM) mode to achieve sensitive and specific detection and quantification of 33 selected steroid metabolites (**Table 5-1**, **Fig. 5-1**).

Table 5-1 Steroid metabolites detected in 24h urine collections by GC-MS, tabulated against the steroid hormones they originate from.

Steroid metabolite	*Metabolite of*
Androgen metabolites	
Androsterone (An)	Androstenedione, testosterone, 5α-dihydrotestosterone
Etiocholanolone (Et)	Androstenedione, testosterone
11β-hydroxyandrosterone (11β-OH-An)	11β-hydroxyandrostenedione
Androgen precursor metabolites	
Dehydroepiandrosterone (DHEA)	DHEA and DHEA sulphate (DHEAS)
16α-hydroxy- DHEA (16α-OH-DHEA)	DHEA + DHEAS
Pregnenetriol (5-PT)	17-hydroxypregnenolone
Pregnenediol (5-PD)/ Pregnadienol	Pregnenolone
Mineralocorticoid metabolites	
Tetrahydro-11-dehydrocorticosterone (THA)	Corticosterone, 11-dehydrocorticosterone
5α- tetrahydro-11-dehydrocorticosterone (5α-THA)	Corticosterone, 11-dehydrocorticosterone
18-hydroxy-dehydrocorticosterone (11-OH-THA)	11-oxo-corticosterone, 11-dehydrocorticosterone
Tetrahydrocorticosterone (THB)	Corticosterone
5α-tetrahydrocorticosterone (5α-THB)	Corticosterone
Tetrahydroaldosterone (3α5β-THALDO)	Aldosterone
Mineralocorticoid precursor metabolites	
Tetrahydro-11- deoxycorticosterone (THDOC)	11-deoxycorticosterone
5α-tetrahydro-11-deoxycorticosterone (5α-THDOC)	11-doxycorticosterone
Gluocorticoid precursor metabolites	
Pregnanediol (PD)	Progesterone
3α, 5α-17-hydroxypregnanolone (3α5α-17HP)	17-hydroxyprogesterone
17-hydroxy-pregnanolone (17HP)	17-hydroxyprogesterone
Pregnanetriol (PT)	17-hydroxyprogesterone
Pregnanetriolone (PTONE)	21-deoxycortisol
Tetrahydro-11-deoxycortisol (THS)	11-deoxycortisol
Total glucocorticoid metabolites	
Cortisol (F)	Cortisol
6β-hydrocortisone (6β-OHF)	Cortisol
Tetrahydrocortisol (THF)	Cortisol
5α-tetrahydrocortisol (5α-THF)	Cortisol
α-cortol	Cortisol
β-cortol	Cortisol
11β-hydroxyetiocholanolone (11β-OH-Etio)	Cortisol
Cortisone (E)	Cortisone
Tetrahydrocortisone (THE)	Cortisone

α-cortolone	Cortisone
β-cortolone	Cortisone
11-oxo-etiocholanolone (11-oxo-Etio)	Cortisol

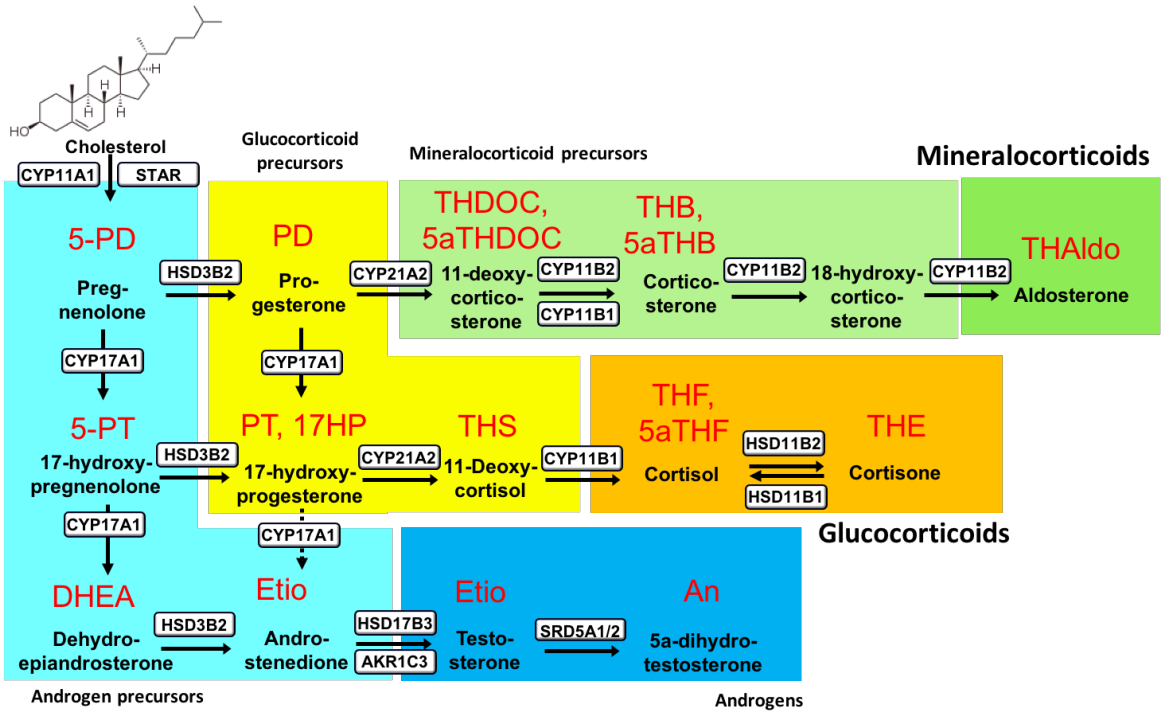

Figure 5-1 Adrenal steroid hormones and precursor hormones along the steroidogenic pathways (small print) and their metabolites detected by GC-MS in urine (coloured bold print). AKR1C3: Alpha-Keto-Reductase Family 1 Member C3.

5.2.3 Expert review of steroid profile

Three clinical endocrinologists with experience in adrenal disease were provided with 24-steroid profiles derived from serial post-operative samples contributed by patients who either a) developed disease recurrence or b) remained recurrence-free over a follow-up period of at least 3 years. The latter comprised a negative control cohort, as the chances of disease recurrence past this time-point are relatively low (Beuschlein et al., 2015). Pre-operative steroid profiles were also provided when available. Clinicians were asked to independently review the longitudinal steroid profile series from each individual patient retrospectively and identify any samples which they considered highly suggestive of disease recurrence. Reference ranges derived from the healthy controls groups were provided for each steroid. All assessors were blinded with regard to clinical information other than basic patient demographics (age, sex), sampling time in relation to surgery and use of mitotane. Recurrence detection was considered successful only if it preceded or coincided with the earliest urine sample collected after the first radiological manifestation of recurrent disease (i.e. late biochemical detections in relation to imaging did not count as true positives).

5.2.4 Statistical analysis

Data analysis and graphic representation was completed using Graphpad Prism Software. Data are summarised as median (IQR) values unless otherwise stated. Two-group comparisons were performed using the Mann-Whitney test. Comparisons between multiple groups were performed using the Kruskal-Wallis test.

5.3 Results

5.3.1 Patient characteristics

129 patients (62 men, 67 women) who had undergone complete (R0) resection of a histologically confirmed ACC provided at least one 24-hour urine sample whilst considered disease-free according to the most recent clinical and radiological assessment and no later than 2 years post-operatively. Median age at diagnosis was 55 years (range 14-80 years). Frequency and total number of urine samples varied considerably among participants. The follow-up period, as determined by perusal of relevant clinical entries on the ENSAT online clinical registry, was variable with a median follow-up of 31 months (IQR 18-42 months). During this period, 41 patients developed disease recurrence; 9 of them had to be excluded as no post-recurrence urine could be provided (**Fig. 5-2**). Two patients developed serial recurrences (with intermediate complete metastasectomy), providing urine samples before and after each one of them, so that the total number of recurrences amounted to 34. Of the remaining patients, 40 were clinically and radiologically followed up for over 3 years; these were considered cured comprising a 'negative control' cohort for the purposes of this study, as the natural history of ACC rarely involves recurrences presenting after this post-operative time-point (Beuschlein et al., 2015). Relevant clinical details for the 32 recurred patients and the 40 disease-free controls are provided in Table 5-1.

Of the 32 recurred patients, 13 had provided a urine sample before resection of the primary tumour; the remaining 19 patients only contributed post-operative urine samples. All samples provided by patients in these two subgroups are depicted in **Fig. 5-3**, plotted against time after surgery.

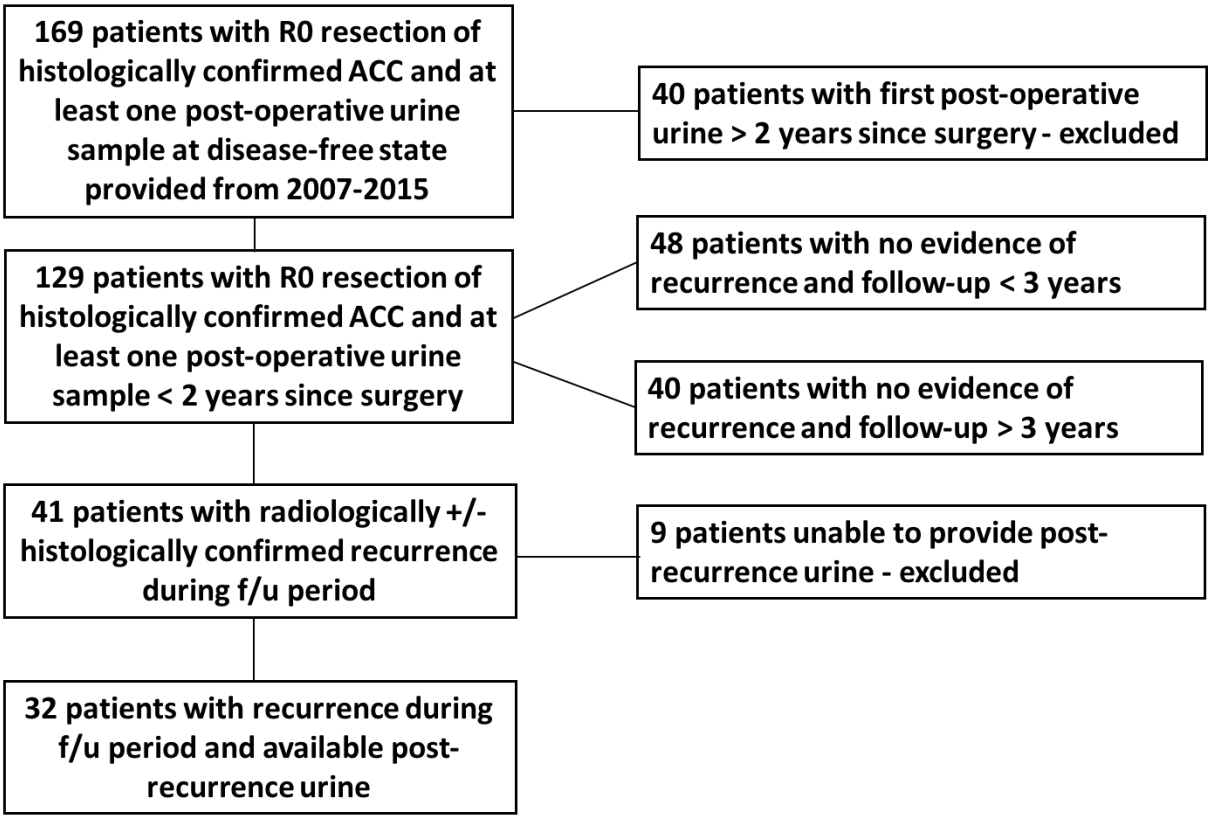

Figure 5-2 Recruitment flow chart. 32 patients with recurrence comprised the 'disease-positive' cohort. 40 patients with no evidence of recurrence for over three years comprised the 'disease-negative' control group.

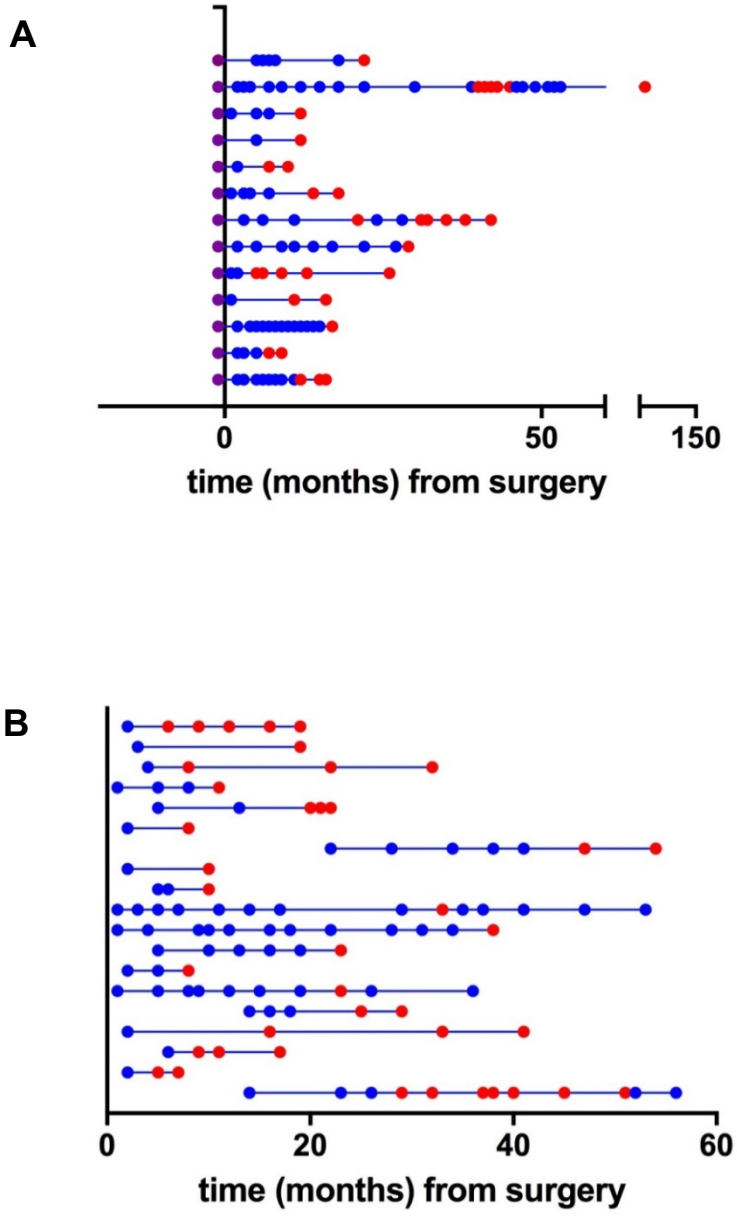

Figure 5-3 Urine samples provided by 32 patients who developed post-operative disease recurrence, plotted against time from surgery. Each line corresponds to a single patient. Red represents samples provided after the first radiological manifestation of recurrent disease; blue represents pre-recurrence samples. Purple dots represent pre-operative samples. A) Patients who provided both pre- and post-operative samples. B) Patients who provided post-op urine samples only.

Table 5-2 Characteristics of study participants who developed ACC recurrence or remained disease-free for at least three years post-operatively.

	Recurred patients	Non-recurred patients
number	32	40
Age (median, range)	52 (22-80)	56 (24-75)
Male (%)	7 (22%)	17 (43%)
Tumour size mm (median, IQR)	94 (70.5-117.5)	80 (75 – 99)
BMI kg/m^2 (median, IQR)	25.2 (21.5-26.8)	22.9 (21.5 – 24.3)
Hormone excess on routine biochemistry (%)	21 (66%)	16 (46%)
Ki67% (median, IQR)	10 (8 – 28)	7 (5-13)
Adj Mitotane (%)	20 (63%)	28 (70%)
Time (months) to recurrence (median, IQR)	14.7 (9.9-24.5)	N/A

5.3.2 Steroid ratios

The expected longitudinal biochemical trail of a gradually enlarging ACC mass (local recurrence or metastasis) would consist in a progressive rise in the value of one or more urinary steroid metabolites. Examples of such trends for some recurred patients in this study are provided in **Figure 5-4**. **Figure 5-5** presents two indicative heat-maps with longitudinal changes in urinary steroid metabolites during follow-up.

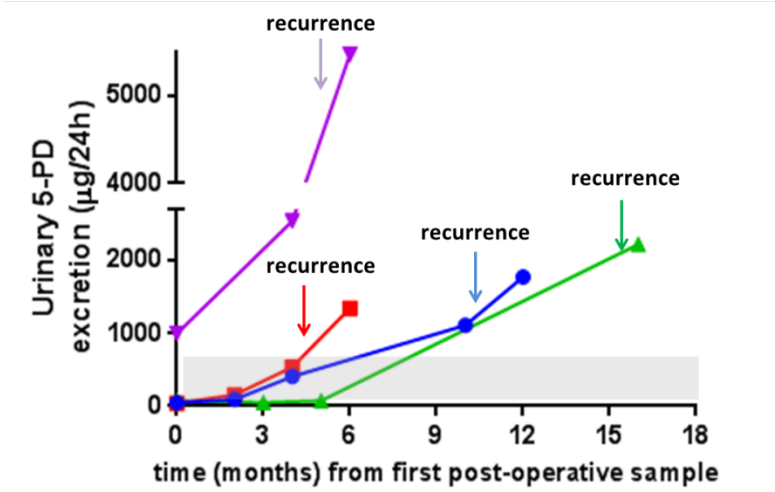

Figure 5-4 Longitudinal post-operative changes in the urinary steroid biomarker 5-PD (pregnenediol) in four female patients who eventually developed disease recurrence. Arrows point to the time of the first radiological detection of recurrent ACC for each patient. The shaded area of the graph represents the 5th-95th centile area for sex-matched healthy controls.

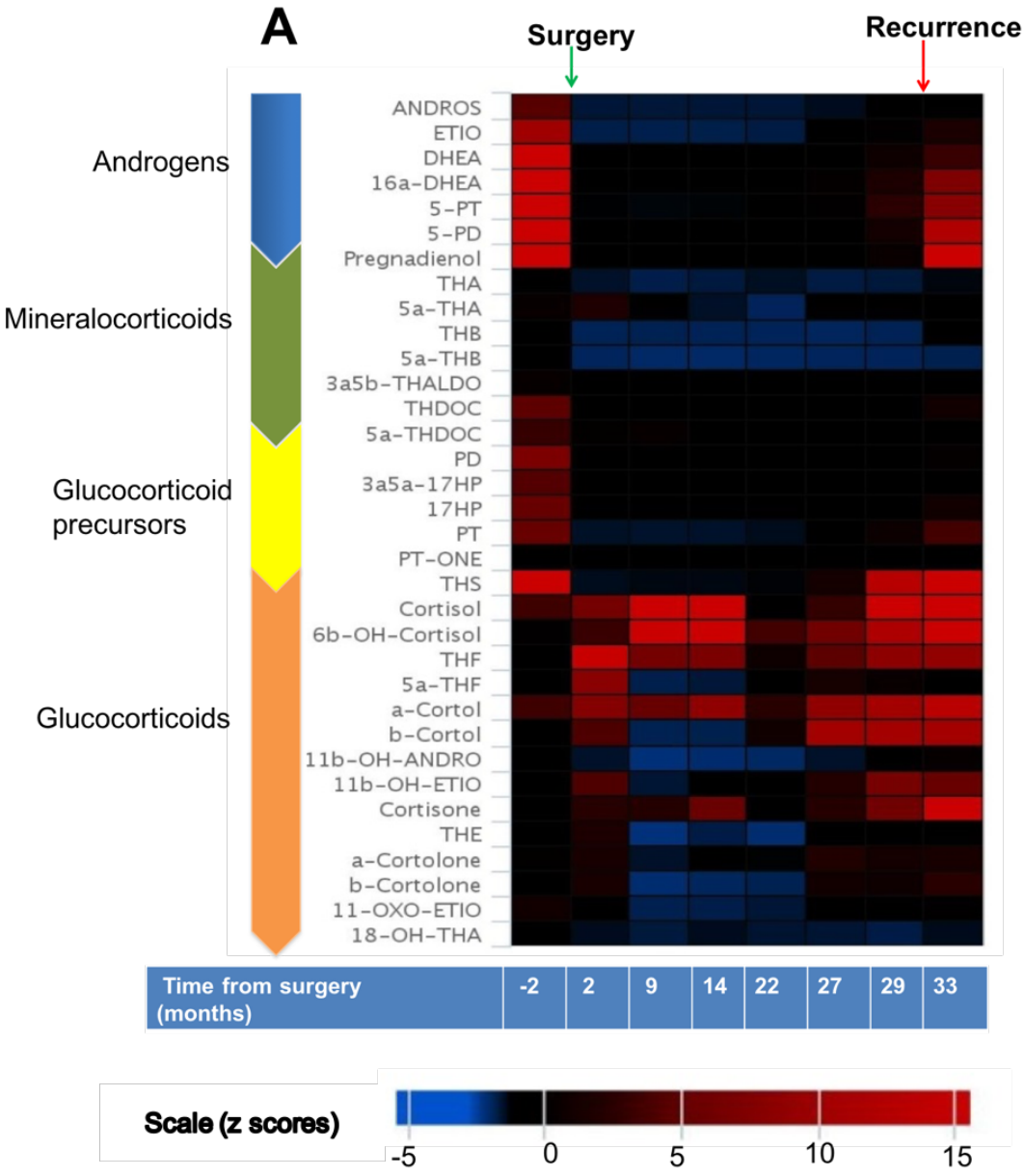
A
Surgery
Recurrence
Androgens
Mineralocorticoids
Glucocorticoid precursors
Glucocorticoids
ANDROS
ETIO
DHEA
16a-DHEA
5-PT
5-PD
Pregnadienol
THA
5a-THA
THB
5a-THB
3a5b-THALDO
THDOC
5a-THDOC
PD
3a5a-17HP
17HP
PT
PT-ONE
THS
Cortisol
6b-OH-Cortisol
THF
5a-THF
a-Cortol
b-Cortol
11b-OH-ANDRO
11b-OH-ETIO
Cortisone
THE
a-Cortolone
b-Cortolone
11-OXO-ETIO
18-OH-THA
Time from surgery (months)
-2
2
9
14
22
27
29
33
Scale (z scores)
-5
0
5
10
15

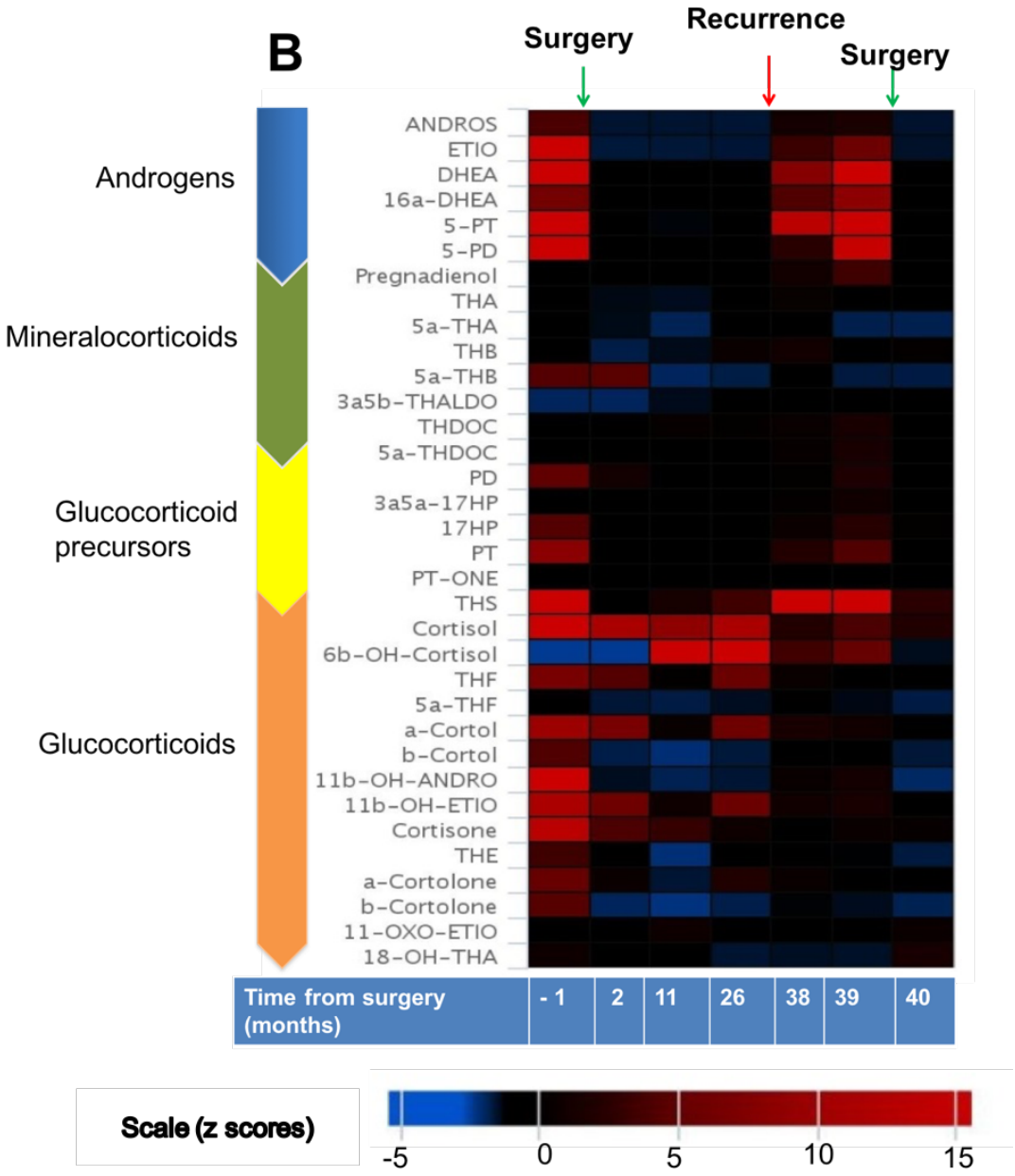

Figure 5-5 Heat-map representation of the longitudinal changes in the urinary steroid metabolome of two ACC patients who eventually developed disease recurrence. Arrows point to the time of surgery or the first radiological evidence of recurrent disease. Red represents metabolites that are raised above the mean control value; blue represents suppressed steroid metabolites.

In the proof-of-concept study for the use of urinary steroid metabolomics for differentiating benign from malignant adrenocortical tumors, Arlt et al. had distinguished 9 steroid biomarkers with the highest diagnostic value in detecting ACC: Etio, 5-PT, 5-PD (androgens and androgen precursors); THDOC, 5α-THA (mineralocorticoids and mineralocorticoid metabolites); PT, PD, THS, 5α-THF (glucocorticoids and glucocorticoid metabolites) (Arlt et al., 2011). 5α-reduced steroid biomarkers 5α-THA and 5α-THF are ill-suited for the specific clinical context of post-operative surveillance, as they are invariably suppressed in patients receiving adjuvant mitotane treatment due to the drug's potent inhibitory effects on 5α-reductase activity (Chortis et al., 2013). In this study, we have thus selected a modified version of this group, substituting DHEA for the two 5α-reduced steroids. DHEA had also been significantly higher in ACCs than in ACAs in the adrenal incidentaloma study and had the highest average absolute excretion values than any other biomarker in ACCs (Arlt et al., 2011).

Considering the first post-operative urine as the 'baseline' sample for each patient, we calculated the following ratios for each of these 8 malignant biomarkers: a) Recurred patients: ratio of steroid excretion in the first post-recurrence sample to excretion of the same steroid in the 'baseline' post-operative sample (n=34 ratios) and b) non-recurred patients: ratio of steroid excretion in each follow-up sample to the the excretion of the same steroid in the 'baseline' sample (n=163 ratios). We then selected the highest of these ratios for each sample. We divided the samples further into four groups, according to recurrence status and mitotane exposure, taking into consideration the inhibitory effect of mitotane on steroidogenesis (**Fig. 5-6**). The median of selected (highest) ratios was significantly higher in samples from recurred than non-recurred patients, in non-mitotane-treated subjects. The same trend was observed in mitotane-treated patients, failing to reach statistical significance. In the sub-group

of patients with available pre-operative urine samples, we tried a different approach, selecting the three highest pre-operative steroid metabolites (when normalised to the 95th percentile of the reference range for the same metabolite). We then looked at the ratio of the value of each of the selected steroid biomarkers in the first post-recurrence urine sample to the value of the same metabolite in the first ('baseline') post-operative urine sample (n=15 ratios). For the four patients with available pre-operative urine in the 'non-recurred' cohort, we followed the same process and calculated the ratio of the value of each of the selected steroid biomarkers in every post-operative urine sample to the value of the same metabolite in the first ('baseline') post-operative urine sample (n=13 ratios). This method produced a better separation between 'recurred' and 'non-recurred' samples (**Fig. 5-7**).

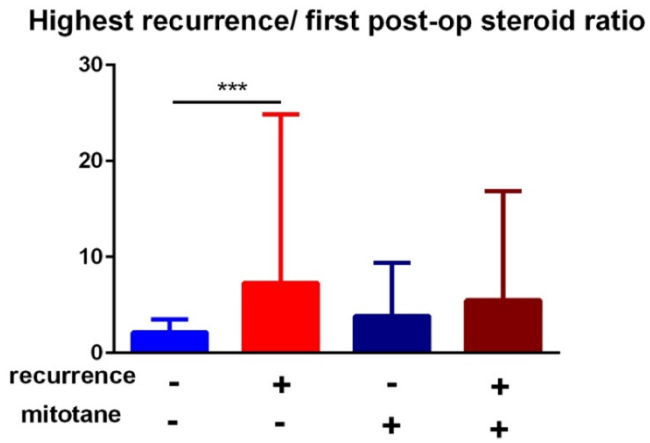

*Figure 5-6 Highest urinary steroid metabolite ratios (recurrence sample to baseline post-operative sample) in recurred patients and non-recurred control patients. Patients have been further classified according to use of adjuvant mitotane. Bars represent median (IQR) values (***p<0.001).*

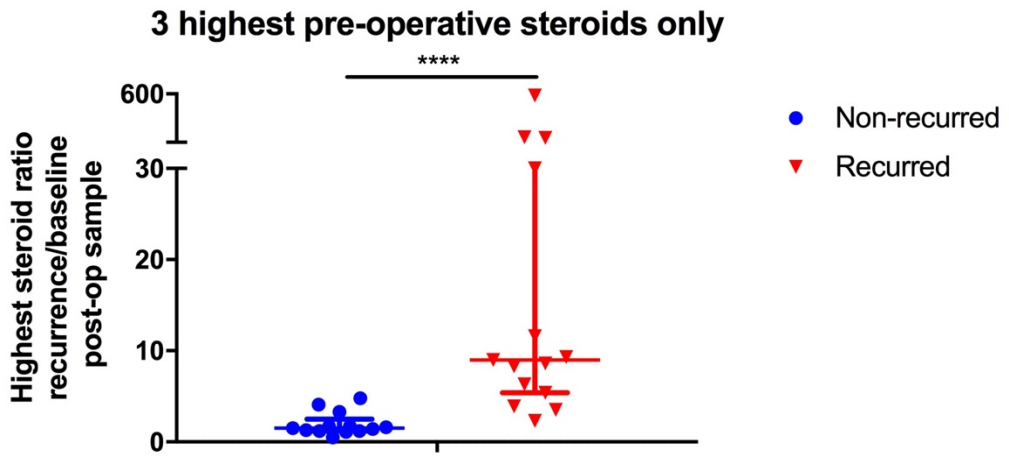

*Figure 5-7 Highest post-operative urinary steroid ratio (recurred sample to first post-operative sample) when focusing on the three steroid biomarkers that were the most elevated in the pre-operative sample. Samples from four non-recurred patients were used as controls. Bars represent median (IQR) values (****p<0.0001).*

5.3.3 Expert review of the urinary steroid metabolome

Longitudinal series of urinary steroid profiles derived from 52 patients (n=32 with documented post-operative recurrence and n=20 with a recurrence-free history of at least three years) were reviewed independently by three clinical endocrinologists in a retrospective and blinded fashion. Only patients who had contributed at least 2 post-operative samples were included, as this was the minimum essential number of samples for patients who recurred according to our inclusion criteria. Clinicians were able to correctly identify recurrent disease by the time of the first post-recurrence sample (defined by reference to the first abnormal surveillance scan) with sensitivities of 65%, 53% and 74%. This improved substantially in the subgroup (n=15 recurrences) of patients who had provided pre-operative urine samples (sensitivities 73-93%) (**Fig. 5-8A**). Of note, 10/15 (67%) of recurrences in these patients were

correctly detected unanimously by all reviewing clinicians. Absence of a pre-operative sample curtailed diagnostic sensitivities to 37-58% **(Fig. 5-8A)**. Specificities, defined as the proportion of non-recurred patients who were correctly identified as such by perusal of the steroid profiles, varied considerably among the assessors (**Fig. 5-8B**). The effect of pre-operative urine availability on specificity could not be reliably assessed as only four non-recurred patients had provided a pre-operative sample. It is worth noting that the diagnostic performance of the steroid profile review was not significantly altered by adjuvant mitotane treatment, despite the drug's known inhibitory effect on steroidogenesis (**Fig. 5-9**). Importantly, the diagnosis of recurrence by assessing clinicians preceded the first radiological evidence of recurrent disease by more than two months in a substantial proportion of cases; with one exception, all these early detections pertained to mitotane-treated patients (**Fig. 5-10**).

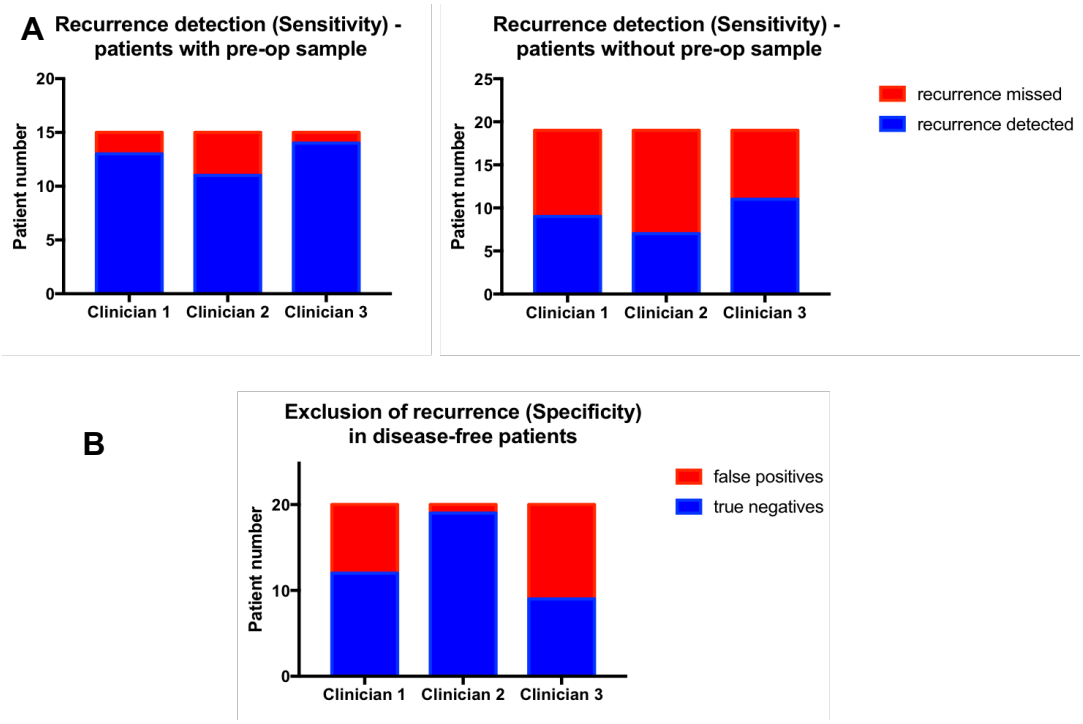

Figure 5-8 Clinician review of serial urinary steroid profiles. A) Recurrence detection (Sensitivity) in ACC patients grouped according to availability of pre-operative urine. B) Recurrence exclusion (Specificity) in disease-free patients

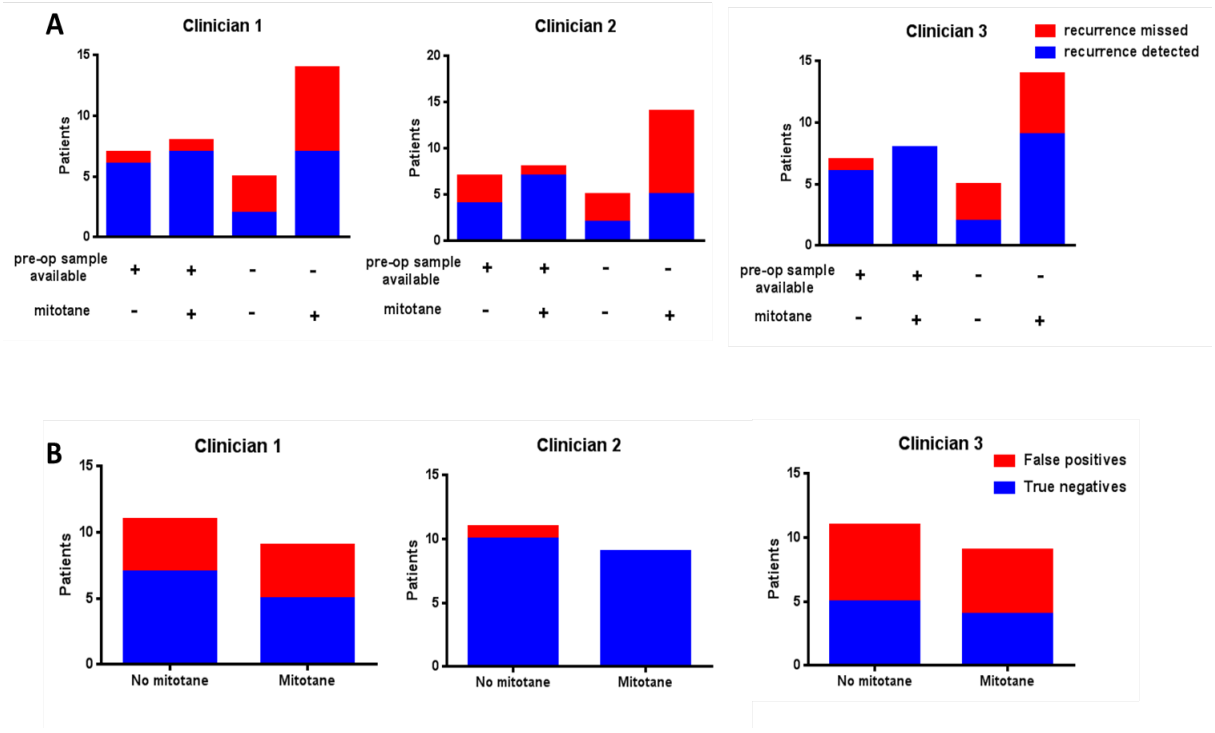

Figure 5-9 Clinician review of serial urinary steroid profiles. A) Recurrence detection (Sensitivity) in ACC patients grouped according to pre-operative urine availability and mitotane treatment. B) Recurrence exclusion (Specificity) in disease-free patients grouped according to mitotane treatment.

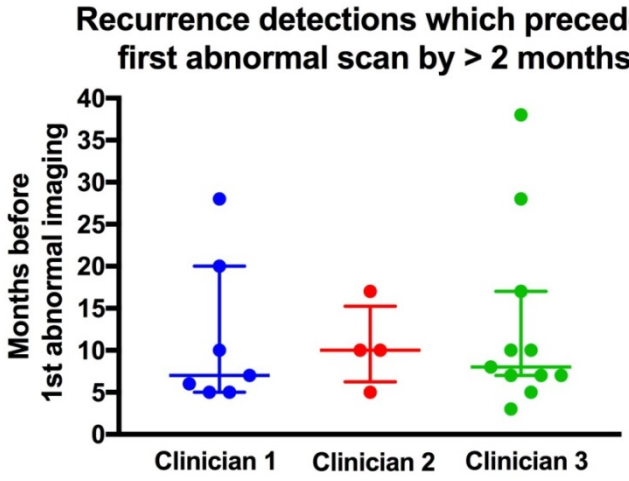

Figure 5-10 Recurrences detected biochemically by assessing clinicians on samples provided > 2 months before the first radiological manifestation of recurrent disease

5.4 Discussion

In this study, we have explored a novel diagnostic tool to facilitate post-operative surveillance for recurrence in patients who have undergone resection of primary ACC. This involved high-sensitivity urinary steroid profiling by GC-MS, a tool which has given highly promising results in the differentiation of benign from malignant adrenal tumours in recent retrospective studies (Arlt et al., 2011). We have assessed the diagnostic potential of urinary steroid profiling in the clinical context of post-operative monitoring in a subjective manner, based on blinded, retrospective clinician review of serial urinary steroid profiles from ACC patients who recurred (positive patient cohort) or remained disease-free for over 3 years (negative control cohort). Our next step will be to develop an automated, machine-learning-based model of analysis; this work has not been completed at the time of writing this thesis.

The need for close post-operative monitoring of ACC patients is dictated by the high rates of disease recurrence, even after microscopically complete (R0) resection. In aggressive tumours (Ki67 > 10%), 5-year recurrence-free survival is lower than 25%. Importantly, histological evidence of less aggressive behaviour (Ki67 < 10%) does not obviate the need for close post-operative follow-up, as recurrence-free survival does not exceed 50% in this patient cohort either (Beuschlein et al., 2015). Current follow-up protocols are based on clinical examination and routine biochemistry orientated towards detecting clinical or biochemical evidence of hormone excess, as well as regular cross-sectional imaging by CT or MRI scans. FDG-PET is also useful in this context but its use is limited by its high cost. Imaging is currently indispensable, as recurrences/ metastases can remain clinically and biochemically inconspicuous until they attain a sizeable volume, which usually exceeds the minimal detection limit of a modern CT/ MRI scan. The frequency of surveillance imaging is however limited by the considerable radiation exposure it ineluctably incurs (CT and FDG-PET scans)

or its high cost (MRI and FDG-PET scans). No consensus exists on the optimal surveillance imaging protocol; however, in most centres this is tailored to match the gradual decline in recurrence rates with time: recurrence rates are highest in the first two years post-operatively, lower in years 3-5 and lowest > 5 years post-operatively (Beuschlein et al., 2015). At University Hospitals Birmingham, the current follow-up protocol entails surveillance CT scans every three months post-operatively in the first two years, every six months in years 3-5 and annually thereafter. Patients who have been disease-free for > 10 years can be discharged as no recurrences have been reported after this time-point.

Our cohort consisted of adult patients with fully resected ACC who were able to provide a 24 h urine sample within two years from surgery and whilst still considered disease free according to the most recent clinical and radiological assessment. This time point was used to increase the yield of recurred patients, as patients who have already been disease-free for two years are less likely to recur. The overall cohort was demographically representative of the general population of ACC patients, with a female preponderance and median age at presentation in the 6th decade of life. Of the 72 patients who completed three years of follow-up, 32 (44%) recurred, a rate that is somewhat lower than previous retrospective studies (Beuschlein et al., 2015, Terzolo et al., 2007). This is likely to be due to selection bias related to the stipulation that a urine sample at a disease-free state must be provided for inclusion to the study – patients who recurred before a 24 h urine sample could be provided were excluded.

On retrospective, blinded assessment of serial 24 h urine collections clinicians were able to detect recurrence by the time of its first radiological manifestation with high sensitivity in cases where a pre-operative urine sample was available. The diagnostic value of a pre-

operative urine sample stems from its ability to impart the individual steroid profile of the particular tumour, which is likely to re-emerge in a future recurrence. With this information to hand, clinicians can focus on steroid biomarkers which were elevated pre-operatively and use a lower threshold to suspect recurrence when changes in their excretion are detected. Of note, 10/15 (67%) of recurrences in these patients were detected unanimously by all reviewing clinicians. In patients who were only able to contribute post-operative urine samples, the ability of clinicians to detect recurrence was substantially lower. Specificity varied considerably among the three clinicians, and correlated inversely to their respective sensitivities. The sub-optimal overall diagnostic accuracy for this patient cohort in comparison to previously reported sensitivities and specificities in patients with adrenal incidentalomas can be explained by the limited disease volume of recurrent/ metastatic ACC, with lesions that are often smaller than 1 cm in maximal diameter at the time of first radiological detection. By comparison, the median ACC size in the 2011 study on adrenal incidentalomas amounted to 9 cm in maximum diameter (Arlt et al., 2011). Consequently, the resulting perturbation of steroidogenesis might be very mild and not always distinguishable from normal sample-to-sample variability.

Interestingly, adjuvant mitotane did not compromise the diagnostic performance of reviewing clinicians, despite the drug's well documented ability to inhibit steroidogenesis. Mitotane interferes with adrenal steroidogenesis in a number of ways, including a) overall suppression of steroidogenesis resulting in lower excretion values for all steroid metabolites, b) rapid glucocorticoid breakdown by CYP3A4 necessitating high-dose hydrocortisone replacement; this means glucocorticoid metabolites are no longer diagnostically relevant in these patients and c) 5α-reductase inhibition, leading to a diminution of 5α-reduced steroids (Chortis et al., 2013). Although mitotane obtunds the ascending trends in steroid biomarkers in recurred

patients, it also suppresses the random sample-to-sample variability (noise), which can be diagnostically opportune.

Obviously, an effective diagnostic tool should be able to produce objective and unbiased outputs which do not rely on the individual clinician's experience and perspicacity. Due to the complexity of the system (multiple biomarkers, modest elevations due to small disease volumes), applying numerical diagnostic cut-offs appears to be too crude a way to predict the underlying disease status. Machine learning-based approaches would offer a good way of utilising the full wealth of information provided by 33-steroid profiles in a systematic, objective and reproducible fashion, as already demonstrated in the case of adrenal incidentalomas (Arlt et al., 2011).

This is the first clinical study exploring the diagnostic potential of urine steroid profiling in the specific clinical setting of post-operative surveillance for recurrence in ACC patients, with only small case series previously reported on this subject. The limitations of our work pertain to the relatively small recurred patient numbers and inconsistency in quality of provided data (e.g. availability of pre-operative urine samples, frequency of post-operative urine samples). After completion of our current analysis by machine learning, we will endeavour to validate these findings in a dedicated prospective study with more stringent inclusion criteria which will address the aforementioned weaknesses (pre-operative urine collection mandatory and short intervals between post-operative urine). Our results so far do not suggest that urinary steroid profiling could obviate the need for follow-up imaging, but it can be useful as a complimentary surveillance tool that could expedite scans in patients with suspicious biochemistry, inform discussions in patients with ambiguous imaging results or suggest the need for institution of adjuvant mitotane treatment.

6 Final conclusions and future directions

6.1 Antioxidant targeting as a novel therapeutic approach in ACC

In this work, we have explored a novel therapeutic avenue in the treatment of ACC. The urgent need to develop new approaches in the management of this rare endocrine malignancy has been highlighted in recent studies demonstrating the disappointing performance of classic combination chemotherapy in patients with advanced disease (Fassnacht et al., 2012). Unfortunately, the substantial progress in our understanding of ACC molecular genetics has so far failed to translate into therapeutic advances. This *in vitro* project draws on recent studies revealing the implication of mitochondrial antioxidant pathway defects in the pathogenesis of congenital adrenal failure. In 2012, genetic studies in patients with Familial Glucocorticoid Deficiency (FGD), a rare hereditary form of adrenal insufficiency, revealed inactivating mutations in the mitochondrial NADPH generator Nicotinamide Nucleotide Transhydrogenase (NNT) (Meimaridou et al., 2012). The biological role of NNT is to provide the mitochondrial antioxidant pathways (glutathione pathway and thioredoxin pathway) with reducing equivalents in the form of NADPH (Rydstrom, 2006). Inactivating mutations of thioredoxin reductase have recently also been discovered in FGD patients. Antioxidant pathways have a crucial biological role within cells, detoxifying Reactive Oxygen Species (ROS), the harmful by-products of aerobic metabolism. Inordinate accumulation of ROS has deleterious effects (oxidative stress), which can culminate to cell death if not counterbalanced by an effective antioxidant defence system. The risk of ROS toxicity is highest in metabolically active tissues such as the adrenal cortex, and most relevant in malignant cells which tend to have higher baseline ROS levels than normal cells. Our hypothesis was that NNT inactivation will compromise the -metabolically highly active- ACC cells' capacity to scavenge ROS, exposing them to oxidative toxicity and, eventually, cell death.

We validated this hypothesis transiently knocking down NNT in NCI-H295R ACC cells *in vitro* (siRNA transfection) and observing an increase in cellular levels of oxidative stress, suppression of cellular proliferation and induction of apoptotic cell death. Furthermore, NNT loss rendered cells sensitive to sub-toxic doses of paraquat, a chemical inducer of oxidative stress. These results provide a first *in vitro* characterisation of the therapeutic potential of NNT in the management of ACC. Next, we employed a long-term silencing model, involving stable NCI-H295R transfection with shRNA against NNT, to delineate the chronic consequences of NNT loss. Here we captured the emergence of a compensated phenotype, with reinstatement of redox homeostasis and abrogation of apoptosis. This compensation was underpinned by higher oxygen consumption and glycolytic rates, indicating higher energy needs. Importantly, a longstanding suppression of proliferation was observed, although this was clearly much less pronounced than the one we observed in the acute setting (**Fig. 6-1**).

A second output of interest was the impact of NNT loss on steroidogenesis; inhibition of steroidogenesis by NNT silencing would be therapeutically useful in patients with adrenal hormone excess, a common clinical and biochemical attribute of ACC. Suppression of steroidogenesis with NNT inactivation appeared theoretically likely, given the glucocorticoid deficiency of NNT mutant patients and the role of NADPH as an essential cofactor to important mitochondrial steroidogenic enzymes (CYP11A1, CYP11B1, CYP11B2). Surprisingly, we observed a paradoxical stimulation of steroidogenesis in the acute setting (siRNA knockdown), with no lingering effect in the long term (shRNA knockdown). Overall, these findings suggest NNT is not a meaningful treatment target as far as inhibition of steroidogenesis is concerned.

We did not exhaust our in vitro work in the study of NNT, but we also selectively inhibited the glutathione pathway (by buthionine sulfoximine, BSO) and the thioredoxin pathway (by auranofin) and monitored the individual impact of these interventions on cellular proliferation and viability. Both drugs demonstrated a cytotoxic potential in clinically attainable doses. Overall, our work suggests that ACC cells are susceptible to pharmacological inhibition of antioxidant pathways. The relative efficiency of the various possible target options (NNT, glutathione pathway, thioredoxin pathway) would need to be explored further with *in vivo* studies, e.g. NCI-H295R xenografts in mice. It is difficult to predict whether a compensated phenotype akin to the one we observed in the stable knockdown model would emerge with *in vivo* inhibition, and if so how long it would take for this to be established. An inducible knockdown model would be particularly attractive given the discrepancy we observed between the acute and chronic NNT knockdown models. Pharmacological inhibition of the glutathione or thioredoxin pathways (e.g. by BSO or auranofin administration) would be more straightforward and *in vivo* studies employing these agents in different malignancies have already been published (Bailey et al., 1994, Bailey, 1998, O'Dwyer et al., 1996, Bailey et al., 1997, Li et al., 2016). Importantly, the ability of malignant cells to adapt to oxidative stress is well described in the literature; therefore, achieving a marked and sustained anti-tumour effect may require concurrent use of a pro-oxidant chemotherapy agent. With this approach, antioxidant targeting would be used as a chemotherapy sensitising strategy. Our *in vitro* results with co-implementation of NNT inhibition and paraquat-induced oxidative stress are promising in this respect. An alternative approach could involve dual inhibition of the glutathione and thioredoxin pathways; this has not been formally explored so far, but recent pilot experiments in our lab have suggested a synergistic effect leading to marked cytotoxicity with low doses of BSO and auranofin.

Ongoing work which is approaching completion comprises RNA sequencing and whole metabolome analysis of both NNT knockdown models (siRNA and shRNA transfected cells). We expect that this additional effort will provide useful mechanistic insights, illuminating the complete molecular impact of NNT inhibition and unravelling the compensatory response which leads to the distinct phenotype of stable NNT silencing.

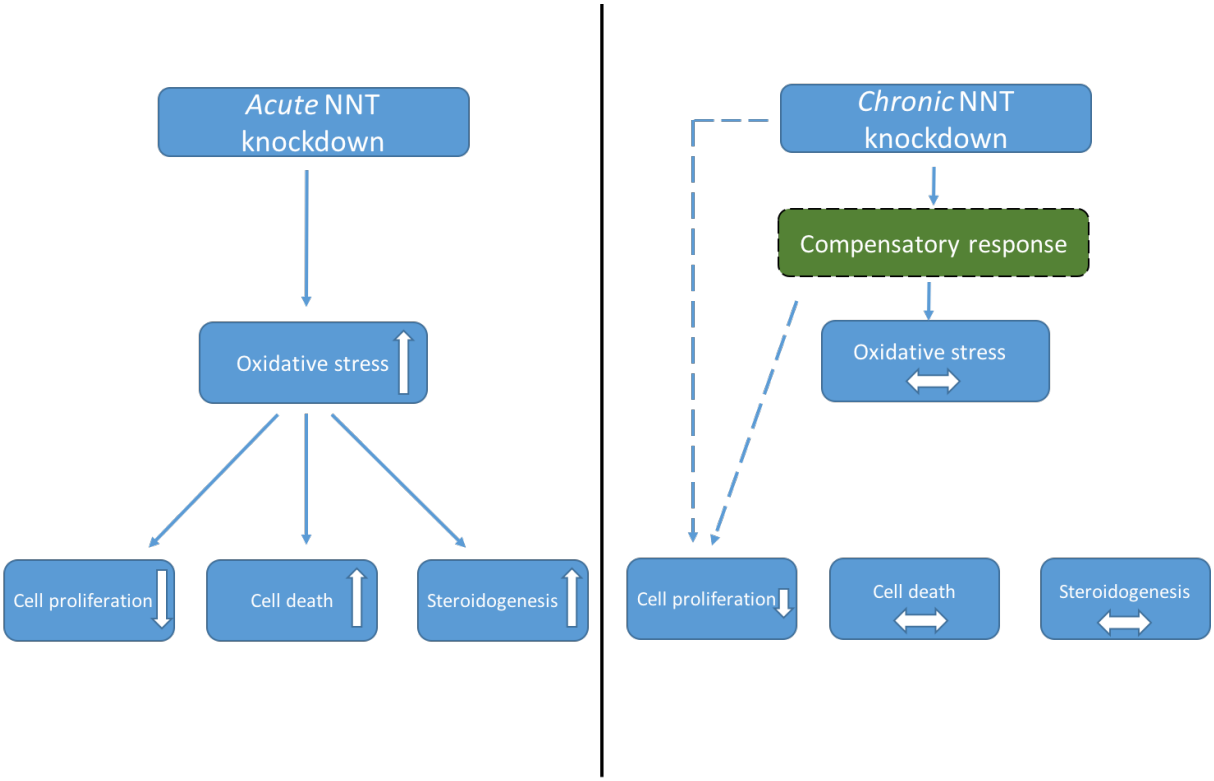

Figure 6-1 Effects of NNT knockdown on ACC cell metabolism, proliferation/viability and steroidogenesis in the acute and chronic setting. Horizontal arrows demonstrate paucity of change in reference to control cells.

6.2 Urine steroid profiling as a new surveillance tool to detect ACC recurrence

Our clinical work followed a different direction, aspiring to develop a novel diagnostic tool to facilitate prompt recurrence detection in operated ACC patients. The majority of patients with resected ACCs will experience post-operative disease recurrence. Therefore, close monitoring is essential for many years. Currently post-operative surveillance is largely imaging-based, with all the limitations this entails in terms of cost, cumulative radiation exposure and diagnostic ambiguity at early recurrence stages. A highly auspicious novel diagnostic modality was recently introduced in the clinical context of adrenal incidentalomas, involving urinary steroid profiling by gas chromatography-mass spectrometry (GC-MS). The sensitivity of GC-MS supersedes the analytical capacity of traditional adrenal biochemistry; the method can quantify up to 34 steroid metabolites in 24h urine collections, spanning the whole spectrum of steroidogenesis. ACC presents a characteristic steroidogenic pattern, with a relative over-abundance of steroid precursors; this can be captured and utilised to differentiate malignant from benign adrenal tumours with high sensitivity and specificity.

In our study, we evaluated the ability of the same technique to serve as a sensitive surveillance tool in the post-operative course of patients who have undergone full resection of ACC. On blinded retrospective review of serial steroid profiles by three clinical endocrinologists, recurrence was detected concurrently with or prior to cross-sectional imaging in the majority of cases. The single most important factor affecting the diagnostic success of subjective urinary steroid profile review was the availability of a pre-operative urine sample, which can reveal the individual steroidogenic fingerprint of the individual tumour. Importantly, adjuvant mitotane treatment did not seem to adversely impact on the results, despite the drug's well-described inhibitory effect on steroidogenesis. We are

currently trying to introduce automated, machine learning-based analysis of the results as an objective and powerful analytical way of processing the complex data sets comprising the urinary steroid profile (urine steroid metabolomics). Upon completion of this work, we will endeavour to validate urine steroid profiling and metabolomics as a diagnostic tool for ACC recurrence detection with a dedicated prospective study with more stringent inclusion criteria (provision of pre-operative urine, high frequency of post-operative urine collection).

REFERENCES

1975. Third national cancer survey: incidence data. *Natl Cancer Inst Monogr*, i-x, 1-454.

ABIVEN, G., COSTE, J., GROUSSIN, L., ANRACT, P., TISSIER, F., LEGMANN, P., DOUSSET, B., BERTAGNA, X. & BERTHERAT, J. 2006. Clinical and biological features in the prognosis of adrenocortical cancer: poor outcome of cortisol-secreting tumors in a series of 202 consecutive patients. *J Clin Endocrinol Metab,* 91**,** 2650-5.

ABRAHAM, J., BAKKE, S., RUTT, A., MEADOWS, B., MERINO, M., ALEXANDER, R., SCHRUMP, D., BARTLETT, D., CHOYKE, P., ROBEY, R., HUNG, E., STEINBERG, S. M., BATES, S. & FOJO, T. 2002. A phase II trial of combination chemotherapy and surgical resection for the treatment of metastatic adrenocortical carcinoma: continuous infusion doxorubicin, vincristine, and etoposide with daily mitotane as a P-glycoprotein antagonist. *Cancer,* 94**,** 2333-43.

ADAMS, J. E., JOHNSON, R. J., RICKARDS, D. & ISHERWOOD, I. 1983. Computed tomography in adrenal disease. *Clin Radiol,* 34**,** 39-49.

ADHIKARY, A., MOHANTY, S., LAHIRY, L., HOSSAIN, D. M., CHAKRABORTY, S. & DAS, T. 2010. Theaflavins retard human breast cancer cell migration by inhibiting NF-kappaB via p53-ROS cross-talk. *FEBS Lett,* 584**,** 7-14.

AGRAWAL, N., DASARADHI, P. V., MOHMMED, A., MALHOTRA, P., BHATNAGAR, R. K. & MUKHERJEE, S. K. 2003. RNA interference: biology, mechanism, and applications. *Microbiol Mol Biol Rev,* 67**,** 657-85.

ALEXANDRE, J., BATTEUX, F., NICCO, C., CHEREAU, C., LAURENT, A., GUILLEVIN, L., WEILL, B. & GOLDWASSER, F. 2006. Accumulation of hydrogen peroxide is an early and crucial step for paclitaxel-induced cancer cell death both in vitro and in vivo. *Int J Cancer,* 119**,** 41-8.

ALEXANDRE, J., HU, Y., LU, W., PELICANO, H. & HUANG, P. 2007. Novel action of paclitaxel against cancer cells: bystander effect mediated by reactive oxygen species. *Cancer Res,* 67**,** 3512-7.

ALLGROVE, J., CLAYDEN, G. S., GRANT, D. B. & MACAULAY, J. C. 1978. Familial glucocorticoid deficiency with achalasia of the cardia and deficient tear production. *Lancet,* 1**,** 1284-6.

ALLOLIO, B. & FASSNACHT, M. 2006. Clinical review: Adrenocortical carcinoma: clinical update. *J Clin Endocrinol Metab,* 91**,** 2027-37.

ANDERSON, C. P., MATTHAY, K. K., PERENTESIS, J. P., NEGLIA, J. P., BAILEY, H. H., VILLABLANCA, J. G., GROSHEN, S., HASENAUER, B., MARIS, J. M., SEEGER, R. C. & REYNOLDS, C. P. 2015. Pilot study of intravenous melphalan combined with continuous infusion L-S,R-buthionine sulfoximine for children with recurrent neuroblastoma. *Pediatr Blood Cancer,* 62**,** 1739-46.

ANDERSON, C. P., TSAI, J. M., MEEK, W. E., LIU, R. M., TANG, Y., FORMAN, H. J. & REYNOLDS, C. P. 1999. Depletion of glutathione by buthionine sulfoxine is cytotoxic for human neuroblastoma cell lines via apoptosis. *Exp Cell Res,* 246**,** 183-92.

ANDREYEV, A. Y., KUSHNAREVA, Y. E. & STARKOV, A. A. 2005. Mitochondrial metabolism of reactive oxygen species. *Biochemistry (Mosc),* 70**,** 200-14.

ARBISER, J. L., PETROS, J., KLAFTER, R., GOVINDAJARAN, B., MCLAUGHLIN, E. R., BROWN, L. F., COHEN, C., MOSES, M., KILROY, S., ARNOLD, R. S. & LAMBETH, J. D. 2002. Reactive oxygen generated by Nox1 triggers the angiogenic switch. *Proc Natl Acad Sci U S A,* 99**,** 715-20.

ARKBLAD, E. L., TUCK, S., PESTOV, N. B., DMITRIEV, R. I., KOSTINA, M. B., STENVALL, J., TRANBERG, M. & RYDSTROM, J. 2005. A Caenorhabditis elegans mutant lacking functional nicotinamide nucleotide transhydrogenase displays increased sensitivity to oxidative stress. *Free Radic Biol Med,* 38**,** 1518-25.

ARLT, W., BIEHL, M., TAYLOR, A. E., HAHNER, S., LIBE, R., HUGHES, B. A., SCHNEIDER, P., SMITH, D. J., STIEKEMA, H., KRONE, N., PORFIRI, E., OPOCHER, G., BERTHERAT, J., MANTERO, F., ALLOLIO, B., TERZOLO, M., NIGHTINGALE, P., SHACKLETON, C. H., BERTAGNA, X., FASSNACHT, M. & STEWART, P. M. 2011. Urine steroid metabolomics as a biomarker tool for detecting malignancy in adrenal tumors. *J Clin Endocrinol Metab,* 96**,** 3775-84.

ARLT, W., REINCKE, M., SIEKMANN, L., WINKELMANN, W. & ALLOLIO, B. 1994. Suramin in adrenocortical cancer: limited efficacy and serious toxicity. *Clin Endocrinol (Oxf),* 41**,** 299-307.

ASSIE, G., ANTONI, G., TISSIER, F., CAILLOU, B., ABIVEN, G., GICQUEL, C., LEBOULLEUX, S., TRAVAGLI, J. P., DROMAIN, C., BERTAGNA, X., BERTHERAT, J., SCHLUMBERGER, M. & BAUDIN, E. 2007. Prognostic parameters of metastatic adrenocortical carcinoma. *J Clin Endocrinol Metab,* 92**,** 148-54.

ASSIE, G., LETOUZE, E., FASSNACHT, M., JOUINOT, A., LUSCAP, W., BARREAU, O., OMEIRI, H., RODRIGUEZ, S., PERLEMOINE, K., RENE-CORAIL, F., ELAROUCI, N., SBIERA, S., KROISS, M., ALLOLIO, B., WALDMANN, J., QUINKLER, M., MANNELLI, M., MANTERO, F., PAPATHOMAS, T., DE KRIJGER, R., TABARIN, A., KERLAN, V., BAUDIN, E., TISSIER, F., DOUSSET, B., GROUSSIN, L., AMAR, L., CLAUSER, E., BERTAGNA, X., RAGAZZON, B., BEUSCHLEIN, F., LIBE, R., DE REYNIES, A. & BERTHERAT, J. 2014. Integrated genomic characterization of adrenocortical carcinoma. *Nat Genet,* 46**,** 607-12.

AUBERT, S., WACRENIER, A., LEROY, X., DEVOS, P., CARNAILLE, B., PROYE, C., WEMEAU, J. L., LECOMTE-HOUCKE, M. & LETEURTRE, E. 2002. Weiss system revisited: a clinicopathologic and immunohistochemical study of 49 adrenocortical tumors. *Am J Surg Pathol,* 26**,** 1612-9.

AZAD, N., IYER, A. K., WANG, L., LU, Y., MEDAN, D., CASTRANOVA, V. & ROJANASAKUL, Y. 2010. Nitric oxide-mediated bcl-2 stabilization potentiates malignant transformation of human lung epithelial cells. *Am J Respir Cell Mol Biol,* 42**,** 578-85.

BAHLIS, N. J., MCCAFFERTY-GRAD, J., JORDAN-MCMURRY, I., NEIL, J., REIS, I., KHARFAN-DABAJA, M., ECKMAN, J., GOODMAN, M., FERNANDEZ, H. F., BOISE, L. H. & LEE, K. P. 2002. Feasibility and correlates of arsenic trioxide combined with ascorbic acid-mediated depletion of intracellular glutathione for the treatment of relapsed/refractory multiple myeloma. *Clin Cancer Res,* 8**,** 3658-68.

BAILEY, H. H. 1998. L-S,R-buthionine sulfoximine: historical development and clinical issues. *Chem Biol Interact,* 111-112**,** 239-54.

BAILEY, H. H., MULCAHY, R. T., TUTSCH, K. D., ARZOOMANIAN, R. Z., ALBERTI, D., TOMBES, M. B., WILDING, G., POMPLUN, M. & SPRIGGS, D. R. 1994. Phase I clinical trial of intravenous L-buthionine sulfoximine and melphalan: an attempt at modulation of glutathione. *J Clin Oncol,* 12**,** 194-205.

BAILEY, H. H., RIPPLE, G., TUTSCH, K. D., ARZOOMANIAN, R. Z., ALBERTI, D., FEIERABEND, C., MAHVI, D., SCHINK, J., POMPLUN, M., MULCAHY, R. T. & WILDING, G. 1997. Phase I study of continuous-infusion L-S,R-buthionine sulfoximine with intravenous melphalan. *J Natl Cancer Inst,* 89**,** 1789-96.

BAKER, A. F., ADAB, K. N., RAGHUNAND, N., CHOW, H. H., STRATTON, S. P., SQUIRE, S. W., BOICE, M., PESTANO, L. A., KIRKPATRICK, D. L. & DRAGOVICH, T. 2013. A phase IB trial of 24-hour intravenous PX-12, a thioredoxin-1 inhibitor, in patients with advanced gastrointestinal cancers. *Invest New Drugs,* 31**,** 631-41.

BANCOS, I., TAMHANE, S., SHAH, M., DELIVANIS, D. A., ALAHDAB, F., ARLT, W., FASSNACHT, M. & MURAD, M. H. 2016. DIAGNOSIS OF ENDOCRINE DISEASE: The diagnostic performance of adrenal biopsy: a systematic review and meta-analysis. *Eur J Endocrinol,* 175**,** R65-80.

BARR, P. M., MILLER, T. P., FRIEDBERG, J. W., PETERSON, D. R., BARAN, A. M., HERR, M., SPIER, C. M., CUI, H., ROE, D. J., PERSKY, D. O., CASULO, C., LITTLETON, J., SCHWARTZ, M., PUVVADA, S., LANDOWSKI, T. H., RIMSZA, L. M., DORR, R. T., FISHER, R. I., BERNSTEIN, S. H. & BRIEHL, M. M. 2014. Phase 2 study of imexon, a prooxidant molecule, in relapsed and refractory B-cell non-Hodgkin lymphoma. *Blood,* 124**,** 1259-65.

BARREAU, O., ASSIE, G., WILMOT-ROUSSEL, H., RAGAZZON, B., BAUDRY, C., PERLEMOINE, K., RENE-CORAIL, F., BERTAGNA, X., DOUSSET, B., HAMZAOUI, N., TISSIER, F., DE REYNIES, A. & BERTHERAT, J. 2013. Identification of a CpG island methylator phenotype in adrenocortical carcinomas. *J Clin Endocrinol Metab,* 98**,** E174-84.

BARZON, L., CHILOSI, M., FALLO, F., MARTIGNONI, G., MONTAGNA, L., PALU, G. & BOSCARO, M. 2001. Molecular analysis of CDKN1C and TP53 in sporadic adrenal tumors. *Eur J Endocrinol,* 145**,** 207-12.

BATES, S. E., SHIEH, C. Y., MICKLEY, L. A., DICHEK, H. L., GAZDAR, A., LORIAUX, D. L. & FOJO, A. T. 1991. Mitotane enhances cytotoxicity of chemotherapy in cell lines expressing a multidrug resistance gene (mdr-1/P-glycoprotein) which is also expressed by adrenocortical carcinomas. *J Clin Endocrinol Metab,* 73**,** 18-29.

BAUDIN, E., DOCAO, C., GICQUEL, C., VASSAL, G., BACHELOT, A., PENFORNIS, A. & SCHLUMBERGER, M. 2002. Use of a topoisomerase I inhibitor (irinotecan, CPT-11) in metastatic adrenocortical carcinoma. *Ann Oncol,* 13**,** 1806-9.

BAUDRY, C., COSTE, J., BOU KHALIL, R., SILVERA, S., GUIGNAT, L., GUIBOURDENCHE, J., ABBAS, H., LEGMANN, P., BERTAGNA, X. & BERTHERAT, J. 2012. Efficiency and tolerance of mitotane in Cushing's disease in 76 patients from a single center. *Eur J Endocrinol,* 167**,** 473-81.

BAUER, G. 2012. Tumor cell-protective catalase as a novel target for rational therapeutic approaches based on specific intercellular ROS signaling. *Anticancer Res,* 32**,** 2599-624.

BEDARD, K. & KRAUSE, K. H. 2007. The NOX family of ROS-generating NADPH oxidases: physiology and pathophysiology. *Physiol Rev,* 87**,** 245-313.

BEHRMAN, H. R. & ATEN, R. F. 1991. Evidence that hydrogen peroxide blocks hormone-sensitive cholesterol transport into mitochondria of rat luteal cells. *Endocrinology,* 128**,** 2958-66.

BERNDTSSON, M., HAGG, M., PANARETAKIS, T., HAVELKA, A. M., SHOSHAN, M. C. & LINDER, S. 2007. Acute apoptosis by cisplatin requires induction of reactive oxygen species but is not associated with damage to nuclear DNA. *Int J Cancer,* 120**,** 175-80.

BERRUTI, A. 2012. Adrenocortical carcinoma. *In:* ELSE, T. (ed.) *Adrenocortical carcinoma.* New York: Elsevier.

BERRUTI, A., FASSNACHT, M., BAUDIN, E., HAMMER, G., HAAK, H., LEBOULLEUX, S., SKOGSEID, B., ALLOLIO, B. & TERZOLO, M. 2010. Adjuvant therapy in patients with adrenocortical carcinoma: a position of an international panel. *J Clin Oncol,* 28**,** e401-2; author reply e403.

BERRUTI, A., SPERONE, P., FERRERO, A., GERMANO, A., ARDITO, A., PRIOLA, A. M., DE FRANCIA, S., VOLANTE, M., DAFFARA, F., GENERALI, D., LEBOULLEUX, S., PEROTTI, P., BAUDIN, E., PAPOTTI, M. & TERZOLO, M. 2012. Phase II study of weekly paclitaxel and sorafenib as second/third-line therapy in patients with adrenocortical carcinoma. *Eur J Endocrinol,* 166**,** 451-8.

BERRUTI, A., TERZOLO, M., PIA, A., ANGELI, A. & DOGLIOTTI, L. 1998. Mitotane associated with etoposide, doxorubicin, and cisplatin in the treatment of advanced adrenocortical carcinoma. Italian Group for the Study of Adrenal Cancer. *Cancer,* 83**,** 2194-200.

BERRUTI, A., TERZOLO, M., SPERONE, P., PIA, A., DELLA CASA, S., GROSS, D. J., CARNAGHI, C., CASALI, P., PORPIGLIA, F., MANTERO, F., REIMONDO, G., ANGELI, A. & DOGLIOTTI, L. 2005. Etoposide, doxorubicin and cisplatin plus mitotane in the treatment of advanced adrenocortical carcinoma: a large prospective phase II trial. *Endocr Relat Cancer,* 12**,** 657-66.

BEUSCHLEIN, F., REINCKE, M., KARL, M., TRAVIS, W. D., JAURSCH-HANCKE, C., ABDELHAMID, S., CHROUSOS, G. P. & ALLOLIO, B. 1994. Clonal composition of human adrenocortical neoplasms. *Cancer Res,* 54**,** 4927-32.

BEUSCHLEIN, F., WEIGEL, J., SAEGER, W., KROISS, M., WILD, V., DAFFARA, F., LIBE, R., ARDITO, A., AL GHUZLAN, A., QUINKLER, M., OSSWALD, A., RONCHI, C. L., DE KRIJGER, R., FEELDERS, R. A., WALDMANN, J., WILLENBERG, H. S., DEUTSCHBEIN, T., STELL, A., REINCKE, M., PAPOTTI, M., BAUDIN, E., TISSIER, F., HAAK, H. R., LOLI, P., TERZOLO, M., ALLOLIO, B., MULLER, H. H. & FASSNACHT, M. 2015. Major prognostic role of Ki67 in localized adrenocortical carcinoma after complete resection. *J Clin Endocrinol Metab,* 100**,** 841-9.

BEUTLER, E. 1996. G6PD: population genetics and clinical manifestations. *Blood Rev,* 10**,** 45-52.

BHOSLE, S. M., PANDEY, B. N., HUILGOL, N. G. & MISHRA, K. P. 2002. Membrane oxidative damage and apoptosis in cervical carcinoma cells of patients after radiation therapy. *Methods Cell Sci,* 24**,** 65-8.

BIENERT, G. P., MOLLER, A. L., KRISTIANSEN, K. A., SCHULZ, A., MOLLER, I. M., SCHJOERRING, J. K. & JAHN, T. P. 2007. Specific aquaporins facilitate the diffusion of hydrogen peroxide across membranes. *J Biol Chem,* 282**,** 1183-92.

BIGLIERI, E. G., HANE, S., SLATON, P. E., JR. & FORSHAM, P. H. 1963. In vivo and in vitro studies of adrenal secretions in Cushing's syndrome and primary aldosteronism. *J Clin Invest,* 42**,** 516-24.

BILIMORIA, K. Y., SHEN, W. T., ELARAJ, D., BENTREM, D. J., WINCHESTER, D. J., KEBEBEW, E. & STURGEON, C. 2008. Adrenocortical carcinoma in the United States: treatment utilization and prognostic factors. *Cancer,* 113**,** 3130-6.

BONACCI, R., GIGLIOTTI, A., BAUDIN, E., WION-BARBOT, N., EMY, P., BONNAY, M., CAILLEUX, A. F., NAKIB, I., SCHLUMBERGER, M. & RESEAU, C. 1998. Cytotoxic therapy with etoposide and cisplatin in advanced adrenocortical carcinoma. *Br J Cancer,* 78**,** 546-9.

BOVIO, S., CATALDI, A., REIMONDO, G., SPERONE, P., NOVELLO, S., BERRUTI, A., BORASIO, P., FAVA, C., DOGLIOTTI, L., SCAGLIOTTI, G. V., ANGELI, A. & TERZOLO, M. 2006. Prevalence of adrenal incidentaloma in a contemporary computerized tomography series. *J Endocrinol Invest,* 29**,** 298-302.

BRAR, S. S., CORBIN, Z., KENNEDY, T. P., HEMENDINGER, R., THORNTON, L., BOMMARIUS, B., ARNOLD, R. S., WHORTON, A. R., STURROCK, A. B., HUECKSTEADT, T. P., QUINN, M. T., KRENITSKY, K., ARDIE, K. G., LAMBETH, J. D. & HOIDAL, J. R. 2003. NOX5 NAD(P)H oxidase regulates growth and apoptosis in DU 145 prostate cancer cells. *Am J Physiol Cell Physiol,* 285**,** C353-69.

BRAUCHLE, M., FUNK, J. O., KIND, P. & WERNER, S. 1996. Ultraviolet B and H2O2 are potent inducers of vascular endothelial growth factor expression in cultured keratinocytes. *J Biol Chem,* 271**,** 21793-7.

BRENTANO, S. T. & MILLER, W. L. 1992. Regulation of human cytochrome P450scc and adrenodoxin messenger ribonucleic acids in JEG-3 cytotrophoblast cells. *Endocrinology,* 131**,** 3010-8.

BROWN, K. K., COX, A. G. & HAMPTON, M. B. 2010. Mitochondrial respiratory chain involvement in peroxiredoxin 3 oxidation by phenethyl isothiocyanate and auranofin. *FEBS Lett,* 584**,** 1257-62.

BUKOWSKI, R. M., WOLFE, M., LEVINE, H. S., CRAWFORD, D. E., STEPHENS, R. L., GAYNOR, E. & HARKER, W. G. 1993. Phase II trial of mitotane and cisplatin in patients with adrenal carcinoma: a Southwest Oncology Group study. *J Clin Oncol,* 11**,** 161-5.

CAWOOD, T. J., HUNT, P. J., O'SHEA, D., COLE, D. & SOULE, S. 2009. Recommended evaluation of adrenal incidentalomas is costly, has high false-positive rates and confers a risk of fatal cancer that is similar to the risk of the adrenal lesion becoming malignant; time for a rethink? *Eur J Endocrinol,* 161**,** 513-27.

CECCARELLI, J., DELFINO, L., ZAPPIA, E., CASTELLANI, P., BORGHI, M., FERRINI, S., TOSETTI, F. & RUBARTELLI, A. 2008. The redox state of the lung cancer microenvironment depends on the levels of thioredoxin expressed by tumor cells and affects tumor progression and response to prooxidants. *Int J Cancer,* 123**,** 1770-8.

CHANDEL, N. S., MCCLINTOCK, D. S., FELICIANO, C. E., WOOD, T. M., MELENDEZ, J. A., RODRIGUEZ, A. M. & SCHUMACKER, P. T. 2000. Reactive oxygen species generated at mitochondrial complex III stabilize hypoxia-inducible factor-1alpha during hypoxia: a mechanism of O2 sensing. *J Biol Chem,* 275**,** 25130-8.

CHEN, E. I., HEWEL, J., KRUEGER, J. S., TIRABY, C., WEBER, M. R., KRALLI, A., BECKER, K., YATES, J. R., 3RD & FELDING-HABERMANN, B. 2007. Adaptation of energy metabolism in breast cancer brain metastases. *Cancer Res,* 67**,** 1472-86.

CHEN, J. & STUBBE, J. 2005. Bleomycins: towards better therapeutics. *Nat Rev Cancer,* 5**,** 102-12.

CHEN, Y., MCMILLAN-WARD, E., KONG, J., ISRAELS, S. J. & GIBSON, S. B. 2008. Oxidative stress induces autophagic cell death independent of apoptosis in transformed and cancer cells. *Cell Death Differ,* 15**,** 171-82.

CHETRAM, M. A., DON-SALU-HEWAGE, A. S. & HINTON, C. V. 2011. ROS enhances CXCR4-mediated functions through inactivation of PTEN in prostate cancer cells. *Biochem Biophys Res Commun,* 410**,** 195-200.

CHORTIS, V., TAYLOR, A. E., SCHNEIDER, P., TOMLINSON, J. W., HUGHES, B. A., O'NEIL, D. M., LIBE, R., ALLOLIO, B., BERTAGNA, X., BERTHERAT, J., BEUSCHLEIN, F., FASSNACHT, M., KARAVITAKI, N., MANNELLI, M., MANTERO, F., OPOCHER, G., PORFIRI, E., QUINKLER, M., SHERLOCK, M.,

TERZOLO, M., NIGHTINGALE, P., SHACKLETON, C. H., STEWART, P. M., HAHNER, S. & ARLT, W. 2013. Mitotane therapy in adrenocortical cancer induces CYP3A4 and inhibits 5alpha-reductase, explaining the need for personalized glucocorticoid and androgen replacement. *J Clin Endocrinol Metab,* 98**,** 161-71.

CHOW, M. S., LIU, L. V. & SOLOMON, E. I. 2008. Further insights into the mechanism of the reaction of activated bleomycin with DNA. *Proc Natl Acad Sci U S A,* 105**,** 13241-5.

CHOW, W. H., HSING, A. W., MCLAUGHLIN, J. K. & FRAUMENI, J. F., JR. 1996. Smoking and adrenal cancer mortality among United States veterans. *Cancer Epidemiol Biomarkers Prev,* 5**,** 79-80.

CHUN, H. G., YAGODA, A., KEMENY, N. & WATSON, R. C. 1983. Cisplatin for adrenal cortical carcinoma. *Cancer Treat Rep,* 67**,** 513-4.

CLARK, A. J., CHAN, L. F., CHUNG, T. T. & METHERELL, L. A. 2009. The genetics of familial glucocorticoid deficiency. *Best Pract Res Clin Endocrinol Metab,* 23**,** 159-65.

COX, A. G., BROWN, K. K., ARNER, E. S. & HAMPTON, M. B. 2008. The thioredoxin reductase inhibitor auranofin triggers apoptosis through a Bax/Bak-dependent process that involves peroxiredoxin 3 oxidation. *Biochem Pharmacol,* 76**,** 1097-109.

COX, A. G., WINTERBOURN, C. C. & HAMPTON, M. B. 2010. Mitochondrial peroxiredoxin involvement in antioxidant defence and redox signalling. *Biochem J,* 425**,** 313-25.

CUSTODIO, G., KOMECHEN, H., FIGUEIREDO, F. R., FACHIN, N. D., PIANOVSKI, M. A. & FIGUEIREDO, B. C. 2012. Molecular epidemiology of adrenocortical tumors in southern Brazil. *Mol Cell Endocrinol,* 351**,** 44-51.

DALBEY, W. E., NETTESHEIM, P., GRIESEMER, R., CATON, J. E. & GUERIN, M. R. 1980. Chronic inhalation of cigarette smoke by F344 rats. *J Natl Cancer Inst,* 64**,** 383-90.

DANIEL, E., AYLWIN, S., MUSTAFA, O., BALL, S., MUNIR, A., BOELAERT, K., CHORTIS, V., CUTHBERTSON, D. J., DAOUSI, C., RAJEEV, S. P., DAVIS, J., CHEER, K., DRAKE, W., GUNGANAH, K., GROSSMAN, A., GURNELL, M., POWLSON, A. S., KARAVITAKI, N., HUGUET, I., KEARNEY, T., MOHIT, K., MEERAN, K., HILL, N., REES, A., LANSDOWN, A. J., TRAINER, P. J., MINDER, A. E. & NEWELL-PRICE, J. 2015. Effectiveness of Metyrapone in Treating Cushing's Syndrome: A Retrospective Multicenter Study in 195 Patients. *J Clin Endocrinol Metab,* 100**,** 4146-54.

DATRICE, N. M., LANGAN, R. C., RIPLEY, R. T., KEMP, C. D., STEINBERG, S. M., WOOD, B. J., LIBUTTI, S. K., FOJO, T., SCHRUMP, D. S. & AVITAL, I. 2012. Operative management for recurrent and metastatic adrenocortical carcinoma. *J Surg Oncol,* 105**,** 709-13.

DE FRAIPONT, F., EL ATIFI, M., CHERRADI, N., LE MOIGNE, G., DEFAYE, G., HOULGATTE, R., BERTHERAT, J., BERTAGNA, X., PLOUIN, P. F., BAUDIN, E., BERGER, F., GICQUEL, C., CHABRE, O. & FEIGE, J. J. 2005. Gene expression profiling of human adrenocortical tumors using complementary deoxyribonucleic Acid microarrays identifies several candidate genes as markers of malignancy. *J Clin Endocrinol Metab,* 90**,** 1819-29.

DE REYNIES, A., ASSIE, G., RICKMAN, D. S., TISSIER, F., GROUSSIN, L., RENE-CORAIL, F., DOUSSET, B., BERTAGNA, X., CLAUSER, E. & BERTHERAT, J. 2009. Gene expression profiling reveals a new classification of adrenocortical tumors and identifies molecular predictors of malignancy and survival. *J Clin Oncol,* 27**,** 1108-15.

DECKER, R. A., ELSON, P., HOGAN, T. F., CITRIN, D. L., WESTRING, D. W., BANERJEE, T. K., GILCHRIST, K. W. & HORTON, J. 1991. Eastern Cooperative

Oncology Group study 1879: mitotane and adriamycin in patients with advanced adrenocortical carcinoma. *Surgery,* 110**,** 1006-13.

DEL RIO, L. A., SANDALIO, L. M., PALMA, J. M., BUENO, P. & CORPAS, F. J. 1992. Metabolism of oxygen radicals in peroxisomes and cellular implications. *Free Radic Biol Med,* 13**,** 557-80.

DENNING, T. L., TAKAISHI, H., CROWE, S. E., BOLDOGH, I., JEVNIKAR, A. & ERNST, P. B. 2002. Oxidative stress induces the expression of Fas and Fas ligand and apoptosis in murine intestinal epithelial cells. *Free Radic Biol Med,* 33**,** 1641-50.

DEROUET-HUMBERT, E., ROEMER, K. & BUREIK, M. 2005. Adrenodoxin (Adx) and CYP11A1 (P450scc) induce apoptosis by the generation of reactive oxygen species in mitochondria. *Biol Chem,* 386**,** 453-61.

DESHPANDE, S. S., QI, B., PARK, Y. C. & IRANI, K. 2003. Constitutive activation of rac1 results in mitochondrial oxidative stress and induces premature endothelial cell senescence. *Arterioscler Thromb Vasc Biol,* 23**,** e1-6.

DI CARLO, I., TORO, A., SPARATORE, F. & CORDIO, S. 2006. Liver resection for hepatic metastases from adrenocortical carcinoma. *HPB (Oxford),* 8**,** 106-9.

DI PIETRO, C., PIRO, S., TABBI, G., RAGUSA, M., DI PIETRO, V., ZIMMITTI, V., CUDA, F., ANELLO, M., CONSOLI, U., SALINARO, E. T., CARUSO, M., VANCHERI, C., CRIMI, N., SABINI, M. G., CIRRONE, G. A., RAFFAELE, L., PRIVITERA, G., PULVIRENTI, A., GIUGNO, R., FERRO, A., CUTTONE, G., LO NIGRO, S., PURRELLO, R., PURRELLO, F. & PURRELLO, M. 2006. Cellular and molecular effects of protons: apoptosis induction and potential implications for cancer therapy. *Apoptosis,* 11**,** 57-66.

DIEMER, T., ALLEN, J. A., HALES, K. H. & HALES, D. B. 2003. Reactive oxygen disrupts mitochondria in MA-10 tumor Leydig cells and inhibits steroidogenic acute regulatory (StAR) protein and steroidogenesis. *Endocrinology,* 144**,** 2882-91.

DINNES, J., BANCOS, I., FERRANTE DI RUFFANO, L., CHORTIS, V., DAVENPORT, C., BAYLISS, S., SAHDEV, A., GUEST, P., FASSNACHT, M., DEEKS, J. J. & ARLT, W. 2016. MANAGEMENT OF ENDOCRINE DISEASE: Imaging for the diagnosis of malignancy in incidentally discovered adrenal masses: a systematic review and meta-analysis. *Eur J Endocrinol,* 175**,** R51-64.

DOERR, H. G., SIPPELL, W. G., DROP, S. L., BIDLINGMAIER, F. & KNORR, D. 1987. Evidence of 11 beta-hydroxylase deficiency in childhood adrenocortical tumors. The plasma corticosterone/11-deoxycorticosterone ratio as a possible marker for malignancy. *Cancer,* 60**,** 1625-9.

DOHNA, M., REINCKE, M., MINCHEVA, A., ALLOLIO, B., SOLINAS-TOLDO, S. & LICHTER, P. 2000. Adrenocortical carcinoma is characterized by a high frequency of chromosomal gains and high-level amplifications. *Genes Chromosomes Cancer,* 28**,** 145-52.

DONADELLI, M., COSTANZO, C., BEGHELLI, S., SCUPOLI, M. T., DANDREA, M., BONORA, A., PIACENTINI, P., BUDILLON, A., CARAGLIA, M., SCARPA, A. & PALMIERI, M. 2007. Synergistic inhibition of pancreatic adenocarcinoma cell growth by trichostatin A and gemcitabine. *Biochim Biophys Acta,* 1773**,** 1095-106.

DUSRE, L., MIMNAUGH, E. G., MYERS, C. E. & SINHA, B. K. 1989. Potentiation of doxorubicin cytotoxicity by buthionine sulfoximine in multidrug-resistant human breast tumor cells. *Cancer Res,* 49**,** 511-5.

DUYNDAM, M. C., HULSCHER, T. M., FONTIJN, D., PINEDO, H. M. & BOVEN, E. 2001. Induction of vascular endothelial growth factor expression and hypoxia-inducible factor 1alpha protein by the oxidative stressor arsenite. *J Biol Chem,* 276**,** 48066-76.

DY, B. M., WISE, K. B., RICHARDS, M. L., YOUNG, W. F., JR., GRANT, C. S., BIBLE, K. C., ROSEDAHL, J., HARMSEN, W. S., FARLEY, D. R. & THOMPSON, G. B. 2013. Operative intervention for recurrent adrenocortical cancer. *Surgery,* 154**,** 1292-9; discussion 1299.

ELSE, T. 2012. Association of adrenocortical carcinoma with familial cancer susceptibility syndromes. *Mol Cell Endocrinol,* 351**,** 66-70.

ELSE, T., KIM, A. C., SABOLCH, A., RAYMOND, V. M., KANDATHIL, A., CAOILI, E. M., JOLLY, S., MILLER, B. S., GIORDANO, T. J. & HAMMER, G. D. 2014. Adrenocortical carcinoma. *Endocr Rev,* 35**,** 282-326.

ERDOGAN, I., DEUTSCHBEIN, T., JUROWICH, C., KROISS, M., RONCHI, C., QUINKLER, M., WALDMANN, J., WILLENBERG, H. S., BEUSCHLEIN, F., FOTTNER, C., KLOSE, S., HEIDEMEIER, A., BRIX, D., FENSKE, W., HAHNER, S., REIBETANZ, J., ALLOLIO, B., FASSNACHT, M. & GERMAN ADRENOCORTICAL CARCINOMA STUDY, G. 2013. The role of surgery in the management of recurrent adrenocortical carcinoma. *J Clin Endocrinol Metab,* 98**,** 181-91.

FAN, J., YE, J., KAMPHORST, J. J., SHLOMI, T., THOMPSON, C. B. & RABINOWITZ, J. D. 2014. Quantitative flux analysis reveals folate-dependent NADPH production. *Nature,* 510**,** 298-302.

FASSNACHT, M. & ALLOLIO, B. 2009. Clinical management of adrenocortical carcinoma. *Best Pract Res Clin Endocrinol Metab,* 23**,** 273-89.

FASSNACHT, M. & ALLOLIO, B. 2011. Epidemiology of Adrenocortical Carcinoma. *In:* HAMMER, G. & ELSE, T. (eds.) *Adrenocortical Carcinoma.* Springer.

FASSNACHT, M., ARLT, W., BANCOS, I., DRALLE, H., NEWELL-PRICE, J., SAHDEV, A., TABARIN, A., TERZOLO, M., TSAGARAKIS, S. & DEKKERS, O. M. 2016. Management of adrenal incidentalomas: European Society of Endocrinology Clinical Practice Guideline in collaboration with the European Network for the Study of Adrenal Tumors. *Eur J Endocrinol,* 175**,** G1-G34.

FASSNACHT, M., BERRUTI, A., BAUDIN, E., DEMEURE, M. J., GILBERT, J., HAAK, H., KROISS, M., QUINN, D. I., HESSELTINE, E., RONCHI, C. L., TERZOLO, M., CHOUEIRI, T. K., POONDRU, S., FLEEGE, T., RORIG, R., CHEN, J., STEPHENS, A. W., WORDEN, F. & HAMMER, G. D. 2015. Linsitinib (OSI-906) versus placebo for patients with locally advanced or metastatic adrenocortical carcinoma: a double-blind, randomised, phase 3 study. *Lancet Oncol,* 16**,** 426-35.

FASSNACHT, M., HAHNER, S., POLAT, B., KOSCHKER, A. C., KENN, W., FLENTJE, M. & ALLOLIO, B. 2006. Efficacy of adjuvant radiotherapy of the tumor bed on local recurrence of adrenocortical carcinoma. *J Clin Endocrinol Metab,* 91**,** 4501-4.

FASSNACHT, M., JOHANSSEN, S., QUINKLER, M., BUCSKY, P., WILLENBERG, H. S., BEUSCHLEIN, F., TERZOLO, M., MUELLER, H. H., HAHNER, S., ALLOLIO, B., GERMAN ADRENOCORTICAL CARCINOMA REGISTRY, G. & EUROPEAN NETWORK FOR THE STUDY OF ADRENAL, T. 2009. Limited prognostic value of the 2004 International Union Against Cancer staging classification for adrenocortical carcinoma: proposal for a Revised TNM Classification. *Cancer,* 115**,** 243-50.

FASSNACHT, M., KROISS, M. & ALLOLIO, B. 2013. Update in adrenocortical carcinoma. *J Clin Endocrinol Metab,* 98**,** 4551-64.

FASSNACHT, M., LIBE, R., KROISS, M. & ALLOLIO, B. 2011. Adrenocortical carcinoma: a clinician's update. *Nat Rev Endocrinol,* 7**,** 323-35.

FASSNACHT, M., TERZOLO, M., ALLOLIO, B., BAUDIN, E., HAAK, H., BERRUTI, A., WELIN, S., SCHADE-BRITTINGER, C., LACROIX, A., JARZAB, B., SORBYE, H., TORPY, D. J., STEPAN, V., SCHTEINGART, D. E., ARLT, W., KROISS, M., LEBOULLEUX, S., SPERONE, P., SUNDIN, A., HERMSEN, I., HAHNER, S., WILLENBERG, H. S., TABARIN, A., QUINKLER, M., DE LA FOUCHARDIERE, C., SCHLUMBERGER, M., MANTERO, F., WEISMANN, D., BEUSCHLEIN, F., GELDERBLOM, H., WILMINK, H., SENDER, M., EDGERLY, M., KENN, W., FOJO, T., MULLER, H. H., SKOGSEID, B. & GROUP, F.-A. S. 2012. Combination chemotherapy in advanced adrenocortical carcinoma. *N Engl J Med,* 366**,** 2189-97.

FORSS-PETTER, S., WERNER, H., BERGER, J., LASSMANN, H., MOLZER, B., SCHWAB, M. H., BERNHEIMER, H., ZIMMERMANN, F. & NAVE, K. A. 1997. Targeted inactivation of the X-linked adrenoleukodystrophy gene in mice. *J Neurosci Res,* 50**,** 829-43.

FRAGOSO, M. C., ALMEIDA, M. Q., MAZZUCO, T. L., MARIANI, B. M., BRITO, L. P., GONCALVES, T. C., ALENCAR, G. A., LIMA LDE, O., FARIA, A. M., BOURDEAU, I., LUCON, A. M., FREIRE, D. S., LATRONICO, A. C., MENDONCA, B. B., LACROIX, A. & LERARIO, A. M. 2012. Combined expression of BUB1B, DLGAP5, and PINK1 as predictors of poor outcome in adrenocortical tumors: validation in a Brazilian cohort of adult and pediatric patients. *Eur J Endocrinol,* 166**,** 61-7.

FREDERIKS, W. M., KUMMERLIN, I. P., BOSCH, K. S., VREELING-SINDELAROVA, H., JONKER, A. & VAN NOORDEN, C. J. 2007. NADPH production by the pentose phosphate pathway in the zona fasciculata of rat adrenal gland. *J Histochem Cytochem,* 55**,** 975-80.

FREEMAN, H. C., HUGILL, A., DEAR, N. T., ASHCROFT, F. M. & COX, R. D. 2006. Deletion of nicotinamide nucleotide transhydrogenase: a new quantitive trait locus accounting for glucose intolerance in C57BL/6J mice. *Diabetes,* 55**,** 2153-6.

FRUEHAUF, J. P. & MEYSKENS, F. L., JR. 2007. Reactive oxygen species: a breath of life or death? *Clin Cancer Res,* 13**,** 789-94.

FUJISAWA, Y., NAPOLI, E., WONG, S., SONG, G., YAMAGUCHI, R., MATSUI, T., NAGASAKI, K., OGATA, T. & GIULIVI, C. 2015. Impact of a novel homozygous mutation in nicotinamide nucleotide transhydrogenase on mitochondrial DNA integrity in a case of familial glucocorticoid deficiency. *BBA Clin,* 3**,** 70-78.

GAMEIRO, P. A., LAVIOLETTE, L. A., KELLEHER, J. K., ILIOPOULOS, O. & STEPHANOPOULOS, G. 2013. Cofactor balance by nicotinamide nucleotide transhydrogenase (NNT) coordinates reductive carboxylation and glucose catabolism in the tricarboxylic acid (TCA) cycle. *J Biol Chem,* 288**,** 12967-77.

GANDIN, V., FERNANDES, A. P., RIGOBELLO, M. P., DANI, B., SORRENTINO, F., TISATO, F., BJORNSTEDT, M., BINDOLI, A., STURARO, A., RELLA, R. & MARZANO, C. 2010. Cancer cell death induced by phosphine gold(I) compounds targeting thioredoxin reductase. *Biochem Pharmacol,* 79**,** 90-101.

GARBARINO, J. A., CARDILE, V., LOMBARDO, L., CHAMY, M. C., PIOVANO, M. & RUSSO, A. 2007. Demalonyl thyrsiflorin A, a semisynthetic labdane-derived diterpenoid, induces apoptosis and necrosis in human epithelial cancer cells. *Chem Biol Interact,* 169**,** 198-206.

GARCIA-CALVO, M., PETERSON, E. P., RASPER, D. M., VAILLANCOURT, J. P., ZAMBONI, R., NICHOLSON, D. W. & THORNBERRY, N. A. 1999. Purification and catalytic properties of human caspase family members. *Cell Death Differ,* 6**,** 362-9.

GAUJOUX, S., TISSIER, F., GROUSSIN, L., LIBE, R., RAGAZZON, B., LAUNAY, P., AUDEBOURG, A., DOUSSET, B., BERTAGNA, X. & BERTHERAT, J. 2008. Wnt/beta-catenin and 3',5'-cyclic adenosine 5'-monophosphate/protein kinase A signaling pathways alterations and somatic beta-catenin gene mutations in the progression of adrenocortical tumors. *J Clin Endocrinol Metab,* 93**,** 4135-40.

GICQUEL, C., BERTAGNA, X., GASTON, V., COSTE, J., LOUVEL, A., BAUDIN, E., BERTHERAT, J., CHAPUIS, Y., DUCLOS, J. M., SCHLUMBERGER, M., PLOUIN, P. F., LUTON, J. P. & LE BOUC, Y. 2001. Molecular markers and long-term recurrences in a large cohort of patients with sporadic adrenocortical tumors. *Cancer Res,* 61**,** 6762-7.

GICQUEL, C., LEBLOND-FRANCILLARD, M., BERTAGNA, X., LOUVEL, A., CHAPUIS, Y., LUTON, J. P., GIRARD, F. & LE BOUC, Y. 1994. Clonal analysis of human adrenocortical carcinomas and secreting adenomas. *Clin Endocrinol (Oxf),* 40**,** 465-77.

GIORDANO, T. J., KUICK, R., ELSE, T., GAUGER, P. G., VINCO, M., BAUERSFELD, J., SANDERS, D., THOMAS, D. G., DOHERTY, G. & HAMMER, G. 2009. Molecular classification and prognostication of adrenocortical tumors by transcriptome profiling. *Clin Cancer Res,* 15**,** 668-76.

GLENNAS, A., KVIEN, T. K., ANDRUP, O., CLARKE-JENSSEN, O., KARSTENSEN, B. & BRODIN, U. 1997. Auranofin is safe and superior to placebo in elderly-onset rheumatoid arthritis. *Br J Rheumatol,* 36**,** 870-7.

GLORIEUX, C., ZAMOCKY, M., SANDOVAL, J. M., VERRAX, J. & CALDERON, P. B. 2015. Regulation of catalase expression in healthy and cancerous cells. *Free Radic Biol Med,* 87**,** 84-97.

GORDAN, J. D., BERTOUT, J. A., HU, C. J., DIEHL, J. A. & SIMON, M. C. 2007. HIF-2alpha promotes hypoxic cell proliferation by enhancing c-myc transcriptional activity. *Cancer Cell,* 11**,** 335-47.

GRINBERG, A. V., HANNEMANN, F., SCHIFFLER, B., MULLER, J., HEINEMANN, U. & BERNHARDT, R. 2000. Adrenodoxin: structure, stability, and electron transfer properties. *Proteins,* 40**,** 590-612.

GRONDAL, S., ERIKSSON, B., HAGENAS, L., WERNER, S. & CURSTEDT, T. 1990. Steroid profile in urine: a useful tool in the diagnosis and follow up of adrenocortical carcinoma. *Acta Endocrinol (Copenh),* 122**,** 656-63.

GUMIREDDY, K., LI, A., CAO, L., YAN, J., LIU, L., XU, X., PAZOLES, C. & HUANG, Q. 2013. NOV-002, A Glutathione Disulfide Mimetic, Suppresses Tumor Cell Invasion and Metastasis. *J Carcinog Mutagen,* 2013.

GUPTA, A., BHATT, M. L. & MISRA, M. K. 2010. Assessment of free radical-mediated damage in head and neck squamous cell carcinoma patients and after treatment with radiotherapy. *Indian J Biochem Biophys,* 47**,** 96-9.

GUPTA, S. C., HEVIA, D., PATCHVA, S., PARK, B., KOH, W. & AGGARWAL, B. B. 2012. Upsides and downsides of reactive oxygen species for cancer: the roles of reactive oxygen species in tumorigenesis, prevention, and therapy. *Antioxid Redox Signal,* 16**,** 1295-322.

GUZY, R. D., MACK, M. M. & SCHUMACKER, P. T. 2007. Mitochondrial complex III is required for hypoxia-induced ROS production and gene transcription in yeast. *Antioxid Redox Signal,* 9**,** 1317-28.

GUZY, R. D. & SCHUMACKER, P. T. 2006. Oxygen sensing by mitochondria at complex III: the paradox of increased reactive oxygen species during hypoxia. *Exp Physiol,* 91**,** 807-19.

HAAK, H. R., CORNELISSE, C. J., HERMANS, J., COBBEN, L. & FLEUREN, G. J. 1993. Nuclear DNA content and morphological characteristics in the prognosis of adrenocortical carcinoma. *Br J Cancer,* 68**,** 151-5.

HABRA, M. A., EJAZ, S., FENG, L., DAS, P., DENIZ, F., GRUBBS, E. G., PHAN, A., WAGUESPACK, S. G., AYALA-RAMIREZ, M., JIMENEZ, C., PERRIER, N. D., LEE, J. E. & VASSILOPOULOU-SELLIN, R. 2013. A retrospective cohort analysis of the efficacy of adjuvant radiotherapy after primary surgical resection in patients with adrenocortical carcinoma. *J Clin Endocrinol Metab,* 98**,** 192-7.

HAHNER, S. & FASSNACHT, M. 2005. Mitotane for adrenocortical carcinoma treatment. *Curr Opin Investig Drugs,* 6**,** 386-94.

HAHNER, S., KREISSL, M. C., FASSNACHT, M., HAENSCHEID, H., KNOEDLER, P., LANG, K., BUCK, A. K., REINERS, C., ALLOLIO, B. & SCHIRBEL, A. 2012. [131I]iodometomidate for targeted radionuclide therapy of advanced adrenocortical carcinoma. *J Clin Endocrinol Metab,* 97**,** 914-22.

HAHNER, S. H., B; HERRMANN, K; BUCK, AK; BLÜMEL, C; HÄNSCHEID, H; BRUMBERG, J; MICHELMANN, D; NANNEN, L; RIES, M; FASSNACHT, M; ALLOLIO, B & SCHIRBEL, A 2015. [123/131I] azetidinylamide a novel radiotracer for diagnosis and treatment of adrenocortical tumours -- from bench to bedside. *Endocrine abstracts,* 37.

HALVEY, P. J., WATSON, W. H., HANSEN, J. M., GO, Y. M., SAMALI, A. & JONES, D. P. 2005. Compartmental oxidation of thiol-disulphide redox couples during epidermal growth factor signalling. *Biochem J,* 386**,** 215-9.

HAMPTON, M. B. & ORRENIUS, S. 1997. Dual regulation of caspase activity by hydrogen peroxide: implications for apoptosis. *FEBS Lett,* 414**,** 552-6.

HAN, D., ANTUNES, F., CANALI, R., RETTORI, D. & CADENAS, E. 2003. Voltage-dependent anion channels control the release of the superoxide anion from mitochondria to cytosol. *J Biol Chem,* 278**,** 5557-63.

HANSEN, J. M., ZHANG, H. & JONES, D. P. 2006. Differential oxidation of thioredoxin-1, thioredoxin-2, and glutathione by metal ions. *Free Radic Biol Med,* 40**,** 138-45.

HANUKOGLU, I. 2006. Antioxidant protective mechanisms against reactive oxygen species (ROS) generated by mitochondrial P450 systems in steroidogenic cells. *Drug Metab Rev,* 38**,** 171-96.

HANUKOGLU, I. & HANUKOGLU, Z. 1986. Stoichiometry of mitochondrial cytochromes P-450, adrenodoxin and adrenodoxin reductase in adrenal cortex and corpus luteum. Implications for membrane organization and gene regulation. *Eur J Biochem,* 157**,** 27-31.

HAQ, M. M., LEGHA, S. S., SAMAAN, N. A., BODEY, G. P. & BURGESS, M. A. 1980. Cytotoxic chemotherapy in adrenal cortical carcinoma. *Cancer Treat Rep,* 64**,** 909-13.

HARING, R., WALLASCHOFSKI, H., TEUMER, A., KROEMER, H., TAYLOR, A. E., SHACKLETON, C. H., NAUCK, M., VOLKER, U., HOMUTH, G. & ARLT, W. 2013. A SULT2A1 genetic variant identified by GWAS as associated with low serum DHEAS does not impact on the actual DHEA/DHEAS ratio. *J Mol Endocrinol,* 50**,** 73-7.

HELLFRITSCH, J., KIRSCH, J., SCHNEIDER, M., FLUEGE, T., WORTMANN, M., FRIJHOFF, J., DAGNELL, M., FEY, T., ESPOSITO, I., KOLLE, P., POGODA, K., ANGELI, J. P., INGOLD, I., KUHLENCORDT, P., OSTMAN, A., POHL, U., CONRAD, M. & BECK, H. 2015. Knockout of mitochondrial thioredoxin reductase stabilizes prolyl

hydroxylase 2 and inhibits tumor growth and tumor-derived angiogenesis. *Antioxid Redox Signal,* 22**,** 938-50.

HERMSEN, I. G., GROENEN, Y. E., DERCKSEN, M. W., THEUWS, J. & HAAK, H. R. 2010. Response to radiation therapy in adrenocortical carcinoma. *J Endocrinol Invest,* 33**,** 712-4.

HERSHKOVITZ, E., ARAFAT, M., LOEWENTHAL, N., HAIM, A. & PARVARI, R. 2015. Combined adrenal failure and testicular adrenal rest tumor in a patient with nicotinamide nucleotide transhydrogenase deficiency. *J Pediatr Endocrinol Metab,* 28**,** 1187-90.

HILL, K. E., MCCOLLUM, G. W., BOEGLIN, M. E. & BURK, R. F. 1997. Thioredoxin reductase activity is decreased by selenium deficiency. *Biochem Biophys Res Commun,* 234**,** 293-5.

HIRSCHMANN, H. & HIRSCHMANN, F. B. 1950. Steroid excretion in a case of adrenocortical carcinoma. V. delta 5-Pregnenetriol-3 beta, 17 alpha, 20 alpha. *J Biol Chem,* 187**,** 137-46.

HO, B. Y., WU, Y. M., CHANG, K. J. & PAN, T. M. 2011. Dimerumic acid inhibits SW620 cell invasion by attenuating H(2)O(2)-mediated MMP-7 expression via JNK/C-Jun and ERK/C-Fos activation in an AP-1-dependent manner. *Int J Biol Sci,* 7**,** 869-80.

HO, J., TURKBEY, B., EDGERLY, M., ALIMCHANDANI, M., QUEZADO, M., CAMPHAUSEN, K., FOJO, T. & KAUSHAL, A. 2013. Role of radiotherapy in adrenocortical carcinoma. *Cancer J,* 19**,** 288-94.

HORNSBY, P. J. 1980. Regulation of cytochrome P-450-supported 11 beta-hydroxylation of deoxycortisol by steroids, oxygen, and antioxidants in adrenocortical cell cultures. *J Biol Chem,* 255**,** 4020-7.

HOSHIDA, Y., MORIYAMA, M., OTSUKA, M., KATO, N., TANIGUCHI, H., SHIRATORI, Y., SEKI, N. & OMATA, M. 2007. Gene expressions associated with chemosensitivity in human hepatoma cells. *Hepatogastroenterology,* 54**,** 489-92.

HSING, A. W., NAM, J. M., CO CHIEN, H. T., MCLAUGHLIN, J. K. & FRAUMENI, J. F., JR. 1996. Risk factors for adrenal cancer: an exploratory study. *Int J Cancer,* 65**,** 432-6.

HSU, C. H., CHEN, C. L., HONG, R. L., CHEN, K. L., LIN, J. F. & CHENG, A. L. 2002. Prognostic value of multidrug resistance 1, glutathione-S-transferase-pi and p53 in advanced nasopharyngeal carcinoma treated with systemic chemotherapy. *Oncology,* 62**,** 305-12.

HU, Y., ROSEN, D. G., ZHOU, Y., FENG, L., YANG, G., LIU, J. & HUANG, P. 2005. Mitochondrial manganese-superoxide dismutase expression in ovarian cancer: role in cell proliferation and response to oxidative stress. *J Biol Chem,* 280**,** 39485-92.

HUANG, L. E., ARANY, Z., LIVINGSTON, D. M. & BUNN, H. F. 1996. Activation of hypoxia-inducible transcription factor depends primarily upon redox-sensitive stabilization of its alpha subunit. *J Biol Chem,* 271**,** 32253-9.

HUEBNER, A., MANN, P., ROHDE, E., KAINDL, A. M., WITT, M., VERKADE, P., JAKUBICZKA, S., MENSCHIKOWSKI, M., STOLTENBURG-DIDINGER, G. & KOEHLER, K. 2006. Mice lacking the nuclear pore complex protein ALADIN show female infertility but fail to develop a phenotype resembling human triple A syndrome. *Mol Cell Biol,* 26**,** 1879-87.

ICARD, P., LOUVEL, A. & CHAPUIS, Y. 1992. Survival rates and prognostic factors in adrenocortical carcinoma. *World J Surg,* 16**,** 753-8.

IRANI, K., XIA, Y., ZWEIER, J. L., SOLLOTT, S. J., DER, C. J., FEARON, E. R., SUNDARESAN, M., FINKEL, T. & GOLDSCHMIDT-CLERMONT, P. J. 1997.

Mitogenic signaling mediated by oxidants in Ras-transformed fibroblasts. *Science,* 275**,** 1649-52.

IVASHCHENKO, O., VAN VELDHOVEN, P. P., BREES, C., HO, Y. S., TERLECKY, S. R. & FRANSEN, M. 2011. Intraperoxisomal redox balance in mammalian cells: oxidative stress and interorganellar cross-talk. *Mol Biol Cell,* 22**,** 1440-51.

JACKSON, A. L. & LINSLEY, P. S. 2010. Recognizing and avoiding siRNA off-target effects for target identification and therapeutic application. *Nat Rev Drug Discov,* 9**,** 57-67.

JAMES, J., MURRY, D. J., TRESTON, A. M., STORNIOLO, A. M., SLEDGE, G. W., SIDOR, C. & MILLER, K. D. 2007. Phase I safety, pharmacokinetic and pharmacodynamic studies of 2-methoxyestradiol alone or in combination with docetaxel in patients with locally recurrent or metastatic breast cancer. *Invest New Drugs,* 25**,** 41-8.

JAZAYERI, O., LIU, X., VAN DIEMEN, C. C., BAKKER-VAN WAARDE, W. M., SIKKEMA-RADDATZ, B., SINKE, R. J., ZHANG, J. & VAN RAVENSWAAIJ-ARTS, C. M. 2015. A novel homozygous insertion and review of published mutations in the NNT gene causing familial glucocorticoid deficiency (FGD). *Eur J Med Genet,* 58**,** 642-9.

JING, Y., DAI, J., CHALMERS-REDMAN, R. M., TATTON, W. G. & WAXMAN, S. 1999. Arsenic trioxide selectively induces acute promyelocytic leukemia cell apoptosis via a hydrogen peroxide-dependent pathway. *Blood,* 94**,** 2102-11.

JO, S. H., SON, M. K., KOH, H. J., LEE, S. M., SONG, I. H., KIM, Y. O., LEE, Y. S., JEONG, K. S., KIM, W. B., PARK, J. W., SONG, B. J. & HUH, T. L. 2001. Control of mitochondrial redox balance and cellular defense against oxidative damage by mitochondrial NADP+-dependent isocitrate dehydrogenase. *J Biol Chem,* 276**,** 16168-76.

JOHANSSEN, S., HAHNER, S., SAEGER, W., QUINKLER, M., BEUSCHLEIN, F., DRALLE, H., HAAF, M., KROISS, M., JUROWICH, C., LANGER, P., OELKERS, W., SPAHN, M., WILLENBERG, H. S., MADER, U., ALLOLIO, B. & FASSNACHT, M. 2010. Deficits in the management of patients with adrenocortical carcinoma in Germany. *Dtsch Arztebl Int,* 107**,** 885-91.

JONES, C. U., HUNT, D., MCGOWAN, D. G., AMIN, M. B., CHETNER, M. P., BRUNER, D. W., LEIBENHAUT, M. H., HUSAIN, S. M., ROTMAN, M., SOUHAMI, L., SANDLER, H. M. & SHIPLEY, W. U. 2011. Radiotherapy and short-term androgen deprivation for localized prostate cancer. *N Engl J Med,* 365**,** 107-18.

JUHLEN, R., IDKOWIAK, J., TAYLOR, A. E., KIND, B., ARLT, W., HUEBNER, A. & KOEHLER, K. 2015. Role of ALADIN in human adrenocortical cells for oxidative stress response and steroidogenesis. *PLoS One,* 10**,** e0124582.

KAIMUL, A. M., NAKAMURA, H., MASUTANI, H. & YODOI, J. 2007. Thioredoxin and thioredoxin-binding protein-2 in cancer and metabolic syndrome. *Free Radic Biol Med,* 43**,** 861-8.

KEBEBEW, E., REIFF, E., DUH, Q. Y., CLARK, O. H. & MCMILLAN, A. 2006. Extent of disease at presentation and outcome for adrenocortical carcinoma: have we made progress? *World J Surg,* 30**,** 872-8.

KERKHOFS, T. M., KERSTENS, M. N., KEMA, I. P., WILLEMS, T. P. & HAAK, H. R. 2015. Diagnostic Value of Urinary Steroid Profiling in the Evaluation of Adrenal Tumors. *Horm Cancer,* 6**,** 168-75.

KERKHOFS, T. M., VERHOEVEN, R. H., VAN DER ZWAN, J. M., DIELEMAN, J., KERSTENS, M. N., LINKS, T. P., VAN DE POLL-FRANSE, L. V. & HAAK, H. R. 2013. Adrenocortical carcinoma: a population-based study on incidence and survival in the Netherlands since 1993. *Eur J Cancer,* 49**,** 2579-86.

KHAN, T. S., IMAM, H., JUHLIN, C., SKOGSEID, B., GRONDAL, S., TIBBLIN, S., WILANDER, E., OBERG, K. & ERIKSSON, B. 2000. Streptozocin and o,p'DDD in the treatment of adrenocortical cancer patients: long-term survival in its adjuvant use. *Ann Oncol,* 11**,** 1281-7.

KHAN, T. S., SUNDIN, A., JUHLIN, C., WILANDER, E., OBERG, K. & ERIKSSON, B. 2004. Vincristine, cisplatin, teniposide, and cyclophosphamide combination in the treatment of recurrent or metastatic adrenocortical cancer. *Med Oncol,* 21**,** 167-77.

KIRSHNER, J. R., HE, S., BALASUBRAMANYAM, V., KEPROS, J., YANG, C. Y., ZHANG, M., DU, Z., BARSOUM, J. & BERTIN, J. 2008. Elesclomol induces cancer cell apoptosis through oxidative stress. *Mol Cancer Ther,* 7**,** 2319-27.

KJELLMAN, M., KALLIONIEMI, O. P., KARHU, R., HOOG, A., FARNEBO, L. O., AUER, G., LARSSON, C. & BACKDAHL, M. 1996. Genetic aberrations in adrenocortical tumors detected using comparative genomic hybridization correlate with tumor size and malignancy. *Cancer Res,* 56**,** 4219-23.

KJELLMAN, M., ROSHANI, L., TEH, B. T., KALLIONIEMI, O. P., HOOG, A., GRAY, S., FARNEBO, L. O., HOLST, M., BACKDAHL, M. & LARSSON, C. 1999. Genotyping of adrenocortical tumors: very frequent deletions of the MEN1 locus in 11q13 and of a 1-centimorgan region in 2p16. *J Clin Endocrinol Metab,* 84**,** 730-5.

KLOOS, R. T., GROSS, M. D., FRANCIS, I. R., KOROBKIN, M. & SHAPIRO, B. 1995. Incidentally discovered adrenal masses. *Endocr Rev,* 16**,** 460-84.

KOKA, P. S., MONDAL, D., SCHULTZ, M., ABDEL-MAGEED, A. B. & AGRAWAL, K. C. 2010. Studies on molecular mechanisms of growth inhibitory effects of thymoquinone against prostate cancer cells: role of reactive oxygen species. *Exp Biol Med (Maywood),* 235**,** 751-60.

KONA, F. R., BUAC, D. & A, M. B. 2011. Disulfiram, and disulfiram derivatives as novel potential anticancer drugs targeting the ubiquitin-proteasome system in both preclinical and clinical studies. *Curr Cancer Drug Targets,* 11**,** 338-46.

KOTAMRAJU, S., CHITAMBAR, C. R., KALIVENDI, S. V., JOSEPH, J. & KALYANARAMAN, B. 2002. Transferrin receptor-dependent iron uptake is responsible for doxorubicin-mediated apoptosis in endothelial cells: role of oxidant-induced iron signaling in apoptosis. *J Biol Chem,* 277**,** 17179-87.

KROISS, M., QUINKLER, M., JOHANSSEN, S., VAN ERP, N. P., LANKHEET, N., POLLINGER, A., LAUBNER, K., STRASBURGER, C. J., HAHNER, S., MULLER, H. H., ALLOLIO, B. & FASSNACHT, M. 2012. Sunitinib in refractory adrenocortical carcinoma: a phase II, single-arm, open-label trial. *J Clin Endocrinol Metab,* 97**,** 3495-503.

KROISS, M., QUINKLER, M., LUTZ, W. K., ALLOLIO, B. & FASSNACHT, M. 2011. Drug interactions with mitotane by induction of CYP3A4 metabolism in the clinical management of adrenocortical carcinoma. *Clin Endocrinol (Oxf),* 75**,** 585-91.

KRYSKO, D. V., VANDEN BERGHE, T., D'HERDE, K. & VANDENABEELE, P. 2008. Apoptosis and necrosis: detection, discrimination and phagocytosis. *Methods,* 44**,** 205-21.

KUNIKOWSKA, J., MATYSKIEL, R., TOUTOUNCHI, S., GRABOWSKA-DERLATKA, L., KOPERSKI, L. & KROLICKI, L. 2014. What parameters from 18F-FDG PET/CT are useful in evaluation of adrenal lesions? *Eur J Nucl Med Mol Imaging,* 41**,** 2273-80.

LA ROCCA, R. V., STEIN, C. A., DANESI, R., JAMIS-DOW, C. A., WEISS, G. H. & MYERS, C. E. 1990a. Suramin in adrenal cancer: modulation of steroid hormone production, cytotoxicity in vitro, and clinical antitumor effect. *J Clin Endocrinol Metab,* 71**,** 497-504.

LA ROCCA, R. V., STEIN, C. A., DANESI, R. & MYERS, C. E. 1990b. Suramin, a novel antitumor compound. *J Steroid Biochem Mol Biol,* 37**,** 893-8.

LAPUNZINA, P. 2005. Risk of tumorigenesis in overgrowth syndromes: a comprehensive review. *Am J Med Genet C Semin Med Genet,* 137C**,** 53-71.

LEE, H. R., CHO, J. M., SHIN, D. H., YONG, C. S., CHOI, H. G., WAKABAYASHI, N. & KWAK, M. K. 2008. Adaptive response to GSH depletion and resistance to L-buthionine-(S,R)-sulfoximine: involvement of Nrf2 activation. *Mol Cell Biochem,* 318**,** 23-31.

LEI, S., ZAVALA-FLORES, L., GARCIA-GARCIA, A., NANDAKUMAR, R., HUANG, Y., MADAYIPUTHIYA, N., STANTON, R. C., DODDS, E. D., POWERS, R. & FRANCO, R. 2014. Alterations in energy/redox metabolism induced by mitochondrial and environmental toxins: a specific role for glucose-6-phosphate-dehydrogenase and the pentose phosphate pathway in paraquat toxicity. *ACS Chem Biol,* 9**,** 2032-48.

LENDERS, J. W., DUH, Q. Y., EISENHOFER, G., GIMENEZ-ROQUEPLO, A. P., GREBE, S. K., MURAD, M. H., NARUSE, M., PACAK, K., YOUNG, W. F., JR. & ENDOCRINE, S. 2014. Pheochromocytoma and paraganglioma: an endocrine society clinical practice guideline. *J Clin Endocrinol Metab,* 99**,** 1915-42.

LERARIO, A. M., WORDEN, F. P., RAMM, C. A., HESSELTINE, E. A., STADLER, W. M., ELSE, T., SHAH, M. H., AGAMAH, E., RAO, K. & HAMMER, G. D. 2014. The combination of insulin-like growth factor receptor 1 (IGF1R) antibody cixutumumab and mitotane as a first-line therapy for patients with recurrent/metastatic adrenocortical carcinoma: a multi-institutional NCI-sponsored trial. *Horm Cancer,* 5**,** 232-9.

LEUNG, J. H., SCHURIG-BRICCIO, L. A., YAMAGUCHI, M., MOELLER, A., SPEIR, J. A., GENNIS, R. B. & STOUT, C. D. 2015. Structural biology. Division of labor in transhydrogenase by alternating proton translocation and hydride transfer. *Science,* 347**,** 178-81.

LEWIS, C. A., PARKER, S. J., FISKE, B. P., MCCLOSKEY, D., GUI, D. Y., GREEN, C. R., VOKES, N. I., FEIST, A. M., VANDER HEIDEN, M. G. & METALLO, C. M. 2014. Tracing compartmentalized NADPH metabolism in the cytosol and mitochondria of mammalian cells. *Mol Cell,* 55**,** 253-63.

LI, H., HU, J., WU, S., WANG, L., CAO, X., ZHANG, X., DAI, B., CAO, M., SHAO, R., ZHANG, R., MAJIDI, M., JI, L., HEYMACH, J. V., WANG, M., PAN, S., MINNA, J., MEHRAN, R. J., SWISHER, S. G., ROTH, J. A. & FANG, B. 2016. Auranofin-mediated inhibition of PI3K/AKT/mTOR axis and anticancer activity in non-small cell lung cancer cells. *Oncotarget,* 7**,** 3548-58.

LI, Y., HUANG, T. T., CARLSON, E. J., MELOV, S., URSELL, P. C., OLSON, J. L., NOBLE, L. J., YOSHIMURA, M. P., BERGER, C., CHAN, P. H., WALLACE, D. C. & EPSTEIN, C. J. 1995. Dilated cardiomyopathy and neonatal lethality in mutant mice lacking manganese superoxide dismutase. *Nat Genet,* 11**,** 376-81.

LIBE, R. 2015. Adrenocortical carcinoma (ACC): diagnosis, prognosis, and treatment. *Front Cell Dev Biol,* 3**,** 45.

LIBE, R., BORGET, I., RONCHI, C. L., ZAGGIA, B., KROISS, M., KERKHOFS, T., BERTHERAT, J., VOLANTE, M., QUINKLER, M., CHABRE, O., BALA, M., TABARIN, A., BEUSCHLEIN, F., VEZZOSI, D., DEUTSCHBEIN, T., BORSON-CHAZOT, F., HERMSEN, I., STELL, A., FOTTNER, C., LEBOULLEUX, S., HAHNER, S., MANNELLI, M., BERRUTI, A., HAAK, H., TERZOLO, M., FASSNACHT, M., BAUDIN, E. & NETWORK, E. 2015. Prognostic factors in stage III-IV adrenocortical carcinomas (ACC): an European Network for the Study of Adrenal Tumor (ENSAT) study. *Ann Oncol,* 26**,** 2119-25.

LIN, J., ZAHURAK, M., BEER, T. M., RYAN, C. J., WILDING, G., MATHEW, P., MORRIS, M., CALLAHAN, J. A., GORDON, G., REICH, S. D., CARDUCCI, M. A. & ANTONARAKIS, E. S. 2013. A non-comparative randomized phase II study of 2 doses of ATN-224, a copper/zinc superoxide dismutase inhibitor, in patients with biochemically recurrent hormone-naive prostate cancer. *Urol Oncol,* 31**,** 581-8.

LIU, S. L., LIN, X., SHI, D. Y., CHENG, J., WU, C. Q. & ZHANG, Y. D. 2002. Reactive oxygen species stimulated human hepatoma cell proliferation via cross-talk between PI3-K/PKB and JNK signaling pathways. *Arch Biochem Biophys,* 406**,** 173-82.

LO-COCO, F., AVVISATI, G., VIGNETTI, M., THIEDE, C., ORLANDO, S. M., IACOBELLI, S., FERRARA, F., FAZI, P., CICCONI, L., DI BONA, E., SPECCHIA, G., SICA, S., DIVONA, M., LEVIS, A., FIEDLER, W., CERQUI, E., BRECCIA, M., FIORITONI, G., SALIH, H. R., CAZZOLA, M., MELILLO, L., CARELLA, A. M., BRANDTS, C. H., MORRA, E., VON LILIENFELD-TOAL, M., HERTENSTEIN, B., WATTAD, M., LUBBERT, M., HANEL, M., SCHMITZ, N., LINK, H., KROPP, M. G., RAMBALDI, A., LA NASA, G., LUPPI, M., CICERI, F., FINIZIO, O., VENDITTI, A., FABBIANO, F., DOHNER, K., SAUER, M., GANSER, A., AMADORI, S., MANDELLI, F., DOHNER, H., EHNINGER, G., SCHLENK, R. F., PLATZBECKER, U., GRUPPO ITALIANO MALATTIE EMATOLOGICHE, D. A., GERMAN-AUSTRIAN ACUTE MYELOID LEUKEMIA STUDY, G. & STUDY ALLIANCE, L. 2013. Retinoic acid and arsenic trioxide for acute promyelocytic leukemia. *N Engl J Med,* 369**,** 111-21.

LOPERT, P. & PATEL, M. 2014. Nicotinamide nucleotide transhydrogenase (Nnt) links the substrate requirement in brain mitochondria for hydrogen peroxide removal to the thioredoxin/peroxiredoxin (Trx/Prx) system. *J Biol Chem,* 289**,** 15611-20.

LU, J., CHEW, E. H. & HOLMGREN, A. 2007. Targeting thioredoxin reductase is a basis for cancer therapy by arsenic trioxide. *Proc Natl Acad Sci U S A,* 104**,** 12288-93.

LUGHEZZANI, G., SUN, M., PERROTTE, P., JELDRES, C., ALASKER, A., ISBARN, H., BUDAUS, L., SHARIAT, S. F., GUAZZONI, G., MONTORSI, F. & KARAKIEWICZ, P. I. 2010. The European Network for the Study of Adrenal Tumors staging system is prognostically superior to the international union against cancer-staging system: a North American validation. *Eur J Cancer,* 46**,** 713-9.

LUTON, J. P., CERDAS, S., BILLAUD, L., THOMAS, G., GUILHAUME, B., BERTAGNA, X., LAUDAT, M. H., LOUVEL, A., CHAPUIS, Y., BLONDEAU, P. & ET AL. 1990. Clinical features of adrenocortical carcinoma, prognostic factors, and the effect of mitotane therapy. *N Engl J Med,* 322**,** 1195-201.

MACCHI, C., REBUFFAT, P., BLANDAMURA, S., PIAZZA, M., MACCHI, V., FIORE, D. & NUSSDORFER, G. G. 1998. Adrenocortical oncocytoma: case report and review of the literature. *Tumori,* 84**,** 403-7.

MADEIRA, J. M., GIBSON, D. L., KEAN, W. F. & KLEGERIS, A. 2012. The biological activity of auranofin: implications for novel treatment of diseases. *Inflammopharmacology,* 20**,** 297-306.

MAEDA, H., HORI, S., OHIZUMI, H., SEGAWA, T., KAKEHI, Y., OGAWA, O. & KAKIZUKA, A. 2004. Effective treatment of advanced solid tumors by the combination of arsenic trioxide and L-buthionine-sulfoximine. *Cell Death Differ,* 11**,** 737-46.

MAGEE, B. J., GATTAMANENI, H. R. & PEARSON, D. 1987. Adrenal cortical carcinoma: survival after radiotherapy. *Clin Radiol,* 38**,** 587-8.

MALKIN, D., LI, F. P., STRONG, L. C., FRAUMENI, J. F., JR., NELSON, C. E., KIM, D. H., KASSEL, J., GRYKA, M. A., BISCHOFF, F. Z., TAINSKY, M. A. & ET AL. 1990.

Germ line p53 mutations in a familial syndrome of breast cancer, sarcomas, and other neoplasms. *Science,* 250**,** 1233-8.

MANTERO, F., TERZOLO, M., ARNALDI, G., OSELLA, G., MASINI, A. M., ALI, A., GIOVAGNETTI, M., OPOCHER, G. & ANGELI, A. 2000. A survey on adrenal incidentaloma in Italy. Study Group on Adrenal Tumors of the Italian Society of Endocrinology. *J Clin Endocrinol Metab,* 85**,** 637-44.

MARI, M., MORALES, A., COLELL, A., GARCIA-RUIZ, C. & FERNANDEZ-CHECA, J. C. 2009. Mitochondrial glutathione, a key survival antioxidant. *Antioxid Redox Signal,* 11**,** 2685-700.

MARTIN, V., HERRERA, F., GARCIA-SANTOS, G., ANTOLIN, I., RODRIGUEZ-BLANCO, J. & RODRIGUEZ, C. 2007. Signaling pathways involved in antioxidant control of glioma cell proliferation. *Free Radic Biol Med,* 42**,** 1715-22.

MARTINDALE, J. L. & HOLBROOK, N. J. 2002. Cellular response to oxidative stress: signaling for suicide and survival. *J Cell Physiol,* 192**,** 1-15.

MEDAN, D., WANG, L., TOLEDO, D., LU, B., STEHLIK, C., JIANG, B. H., SHI, X. & ROJANASAKUL, Y. 2005. Regulation of Fas (CD95)-induced apoptotic and necrotic cell death by reactive oxygen species in macrophages. *J Cell Physiol,* 203**,** 78-84.

MEHTA, M. P., SHAPIRO, W. R., PHAN, S. C., GERVAIS, R., CARRIE, C., CHABOT, P., PATCHELL, R. A., GLANTZ, M. J., RECHT, L., LANGER, C., SUR, R. K., ROA, W. H., MAHE, M. A., FORTIN, A., NIEDER, C., MEYERS, C. A., SMITH, J. A., MILLER, R. A. & RENSCHLER, M. F. 2009. Motexafin gadolinium combined with prompt whole brain radiotherapy prolongs time to neurologic progression in non-small-cell lung cancer patients with brain metastases: results of a phase III trial. *Int J Radiat Oncol Biol Phys,* 73**,** 1069-76.

MEIMARIDOU, E., HUGHES, C. R., KOWALCZYK, J., GUASTI, L., CHAPPLE, J. P., KING, P. J., CHAN, L. F., CLARK, A. J. & METHERELL, L. A. 2013. Familial glucocorticoid deficiency: New genes and mechanisms. *Mol Cell Endocrinol,* 371**,** 195-200.

MEIMARIDOU, E., KOWALCZYK, J., GUASTI, L., HUGHES, C. R., WAGNER, F., FROMMOLT, P., NURNBERG, P., MANN, N. P., BANERJEE, R., SAKA, H. N., CHAPPLE, J. P., KING, P. J., CLARK, A. J. & METHERELL, L. A. 2012. Mutations in NNT encoding nicotinamide nucleotide transhydrogenase cause familial glucocorticoid deficiency. *Nat Genet,* 44**,** 740-2.

METHERELL, L. A., CHAPPLE, J. P., COORAY, S., DAVID, A., BECKER, C., RUSCHENDORF, F., NAVILLE, D., BEGEOT, M., KHOO, B., NURNBERG, P., HUEBNER, A., CHEETHAM, M. E. & CLARK, A. J. 2005. Mutations in MRAP, encoding a new interacting partner of the ACTH receptor, cause familial glucocorticoid deficiency type 2. *Nat Genet,* 37**,** 166-70.

MIHAI, R. 2015. Diagnosis, treatment and outcome of adrenocortical cancer. *Br J Surg,* 102**,** 291-306.

MILLER, W. L. 2005. Minireview: regulation of steroidogenesis by electron transfer. *Endocrinology,* 146**,** 2544-50.

MINOWADA, S., KINOSHITA, K., HARA, M., ISURUGI, K., UCHIKAWA, T. & NIIJIMA, T. 1985. Measurement of urinary steroid profile in patients with adrenal tumor as a screening method for carcinoma. *Endocrinol Jpn,* 32**,** 29-37.

MONTANARO, D., MAGGIOLINI, M., RECCHIA, A. G., SIRIANNI, R., AQUILA, S., BARZON, L., FALLO, F., ANDO, S. & PEZZI, V. 2005. Antiestrogens upregulate

estrogen receptor beta expression and inhibit adrenocortical H295R cell proliferation. *J Mol Endocrinol,* 35**,** 245-56.

MONTERO, A. J., DIAZ-MONTERO, C. M., DEUTSCH, Y. E., HURLEY, J., KONIARIS, L. G., RUMBOLDT, T., YASIR, S., JORDA, M., GARRET-MAYER, E., AVISAR, E., SLINGERLAND, J., SILVA, O., WELSH, C., SCHUHWERK, K., SEO, P., PEGRAM, M. D. & GLUCK, S. 2012. Phase 2 study of neoadjuvant treatment with NOV-002 in combination with doxorubicin and cyclophosphamide followed by docetaxel in patients with HER-2 negative clinical stage II-IIIc breast cancer. *Breast Cancer Res Treat,* 132**,** 215-23.

MONTERO, A. J. & JASSEM, J. 2011. Cellular redox pathways as a therapeutic target in the treatment of cancer. *Drugs,* 71**,** 1385-96.

MOORE, C. B., GUTHRIE, E. H., HUANG, M. T. & TAXMAN, D. J. 2010. Short hairpin RNA (shRNA): design, delivery, and assessment of gene knockdown. *Methods Mol Biol,* 629**,** 141-58.

MUSTACICH, D. & POWIS, G. 2000. Thioredoxin reductase. *Biochem J,* 346 Pt 1**,** 1-8.

NA, A. R., CHUNG, Y. M., LEE, S. B., PARK, S. H., LEE, M. S. & YOO, Y. D. 2008. A critical role for Romo1-derived ROS in cell proliferation. *Biochem Biophys Res Commun,* 369**,** 672-8.

NAGEM, R. A., MARTINS, E. A., GONCALVES, V. M., APARICIO, R. & POLIKARPOV, I. 1999. Crystallization and preliminary X-ray diffraction studies of human catalase. *Acta Crystallogr D Biol Crystallogr,* 55**,** 1614-5.

NAING, A., LORUSSO, P., FU, S., HONG, D., CHEN, H. X., DOYLE, L. A., PHAN, A. T., HABRA, M. A. & KURZROCK, R. 2013. Insulin growth factor receptor (IGF-1R) antibody cixutumumab combined with the mTOR inhibitor temsirolimus in patients with metastatic adrenocortical carcinoma. *Br J Cancer,* 108**,** 826-30.

NAIR, R. R., EMMONS, M. F., CRESS, A. E., ARGILAGOS, R. F., LAM, K., KERR, W. T., WANG, H. G., DALTON, W. S. & HAZLEHURST, L. A. 2009. HYD1-induced increase in reactive oxygen species leads to autophagy and necrotic cell death in multiple myeloma cells. *Mol Cancer Ther,* 8**,** 2441-51.

NIEMAN, L. K., BILLER, B. M., FINDLING, J. W., MURAD, M. H., NEWELL-PRICE, J., SAVAGE, M. O., TABARIN, A. & ENDOCRINE, S. 2015. Treatment of Cushing's Syndrome: An Endocrine Society Clinical Practice Guideline. *J Clin Endocrinol Metab,* 100**,** 2807-31.

NIKIFOROV, A., DOLLE, C., NIERE, M. & ZIEGLER, M. 2011. Pathways and subcellular compartmentation of NAD biosynthesis in human cells: from entry of extracellular precursors to mitochondrial NAD generation. *J Biol Chem,* 286**,** 21767-78.

NIU, C., YAN, H., YU, T., SUN, H. P., LIU, J. X., LI, X. S., WU, W., ZHANG, F. Q., CHEN, Y., ZHOU, L., LI, J. M., ZENG, X. Y., YANG, R. R., YUAN, M. M., REN, M. Y., GU, F. Y., CAO, Q., GU, B. W., SU, X. Y., CHEN, G. Q., XIONG, S. M., ZHANG, T. D., WAXMAN, S., WANG, Z. Y., CHEN, Z., HU, J., SHEN, Z. X. & CHEN, S. J. 1999. Studies on treatment of acute promyelocytic leukemia with arsenic trioxide: remission induction, follow-up, and molecular monitoring in 11 newly diagnosed and 47 relapsed acute promyelocytic leukemia patients. *Blood,* 94**,** 3315-24.

NOVOSELOVA, T. V., RATH, S. R., CARPENTER, K., PACHTER, N., DICKINSON, J. E., PRICE, G., CHAN, L. F., CHOONG, C. S. & METHERELL, L. A. 2015. NNT pseudoexon activation as a novel mechanism for disease in two siblings with familial glucocorticoid deficiency. *J Clin Endocrinol Metab,* 100**,** E350-4.

O'DWYER, P. J., HAMILTON, T. C., LACRETA, F. P., GALLO, J. M., KILPATRICK, D., HALBHERR, T., BRENNAN, J., BOOKMAN, M. A., HOFFMAN, J., YOUNG, R. C., COMIS, R. L. & OZOLS, R. F. 1996. Phase I trial of buthionine sulfoximine in combination with melphalan in patients with cancer. *J Clin Oncol,* 14**,** 249-56.

OH, S. Y., SOHN, Y. W., PARK, J. W., PARK, H. J., JEON, H. M., KIM, T. K., LEE, J. S., JUNG, J. E., JIN, X., CHUNG, Y. G., CHOI, Y. K., YOU, S., LEE, J. B. & KIM, H. 2007. Selective cell death of oncogenic Akt-transduced brain cancer cells by etoposide through reactive oxygen species mediated damage. *Mol Cancer Ther,* 6**,** 2178-87.

OHGAKI, H., KLEIHUES, P. & HEITZ, P. U. 1993. p53 mutations in sporadic adrenocortical tumors. *Int J Cancer,* 54**,** 408-10.

OKADA, M., FUKUSHIMA, D. K. & GALLAGHER, T. F. 1959. Isolation and characterization of 3 beta-hydroxy-delta 5-steroids in adrenal carcinoma. *J Biol Chem,* 234**,** 1688-92.

OP DEN WINKEL, J., PFANNSCHMIDT, J., MULEY, T., GRUNEWALD, C., DIENEMANN, H., FASSNACHT, M. & ALLOLIO, B. 2011. Metastatic adrenocortical carcinoma: results of 56 pulmonary metastasectomies in 24 patients. *Ann Thorac Surg,* 92**,** 1965-70.

PAPOTTI, M., LIBE, R., DUREGON, E., VOLANTE, M., BERTHERAT, J. & TISSIER, F. 2011. The Weiss score and beyond--histopathology for adrenocortical carcinoma. *Horm Cancer,* 2**,** 333-40.

PARK, E. J., CHOI, K. S. & KWON, T. K. 2011. beta-Lapachone-induced reactive oxygen species (ROS) generation mediates autophagic cell death in glioma U87 MG cells. *Chem Biol Interact,* 189**,** 37-44.

PARK, S. J. & KIM, I. S. 2005. The role of p38 MAPK activation in auranofin-induced apoptosis of human promyelocytic leukaemia HL-60 cells. *Br J Pharmacol,* 146**,** 506-13.

PARKER, N., VIDAL-PUIG, A. J., AZZU, V. & BRAND, M. D. 2009. Dysregulation of glucose homeostasis in nicotinamide nucleotide transhydrogenase knockout mice is independent of uncoupling protein 2. *Biochim Biophys Acta,* 1787**,** 1451-7.

PAYNE, A. H. & HALES, D. B. 2004. Overview of steroidogenic enzymes in the pathway from cholesterol to active steroid hormones. *Endocr Rev,* 25**,** 947-70.

PELICANO, H., FENG, L., ZHOU, Y., CAREW, J. S., HILEMAN, E. O., PLUNKETT, W., KEATING, M. J. & HUANG, P. 2003. Inhibition of mitochondrial respiration: a novel strategy to enhance drug-induced apoptosis in human leukemia cells by a reactive oxygen species-mediated mechanism. *J Biol Chem,* 278**,** 37832-9.

PERON, F. G., HAKSAR, A. & LIN, M. 1975. Sources of reducing equivalents for cytochrome P-450 mitochondrial steroid hydroxylations in rat adrenal cortex cells. *J Steroid Biochem,* 6**,** 411-7.

PHELPS, D. C. & HATEFI, Y. 1981. Inhibition of the mitochondrial nicotinamide nucleotide transhydrogenase by dicyclohexylcarbodiimide and diethylpyrocarbonate. *J Biol Chem,* 256**,** 8217-21.

PICARD, M., MCMANUS, M. J., GRAY, J. D., NASCA, C., MOFFAT, C., KOPINSKI, P. K., SEIFERT, E. L., MCEWEN, B. S. & WALLACE, D. C. 2015. Mitochondrial functions modulate neuroendocrine, metabolic, inflammatory, and transcriptional responses to acute psychological stress. *Proc Natl Acad Sci U S A,* 112**,** E6614-23.

POLAT, B., FASSNACHT, M., PFREUNDNER, L., GUCKENBERGER, M., BRATENGEIER, K., JOHANSSEN, S., KENN, W., HAHNER, S., ALLOLIO, B. & FLENTJE, M. 2009. Radiotherapy in adrenocortical carcinoma. *Cancer,* 115**,** 2816-23.

POLICASTRO, L., MOLINARI, B., LARCHER, F., BLANCO, P., PODHAJCER, O. L., COSTA, C. S., ROJAS, P. & DURAN, H. 2004. Imbalance of antioxidant enzymes in tumor cells and inhibition of proliferation and malignant features by scavenging hydrogen peroxide. *Mol Carcinog,* 39**,** 103-13.

POLLAK, N., NIERE, M. & ZIEGLER, M. 2007. NAD kinase levels control the NADPH concentration in human cells. *J Biol Chem,* 282**,** 33562-71.

POMMIER, R. F. & BRENNAN, M. F. 1992. An eleven-year experience with adrenocortical carcinoma. *Surgery,* 112**,** 963-70; discussion 970-1.

POWIS, G. & MONTFORT, W. R. 2001. Properties and biological activities of thioredoxins. *Annu Rev Biophys Biomol Struct,* 30**,** 421-55.

PRASAD, R., CHAN, L. F., HUGHES, C. R., KASKI, J. P., KOWALCZYK, J. C., SAVAGE, M. O., PETERS, C. J., NATHWANI, N., CLARK, A. J., STORR, H. L. & METHERELL, L. A. 2014a. Thioredoxin Reductase 2 (TXNRD2) mutation associated with familial glucocorticoid deficiency (FGD). *J Clin Endocrinol Metab,* 99**,** E1556-63.

PRASAD, R., KOWALCZYK, J. C., MEIMARIDOU, E., STORR, H. L. & METHERELL, L. A. 2014b. Oxidative stress and adrenocortical insufficiency. *J Endocrinol,* 221**,** R63-73.

PRASAD, R., METHERELL, L. A., CLARK, A. J. & STORR, H. L. 2013. Deficiency of ALADIN impairs redox homeostasis in human adrenal cells and inhibits steroidogenesis. *Endocrinology,* 154**,** 3209-18.

PUGH, C. W. & RATCLIFFE, P. J. 2003. Regulation of angiogenesis by hypoxia: role of the HIF system. *Nat Med,* 9**,** 677-84.

QU, Y., WANG, J., RAY, P. S., GUO, H., HUANG, J., SHIN-SIM, M., BUKOYE, B. A., LIU, B., LEE, A. V., LIN, X., HUANG, P., MARTENS, J. W., GIULIANO, A. E., ZHANG, N., CHENG, N. H. & CUI, X. 2011. Thioredoxin-like 2 regulates human cancer cell growth and metastasis via redox homeostasis and NF-kappaB signaling. *J Clin Invest,* 121**,** 212-25.

QUINKLER, M., HAHNER, S., WORTMANN, S., JOHANSSEN, S., ADAM, P., RITTER, C., STRASBURGER, C., ALLOLIO, B. & FASSNACHT, M. 2008. Treatment of advanced adrenocortical carcinoma with erlotinib plus gemcitabine. *J Clin Endocrinol Metab,* 93**,** 2057-62.

RADISKY, D. C., LEVY, D. D., LITTLEPAGE, L. E., LIU, H., NELSON, C. M., FATA, J. E., LEAKE, D., GODDEN, E. L., ALBERTSON, D. G., NIETO, M. A., WERB, Z. & BISSELL, M. J. 2005. Rac1b and reactive oxygen species mediate MMP-3-induced EMT and genomic instability. *Nature,* 436**,** 123-7.

RAGAZZON, B., LIBE, R., GAUJOUX, S., ASSIE, G., FRATTICCI, A., LAUNAY, P., CLAUSER, E., BERTAGNA, X., TISSIER, F., DE REYNIES, A. & BERTHERAT, J. 2010. Transcriptome analysis reveals that p53 and {beta}-catenin alterations occur in a group of aggressive adrenocortical cancers. *Cancer Res,* 70**,** 8276-81.

RAINERI, I., CARLSON, E. J., GACAYAN, R., CARRA, S., OBERLEY, T. D., HUANG, T. T. & EPSTEIN, C. J. 2001. Strain-dependent high-level expression of a transgene for manganese superoxide dismutase is associated with growth retardation and decreased fertility. *Free Radic Biol Med,* 31**,** 1018-30.

RAJAMOHAN, S. B., RAGHURAMAN, G., PRABHAKAR, N. R. & KUMAR, G. K. 2012. NADPH oxidase-derived H(2)O(2) contributes to angiotensin II-induced aldosterone synthesis in human and rat adrenal cortical cells. *Antioxid Redox Signal,* 17**,** 445-59.

RAMANATHAN, B., JAN, K. Y., CHEN, C. H., HOUR, T. C., YU, H. J. & PU, Y. S. 2005. Resistance to paclitaxel is proportional to cellular total antioxidant capacity. *Cancer Res,* 65**,** 8455-60.

RAMEZANI, A. & HAWLEY, R. G. 2002. Overview of the HIV-1 Lentiviral Vector System. *Curr Protoc Mol Biol,* Chapter 16**,** Unit 16 21.

RAPOPORT, R., SKLAN, D. & HANUKOGLU, I. 1995. Electron leakage from the adrenal cortex mitochondrial P450scc and P450c11 systems: NADPH and steroid dependence. *Arch Biochem Biophys,* 317**,** 412-6.

RAZA, A., GALILI, N., CALLANDER, N., OCHOA, L., PIRO, L., EMANUEL, P., WILLIAMS, S., BURRIS, H., 3RD, FADERL, S., ESTROV, Z., CURTIN, P., LARSON, R. A., KECK, J. G., JONES, M., MENG, L. & BROWN, G. L. 2009. Phase 1-2a multicenter dose-escalation study of ezatiostat hydrochloride liposomes for injection (Telintra, TLK199), a novel glutathione analog prodrug in patients with myelodysplastic syndrome. *J Hematol Oncol,* 2**,** 20.

REAM, J. M., GAING, B., MUSSI, T. C. & ROSENKRANTZ, A. B. 2015. Characterization of adrenal lesions at chemical-shift MRI: a direct intraindividual comparison of in- and opposed-phase imaging at 1.5 T and 3 T. *AJR Am J Roentgenol,* 204**,** 536-41.

REBRIN, I. & SOHAL, R. S. 2008. Pro-oxidant shift in glutathione redox state during aging. *Adv Drug Deliv Rev,* 60**,** 1545-52.

REIBETANZ, J., JUROWICH, C., ERDOGAN, I., NIES, C., RAYES, N., DRALLE, H., BEHREND, M., ALLOLIO, B., FASSNACHT, M. & GERMAN, A. C. C. S. G. 2012. Impact of lymphadenectomy on the oncologic outcome of patients with adrenocortical carcinoma. *Ann Surg,* 255**,** 363-9.

REINCKE, M., KARL, M., TRAVIS, W. H., MASTORAKOS, G., ALLOLIO, B., LINEHAN, H. M. & CHROUSOS, G. P. 1994. p53 mutations in human adrenocortical neoplasms: immunohistochemical and molecular studies. *J Clin Endocrinol Metab,* 78**,** 790-4.

REINCKE, M., WACHENFELD, C., MORA, P., THUMSER, A., JAURSCH-HANCKE, C., ABDELHAMID, S., CHROUSOS, G. P. & ALLOLIO, B. 1996. p53 mutations in adrenal tumors: Caucasian patients do not show the exon 4 "hot spot" found in Taiwan. *J Clin Endocrinol Metab,* 81**,** 3636-8.

REINEHR, R., BECKER, S., EBERLE, A., GRETHER-BECK, S. & HAUSSINGER, D. 2005. Involvement of NADPH oxidase isoforms and Src family kinases in CD95-dependent hepatocyte apoptosis. *J Biol Chem,* 280**,** 27179-94.

RENSCHLER, M. F. 2004. The emerging role of reactive oxygen species in cancer therapy. *Eur J Cancer,* 40**,** 1934-40.

RIPLEY, R. T., KEMP, C. D., DAVIS, J. L., LANGAN, R. C., ROYAL, R. E., LIBUTTI, S. K., STEINBERG, S. M., WOOD, B. J., KAMMULA, U. S., FOJO, T. & AVITAL, I. 2011. Liver resection and ablation for metastatic adrenocortical carcinoma. *Ann Surg Oncol,* 18**,** 1972-9.

RIPOLL, V. M., MEADOWS, N. A., BANGERT, M., LEE, A. W., KADIOGLU, A. & COX, R. D. 2012. Nicotinamide nucleotide transhydrogenase (NNT) acts as a novel modulator of macrophage inflammatory responses. *FASEB J,* 26**,** 3550-62.

RITCHIE, J. & BALASUBRAMANIAN, S. 2011. Anatomy of the pituitary, thyroid, parathyroid and adrenal glands. *Surgery (Oxf),* 29**,** 403-407.

RONCHI, J. A., FIGUEIRA, T. R., RAVAGNANI, F. G., OLIVEIRA, H. C., VERCESI, A. E. & CASTILHO, R. F. 2013. A spontaneous mutation in the nicotinamide nucleotide transhydrogenase gene of C57BL/6J mice results in mitochondrial redox abnormalities. *Free Radic Biol Med,* 63**,** 446-56.

ROUCHER-BOULEZ, F., MALLET-MOTAK, D., SAMARA-BOUSTANI, D., JILANI, H., LADJOUZE, A., SOUCHON, P. F., SIMON, D., NIVOT, S., HEINRICHS, C., RONZE,

M., BERTAGNA, X., GROISNE, L., LEHEUP, B., NAUD-SAUDREAU, C., BLONDIN, G., LEFEVRE, C., LEMARCHAND, L. & MOREL, Y. 2016. NNT mutations: a cause of primary adrenal insufficiency, oxidative stress and extra-adrenal defects. *Eur J Endocrinol,* 175**,** 73-84.

RUDIN, C. M., YANG, Z., SCHUMAKER, L. M., VANDERWEELE, D. J., NEWKIRK, K., EGORIN, M. J., ZUHOWSKI, E. G. & CULLEN, K. J. 2003. Inhibition of glutathione synthesis reverses Bcl-2-mediated cisplatin resistance. *Cancer Res,* 63**,** 312-8.

RUIZ-RAMOS, R., LOPEZ-CARRILLO, L., RIOS-PEREZ, A. D., DE VIZCAYA-RUIZ, A. & CEBRIAN, M. E. 2009. Sodium arsenite induces ROS generation, DNA oxidative damage, HO-1 and c-Myc proteins, NF-kappaB activation and cell proliferation in human breast cancer MCF-7 cells. *Mutat Res,* 674**,** 109-15.

RYDSTROM, J. 1972. Site-specific inhibitors of mitochondrial nicotinamide-nucleotide transhydrogenase. *Eur J Biochem,* 31**,** 496-504.

RYDSTROM, J. 1974. Evidence for a proton-dependent regulation of mitochondrial nicotinamide-nucleotide transhydrogenase. *Eur J Biochem,* 45**,** 67-76.

RYDSTROM, J. 2006. Mitochondrial NADPH, transhydrogenase and disease. *Biochim Biophys Acta,* 1757**,** 721-6.

RYDSTROM, J., HU, X., FJELLSTROM, O., MEULLER, J., ZHANG, J., JOHANSSON, C. & BIZOUARN, T. 1998. Domains, specific residues and conformational states involved in hydride ion transfer and proton pumping by nicotinamide nucleotide transhydrogenase from Escherichia coli. *Biochim Biophys Acta,* 1365**,** 10-6.

SABHARWAL, S. S. & SCHUMACKER, P. T. 2014. Mitochondrial ROS in cancer: initiators, amplifiers or an Achilles' heel? *Nat Rev Cancer,* 14**,** 709-21.

SAUER, U., CANONACO, F., HERI, S., PERRENOUD, A. & FISCHER, E. 2004. The soluble and membrane-bound transhydrogenases UdhA and PntAB have divergent functions in NADPH metabolism of Escherichia coli. *J Biol Chem,* 279**,** 6613-9.

SAUNDERS, J. A., ROGERS, L. C., KLOMSIRI, C., POOLE, L. B. & DANIEL, L. W. 2010. Reactive oxygen species mediate lysophosphatidic acid induced signaling in ovarian cancer cells. *Free Radic Biol Med,* 49**,** 2058-67.

SBIERA, S., LEICH, E., LIEBISCH, G., SBIERA, I., SCHIRBEL, A., WIEMER, L., MATYSIK, S., ECKHARDT, C., GARDILL, F., GEHL, A., KENDL, S., WEIGAND, I., BALA, M., RONCHI, C. L., DEUTSCHBEIN, T., SCHMITZ, G., ROSENWALD, A., ALLOLIO, B., FASSNACHT, M. & KROISS, M. 2015. Mitotane Inhibits Sterol-O-Acyl Transferase 1 Triggering Lipid-Mediated Endoplasmic Reticulum Stress and Apoptosis in Adrenocortical Carcinoma Cells. *Endocrinology,* 156**,** 3895-908.

SBIERA, S., SCHMULL, S., ASSIE, G., VOELKER, H. U., KRAUS, L., BEYER, M., RAGAZZON, B., BEUSCHLEIN, F., WILLENBERG, H. S., HAHNER, S., SAEGER, W., BERTHERAT, J., ALLOLIO, B. & FASSNACHT, M. 2010. High diagnostic and prognostic value of steroidogenic factor-1 expression in adrenal tumors. *J Clin Endocrinol Metab,* 95**,** E161-71.

SCHAFER, F. Q. & BUETTNER, G. R. 2001. Redox environment of the cell as viewed through the redox state of the glutathione disulfide/glutathione couple. *Free Radic Biol Med,* 30**,** 1191-212.

SCHIEBER, M. & CHANDEL, N. S. 2014. ROS function in redox signaling and oxidative stress. *Curr Biol,* 24**,** R453-62.

SCHLUMBERGER, M., BRUGIERES, L., GICQUEL, C., TRAVAGLI, J. P., DROZ, J. P. & PARMENTIER, C. 1991. 5-Fluorouracil, doxorubicin, and cisplatin as treatment for adrenal cortical carcinoma. *Cancer,* 67**,** 2997-3000.

SCHNELLDORFER, T., GANSAUGE, S., GANSAUGE, F., SCHLOSSER, S., BEGER, H. G. & NUSSLER, A. K. 2000. Glutathione depletion causes cell growth inhibition and enhanced apoptosis in pancreatic cancer cells. *Cancer,* 89**,** 1440-7.

SCHTEINGART, D. E., DOHERTY, G. M., GAUGER, P. G., GIORDANO, T. J., HAMMER, G. D., KOROBKIN, M. & WORDEN, F. P. 2005. Management of patients with adrenal cancer: recommendations of an international consensus conference. *Endocr Relat Cancer,* 12**,** 667-80.

SCHULICK, R. D. & BRENNAN, M. F. 1999. Long-term survival after complete resection and repeat resection in patients with adrenocortical carcinoma. *Ann Surg Oncol,* 6**,** 719-26.

SCHULTE, H. M., BENKER, G., REINWEIN, D., SIPPELL, W. G. & ALLOLIO, B. 1990. Infusion of low dose etomidate: correction of hypercortisolemia in patients with Cushing's syndrome and dose-response relationship in normal subjects. *J Clin Endocrinol Metab,* 70**,** 1426-30.

SCHUMACKER, P. T. 2006. Reactive oxygen species in cancer cells: live by the sword, die by the sword. *Cancer Cell,* 10**,** 175-6.

SECCIA, T. M., FASSINA, A., NUSSDORFER, G. G., PESSINA, A. C. & ROSSI, G. P. 2005. Aldosterone-producing adrenocortical carcinoma: an unusual cause of Conn's syndrome with an ominous clinical course. *Endocr Relat Cancer,* 12**,** 149-59.

SEQUIST, L. V., FIDIAS, P. M., TEMEL, J. S., KOLEVSKA, T., RABIN, M. S., BOCCIA, R. V., BURRIS, H. A., BELT, R. J., HUBERMAN, M. S., MELNYK, O., MILLS, G. M., ENGLUND, C. W., CALDWELL, D. C., KECK, J. G., MENG, L., JONES, M., BROWN, G. L., EDELMAN, M. J. & LYNCH, T. J. 2009. Phase 1-2a multicenter dose-ranging study of canfosfamide in combination with carboplatin and paclitaxel as first-line therapy for patients with advanced non-small cell lung cancer. *J Thorac Oncol,* 4**,** 1389-96.

SHACKLETON, C. H. & SNODGRASS, G. H. 1974. Steroid excretion by an infant with an unusual salt-losing syndrome: a gas chromatographic-mass spectrometric study. *Ann Clin Biochem,* 11**,** 91-9.

SHEN, Z. X., CHEN, G. Q., NI, J. H., LI, X. S., XIONG, S. M., QIU, Q. Y., ZHU, J., TANG, W., SUN, G. L., YANG, K. Q., CHEN, Y., ZHOU, L., FANG, Z. W., WANG, Y. T., MA, J., ZHANG, P., ZHANG, T. D., CHEN, S. J., CHEN, Z. & WANG, Z. Y. 1997. Use of arsenic trioxide (As2O3) in the treatment of acute promyelocytic leukemia (APL): II. Clinical efficacy and pharmacokinetics in relapsed patients. *Blood,* 89**,** 3354-60.

SHIL, P., SANGHVI, S. H., VIDYASAGAR, P. B. & MISHRA, K. P. 2005. Enhancement of radiation cytotoxicity in murine cancer cells by electroporation: in vitro and in vivo studies. *J Environ Pathol Toxicol Oncol,* 24**,** 291-8.

SHIMOMURA, K., GALVANOVSKIS, J., GOLDSWORTHY, M., HUGILL, A., KAIZAK, S., LEE, A., MEADOWS, N., QUWAILID, M. M., RYDSTROM, J., TEBOUL, L., ASHCROFT, F. & COX, R. D. 2009. Insulin secretion from beta-cells is affected by deletion of nicotinamide nucleotide transhydrogenase. *Methods Enzymol,* 457**,** 451-80.

SHRIVASTAVA, A., KUZONTKOSKI, P. M., GROOPMAN, J. E. & PRASAD, A. 2011. Cannabidiol induces programmed cell death in breast cancer cells by coordinating the cross-talk between apoptosis and autophagy. *Mol Cancer Ther,* 10**,** 1161-72.

SJOVALL, J. 1975. Analysis of steroids by liquid-gel chromatography and computerized gas chromatography-mass spectrometry. *J Steroid Biochem,* 6**,** 227-32.

SOBHAKUMARI, A., LOVE-HOMAN, L., FLETCHER, E. V., MARTIN, S. M., PARSONS, A. D., SPITZ, D. R., KNUDSON, C. M. & SIMONS, A. L. 2012. Susceptibility of human head and neck cancer cells to combined inhibition of glutathione and thioredoxin metabolism. *PLoS One,* 7**,** e48175.

SOGA, H., TAKENAKA, A., OOBA, T., NAKANO, Y., MIYAKE, H., TAKEDA, M., TANAKA, K., HARA, I. & FUJISAWA, M. 2009. A twelve-year experience with adrenal cortical carcinoma in a single institution: long-term survival after surgical treatment and transcatheter arterial embolization. *Urol Int,* 82**,** 222-6.

SOMJEN, D., STERN, N., KNOLL, E., SHARON, O., GAYER, B., KULIK, T. & KOHEN, F. 2003. Carboxy derivatives of isoflavones as affinity carriers for cytotoxic drug targeting in adrenocortical H295R carcinoma cells. *J Endocrinol,* 179**,** 395-403.

SPERONE, P., FERRERO, A., DAFFARA, F., PRIOLA, A., ZAGGIA, B., VOLANTE, M., SANTINI, D., VINCENZI, B., BADALAMENTI, G., INTRIVICI, C., DEL BUONO, S., DE FRANCIA, S., KALOMIRAKIS, E., RATTI, R., ANGELI, A., DOGLIOTTI, L., PAPOTTI, M., TERZOLO, M. & BERRUTI, A. 2010. Gemcitabine plus metronomic 5-fluorouracil or capecitabine as a second-/third-line chemotherapy in advanced adrenocortical carcinoma: a multicenter phase II study. *Endocr Relat Cancer,* 17**,** 445-53.

ST-PIERRE, J., BUCKINGHAM, J. A., ROEBUCK, S. J. & BRAND, M. D. 2002. Topology of superoxide production from different sites in the mitochondrial electron transport chain. *J Biol Chem,* 277**,** 44784-90.

STOCCO, D. M. & ASCOLI, M. 1993. The use of genetic manipulation of MA-10 Leydig tumor cells to demonstrate the role of mitochondrial proteins in the acute regulation of steroidogenesis. *Endocrinology,* 132**,** 959-67.

STOCCO, D. M., WELLS, J. & CLARK, B. J. 1993. The effects of hydrogen peroxide on steroidogenesis in mouse Leydig tumor cells. *Endocrinology,* 133**,** 2827-32.

STOJADINOVIC, A., GHOSSEIN, R. A., HOOS, A., NISSAN, A., MARSHALL, D., DUDAS, M., CORDON-CARDO, C., JAQUES, D. P. & BRENNAN, M. F. 2002. Adrenocortical carcinoma: clinical, morphologic, and molecular characterization. *J Clin Oncol,* 20**,** 941-50.

STURGEON, C., SHEN, W. T., CLARK, O. H., DUH, Q. Y. & KEBEBEW, E. 2006. Risk assessment in 457 adrenal cortical carcinomas: how much does tumor size predict the likelihood of malignancy? *J Am Coll Surg,* 202**,** 423-30.

SULLIVAN, R. & GRAHAM, C. H. 2008. Chemosensitization of cancer by nitric oxide. *Curr Pharm Des,* 14**,** 1113-23.

SUN, J. S., TSUANG, Y. H., HUANG, W. C., CHEN, L. T., HANG, Y. S. & LU, F. J. 1997. Menadione-induced cytotoxicity to rat osteoblasts. *Cell Mol Life Sci,* 53**,** 967-76.

SWEENEY, C., LIU, G., YIANNOUTSOS, C., KOLESAR, J., HORVATH, D., STAAB, M. J., FIFE, K., ARMSTRONG, V., TRESTON, A., SIDOR, C. & WILDING, G. 2005. A phase II multicenter, randomized, double-blind, safety trial assessing the pharmacokinetics, pharmacodynamics, and efficacy of oral 2-methoxyestradiol capsules in hormone-refractory prostate cancer. *Clin Cancer Res,* 11**,** 6625-33.

TADJINE, M., LAMPRON, A., OUADI, L. & BOURDEAU, I. 2008. Frequent mutations of beta-catenin gene in sporadic secreting adrenocortical adenomas. *Clin Endocrinol (Oxf),* 68**,** 264-70.

TAGDE, A., SINGH, H., KANG, M. H. & REYNOLDS, C. P. 2014. The glutathione synthesis inhibitor buthionine sulfoximine synergistically enhanced melphalan activity against preclinical models of multiple myeloma. *Blood Cancer J,* 4**,** e229.

TALBOT, S., NELSON, R. & SELF, W. T. 2008. Arsenic trioxide and auranofin inhibit selenoprotein synthesis: implications for chemotherapy for acute promyelocytic leukaemia. *Br J Pharmacol,* 154**,** 940-8.

TATTERSALL, M. H., LANDER, H., BAIN, B., STOCKS, A. E., WOODS, R. L., FOX, R. M., BYRNE, E., TROTTEN, J. R. & ROOS, I. 1980. Cis-platinum treatment of metastatic adrenal carcinoma. *Med J Aust,* 1**,** 419-21.

TAYLOR, A. E., KEEVIL, B. & HUHTANIEMI, I. T. 2015. Mass spectrometry and immunoassay: how to measure steroid hormones today and tomorrow. *Eur J Endocrinol,* 173**,** D1-12.

TERZOLO, M. 2012. Adrenocortical carcinoma. *In:* ELSE, T. (ed.) *Adrenocortical carcinoma.* New York: Elsevier.

TERZOLO, M., ANGELI, A., FASSNACHT, M., DAFFARA, F., TAUCHMANOVA, L., CONTON, P. A., ROSSETTO, R., BUCI, L., SPERONE, P., GROSSRUBATSCHER, E., REIMONDO, G., BOLLITO, E., PAPOTTI, M., SAEGER, W., HAHNER, S., KOSCHKER, A. C., ARVAT, E., AMBROSI, B., LOLI, P., LOMBARDI, G., MANNELLI, M., BRUZZI, P., MANTERO, F., ALLOLIO, B., DOGLIOTTI, L. & BERRUTI, A. 2007. Adjuvant mitotane treatment for adrenocortical carcinoma. *N Engl J Med,* 356**,** 2372-80.

TIU, S. C., CHAN, A. O., TAYLOR, N. F., LEE, C. Y., LOUNG, P. Y., CHOI, C. H. & SHEK, C. C. 2009. Use of urinary steroid profiling for diagnosing and monitoring adrenocortical tumours. *Hong Kong Med J,* 15**,** 463-70.

TOUCHSTONE, J. C., RICHARDSON, E. M., BULASCHENKO, H., LANDOLT, I. & DOHAN, F. C. 1954. Isolation of pregnane-3-alpha, 17-alpha, 21-triol-20-one (tetrahydro compound S) from the urine of a woman with metastatic adrenocortical carcinoma. *J Clin Endocrinol Metab,* 14**,** 676-8.

TOWNSEND, D. M. & TEW, K. D. 2009. Pharmacology of a mimetic of glutathione disulfide, NOV-002. *Biomed Pharmacother,* 63**,** 75-8.

TOYE, A. A., LIPPIAT, J. D., PROKS, P., SHIMOMURA, K., BENTLEY, L., HUGILL, A., MIJAT, V., GOLDSWORTHY, M., MOIR, L., HAYNES, A., QUARTERMAN, J., FREEMAN, H. C., ASHCROFT, F. M. & COX, R. D. 2005. A genetic and physiological study of impaired glucose homeostasis control in C57BL/6J mice. *Diabetologia,* 48**,** 675-86.

TRACHOOTHAM, D., ALEXANDRE, J. & HUANG, P. 2009. Targeting cancer cells by ROS-mediated mechanisms: a radical therapeutic approach? *Nat Rev Drug Discov,* 8**,** 579-91.

TRACHOOTHAM, D., ZHOU, Y., ZHANG, H., DEMIZU, Y., CHEN, Z., PELICANO, H., CHIAO, P. J., ACHANTA, G., ARLINGHAUS, R. B., LIU, J. & HUANG, P. 2006. Selective killing of oncogenically transformed cells through a ROS-mediated mechanism by beta-phenylethyl isothiocyanate. *Cancer Cell,* 10**,** 241-52.

TRAVERSO, N., RICCIARELLI, R., NITTI, M., MARENGO, B., FURFARO, A. L., PRONZATO, M. A., MARINARI, U. M. & DOMENICOTTI, C. 2013. Role of glutathione in cancer progression and chemoresistance. *Oxid Med Cell Longev,* 2013**,** 972913.

UCHIKURA, K., WADA, T., HOSHINO, S., NAGAKAWA, Y., AIKO, T., BULKLEY, G. B., KLEIN, A. S. & SUN, Z. 2004. Lipopolysaccharides induced increases in Fas ligand expression by Kupffer cells via mechanisms dependent on reactive oxygen species. *Am J Physiol Gastrointest Liver Physiol,* 287**,** G620-6.

UEDA, S., MASUTANI, H., NAKAMURA, H., TANAKA, T., UENO, M. & YODOI, J. 2002. Redox control of cell death. *Antioxid Redox Signal,* 4**,** 405-14.

URSINI, M. V., PARRELLA, A., ROSA, G., SALZANO, S. & MARTINI, G. 1997. Enhanced expression of glucose-6-phosphate dehydrogenase in human cells sustaining oxidative stress. *Biochem J,* 323 (Pt 3)**,** 801-6.

UYS, J. D., MANEVICH, Y., DEVANE, L. C., HE, L., GARRET, T. E., PAZOLES, C. J., TEW, K. D. & TOWNSEND, D. M. 2010. Preclinical pharmacokinetic analysis of NOV-002, a glutathione disulfide mimetic. *Biomed Pharmacother,* 64**,** 493-8.

VAN ROERMUND, C. W., VISSER, W. F., IJLST, L., VAN CRUCHTEN, A., BOEK, M., KULIK, W., WATERHAM, H. R. & WANDERS, R. J. 2008. The human peroxisomal ABC half transporter ALDP functions as a homodimer and accepts acyl-CoA esters. *FASEB J,* 22**,** 4201-8.

VAN SLOOTEN, H. & VAN OOSTEROM, A. T. 1983. CAP (cyclophosphamide, doxorubicin, and cisplatin) regimen in adrenal cortical carcinoma. *Cancer Treat Rep,* 67**,** 377-9.

VANDER HEIDEN, M. G., CANTLEY, L. C. & THOMPSON, C. B. 2009. Understanding the Warburg effect: the metabolic requirements of cell proliferation. *Science,* 324**,** 1029-33.

VELIKANOVA, L. I., SHAFIGULLINA, Z. R., LISITSIN, A. A., VOROKHOBINA, N. V., GRIGORYAN, K., KUKHIANIDZE, E. A., STRELNIKOVA, E. G., KRIVOKHIZHINA, N. S., KRASNOV, L. M., FEDOROV, E. A., SABLIN, I. V., MOSKVIN, A. L. & BESSONOVA, E. A. 2016. Different Types of Urinary Steroid Profiling Obtained by High-Performance Liquid Chromatography and Gas Chromatography-Mass Spectrometry in Patients with Adrenocortical Carcinoma. *Horm Cancer,* 7**,** 327-335.

VERGOTE, I., FINKLER, N., DEL CAMPO, J., LOHR, A., HUNTER, J., MATEI, D., KAVANAGH, J., VERMORKEN, J. B., MENG, L., JONES, M., BROWN, G., KAYE, S. & GROUP, A.-S. 2009. Phase 3 randomised study of canfosfamide (Telcyta, TLK286) versus pegylated liposomal doxorubicin or topotecan as third-line therapy in patients with platinum-refractory or -resistant ovarian cancer. *Eur J Cancer,* 45**,** 2324-32.

WAJCHENBERG, B. L., ALBERGARIA PEREIRA, M. A., MEDONCA, B. B., LATRONICO, A. C., CAMPOS CARNEIRO, P., ALVES, V. A., ZERBINI, M. C., LIBERMAN, B., CARLOS GOMES, G. & KIRSCHNER, M. A. 2000. Adrenocortical carcinoma: clinical and laboratory observations. *Cancer,* 88**,** 711-36.

WANG, G. L., JIANG, B. H. & SEMENZA, G. L. 1995. Effect of altered redox states on expression and DNA-binding activity of hypoxia-inducible factor 1. *Biochem Biophys Res Commun,* 212**,** 550-6.

WANG, T. & RAINEY, W. E. 2012. Human adrenocortical carcinoma cell lines. *Mol Cell Endocrinol,* 351**,** 58-65.

WANG, X., SON, Y. O., CHANG, Q., SUN, L., HITRON, J. A., BUDHRAJA, A., ZHANG, Z., KE, Z., CHEN, F., LUO, J. & SHI, X. 2011. NADPH oxidase activation is required in reactive oxygen species generation and cell transformation induced by hexavalent chromium. *Toxicol Sci,* 123**,** 399-410.

WANGBERG, B., KHORRAM-MANESH, A., JANSSON, S., NILSSON, B., NILSSON, O., JAKOBSSON, C. E., LINDSTEDT, S., ODEN, A. & AHLMAN, H. 2010. The long-term survival in adrenocortical carcinoma with active surgical management and use of monitored mitotane. *Endocr Relat Cancer,* 17**,** 265-72.

WATSON, J. 2013. Oxidants, antioxidants and the current incurability of metastatic cancers. *Open Biol,* 3**,** 120144.

WEINBERG-SHUKRON, A., ABU-LIBDEH, A., ZHADEH, F., CARMEL, L., KOGOT-LEVIN, A., KAMAL, L., KANAAN, M., ZELIGSON, S., RENBAUM, P., LEVY-

LAHAD, E. & ZANGEN, D. 2015. Combined mineralocorticoid and glucocorticoid deficiency is caused by a novel founder nicotinamide nucleotide transhydrogenase mutation that alters mitochondrial morphology and increases oxidative stress. *J Med Genet,* 52**,** 636-41.

WEIR, S. J., DEGENNARO, L. J. & AUSTIN, C. P. 2012. Repurposing approved and abandoned drugs for the treatment and prevention of cancer through public-private partnership. *Cancer Res,* 72**,** 1055-8.

WEISS, L. M. 1984. Comparative histologic study of 43 metastasizing and nonmetastasizing adrenocortical tumors. *Am J Surg Pathol,* 8**,** 163-9.

WEISS, L. M., MEDEIROS, L. J. & VICKERY, A. L., JR. 1989. Pathologic features of prognostic significance in adrenocortical carcinoma. *Am J Surg Pathol,* 13**,** 202-6.

WHATLEY, S. A., CURTI, D., DAS GUPTA, F., FERRIER, I. N., JONES, S., TAYLOR, C. & MARCHBANKS, R. M. 1998. Superoxide, neuroleptics and the ubiquinone and cytochrome b5 reductases in brain and lymphocytes from normals and schizophrenic patients. *Mol Psychiatry,* 3**,** 227-37.

WIEDEMANN, H. R. 1997. Frequency of Wiedemann-Beckwith syndrome in Germany; rate of hemihyperplasia and of tumours in affected children. *Eur J Pediatr,* 156**,** 251.

WILLIAMSON, S. K., LEW, D., MILLER, G. J., BALCERZAK, S. P., BAKER, L. H. & CRAWFORD, E. D. 2000. Phase II evaluation of cisplatin and etoposide followed by mitotane at disease progression in patients with locally advanced or metastatic adrenocortical carcinoma: a Southwest Oncology Group Study. *Cancer,* 88**,** 1159-65.

WONDRAK, G. T. 2009. Redox-directed cancer therapeutics: molecular mechanisms and opportunities. *Antioxid Redox Signal,* 11**,** 3013-69.

WONG, D. D., SPAGNOLO, D. V., BISCEGLIA, M., HAVLAT, M., MCCALLUM, D. & PLATTEN, M. A. 2011. Oncocytic adrenocortical neoplasms--a clinicopathologic study of 13 new cases emphasizing the importance of their recognition. *Hum Pathol,* 42**,** 489-99.

WOOD, M. A. & HAMMER, G. D. 2011. Adrenocortical stem and progenitor cells: unifying model of two proposed origins. *Mol Cell Endocrinol,* 336**,** 206-12.

WOOTEN, M. D. & KING, D. K. 1993. Adrenal cortical carcinoma. Epidemiology and treatment with mitotane and a review of the literature. *Cancer,* 72**,** 3145-55.

WORTMANN, S., QUINKLER, M., RITTER, C., KROISS, M., JOHANSSEN, S., HAHNER, S., ALLOLIO, B. & FASSNACHT, M. 2010. Bevacizumab plus capecitabine as a salvage therapy in advanced adrenocortical carcinoma. *Eur J Endocrinol,* 162**,** 349-56.

WU, C. C., SHETE, S., AMOS, C. I. & STRONG, L. C. 2006. Joint effects of germ-line p53 mutation and sex on cancer risk in Li-Fraumeni syndrome. *Cancer Res,* 66**,** 8287-92.

XIAO, Q., YANG, Y. A., ZHAO, X. Y., HE, L. S., QIN, Y., HE, Y. H., ZHANG, G. P. & LUO, J. D. 2015. Oxidative stress contributes to the impaired sonic hedgehog pathway in type 1 diabetic mice with myocardial infarction. *Exp Ther Med,* 10**,** 1750-1758.

XIE, C. M., CHAN, W. Y., YU, S., ZHAO, J. & CHENG, C. H. 2011. Bufalin induces autophagy-mediated cell death in human colon cancer cells through reactive oxygen species generation and JNK activation. *Free Radic Biol Med,* 51**,** 1365-75.

XING, Y., EDWARDS, M. A., AHLEM, C., KENNEDY, M., COHEN, A., GOMEZ-SANCHEZ, C. E. & RAINEY, W. E. 2011. The effects of ACTH on steroid metabolomic profiles in human adrenal cells. *J Endocrinol,* 209**,** 327-35.

YAMAGUCHI, M., HATEFI, Y., TRACH, K. & HOCH, J. A. 1988. The primary structure of the mitochondrial energy-linked nicotinamide nucleotide transhydrogenase deduced from the sequence of cDNA clones. *J Biol Chem,* 263**,** 2761-7.

YAMAGUCHI, R., KATO, F., HASEGAWA, T., KATSUMATA, N., FUKAMI, M., MATSUI, T., NAGASAKI, K. & OGATA, T. 2013. A novel homozygous mutation of the nicotinamide nucleotide transhydrogenase gene in a Japanese patient with familial glucocorticoid deficiency. *Endocr J,* 60**,** 855-9.

YAN, B., PENG, Y. & LI, C. Y. 2009. Molecular analysis of genetic instability caused by chronic inflammation. *Methods Mol Biol,* 512**,** 15-28.

YANG, C., JO, S. H., CSERNUS, B., HYJEK, E., LIU, Y., CHADBURN, A. & WANG, Y. L. 2007. Activation of peroxisome proliferator-activated receptor gamma contributes to the survival of T lymphoma cells by affecting cellular metabolism. *Am J Pathol,* 170**,** 722-32.

YIN, F., SANCHETI, H. & CADENAS, E. 2012. Silencing of nicotinamide nucleotide transhydrogenase impairs cellular redox homeostasis and energy metabolism in PC12 cells. *Biochim Biophys Acta,* 1817**,** 401-9.

YING, W. 2008. NAD+/NADH and NADP+/NADPH in cellular functions and cell death: regulation and biological consequences. *Antioxid Redox Signal,* 10**,** 179-206.

ZHAO, Y., AO, H., CHEN, L., SOTTAS, C. M., GE, R. S., LI, L. & ZHANG, Y. 2012. Mono-(2-ethylhexyl) phthalate affects the steroidogenesis in rat Leydig cells through provoking ROS perturbation. *Toxicol In Vitro,* 26**,** 950-5.

ZHENG, S., CHERNIACK, A. D., DEWAL, N., MOFFITT, R. A., DANILOVA, L., MURRAY, B. A., LERARIO, A. M., ELSE, T., KNIJNENBURG, T. A., CIRIELLO, G., KIM, S., ASSIE, G., MOROZOVA, O., AKBANI, R., SHIH, J., HOADLEY, K. A., CHOUEIRI, T. K., WALDMANN, J., METE, O., ROBERTSON, A. G., WU, H. T., RAPHAEL, B. J., SHAO, L., MEYERSON, M., DEMEURE, M. J., BEUSCHLEIN, F., GILL, A. J., SIDHU, S. B., ALMEIDA, M. Q., FRAGOSO, M. C., COPE, L. M., KEBEBEW, E., HABRA, M. A., WHITSETT, T. G., BUSSEY, K. J., RAINEY, W. E., ASA, S. L., BERTHERAT, J., FASSNACHT, M., WHEELER, D. A., CANCER GENOME ATLAS RESEARCH, N., HAMMER, G. D., GIORDANO, T. J. & VERHAAK, R. G. 2016. Comprehensive Pan-Genomic Characterization of Adrenocortical Carcinoma. *Cancer Cell,* 30**,** 363.

ZHOU, Y., HILEMAN, E. O., PLUNKETT, W., KEATING, M. J. & HUANG, P. 2003. Free radical stress in chronic lymphocytic leukemia cells and its role in cellular sensitivity to ROS-generating anticancer agents. *Blood,* 101**,** 4098-104.

ZIEGLER, G. A., VONRHEIN, C., HANUKOGLU, I. & SCHULZ, G. E. 1999. The structure of adrenodoxin reductase of mitochondrial P450 systems: electron transfer for steroid biosynthesis. *J Mol Biol,* 289**,** 981-90.